Tidal Bridge

Improvement of the operating reliability by reducing the dynamic response due to waves

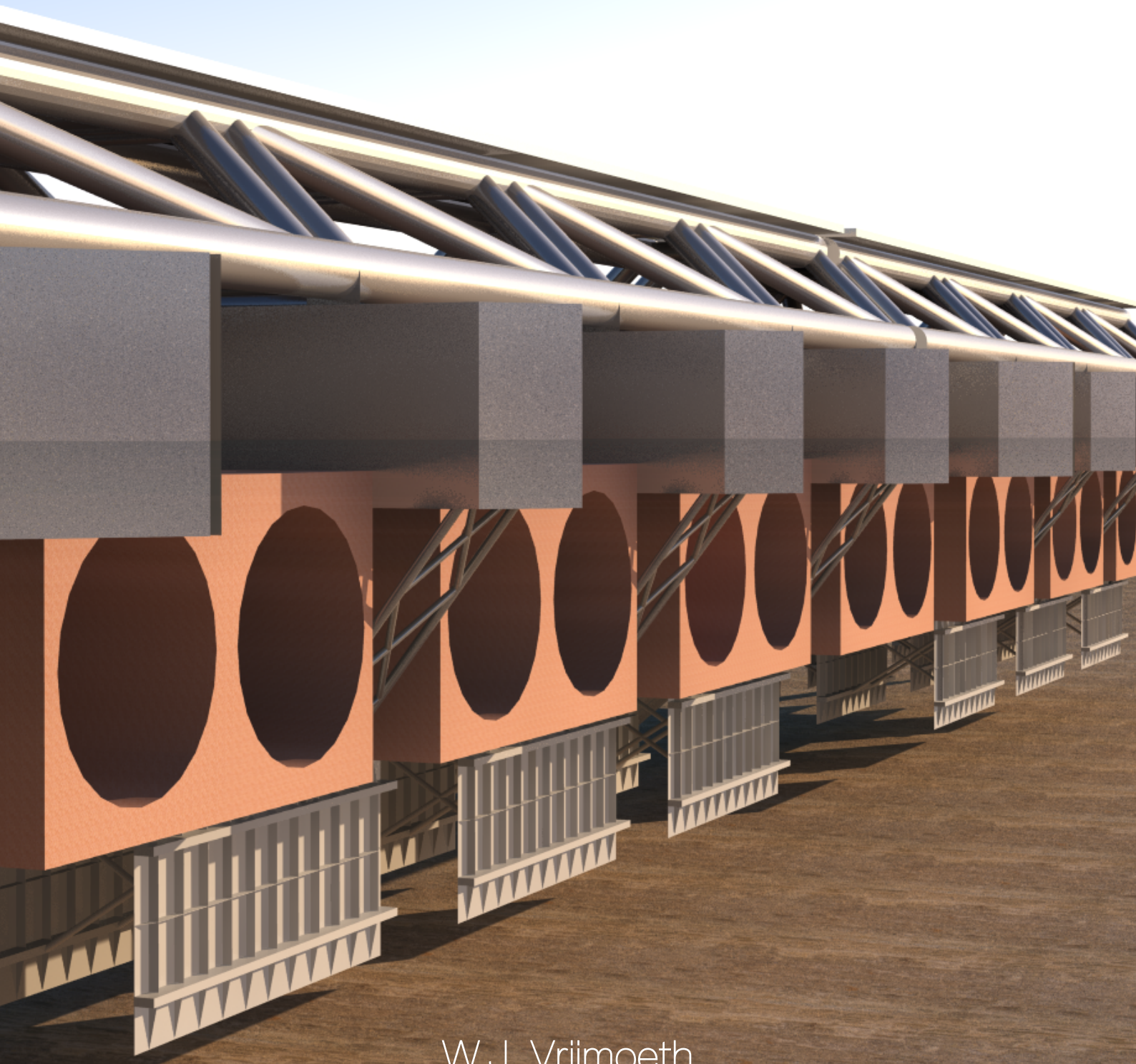

W.J. Vrijmoeth

bam

TU Delft

The image on the cover page shows an idea of the resulting design of this report.

The Tidal Bridge

Improvement of the operating reliability by reducing the dynamic response due to waves

A patented concept held by the Royal BAM Group of a floating bridge combined with the world's largest tidal power plant located in the Strait of Larantuka, Indonesia

W.J. (Wessel) Vrijmoeth

to obtain the degree of,
Master of Science in Civil Engineering,
track Hydraulic Engineering,
at the Delft University of Technology,
to be defended publicly on Thursday December 17, 2020 at 12:00.

Student number:	4367014
Student email:	w.j.vrijmoeth@student.tudelft.nl
Project start:	March 1, 2020

Examination committee:

Dr. ir. J.D. Bricker (chair), *Associate professor, Hydraulic Engineering,*	*Delft University of Technology*
Dr. ing. M.Z. Voorendt, *Researcher and Lecturer of Hydraulic Structures,*	*Delft University of Technology*
Dr. ir. H. Hendrikse, *Assistant Professor Offshore Engineering,*	*Delft University of Technology*
Ir. D.J. de Jong, *Design Manager,*	*BAM Infraconsult bv*

An electronic version of this thesis is available at http://repository.tudelft.nl/.

Preface

This thesis presents the design report on the improvement of the operating reliability of the BAM Tidal Bridge by reducing the dynamic response due to waves. It delivers the last part of the master program of Civil Engineering at Delft University of Technology (DUT). The thesis has been accomplished in close collaboration with the Royal BAM Group which develops the patented Tidal Bridge concept. The thesis follows upon two earlier theses of F.F.H.M. Hoogsteder and G. Dorgelo. They studied the Tidal Bridge dynamics before, guided by the Delft University of Technology and the Royal BAM Group as well. These theses, including this thesis, are one step ahead in the development of the Tidal Bridge concept as the Royal BAM Group is still working on contractual phase of the project.

The thesis contributes to the BAM Tidal Bridge team in providing in depth knowledge about the physical processes that drive the dynamic behaviour of the Tidal Bridge, and in providing possible mitigation strategies which may or may not be effective. The thesis also contributes to future students that are willing to study the Tidal Bridge or differently shaped floating structures. Basic foreknowledge is recommended in environmental fluid mechanics, fluid-structure interactions, dynamics of structures, and hydraulic structures.

I would like to express my sincere gratitude towards those who have contributed and supported me in accomplishing this thesis. Jeremy Bricker (DUT) is greatly appreciated in chairing the thesis committee and his constructive feedback. Mark Voorendt (DUT) as daily supervisor showed to be exceptionally valuable in his analytic thinking and his guidance about the optimal methodology, terminology, and outline which covers a large part of the thesis. Dick de Jong (BAM) as daily supervisor contributed greatly in sharing his hands-on engineering approach, and his divers experience of designing complex structures. Hayo Hendrikse (DUT) has been very devoted in sharing his expertise in the dynamics of structures and in guiding me in improving the complex structural dynamics model. Martijn Meijer (BAM) is acknowledged for providing the opportunity to contribute to his team as a graduate intern which I enjoyed very much.

I would also like to share my gratefulness for the people around me who have supported me personally. My parents have invested plentifully in my personal and educational development. I acknowledge the graduation from university to be one of their successes in my rich maturation. Eline has provided the best emotional support to get me through the challenging process of writing a thesis. Also, my roommates of The Golden Lion are greatly appreciated for their never-ending humour and positive vibe during these times of the pandemic.

I am grateful for the opportunity to develop myself as a hydraulic engineer at Delft University of Technology. This has contributed greatly in my passion to keep exploring for durable solutions to foster a sustainable planet for each individual.

Wessel Vrijmoeth

Delft
December, 2020

Abstract

This document is a design report on the dynamic response of and the potential enhancements to the Tidal Bridge concept in the Strait of Larantuka (Indonesia).

The Tidal Bridge that is the focus of this investigation is a proposed bifunctional concept of a bridge connection between two Indonesian islands, and the world's largest tidal power plant. It is projected to cross the Strait of Larantuka, which has a minimum width of 600 meters and maximum depth of 35 meters. The combination of the large depth and strong currents through the strait makes a traditional bottom-founded bridge too expensive for its use.

The total Tidal Bridge project from shore to shore consists of four floating elements to span the middle part of the strait and two regular bridges to connect the shores to the four floating elements. These floating elements are mainly kept in place by the pendulum forces and the buoyancy force. One of these floating elements is displayed in Figure 1. The large current potential is harvested by the bi-directional free-flow turbines.

Waves propagate into the strait and force the floating elements into a dynamic response. This may lead to exceeding the combined acceleration serviceability limit of 0.7 m/s^2 which defines intolerable situations with regard to user's comfort and safety. Preferably, the extent to which the limit is exceeded is quantified and reduced with a solution. The objective of the report is therefore:

> *to design an additional structure or modification to the Tidal Bridge that reduces the dynamic response to the wave forcing. The downtime must be reduced to a maximum of five days per year based on a 50% confidence interval.*

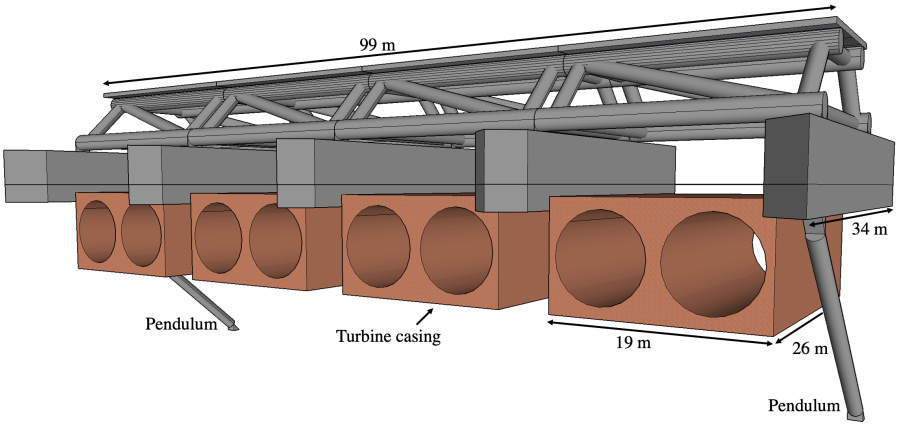

Figure 1 Perspective sketch with some dimensions of the original floating element design of the Tidal Bridge with its yellow coloured FishFlow turbines

The methodology of this design report is based on the systems engineering design process. Three substantive design loops develop a working principle into the subsequent design stages of a concept (design loop 1), alternative (design loop 2), variant (design loop 3), and the resulting design to end with. A numeric structural dynamics model is developed to explore the dynamic response of the original Tidal Bridge design and of the proposed design optimizations.

The preparatory exploration of the dynamic response shows that the original floating element design is significantly impacted by inertia forces over drag forces ($KC \approx 0.1 - 0.3$). The inertia wave forces, as described by the used Morison equation, are linearly dependent to added mass and the fluid particle acceleration. This part of the Morison equation helps to explain the dynamic response of the original design and the significant contribution of the turbines to the dynamic response. The large submerged turbine casings include relatively much added mass in the region with the largest wave related fluid particle accelerations (close to the free surface). This leads to a determined downtime of the Tidal Bridge of 23 days per year whereas it would have been 0 days per year for a Tidal Bridge design without turbines.

A sensitivity analysis to the design parameters shows the floater length to be relatively influential in the dynamic response of the original design. More elaborate tests on the promising and optimized floater length showed a marginal improvement and such an optimization in mass and stiffness does not lead to the objected improvement. Therefore, the design scope is narrowed to solutions in the form of additional structures leaving solutions in the form of design modifications aside. Further analysis also showed that the sway degree of freedom has the largest contribution to exceeding the serviceability limit.

Results from the process of the three substantive design loops lead to selecting the best developed variants. The resulting design consists of three sway plates hanging below each of the three floaters shown in Figure 2. This design anticipates well to the inertia dominance and to the limiting degree of freedom by generating much added mass in the sway direction. The fluid particle acceleration as a result of the waves at the depth of the centre of the sway plate is about 5% of the acceleration at the free surface. Hence, the additional inertia of the plate is greatly contributes to the total sway and rotational inertia of the complete structure and practically not contributing to additional forcing due to waves.

The sway plates and their supporting structure is structurally developed to the ultimate limit state. The forcing resulting from the dynamic response due to the waves and a static drag forcing due to the large tidal currents are both taken into consideration for the structural calculation. The additional loads of the sway plates on the original design are transferred by the pendulums and foundations without a need for adaptations, while the truss structure needs some simple adaptations in the truss design. The hinge location, which controls the permanent roll displacement due to current-related drag forces, moves from 6.5 to 13.5 meters relative to the middle of the floater and can stay connected to the bottom plate of the side floaters.

The resulting design successfully fulfills the objective by reducing the downtime to 0 days per year with a 50% confidence interval. With this reduction, all the downtime of 23 days per year has been resolved. The resulting design has some significant advantages compared to the other proposed variants, namely a great effectivity relative to the steel need, modular possibilities and an increased energy yield of the turbines.

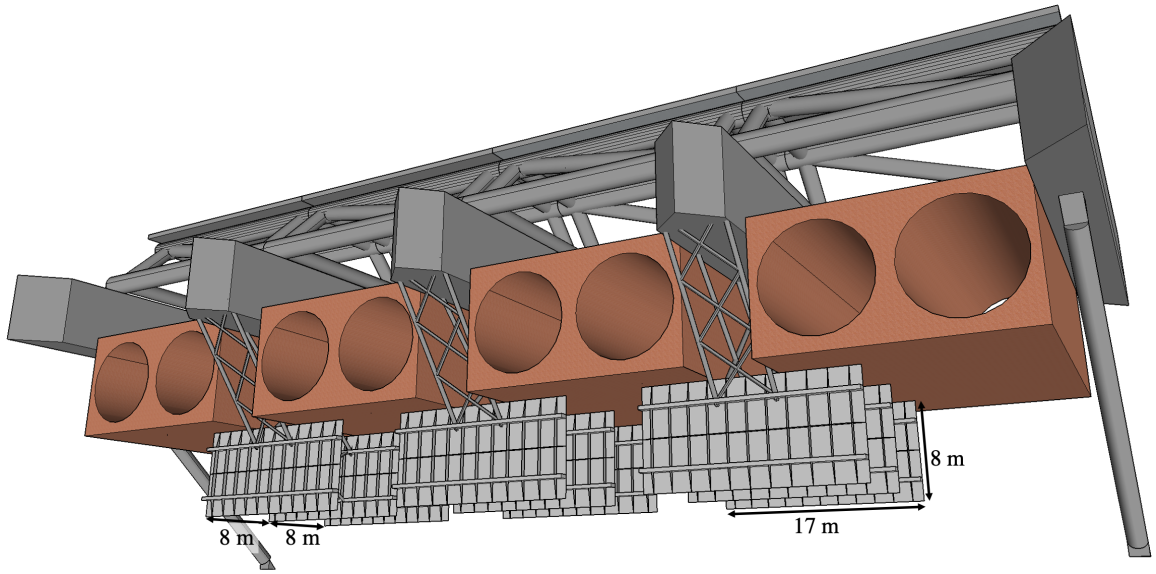

Figure 2 Perspective sketch with some measurements of the resulting design integrate in the floating element of the Tidal Bridge

Contents

1 | Introduction

This chapter introduces the Tidal Bridge project in the Indonesian archipelago. It includes a brief summary of the Tidal Bridge project and design, analyzes the concerned stakeholders, shows the connection to the preceding theses, describes the problem, objective, scope and methodology for the thesis.

1.1 Connecting Flores and Adonara

Flores and Adonara are two islands in the Indonesian archipelago divided by the Strait of Larantuka. The islands have two million and one hundred thousand inhabitants respectively. Adonara is positioned on the east side of Flores and the two islands form a strait with a minimum width of 600 meters and maximum depth of 35 meters. Figure 1.1 gives a geographical overview of the project site. There are advanced plans to connect those islands with a bridge (De Rijke, Koot, & Sengers, 2017). The connection would accelerate infrastructure development, offer more economic development through tourism, and make use of the enhanced local potential of the two islands.

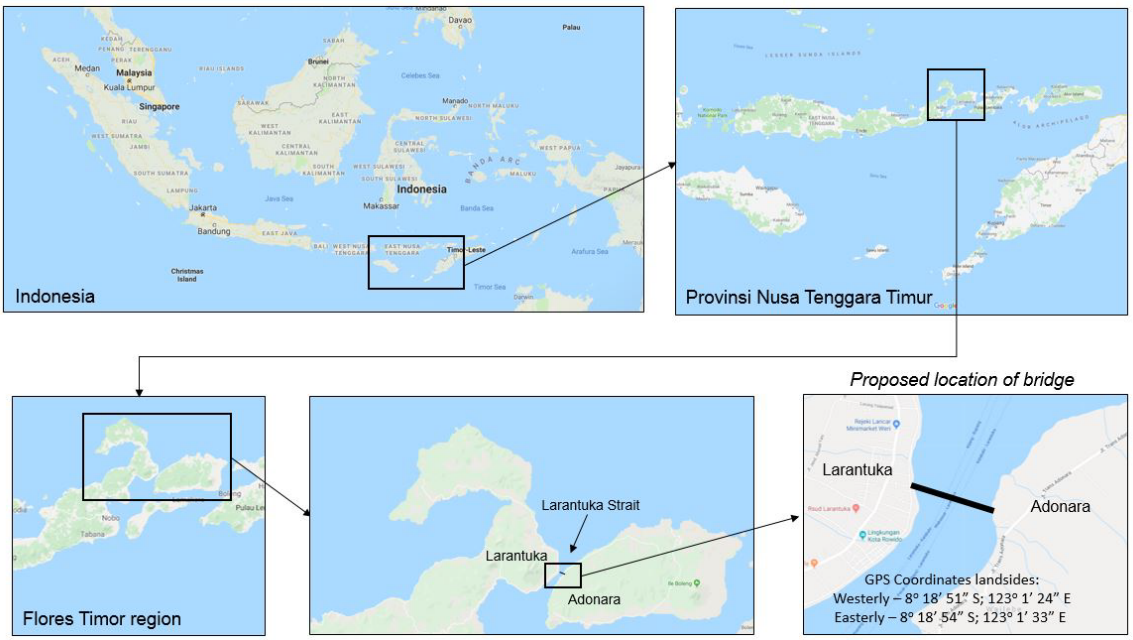

Figure 1.1 The position of the islands Flores and Adonara in the Indonesian archipelago (Hoogsteder, 2019).

A feasibility study concludes that a floating bridge is a more economical solution compared to a static bridge design (De Rijke et al., 2017). The large water depth and the high flow velocities which reach 4.0 m/s increase the cost for a static design. The feasibility study proposes to connect turbines to the bridge to make use of the enormous energy potential of the tidal currents through the strait. The turbines reduce the total costs of the bridge on the long term and they contribute to connect many households to the energy grid for the first time. Theoretical feasibility studies and on site investigations show that the project may have much potential to be

beneficial for the many involved actors (De Rijke et al., 2017; Orhan & Mayerle, 2020). The original floating bridge design with the energy harvesting possibility is called the Palmerah Tidal Bridge, with a total projected costs of about 225 million USD. In this report it is referred to as Tidal Bridge (Tidal Bridge, 2020).

The original Tidal Bridge design is roughly restricted to move in only three of the six degrees of freedom. These three degrees of freedom are predominantly (in this report: exclusively) excited by the waves within the strait. Earlier research shows that these waves have a significant impact on the dynamic behaviour of the bridge (Dorgelo, 2020; Hoogsteder, 2019). An additional study that focuses on the severity of the dynamic problem and focuses on the mitigation of the dynamics would contribute to the development of the Tidal Bridge project.

1.2 Problem analysis

1.2.1 The original Tidal Bridge design

Project location

Antea determined the optimal location of the bridge based on many evaluation criteria. The total length of the bridge at this location is about 860 meters from shore to shore. This location is displayed in Figure 1.2 and is pointed out with a number one (Vos, Seinen, & Van den Eijnden, 2017).

Figure 1.2 The optimal location for the Tidal bridge is displayed in the Figure with the number one.

Bridge outline

Antea proposes a bridge outline in the feasibility study that suits the most important needs for the bridge namely: functional, economical and feasible (De Rijke et al., 2017). The outline of this initial design with the different sections and different lengths is displayed in Figure 1.3 (Vos, Hoogeveen, & Van den Eijnden, 2017).

Floating elements: In the middle of the bridge, there are four floating elements with a length of 100 meters each. The floating elements are completely constructed out of steel and displayed in Figure 1.4. One bridge element consists of five floaters, a truss structure and a deck. Four of these floating elements form the core and technically the most challenging part of the bridge. The floating elements have a connection to the other elements that prevent for vertical and horizontal movements and allow for rotational movements. The elements are connected to the sea bed with a pendulum on each each side of the floating element. These floating elements are elaborated upon further in Section 1.2.1 more thoroughly.

Roll-on Roll-off elements: The roll-on roll-off (RoRo) elements connect the floating elements to the static civil bridge parts at the abutments. The RoRo connections have a length of about 30 meters and form a smooth transition between the static civil bridge and the free-moving floating elements.

Civil bridge: The civil bridge is a static bridge at both sides of the shore of the strait with lengths of 250 meters each. The depth and current velocities closer to the shore take limited magnitudes and a static design is an economical more feasible solution. The civil bridges have an architectural interesting super structure to make the bridge iconic for its region.

Landfall: On both sides, the civil bridge is connected to the shore with landfall structures. These form the transition between the regular road and the civil bridge.

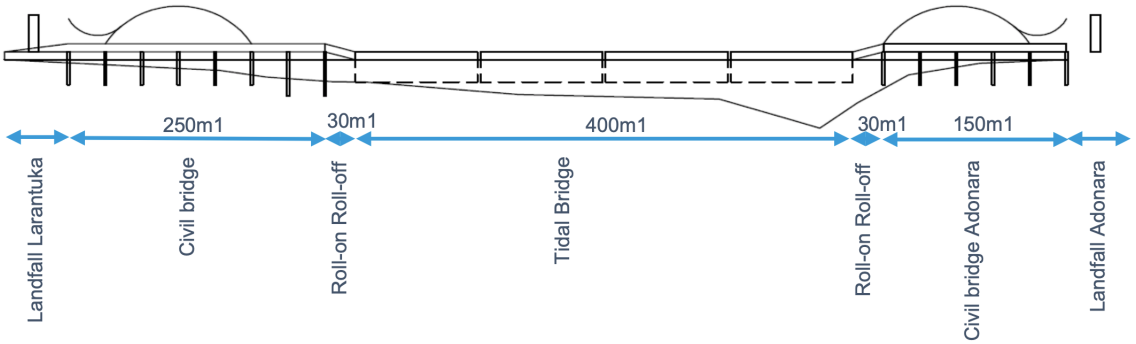

Figure 1.3 Overview of the Tidal Bridge design (Vos, Seinen, & Van den Eijnden, 2017)

The large floating elements are favourable over small floating elements, as they decrease the number of anchors, and the number of connections between moving elements. The pendulums are well able to manage the changing surface elevation of the tides and the forces of the currents. This solution guarantees less side-way movements compared to a cable stabilizing solution.

Hoogsteder (2019) and Dorgelo (2020) performed studies to the dynamic behaviour of the Tidal Bridge. The performed research shows that the elements start moving by the wave forcing predominantly and not so much due to the current, wind or traffic forcing. The floaters underneath the floating elements can be compared with boats. The flow of water along the boat due to the boat's speed does not excite the boat, while waves have a great impact on the boat's movements. The analogy works well for the Tidal Bridge as well.

Floating element design

One floating element has a steel truss as backbone of the structure and is displayed in Figure 1.4. The deck of the bridge is placed on top of the truss and five floaters are connected to the bottom of the truss. The middle three floaters (number 2, 3, and 4) are wider ones than the two floaters on the sides (number 1 and 5). A specific layout of the floaters may be found in Appendix A.1. The spaces between the floaters are partially filled with the four turbine casings developed by FishFlow innovations and those four casings hold eight turbines in total. This system of the truss, the deck, five floaters, and eight turbines form one floating element of the Tidal Bridge.

The floating element is connected to the foundation with two pendulums. The first pendulum is connected to floater number 1 and the other pendulum is connected to floater number 5. Both pendulums are connected to one of the 3 tripods which are founded in the bed of the strait. Two pendulums are connected to each tripod as every tripod is giving support to two floating elements. The two floating elements on the shore sides are connected to spud poles which is elaborated upon in the Section 3.1.3

Pendulum design

Each floating element is connected to the bed with one pendulum on each side of the floating element. The forces within the pendulum may be tension or compression forces and can reach values op to 10 MN (Dorgelo, 2020; Vos, Hoogeveen, & Van den Eijnden, 2017). The pendulum angle with respect to the ground as specified in Figure 1.5 may deviate some degrees as the current changes from direction or as the surface elevation differs due to the tides. The pendulum angle does not change radically with values of about 90°as a consequence of the changing current direction.

Figure 1.6 shows the rotational balance of drag forces. The floaters and turbines experience drag forces which are specified with the red colour in Figure 1.6. These drag forces scale with the current velocity squared.

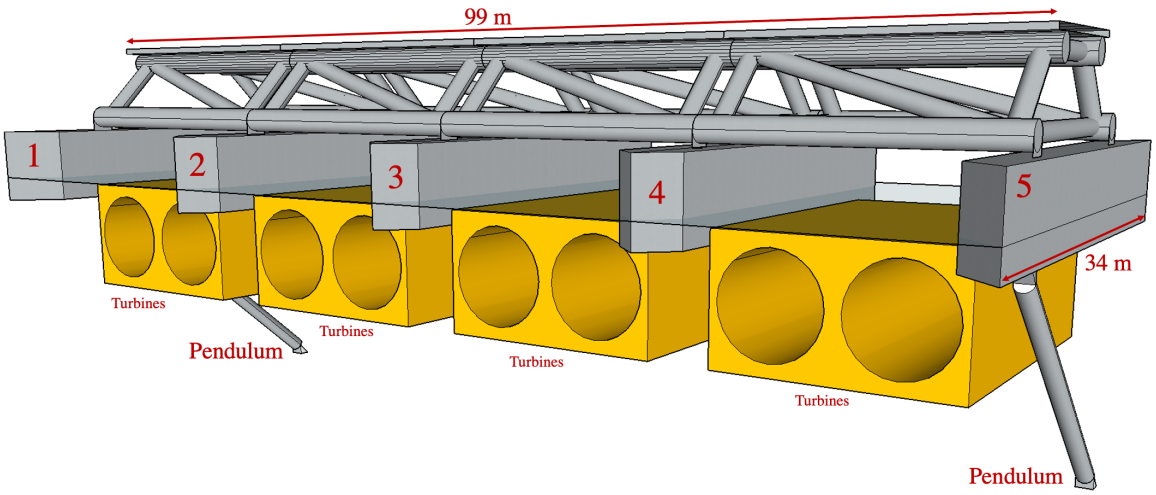

Figure 1.4 Perspective sketch of one floating element with some dimensions

The horizontal reactive force scales with the velocity squared as well since this is purely a reactive force and always equal and opposite to the resultant horizontal drag force of the floater and the turbine. The vertical pendulum force is a fixed ratio of the horizontal force depending on the pendulum angle and scales with velocity squared as well. Hence, the moment induced by the pendulum is dependent on the velocity squared as well. As long as the pendulum is connected to this specific location to the floater, the floating element stays horizontal regardless of the current direction or current velocity. This balance of moments is disrupted somewhat by the changing pendulum angle upon the tidal differences. The resulting roll displacement following upon the unbalance of moments are assumed to stay within the tolerable limits.

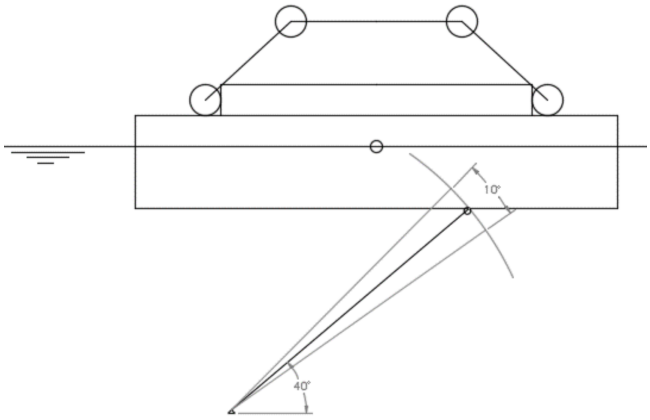

Figure 1.5 The pendulum is able to adapt to the different surface elevations as a result of the tides (De Rijke et al., 2017).

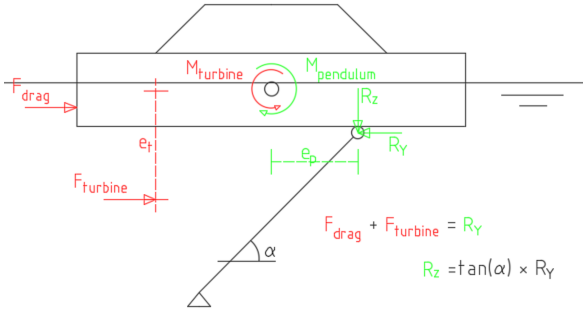

Figure 1.6 The balance of moments existing of the current related drag forces and the reactive pendulum force (De Rijke et al., 2017). This balance leading to zero rotation is only valid for one defined pendulum angle and an unbalance arises with the changing pendulum angle of the high and low tides.

The pendulum design has been chosen over a cable stabilizing design to prevent for horizontal movements more strictly. Figure 1.5 shows how the pendulum design can adapt well to the current direction change and the change in surface elevation due to the tides.

1.2.2 Stakeholder analysis

The design report represents the weighed interest of the stakeholders concerned. The stakeholder analysis forms the basis for the design requirements and the evaluation criteria. Appendix A.2 gives an concise overview of the stakeholders involved in the Tidal Bridge project.

The most important stakeholder is the client of the project: Perusahaan Listrik Negara (PLN), the local

electricity supplier. This stakeholder has the largest interest and also the largest power to enforce changes in the design. The interest of PLN is mostly focused on connecting many Indonesians to a stable electricity grid. BAM, the contractor of the project, and the Indonesian government also have a significant interest and power in the project process and should be managed closely. The other stakeholders have been subdivided in stakeholders that should be informed, kept satisfied, and be monitored. These grouping of the stakeholders and their interest may be found in Appendix A.2.

The most significant interests of the stakeholders has been summarized below. The Tidal Bridge should:

1. offer a safe connection from Flores to Adonara;
2. yield energy to connect the surrounding citizens to the electricity grid;
3. be an economical solution;
4. fit well in the region according to the locals.

These interest are included in the report in Chapter 2 by describing the requirements and evaluation criteria.

1.2.3 Analyzing previous theses

Hoogsteder (2019) and Dorgelo (2020) both performed research on describing the dynamic behaviour of the Tidal Bride design. This design report continues their research by quantifying and optimizing the dynamic behaviour that they have made tangible. The paragraphs below summarize the conclusions of Hoogsteder and Dorgelo in order to facilitate a seamless step from the previous theses to this thesis. Initially, the work of Hoogsteder is summarized as she was the first researching the dynamic behaviour. A larger summary of their work may be found in Appendix A.3 and the complete may be found on the Repository of Delft University of Technology.

Hoogsteder's thesis

Hoogsteder performed a general study to the complete dynamical system of the four floating elements of the Tidal Bridge due to the forcing of the waves and the current. She studied whether this dynamic response leads to exceeding the traffic serviceability limits. Unfortunately, the used models showed unrealistic results for a situation with a current forcing and the verification of the models could not be completed. However, Hoogsteder laid the basis for studying the dynamic behaviour of the Tidal Bridge and she framed the initial insights needed to head start further research.

Dorgelo's thesis

Dorgelo continued to study the dynamics of the Tidal Bridge as many questions were left unanswered. Dorgelo's approach focuses on modelling one single floating element instead of the four floating elements. He tried to model this aspect with a numerical python model. He succeed in integrating and verifying the wave, current and other forcing types. However, there are missed opportunities in the model as he did not model the boundary conditions imposed by the adjacent floating elements. Furthermore, he did not model the FishFlow turbines which heavily influence the dynamic behaviour as well. He succeeded in demonstrating the sensitivity to the design parameters which lead to suggestion to refine the Tidal Bridge design.

Evident continuation of the study

The thesis of Hoogsteder gave the initial insights in the complete system of the Tidal Bridge and how those exceed the serviceability limits. The thesis of Dorgelo provided much more specific information on the dynamic behaviour of one floating element. An evident continuation of these focuses on improving and using the model for optimizations of the Tidal Bridge design. Dorgelo's numerical model forms a computational laboratory in which new ideas and developments may be tested. This project seamlessly continues the previous theses by using Dorgelo's numerical model to design improvements, such that the serviceability limits of the Tidal Bridge may be exceeded less.

1.2.4 The minor shortcomings of the original design

An economical solution for the connection between the shores of Flores and Adonara is the main advantage of the present Tidal Bridge design. Unfortunately, this innovative and economical solution of the Tidal Bridge introduces disadvantages that come along with the dynamic behaviour which are listed below.

1. **Fatigue damage:** A dynamically active system experiences fatigue damage. The many repetitions of the

wave forcing damages the structure on the microscopic level although these wave forces do not exceed the yield strength. Microscopic cracks and sharp edges in the geometry concentrate forces to specific tensile members and the material locally damages, called fatigue damage. The present Tidal Bridge design needs to deal with fatigue damage as well as due to the many repetitions and the large forces through the floating element.

2. **Large element connection force:** The middle two of the four Tidal Bridge floating elements are connected to the adjacent floating elements. These inter-element connections couple the sway and heave movements of the adjacent element. The forces on these inter-element connections are negatively influenced by larger element dynamics.

3. **User discomfort:** Appendix B.1 elaborates upon the maximum combined acceleration values that traffic is allowed to experience as comfortable and safe limits. Appendix B.1 also concludes that user comfort and user safety enhances with smaller floating element dynamics. Furthermore, transitions from the one floating element to the other floating element lead to short and undesired peak accelerations that exceed the serviceability limits. Users would benefit much from bridge elements that are as less dynamic as possible such that the user comfort and safety enhances.

1.2.5 The major shortcoming of the original design

The major shortcoming of the original design of the Tidal Bridge has to do with the downtime. The bridge may need to be out of service for a limited amount of days to guarantee its users' safety at days with extreme physical conditions. The accepted maximum number of days has been determined to be five days per year. This number has been found acceptable for its region (Hoogsteder, 2019).

Hoogsteder and (Dorgelo, 2020) both conclude that the dynamic behaviour of the Tidal Bridge exceeds the serviceability limits. Both authors did not determine the yearly downtime which is specified by the number of days that the bridge would be out of service yearly. Downtime of the Tidal Bridge is greatly undesirable as it hinders the Tidal Bridge's users, leads to a loss of confidence in the availability of the bridge, and leads to economic loses and missed opportunities. The downtime of the bridge needs to be quantified in order to decide whether the Tidal Bridge functions as expected and whether the Tidal Bridge is worth the investment. The design should be optimized if the Tidal Bridge is out of service for more than five days yearly.

1.3 Problem definition

The plans to realize a connection between the islands Flores and Adonara could accelerate infrastructure development on both islands, offer economic development to the region, enhance the local potential of the two islands, and provide electrification for many households around the Larantuka Strait. The generated electricity contributes covering the cost of the investment and hence, the project offers much value to the region.

A thorough study to quantify the downtime and to enhance the dynamic behaviour of the Tidal Bridge has not been performed yet by either BAM, Hoogsteder (2019) or Dorgelo (2020). In the ideal bridge design, the Tidal Bridge does not need to be taken out of service. In that case, the advantages of a static bridge are combined with the economical benefits of the floating concept. The discrepancy between this ideal bridge design and the original dynamically too active Tidal Bridge design drive the problem. This problem is summarized below:

> *The original floating Tidal Bridge design is the preferred solution for a crossing between Flores and Adonara concerned the total design cost. The operational reliability of the original design is unknown and may need to be enhanced.*

1.4 Objective

The problem statement introduced a relevance for a design report which looks into reducing the downtime to tolerable limits. These tolerable limits for the downtime have been presented before to be maximum five days per year. The downtime should preferably be determined with a confidence interval of at least 50% to have idea about the quality of the outcome. The design may take the form of an additional structure or a modification of the original Tidal Bridge design. Further requirements about the design should follow the design requirements of the Tidal Bridge. This leads to the thesis objective which is identical to the design objective:

> *The objective of the thesis is to design an additional structure or modification to the Tidal Bridge that reduces the dynamic behaviour as a response of the wave forcing. The downtime must be reduced to a maximum of five days per year based on a 50% confidence interval. The design must respect the original Tidal Bridge design and follow the design requirements of the original Tidal Bridge design such as the lifetime, maintainability and constructability.*

1.5 Scope

The thesis scopes defines the items which are covered by this design report:

- Only the middle two elements of the four floating elements are taken into account;
- The original Tidal Bridge design and its location are taken as a starting point;
- The requirements concerning the maximum tolerable dynamic response is defined by the serviceability limits;
- Both design optimizations or design additions are considered in this design report.
- The wave loading is the driving force for the dynamic behaviour of the Tidal Bridge. For this investigation the wind and traffic forces are supposed to be negligible;
- The currents through the strait lead to a constant drag force on the Tidal Bridge;
- Current induced dynamic forces of instabilities or vortex shedding are not taken into account;
- Extreme weather events like tsunamis, tropical cyclones, and earthquakes are not taken into account for the ULS calculations;
- The loading conditions of the construction and transportation phase are not taken into account for the ULS calculations;
- The numeric model of Dorgelo (2020) is the starting point of the needed structural dynamics model;
- Open source wind data are taken as input for the wave characteristics model;

Preferably, the thesis scope defines which working principle is chosen to further elaborate upon in the design report. However, the dynamic behaviour of the original Tidal Bridge design has not been analyzed and a suitable working principle for this design report cannot be determined yet. The thesis scope will be narrowed down further after analyzing the dynamic behaviour of the Tidal Bridge.

1.6 Methodology and report outline

The systems engineering design method as described by Molenaar and Voorendt (2020) offers a structured approach to a find the optimal design solution that fulfills the design objective. The systems engineering design method is a systematic and structured approach that fits well for unique and and complex designs like civil engineering structures. The method helps to design from a general idea into a detailed idea which is the case for this design report as well.

The systems engineering design method as described by Molenaar and Voorendt (2020) is adapted such that it suits the need of the design objective better. The adapted methodology is written down per step in the list below.

- **Defining the basis of the design** **Chapter 2**
  The objective of this step is to define the requirements, evaluation criteria and boundary conditions for the design. The wave characteristics needed to determine the downtime of the original Tidal Bridge design

and design optimizations, are developed in this step.

– **Developing the structural dynamics model** **Chapter 3**
The objective of this step is to gather all relevant physics and to supplement and optimize the structural dynamics model. Initially, the mechanical system of the Tidal Bridge is described. Consequently, all relevant physical phenomena are formulated theoretically to construct the structural dynamics model with.

– **Narrowing the design space** **Chapter 4**
The structural dynamics model is used to define the dynamic behaviour of the original Tidal Bridge design. The balance of the dynamic properties of mass and stiffness are explored to determine whether optimizations in those would lead to fulfilling the design objective. The acquainted knowledge about the original situations helps to refine the thesis scope. After these steps, all preparatory work is conducted and the designing through loops can be initiated.

– **Developing qualitative designs - design loop 1** **Chapter 5**
The objective of this first design loop is to develop, verify, evaluate and select **concepts**. The concepts describe a working principle that may eventually lead to a design after two additional design loops. The step delivers three concepts that are developed into alternatives in the next step.

– **Developing quantitative designs - design loop 2** **Chapter 6**
The objective of the second design loop is to develop, verify, and select **alternatives**. The three alternatives are developed concepts that receive dimensions and mass. Consequently, the alternatives are tested with the structural dynamics model to verify the performance. Alternatives that show a significant optimization of the dynamic behaviour of the Tidal Bridge are developed into variants in the next step.

– **Detailing the design - design loop 3** **Chapter 7**
The objective of this design loop is to develop, verify, and evaluate the **variants**. The variants are developed from the alternatives. The variants have clearly defined dimensions and those are checked structurally to strength, stiffness and stability. The variants are tested with the structural dynamics model to verify their performance. A process of verification, evaluation and selection leads to choosing one variant which is developed further in the next step.

– **Resulting design** **Chapter 8**
The objective of this step is to develop further and present the **resulting design**. The resulting design is the chosen variant from the preceding step. The resulting design receives some additional detailing, 3D sketches and a construction method.

2 | The basis of the design

This chapter describes the framework of the requirements, the evaluation criteria, the boundary conditions and the assumptions that must be taken into account in the design process. The wave characteristics model, which takes an important roll in the used report analysis, is developed and described in this chapter as part of the boundary conditions.

2.1 Requirements

This section provides an overview of the requirements needed to reach the design objective of Section 1.4. The functional requirements translate the design objective into more specified and testable requirements. The structural requirements follow upon the functional requirements as structural requirements are inherent to a well functioning structure. The geometrical requirements describe the physical design space of the Tidal Bridge structure with its FishFlow turbines.

2.1.1 Functional requirements

The design optimization or additional structure must:

- reduce the dynamic response of the Tidal Bridge's traffic deck such that serviceability limits of the bridge are solely exceeded for a maximum of five days per year 50% confidence interval. The governing serviceability limits[1] are the combined acceleration limit[2] of 0.7 m/s^2 and the maximum roll displacement limit of 0.06 rad;
- function for various wave lengths and wave heights;
- respect the original materials and design principles;
- have a lifetime of 50 years (Hoogsteder, 2019);
- be durable and sustainable with a minimized impact on the world environmental system;
- not harm or hinder the surrounding flora and fauna;
- not be dangerous for humans;
- be replaceable;
- have the possibility to be inspected while the bridge is operational;
- have the possibility to be maintained while the bridge is operational;
- be redundant to sea level rise;
- be computable.

2.1.2 Structural Requirements

The design optimization or additional structure must:

- have a floating stability defined by a metacentre that is at least 2 meters above the centre of gravity;
- be strong, stable and stiff enough following the Eurocode 3;
- be constructed following the norms that belong to consequence class 3 (Nederlands Normalisatie-instituut, 2019);
- survive extreme wave events that have a return period of once in 1000 years;

[1] A motivation for the chosen serviceability limits may be found in Appendix B.1

[2] The combined acceleration limit consists of the sway acceleration, heave acceleration and roll rotational acceleration. The roll rotational acceleration is transformed into a translational acceleration in the sway and heave directions. The rotational acceleration is multiplied with a sway and heave lever arm representing the distance between the centre of gravity and the edge of the traffic deck.

- take corrosion rates into account of 1.75 mm per 50 years for permanently immersed structures and 3.75 mm per 50 years for structures in the splash zone (BSI, 2009);
- take fatigue damage qualitatively into account;
- make use of the S355 steel class;
- take the mass of the design optimization or additional structure into account in the dynamic calculation;
- not transfer loads to the turbines[3];
- not have an additional anchor or foundation;
- be constructable.

2.1.3 Geometrical requirements

The design optimization or additional structure must:

- be integrated in the original Tidal Bridge design. The floating elements have a length of 99 meters, have two pendulums, have five floaters, have a truss structure that connects all structural elements, have four FishFlow turbine casings with eight turbines in it;
- be spatially realistic.

2.2 Evaluation criteria

The evaluation criteria are used to compare and evaluate the concepts and variants in two of the three design loops after verifying the concepts and variants to the requirements. The first set of evaluation criteria is used in the first design loop of Chapter 5 to evaluate the concepts. The second set of evaluation criteria is used in the third design loop of Chapter 7 to evaluate the variants. The second design loop filters its alternatives by only verifying the performance of the alternatives solely, and an evaluation of the alternative is not needed.

Evaluation criteria of the first design loop

Preferably, the design:

- can easily be maintained;
- avoids wear, cyclic loading, corrosion or erosion;
- has a working principle that is as simple as possible;
- makes use of existing structural elements which are readily available;
- has little to no mechanical parts;
- has a passive damping system;
- can mitigate the dynamic behaviour due to waves with various heights and periods;
- can be adapted easily to reduce the dynamical behaviour of the Tidal Bridge better after brought into place;
- is sustainable;
- is durable;
- does not increase the forces on the pendulums;
- is not visible for its users or does not hinder the user's view from the bridge.

[3]The turbines are constructed by a third party. The structural capacity for additional loads is unknown.

Evaluation criteria of the third design loop

Preferably, the design:
- has the best dynamic performance compared to the steel need;
- functions well with a changing depth;
- contributes positively to the energy yield of the turbines;
- needs less efforts to construct;
- does not influence the dynamic coastal equilibrium;
- has redundancy capacities for possible failure mechanisms;
- does not complicate the determination of the upper hinge location.

2.3 Boundary conditions

The boundary conditions define the limits of the figurative design space. These limits may be defined by nature such as bathymetry, waves, tides and currents. This section initially gathers information about the waves by constructing the wave characteristics model. The section continues to elaborate upon the depth, water levels, and currents.

2.3.1 The probable wave characteristics

Data of field experiments to wave characteristics at the project site is unfortunately not existing. An idea about the wave characteristics is important as the waves are governing in the dynamic behaviour of the Tidal Bridge. Probabilistic wave data is needed to know how many days per year the Tidal Bridge needs to be shut of due to exceeding the serviceability limits.

Initial prediction of the wave height

Vos, Hoogeveen, and Van den Eijnden (2017) performed an initial prediction of the wave heights by calculating wave heights based on wind velocities, fetch, average depth, and the formula's of Bretschneider. They calculated the wave height for a probability of occurrence of once per year and once in 100 years for eight different wind directions. The results are useful for an initial prediction of the wave height. However, the generated data would not suffice for this design report. This design reports needs: a continuous data instead of a discrete data set, the integration of the probability of occurrence of the wind direction, and the integration of near shore processes.

Constructing of the wave characteristics model

A wave characteristics model is needed that defines the probability of exceedance for a wave height at the project location. Such a model would collaborate well with the structural dynamics model to calculate the downtime of the original or optimized design of the Tidal Bridge. Figure 2.1 shows the necessary steps to find the probability of exceedance of a defined wave height at the project location. The model is explained in depth in Appendix B.2. The list below shortly explains the steps that the model takes:

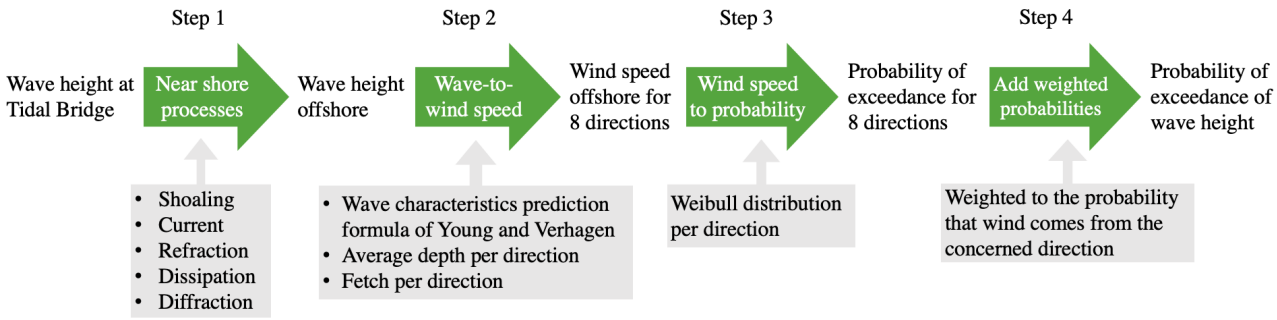

Figure 2.1 Flow chart of the steps executed by the wave characteristics model to find the probability of exceedance of a defined wave height at the project site

1. **Transforming near shore wave heights into offshore wave heights**
   Wave characteristics of waves offshore can be predicted by using wind data. Therefore, the wave height at the Tidal Bridge project site needs to be transformed from near shore wave heights into offshore wave heights. The transformation is being done by making predictions of the various near shore influences. The considered near shore processes are: shoaling, wave-current interaction, refraction, dissipation and diffraction.

2. **Transforming offshore wave heights into wind speeds of eight different directions**
   Waves offshore are mostly formed by wind. A formula that expresses the wave height as a dependency of the wind velocity, a fetch and an average depth has been developed and improved by Young and Verhagen in 1996. This formula is used to calculate eight wind velocities as if the wave originates from the eight different directions at the same time.

3. **Transforming winds speeds of eight directions into eight probabilities**
   The wind characteristics occur with fixed probabilities yearly. This probability information can be used to calculate the probability of occurrence of the just calculated wind speeds. Wind data is extracted from the Climate Forecast System of NOAA[4] which models the global interaction between the ocean, land, and atmosphere. This model results about the wind probability in the region is used to calculate the probability of occurrence of the calculated wind velocities.

4. **Combining the eight probabilities into one probability of exceedance**
   The wind data also provides information about the probability of the wind direction. The total probability of exceedance of a wave height at the Tidal Bridge project site can be determined by including the probability of the wind direction.

The outcomes of the wave characteristics model

The most relevant findings of the wave characteristics model are graphically visualized with Figure 2.2a and 2.2b. Figure 2.2a shows the probability of exceedance of a defined wave height. The grey margin originates from the uncertainty introduced by the prediction of the near shore processes. The grey lines around the black probability of exceedance line define the 5% confidence intervals.

Figure 2.2b shows the most probable wave height plotted to the wave period. The wave height and wave period are coupled to each other through the formula of Young and Verhagen and define this presented relation. The grey region defines the uncertainty of the prediction of near shore processes.

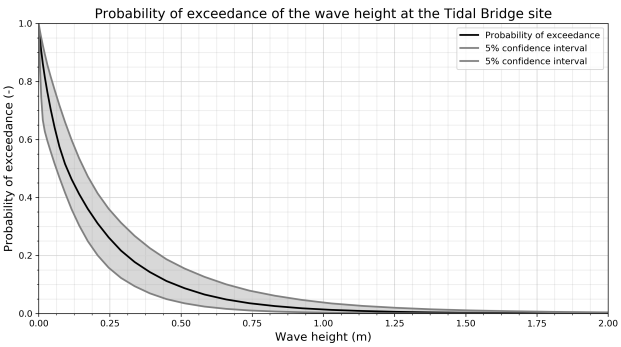

(a) Probability of exceedance of a significant wave height at the Tidal Bridge location

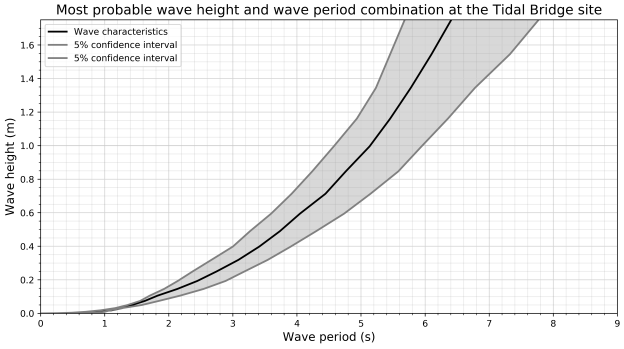

(b) Most probable wave height and wave period combination at the Tidal Bridge project site

Functionality of the wave characteristics model

Figure 2.2a and 2.2b are both used to estimate the downtime of a design of the Tidal Bridge. The structural dynamics model can plot the wave characteristics that lead to exceeding the serviceability limit into Figure 2.2b. The probability of exceedance of the limiting wave characteristics can be evaluated with Figure 2.2a. The downtime can be derived from the probability of exceedance of Figure B.8) and the desired yearly downtime

[4]National Oceanic and Atmospheric Administration

has been found by multiplying the result by 365 days. A more detailed explanation of the wave characteristics model is noted in Appendix B.2.

2.3.2 Other boundary conditions

The other relevant boundary conditions are elaborated upon in the underlying itemization. Appendix B.3 describes those boundary conditions more in detail. The most relevant findings for this design report are presented in the list below:

- **Depth:** The minimum keel clearance is 15 meters and the maximum keel clearance is 28.6 meters below the floaters. A margin for the low tide and inaccuracies in the surveying have already been taken into account in these specified minimum keel clearances.
- **Water levels:** The tidal climate around the Tidal Bridge is a mixed, mainly semi-diurnal tidal climate. The largest possible tidal amplitude is 1.58 meters relative to mean sea level.
- **Currents:** The high current velocities are mostly driven by the phase difference of about 45°of the M_2-tidal constituent that has an amplitude of 0.76 m. Measured and calculated data available about the strait show different results about the maximum current. The maximum current of on site measurements are in the order of 4.5 m/s and the maximum current calculated is in the order 3.5 m/s. The maximum current is assumed to be 4 m/s in this design report which corresponds to the maximum measured current in which the outliers are not taken into account.
- **Waves:** The wave characteristics have been explained in Section 2.3.1. The wave height used for the ultimate limit state check has a return period of 1000 years and a height of 2 meters.

2.4 Assumptions

The assumptions consist of a list of used claims which are mostly plausible and are theoretically not supported further in the report. The assumptions help to effectively work on the design objective without spending time to claims that fall outside the project scope. Assumptions which are not necessarily plausible are elaborated upon in the Appendix I.

- Forces on the Tidal Bridge only occur in the plane perpendicular to the longitudinal axis of the bridge;
- Vortex induced vibrations behind the pendulums, floaters or turbines are not causing relevant forces on the structure;
- Sea level rise has the order of magnitude of 0.5 meters in the upcoming 50 years;
- The steady-state response of regular waves lead to the same maximum combined acceleration as the response of an irregular wave spectrum with a significant wave height equal to the regular wave height;
- Tidal currents through the Strait of Larantuka do not contribute to the governing situation for exceeding the serviceability limits;
- The forces of traffic and wind are insignificant in the dynamic behaviour of the Tidal Bridge[5];
- The one pendulum of the Tidal Bridge adopts the pendulum angle of the second pendulum. The pendulum angle changes over time depending on the displacement of the Tidal Bridge;
- Diffraction effects do not have a significant effect to the dynamic behaviour of the Tidal Bridge;
- The waves at the Tidal Bridge project site are wind-waves generated offshore within a radius of 600 km. Swell ways from outside this 600 km radius are not taken into account;
- Displacements in the x-direction of all the floating elements are completely restricted by one of the spud poles.

[5]As concluded by Dorgelo (2020)

3 | Developing the structural dynamics model

The structural dynamics model is developed and improved in this chapter as it is needed in the subsequent chapters to analyze the dynamic response of the original design and the response of the design optimizations. The previous chapter was essential for this chapter as it defines the input parameters for the structural dynamics model. Initially, the original mechanical system of the Tidal Bridge is sorted out as this mechanical system defines the basis of the numerical model. Consequently, the relevant physical phenomena that should be included in the model are gathered and explored. Finally, the numerical structural dynamics model is developed, improved, and described.

3.1 The Tidal Bridge mechanical system

3.1.1 The coordinate system

Figure 3.1 shows the coordinate system that applies for all calculations, figures and text of this design report. The coordinate system is introduced by Hoogsteder (2019) and later improved by Dorgelo (2020). The translational degree of freedom surge and the rotational degrees of freedom pitch and yaw are mostly restricted due to the large stiffness that comes along with the design. The translational degrees of freedom heave and sway, and the rotational degree of freedom roll are not restricted by the design. Furthermore, the dominating forces of the current and the waves excite the structure in the sway, heave and roll degrees of freedom. The two dimensional plane of the sway, heave and roll degrees of freedom is therefore taken into account in this design report.

The origin of the coordinate system for a floating element is in the centre of gravity of the middle floater. This floater is pointed out in Figure 1.4 with the number three. Positive directed waves and a positive directed currents propagate along the positive y-axis direction. The y-axis is pointing south-southwest and the x-axis is pointing west-northwest. The perspective of Figure 3.1 is taken from the north. The most significant waves come from the north-northeast side of the strait as this part is connected to the open ocean as may be seen in Figure 1.1. These waves are travelling in the positive direction. The south side of the strait is connected to a shelter part of the sea and waves over here are much smaller compared to the waves coming from the north-northeast of the strait.

3.1.2 The geometry, mass and mass moment of inertia

The report from Antea describes the dimensions and materials used for the Tidal Bridge floating element (De Rijke et al., 2017). Dorgelo (2020) calculated the mass and the mass moment of inertia of the different parts of the structure. Table 3.1 shows a summary of the geometry, masses and moment of inertia of the significant objects of one Tidal Bridge floating element. The table takes the FishFlow turbines into account which resulted in a lowered centre of gravity and an increased mass moment of inertia compared to the results of Dorgelo (2020). An elaborate version of this table specifying each object individually may be found in Section C.1.1.

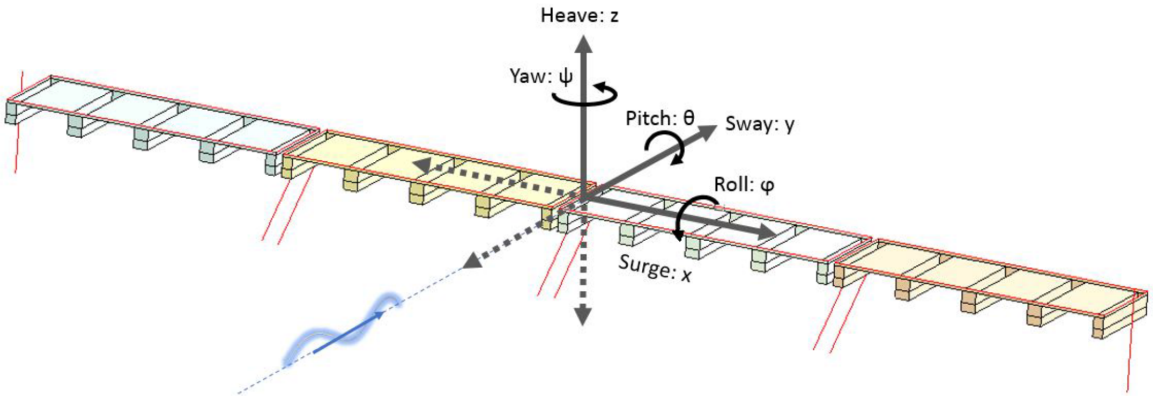

Figure 3.1 The coordinate system as specified by Dorgelo (2020)

Component	**Size** [x,y,z] (m)	**Centre of mass** [x,y,z] (m)	**Mass** (kg)	**Mass moment of inertia** [x,y,z] (10^6 kg·m^2)
Road	[99, 11, 2]	[0, 0, 10.5]	400,000	[48, 378, 337]
Truss	[99, 22, 5.5]	[0, 0, 7.3]	900,000	[87, 800, 786]
3 x small floater	[3.5, 34, 6.55]	[-, 0, 0]	3 x 48,000	3 x [5, -, -]
2 x large floater	[5, 34, 6.55]	[-, 0, 0]	2 x 68,000	2 x [7, -, -]
4 x two turbines	[19, 43.5, 10]	[-, 0, -7.5]	4 x 320,000	4 x [73, -, -]
Equipment	[2.3, 12, 3]	[0, 0, 4.4]	120,000	[4, 2, 1]
Total		**[0.0, 0.0, 0.0]**	**3,000,000**	**[461, 2586, 2670]**

Table 3.1 Summary of the geometry, mass and mass moment of inertia of the most significant objects within a Tidal Bridge floating element. The dashes suggest that number varies over the different floater- or turbine positions.

3.1.3 Technical aspects of the Tidal Bridge

Inter-connection design

The inter-connections of the floating elements restrict all translational movements and allows for all rotational movements. Figure 3.2 shows the rotational degrees of freedom with the coloured accents that may freely move and shows the translational degrees of freedom with the black lines that are restricted to move freely. The design of this inter-connection is adopted from the offshore industry (Vos, Hoogeveen, & Van den Eijnden, 2017). The inter-connection designs are important for the boundary conditions of the structural dynamics model.

Spud pole design

The translational restriction of the floating element adjacent to the civil bridge in the y-direction is not maintained with a pendulum. The pendulum structure introduces horizontal movements upon changes in the surface elevation due to tides. The elements connected to the RoRo element preferably do not translate in the y-direction in order to ease the passage onto the floating element. This translational restriction is ensured with one spud pole on the RoRo sides of the floating elements. One of the two spud poles solely prevents the element to translate in the y-direction. The other spud pole also prevents the element to translate in the x-direction to secure this degree of freedom for the four floating elements. Both spud poles and their corresponding restrictions may be observed in Figure 3.3. The first figure shows the restriction of two translational degrees of freedom and the second figure shows the restriction of only one degree of freedom. This design report assumes no displacements in the x-direction due to an effective spud pole design.

Pendulum stiffness

The Tidal Bridge elements stay in place due to the 31 meter long pendulums that are connected between a hinge on the outer floaters and the ground foundation. More in depth information about the foundation may be found in Appendix C.1.1. The pendulum introduces a significant coupling in the observed three degrees of freedom and is therefore important in the structural dynamics model. The pendulum stiffness is important to

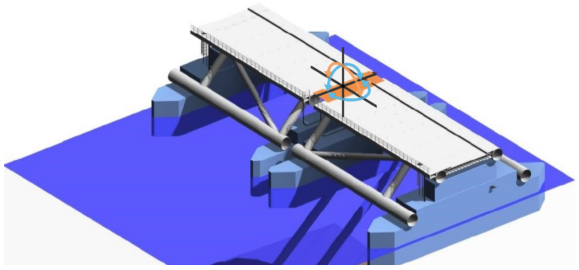

Figure 3.2 The connection between the floating elements restricts translational movements and allows for rotational movements (Vos, Hoogeveen, & Van den Eijnden, 2017).

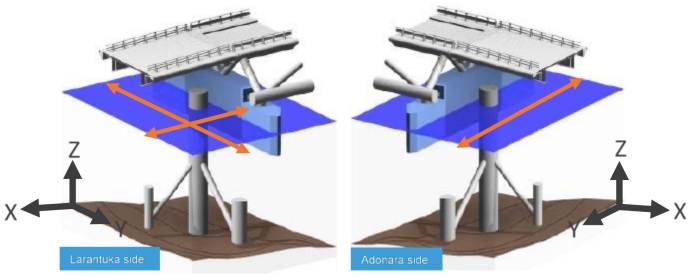

Figure 3.3 The orange arrows show the restriction of movements that the spud pole provides to the floating elements (Vos, Hoogeveen, & Van den Eijnden, 2017).

specify as this influences this dynamic coupling. The pendulum stiffness is dependent on the stiffness of the steel pendulum tube and on the stiffness of the foundation of the pendulum. Dorgelo (2020) estimated that this total stiffness is estimated to be $1 \cdot 10^8$ N/m.

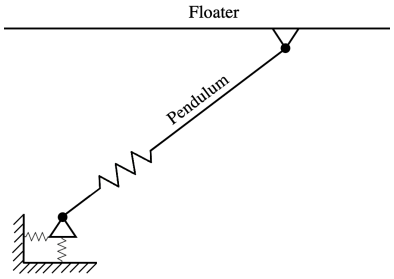

Figure 3.4 Symbolic sketch of the pendulum showing the stiffness of the steel rod and the stiffness of the foundation

FishFlow turbines

The FishFlow turbines from FishFlow Innovations BV have a significant effect on the dynamic behaviour of the Tidal Bridge. The turbines are large objects, rigidly connected to the Tidal Bridge, and come in pairs of two turbines within one casing. This casing displaces enough water to generate the buoyancy forces needed to carry the weight of the turbine impellers and casings.

Figure 3.5 shows a step of the construction method of the turbines. After installing the Tidal Bridge, the turbines are floated below the Tidal Bridge and connected to the truss structure. Figure 3.6 shows the dimensions of the turbine with its casing. More figures can be found in Appendix C.1.1. The total length of the the turbines is larger than the length of the floaters. The turbine casing has a length of 43.5 meters, a width of 19 meters and a height of more than 13 meters.

The turbines function physically as large sails that transfer much wave energy into the dynamic system of the Tidal Bridge. The damping effect of the impeller and the drag of the turbine casing has a limited effect in the reduction of the dynamics. More information about the influence of the turbines to the dynamic behaviour is to be found in Section 4.1.

Stability of the Tidal Bridge element

Appendix C.1.1 shows a hand calculation about the stability of the Tidal Bridge element. The result of the calculation shows that the structure is very stable as it has a GM distance of approximately 42 meters. This stability value suggest that the rotational stiffness is very large as well which has a major influence to the Tidal Bridge dynamic behaviour. However, the rotational stiffness should be compared to the mass moment of inertia in order to evaluate either stiffness or mass dominance.

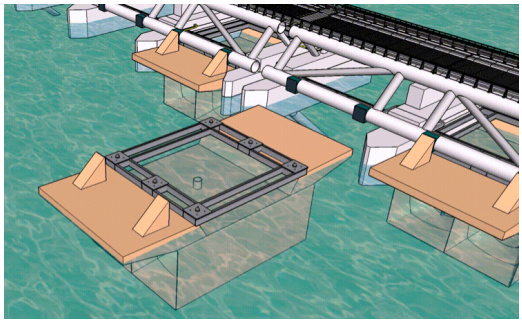

Figure 3.5 figure a (Manshanden, 2020)

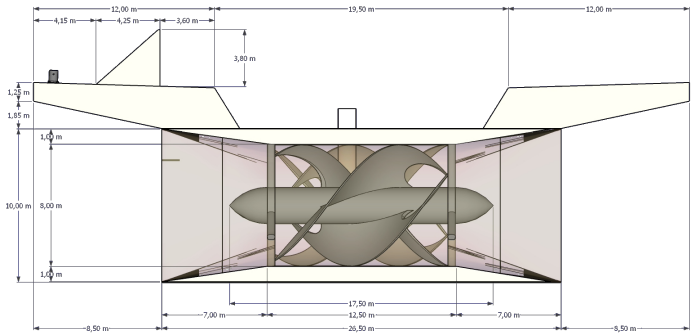

Figure 3.6 figure b (Manshanden, 2020)

3.2 Gathering the relevant physical phenomena

A structural dynamics model is needed to investigate and describe the original dynamic behaviour of the Tidal Bridge and to investigate how well a proposed design solutions works. This section gathers the relevant physical phenomena to construct this structural dynamics model. The classic formulation of the equation of motion represented with Equation 3.1 helps to define all relevant parameters needed for this structural dynamics model and is leading in this section. This formulation can be composed with the help of Newton's second law. The formulation describes the variable $\boldsymbol{x}$ that defines either the displacement, velocity or the acceleration of the structure. The variable $\boldsymbol{x}$ can be calculated with the help of the matrices $\boldsymbol{M}$, $\boldsymbol{C}$, $\boldsymbol{K}$, and the vector $\boldsymbol{F}$. This section is about gathering the relevant physical phenomena that form the foundation of the matrices $\boldsymbol{M}$, $\boldsymbol{C}$, $\boldsymbol{K}$, and the vector $\boldsymbol{F}$.

$$\boldsymbol{M}\ddot{\boldsymbol{x}} + \boldsymbol{C}\dot{\boldsymbol{x}} + \boldsymbol{K}\boldsymbol{x} = \boldsymbol{F} \tag{3.1}$$

This section starts to identify the three matrices $\boldsymbol{M}$, $\boldsymbol{C}$, $\boldsymbol{K}$ first. The mass matrix $\boldsymbol{M}$ is composed of the mass of the structure and the added mass. Consequently, the damping matrix $\boldsymbol{C}$ is composed of radiation damping contributions. Afterwards, the stiffness matrix $\boldsymbol{K}$ describes the stiffness due to the pendulum and the buoyancy forces. Last, the vector $\boldsymbol{F}$ describes the hydraulic forces which are approached by the Morison equation.

3.2.1 The mass matrix M

The mass matrix contains all contributions that form a force by multiplying the contribution with the structure's acceleration. Practically, this matrix is composed of all inertia terms within the dynamical problem which are formed by the mass, the mass moment of inertia, the added mass and the added mass moment of inertia. The mass and the mass moment of inertia is presented with Table 3.1.

The added mass and the added mass moment of inertia describe the mass of the water that needs to move along with the structure's movements. The added mass and the added mass moment of inertia is mostly dependent to the geometry of the structure. Section 3.2.7 specifies more clearly how the added mass and added mass moment of inertia is defined for the Tidal Bridge structure.

3.2.2 The damping matrix C

The damping matrix contains all contributions that form a force by multiplying the contributions with the structure's velocity. Practically, the contributions are solely composed of the radiation damping effects. Radiation damping is the loss of energy in the form of generation of waves. A structure that oscillates in the water generates waves that propagate away from the structure. Potential and kinetic energy is converted to some extent into wave energy. This loss of energy is related to the velocity and therefore defined by the damping matrix.

Vugts (1968) has been doing research to this phenomenon of radiation damping and tried to quantify the radiation damping with experiments. Vugts (1968) quantified the radiation damping per unit length of the floating object like a ship. The width and the draught are leading parameters in determining the magnitude

of the radiation damping. Figure 3.7 shows the results of these experiments for the relevant three degrees of freedom.

These experimentally determined results can be used to quantify the radiation damping for the floaters of the Tidal Bridge and the turbines hanging below the Tidal Bridge. The usage of the results of Vugts (1968) for the submerged turbines should be done with care. The results of Vugts (1968) have been obtained for floating bodies instead of fully submerged bodies. The turbine is just submerged for one meter and the results of Vugts (1968) probably evaluate the damping coefficient neatly.

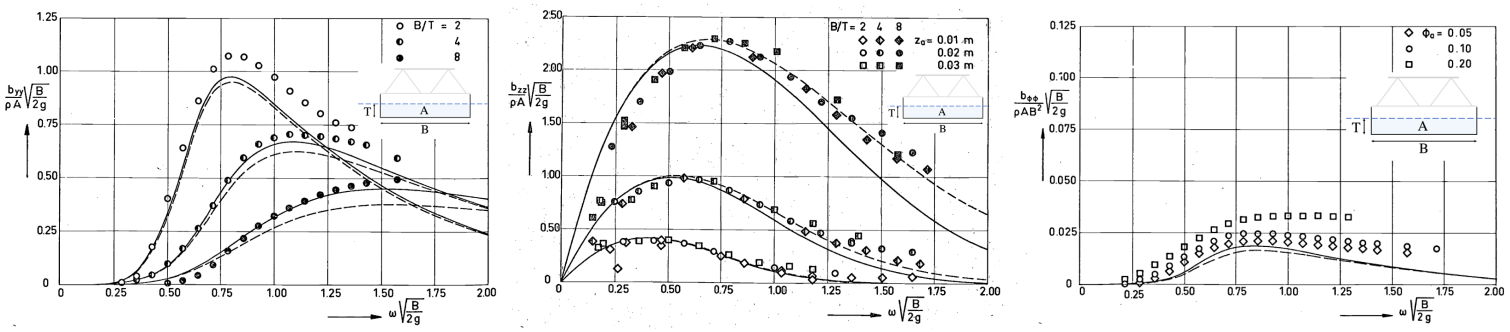

(a) Sway **(b)** Heave **(c)** Roll

Figure 3.7 Experimentally determined radiation damping coefficients for the three relevant degrees of freedom (Vugts, 1968)

Where:	b_{yy}	$[\frac{kg}{m \cdot s}]$	=	radiation damping per unit strip width for the sway degree of freedom
	b_{zz}	$[\frac{kg}{m \cdot s}]$	=	radiation damping per unit strip width for the heave degree of freedom
	$b_{\phi\phi}$	$[\frac{kg}{s}]$	=	radiation damping per unit strip width for the roll degree of freedom
	B	[m]	=	breadth
	T	[m]	=	draught
	A	[m^2]	=	cross sectional area of the submerged part of the strip
	ω	[rad/s]	=	wave frequency
	ρ	[kg/m^3]	=	density of the water
	g	[m/s^2]	=	gravitational acceleration

3.2.3 The stiffness matrix K

The stiffness matrix contains all contributions that form a force by multiplying the contribution with the structure's displacement. Practically, these contributions are composed of the hydraulic stiffness of the buoyancy force and the stiffness of the pendulum. Both stiffness contributions may be found by using the well known displacement method.

3.2.4 The force vector F

The force vector contains all force contributions that are not dependent to the structure's acceleration, velocity or displacement. The types of forcing that belong to the force vector for the Tidal Bridge are: constant forces not dependent on any parameter, and wave[1] forces that scale with the kinematic characteristics of the water particles or the local pressure distributions. This section does not elaborate upon the constant forcing contributions as the integration of those is trivial. The wave forces consist of three contributions that can be approached independently:

1. The first contribution consists of the drag forces that scale with the relative fluid particle velocity squared. This relative particle velocity integrates the relative difference between the water particle velocity and the velocity of the structure.

2. The second contribution consists of the Froude-Krylov force and the hydrodynamic force that both scale with the water particle accelerations.

[1]The current influences are considered to be integrated automatically in the description of the wave fluid particle kinematics.

3. The third contribution consists of a force followed upon the local pressure distribution affected by the waves.

This subsequent section describes the Morison equation which captures the first two contributions. The section afterwards describes the particle kinematics needed for the Morison equation and for the third contribution of the local pressure distribution forcing.

3.2.5 The Morison equation

Approximating the wave force

The Morison equation provides a good first approximation for approaching the wave forces without using complicated computational fluid dynamics software that solve the three-dimensional Navier-Stokes equations. The Morison equation, as displayed in Equation 3.2, captures the first two contributions of the wave forces as described in Section 3.2.4. The Morison equation can be applied for the three translational degrees of freedom separately. Equation 3.2 shows the forcing component of the sway direction.

The first term of Equation 3.2 calculates the first contribution of the wave forcing of Section 3.2.4, drag forces to the floaters, turbines, and pendulums. The drag is quadratically related to the relative velocity of the water particles. The second term and third term represents the hydrodynamic and Froude-Krylov force respectively which form the second contribution of the wave forcing of Section 3.2.4. The hydrodynamic force is dependent to the relative acceleration of the water particles to the concerned structure. The Froude-Krylov force is solely dependent to the water particle acceleration. The physical interpretation of the three terms of the Morison Equation are elaborated upon in the next sections. (Journée & Massie, 2008)

$$\begin{aligned} F_y &= F_{drag,y} + F_{hydro,y} + F_{Krylov,y} \\ &= \underbrace{\frac{1}{2}\rho C_d A\,(u-v)\,|\,(u-v)\,|}_{Drag\ force} + \underbrace{m_a\,(\dot{u}-\dot{v})}_{Hydrodynamic\ force} + \underbrace{\rho V \dot{u}}_{Froude-Krylov\ force} \\ &= \frac{1}{2}\rho C_d A\,(u-v)\,|\,(u-v)\,| + C_m \rho V \dot{u} \end{aligned} \tag{3.2}$$

Where:

F_y		[N]	=	horizontal wave forcing
ρ		[kg/m^4]	=	density of the water
C_d		[-]	=	drag coefficient
A		[m^2]	=	drag surface area
u		[m/s]	=	flow velocity
$\dot{u}$		[m/s^2]	=	flow acceleration
v		[m/s]	=	structure velocity
$\dot{v}$		[m/s^2]	=	structure acceleration
m_a		[-]	=	added mass for the sway degree of freedom
V		[m^3]	=	displaced volume of water
$C_m = \left(1 + \frac{m_a}{\rho V}\right)$		[-]	=	inertia coefficient

Explaining the first term: the drag force

An object in a flow generates disturbances leading to a force. The drag force is directed parallel to the flow and is directed in the flow direction. The physical principle leading to the drag force is to be found in the stagnation pressure that arises in front of and behind the object defined with $p = \frac{1}{2} \cdot \rho \cdot U^2$. The drag coefficient C_d integrates the physical principles that influence the drag force such as the Reynolds number, the cylinder's roughness and the turbulence of the incident flow (Journée & Massie, 2008). This drag coefficient is determined in Section 3.2.5. The drag coefficient of the turbine impeller may be approached with the analytic formula of 3.3 (Zaaijer & Viré, 2019). The turbine induction factor has been determined to be a = 0.188 with help of the provided information about the Turbines of FishFlow innovations (Manshanden, 2020). The motivation for this number may be found in Appendix C.2.2. The drag forces are relevant for the floaters, turbines and pendulums. Another form of drag is friction drag. This type of drag is negligible compared to the disturbance drag force.

$$C_t = 4a(1-a) \approx 0.61 \tag{3.3}$$

Where:

C_t		[-]	=	turbine thrust coefficient
$a = 0.18$		[-]	=	turbine induction factor

Explaining the second term: the hydrodynamic force

The hydrodynamic force can also be called the disturbance force. The relative acceleration of an object with respect to the water particles forces the water to move around the object. The force needed to move the water around the object is called the hydrodynamic force. This force is linearly dependent to the relative acceleration and the total mass of the water that is influenced by the object. This total mass of water is also called the added mass. The part of the hydrodynamic force related to the structure's acceleration is already included in the equation of motion by adding the added mass to the mass matrix. The hydrodynamic force contributing to the force vector of the structural dynamics model should therefore only be dependent to the water particle acceleration and not to the structure's acceleration.

Explaining the third term: the Froude-Krylov force

The Froude-Krylov force can also be called the pressure gradient force. An object that is situated within a pressure gradient field experiences different pressures on both sides of the object. The difference between these pressures result in a force, the Froude-Krylov force. A visual representation of this Froude-Krylov force is to be seen in Figure 3.8. The force is linearly dependent to the displaced water mass of the object and the acceleration of the water around the object, which is the same as a pressure gradient field around the object. The force only exists for accelerating water particles around the object and does not depend on the acceleration of a structure through a still fluid. A still fluid does not have a pressure gradient regardless of the existence of an accelerating object through the fluid. The coupling between the pressure difference and the acceleration has been written down with Equation 3.4.

$$\frac{\delta p}{\delta x} = \rho \frac{du}{dt} = \rho \dot{u} \tag{3.4}$$

Where:

p	[N/m^2]	=	pressure
x	[m]	=	distance
ρ	[kg/m^4]	=	density of the water
u	[m/s]	=	flow velocity
$\dot{u}$	[m/s^2]	=	flow acceleration

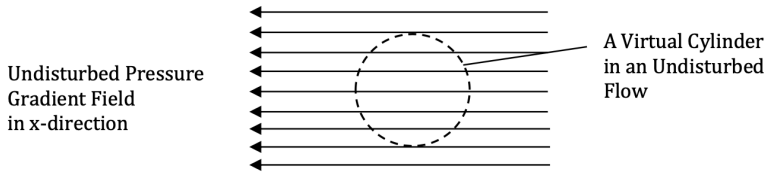

Figure 3.8 Object disturbing pressure gradient resulting in a Froude-Krylov force (Drost, 2018)

Motivating the use of the three terms

The Keulegan-Carpenter (KC) number describes whether the flow around an object is mostly dominated by drag or inertia forces. The KC number for the Tidal Bridge structure is calculated by Equation 3.5. Figure 3.9 gives a visual representation of the definition of the KC number. The KC number compares the total travelled distance of either the structure or the water particles as a ratio of the structure length in the direction of the structure or water movement. Equation 3.5 defines the KC number to be in the range of 0.1 to 0.3 for the situation of the Tidal Bridge.

$$KC = \frac{U_m \cdot T_w}{D} = \frac{2\pi a}{D} \approx 0.1 - 0.3 \tag{3.5}$$

Where:

KC	[-]	=	Keulegan-Carpenter number
U_m	[m/s]	=	maximum velocity
T_w	[s]	=	Wave period
D	[m]	=	Length scale of the object in the direction of the flow velocity
a	[m]	=	Wave amplitude

Flow separation does not occur for small KC values. In those cases drag plays a negligible role. Mutlu Sumer and Fredsoe (2006) defines structures to be inertia dominated with KC numbers of $0 \leq KC \leq 20$ and to be

drag dominated with $KC \geq 30$. Equation 3.5 shows clearly that the Tidal Bridge structure falls in the inertia dominated regime and drag forces could be neglected for the simulation of the wave forcing on the Tidal Bridge structure. However, large current velocities may occur in the Strait of Larantuka due to the tides. These non oscillating current velocities lead to flow separation around the turbines and floaters. The flow separation lead to drag forces which cannot been neglected. Therefore, the drag force is not neglected and the full Morison equation integrating drag and inertia forces is integrated in the model. (Journée & Massie, 2008)

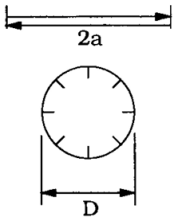

Figure 3.9 Visual representation of the definition of the Keulegan-Carpenter number

Determining the drag and inertia coefficients

The Keulegan-Carpenter number is generally the primary parameter to define the drag and inertia coefficients. In case of a need for more precision, then the drag and inertia coefficients can be further refined by involving the dependencies to the Reynolds number, the Sarpkaya Beta number, or the dimensionless roughness (Journée & Massie, 2008). Due to the large variations in the used wave height, wave period and the current velocity, the preference goes to using a more general value of the drag and inertia coefficients that stay constant throughout the simulations. Such values for the drag and inertia coefficient may be found in the norms of DNV which are widely accepted in offshore structures (DNV, 2011).

The drag coefficient is determined for the pendulum, floaters and turbines separately as those structural elements differ significantly to each other in shape. The drag coefficient is chosen depending on the geometry of the structural element and the concerned degree of freedom for the drag direction. The drag coefficients that were relevant to model the Tidal Bridge structural elements are included in Table C.2 of Appendix C.2.1. The inertia coefficient is dependent on the mass of the displaced volume and the added mass. Those two types of masses can better be determined separately and more accurate instead of using a general inertia coefficient of a design code. The mass of the displaced volume can be determined quiet accurately based on submerged volume of the structure. Section 3.2.7 elaborates further upon the determination of the added mass, which is a more complex parameter to calculate.

Evaluating the Morison equation

So far, the Morison equation seemed to be utterly suitable to model the wave forcing to the Tidal Bridge structure. The needed calculations are convenient and accessible. However, there are some limitations of the formula that should be taken into account and lead to a more complex application of the equation in the structural dynamics model.

The Morison equation is developed to model the wave loads on vertical slender cylinders. The Morison equation can be applied for different shapes, but the determination of the drag and inertia coefficient is not a strait forward process anymore. Inaccuracies are introduced upon determining the drag and inertia coefficient for other more complex shapes than the vertical slender cylinder. Furthermore, the Morison equation showed to model the wave forcing well for waves with a wave length of at least five times the diameter of the vertical cylinder. The evaluated and used particle acceleration for the Morison equation is valid on solely the evaluated position. Or differently stated, every location around the structure has a different corresponding particle acceleration. Too much inaccuracy is introduced upon assuming one particle acceleration to be accurate and valid for the complete structure in a situation of a structure larger than a fifth of the wave length. This problem can be overcome by using grid cells that are all individually shorter than a fifth of the wave length. This numeric trick is used in the structural dynamics model as well.

A shortcoming of the Morison equation which cannot be overcome has to do with diffraction effects. Diffraction effects contain of the physical phenomenon of waves that become affected by the structure resulting in differently expected wave particle kinematics. Taking account of diffraction effects is only possible in a

computational fluid dynamics program due to the complexity of the phenomenon. Dorgelo (2020) found in literature that the forces are probably over predicted in the situation of ignoring the diffraction effects and the model would likely over estimate slightly the dynamic response of the Tidal Bridge.

Conclusion

The Morison equation is a powerful and simple method to approach wave forces on structures. The formula was originally developed to approach the wave forcing on a vertical slender cylinder and the usage for differently shaped structures should be done with care. The drag and inertia coefficient should correspond the structure geometry and the forcing characteristics. Furthermore, a grid that contributes to evaluating the Morison equation for smaller parts of the structures should be adopted.

Three types of input values are needed for using the Morison equation: constants ($\frac{1}{2}$, ρ, geometries (A, V), particle kinematics (u, $\dot{u}$) and coefficients (C_d, C_m). The values of the constants and geometries are trivial to the problem. The particle kinematics are found with wave theory in Section 3.2.6. The drag coefficient is suggested by the norms of the DNV (2011) and the unknown part of the inertia coefficient, namely the added mass, is elaborated upon in Section 3.2.7.

3.2.6 The particle kinematics

Classification of the types of waves around the Tidal Bridge

The needed wave theory formulas depends on the depth, wave height, and wave period. Figure 3.10 shows the different regimes that correspond to different sets of formulas for describing the wave characteristics (Sadeghi, Dzayi, & Alothman, 2017). Section 2.3 elaborated upon the most probable wave height and wave period combinations. These probable wave height and wave period combinations define the limits that are displayed with the horizontal dotted lines in Figure 3.10. The depth below the floating elements of the Tidal Bridge varies between 20 and 33 meters. The depth defines the limits displayed with the vertical dotted lines within Figure 3.10. The area in Figure 3.10 shows that second order Stokes influences should be added to the regular linear wave theory formulas.

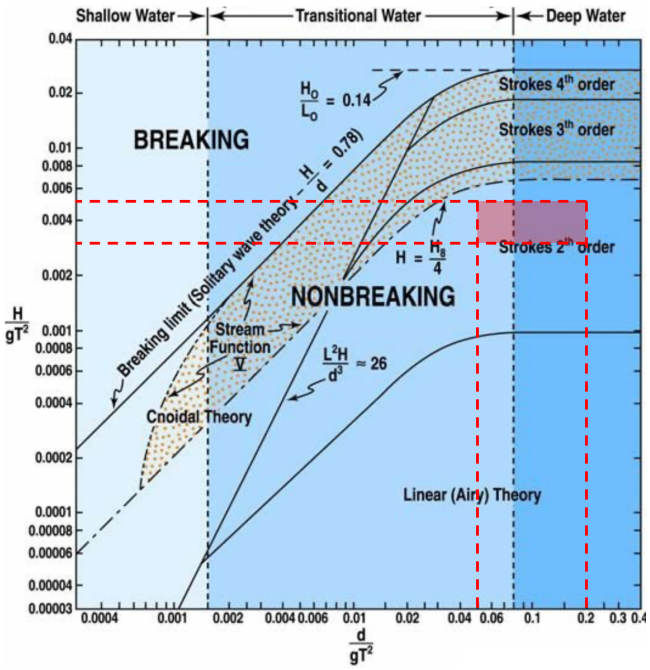

Figure 3.10 Figure displaying the various wave theory regimes (Sadeghi et al., 2017). The red dotted lines define the relevant limits for the situation of the Tidal Bridge.

Stoke's theory

Following Stoke's theory, all waves have one basic harmonic. This basic harmonic of the surface elevation is described with Equation 3.6:

$$\begin{aligned} \eta(y,t) &= a\ cos(\omega t - ky) = \varepsilon\eta_1(y,t) \\ \varepsilon &= ak \end{aligned} \tag{3.6}$$

Where:

$\eta(y,t)$	[m]	=	wave surface elevation of second order Stokes waves dependent on position and time
a	[m]	=	regular wave amplitude
ω	[rad/s$^-$1]	=	wave frequency
k	[rad/m]	=	wave number
ε	[m^2/rad]	=	wave steepness

Higher harmonics are introduced as the depth decreases and waves start to transform into a different shape. Stoke's theory describes formulas for these higher harmonics and adds those higher harmonics as corrections to the linear wave formulas. Equation 3.7 shows how those corrections are added to linear wave (Holthuijsen, 2007).

$$\eta(y,t) = \underbrace{\varepsilon\eta_1(y,t)}_{Linear\ wave} + \underbrace{\varepsilon^2\eta_2(y,t)}_{Second-order\ correction} + \underbrace{\varepsilon^3\eta_3(y,t)}_{Third-order\ correction} + \underbrace{\varepsilon^4\eta_4(y,t)}_{Fourth-order\ correction} + ... \tag{3.7}$$

Figure 3.10 shows that only the second order Stoke's correction is needed to accurately describe the waves at the location of the Tidal Bridge. Higher harmonics may be neglected as those will not occur at the project site. The surface elevation at the project site is described by Equation 3.8.

$$= \underbrace{a\cos(\omega t - ky)}_{Linear\ wave} + \underbrace{ka^2\frac{\cosh(kd)}{4\sinh^3(kd)}(2+\cosh(2kd))\cos(2(\omega t - ky))}_{Second-order\ Stokes\ addition} \tag{3.8}$$

Where: d [m] = depth

Summarizing the wave formulas

Appendix C.2.3 summarizes the second-order wave formulas which are used in the structural dynamics model. The appendix provides formulas for the wave surface elevation, the wave pressure, the particle velocity, and the particle acceleration. The wave surface elevation formula is needed to define whether water is present at a certain location around the floater. The wave pressure formula is needed to calculate the variable buoyancy forces below the floaters. The particle velocity formulas are needed to define the velocity dependent drag to the pendulums, floaters and turbines. The particle acceleration formulas are needed to calculate the water inertia forces to the floaters and to the turbines.

3.2.7 Determination of the added mass coefficient

The phenomenon of added mass

The added mass defines the additional inertia generated by the surrounding fluid that needs to accelerate upon accelerations of the structure. Kolkman and Jongeling (2007) used an interesting analogy of a piston and a cylinder to describe the phenomenon of added mass. A body of water is placed on top of a piston within a cylinder with an open top and bottom[2]. The mass of the water body on top of the piston adds to the total inertia that the piston experiences upon accelerating either up or down.

The mass of the water body around a structure needs to accelerate upon the structure's accelerations as well. Strictly speaking, the fluid particles around the structure all accelerate with a different magnitudes depending on the distance to the structure. The added mass is "a weighted integration of this entire mass" (Kolkman & Jongeling, 2007).

[2]Surrounded by air

Motivating the use of the formulas of the DNV design code

The determination of the added mass can be done with analytically determined formulas. The DNV (2011) provides those analytically determined formulas in the appendix of their design code "Modelling and Analysis of Marine Operations." These formulas are valid for volumes that do not have interference with the free surface nor the bottom. Practically, these formulas work well to calculate the added mass of offshore structures and equipment for a considerable depth. Analytically determining the added mass of structures that have interference with the surface elevation or the bottom is very complex and the use a computational fluid dynamics program for such added mass determination is highly recommended.

The determination of the added mass for structural elements of the Tidal Bridge is preferably done with the formulas of the DNV to keep the structural dynamics model transparent, straightforward, and parametric. Unfortunately, choosing for the ease of the DNV formulas means that insurmountably errors are introduced in the results of the model. The model, supporting the process of finding a design solution, mostly benefits from a transparent, straightforward and parametric model over a very accurate model, which justifies to choice for the formulas of the DNV.

Determining the added mass with the DNV design code

Generally speaking, the added mass can be approached by calculating the mass of the water contained by a virtual cylinder that encircles the frontal width of the concerned object relative to the oscillation direction. Figure 3.11 shows the added mass per unit length for two-dimensional bodies. The added mass is defined by the mass of water within a cylinder that encircles the width of the object. The width of the three displayed objects is all 2a. However, the frontal width of the objects is for two objects 2a and for the other one approaching 0. The two objects on the left side of the figure have an added mass described by the encircled width and the third object does not have added mass. The vertical oscillations of the rightward plate is not going to move the surrounding water.

The structural elements of the Tidal Bridge are generally three-dimensional objects for which an equivalent calculation strategy can be used. The added mass of a plate like the one of Figure 3.12 can be calculated by drawing half cylinders to the surfaces of the object and calculate the mass of the water within the cylinder's volume. The cylinder's diameter takes the magnitude of the shortest length of either length a or length b of the plate. *Hence, the added mass scales quadratically with the shortest distance of an rectangle.*

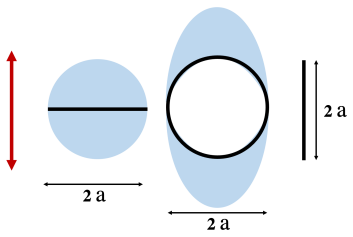

Figure 3.11 The added mass of three two-dimensional bodies for oscillations in the direction of the red double arrow is specified with the blue region. This region has a value of $\rho\pi a^2$ kg/m for the two left objects (DNV, 2011).

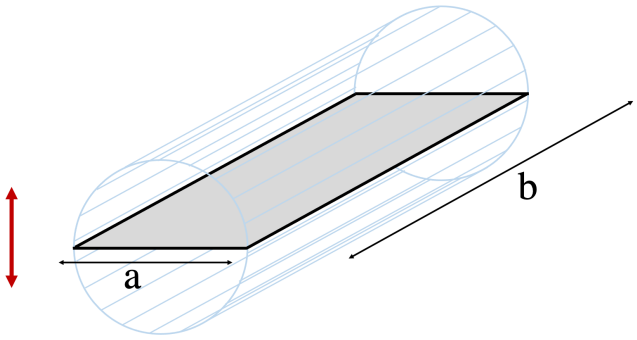

Figure 3.12 The added mass of a plate in the direction of the red double arrow is $\rho\frac{1}{4}\pi a^2 b$ kg/m (DNV, 2011)

The explained calculation strategy of Figure 3.11 and 3.12 has been used to calculate the added mass of most of the structural elements of the Tidal Bridge in the structural dynamics program. The DNV norm suggest some added mass coefficients that can be used to approach the added mass for structures of which the length A approaches B of Figure 3.12. Those coefficients have been used to make the added mass predictions slightly more accurate. The added mass of more complex shapes, like the FishFlow turbines, may differ from this explained theory. In those cases, the added mass is based on good engineering estimates that are in line with the theory about the added mass.

Determining the added mass for the turbine shape

The elaborated theory of Section 3.2.7 relates well to the structure geometry of the tube shaped pendulum and the rectangular shaped floaters of the Tidal Bridge. The added mass of those structures can easily be calculated. The determination of the added mass of the turbines is more complicated due to the shape of the turbine. This section identifies a method to come to an estimation of the added mass of the turbines.

The amount of fluid that accelerates along with the structure depends on the degree of freedom of the movement. Fort this reason, the direction of the movements has been specified in Figure 3.11 and 3.12. The added mass of the turbines is therefore been determined for the three degrees of freedom separately. Figure 3.13 gives an indication of the geometry of the casing geometry.

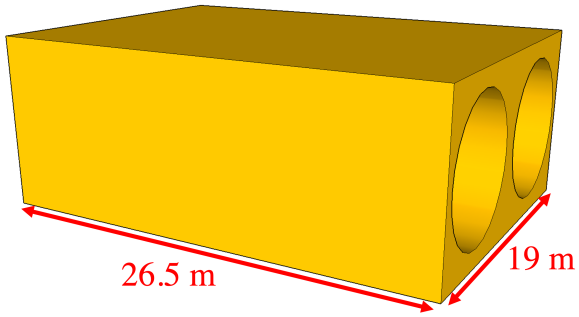

Figure 3.13 Coarse sketch of two turbines within one casing and the casing's geometry

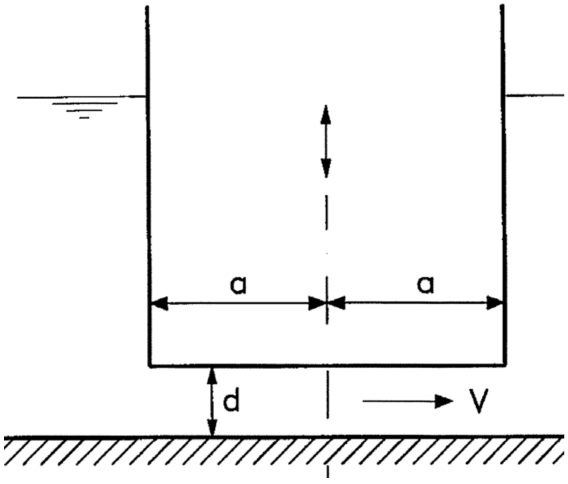

Figure 3.14 A heaving structure in the proximity of bottom experiences an enlarged added mass effect.

Heave The added mass of the turbines for the heave degree of freedom may be split up in three separate parts, the water body: above, within, and below the turbine. Figures 3.15 and 3.16 support the chosen added mass volumes with sketches. The added mass of each of those parts is defined as followed:

1. **Above the turbine:** The water body above the turbine cannot flow off the turbine within half an oscillation period upon a heave displacement of the turbine. Therefore, the mass of all the water above the turbines is taken into account for the added mass in the heave direction.
2. **Within the turbine:** The water body within the turbine is expected to follow the movements of the turbines concerning the vertical direction. All water within the turbine is taken into account for the added mass in heave direction.
3. **Below the turbine:** The added mass of the water body below the turbine is calculated with help of the theory explained in Section 3.2.7. A mass with a volume of the a half cylinder that sticks to the bottom of the turbine casing is taken into account as can be observed in Figure 3.15. For this geometry, the DNV suggests two coefficients which both have been taken into account. The first coefficient takes into account that the geometry of the rectangular bottom plate of the turbine casing approaches a square. The other coefficient takes into account that the fluid is hindered to flow to the other sides of the bottom plates due to the side plates of the turbine casing upon a downward movement. Both coefficients add up to approximately 1.0.

Sway The added mass of the turbine related to the sway degree of freedom is only due to the frontal surface area of the turbine. This frontal surface area is to be viewed well in Figure 3.17. The DNV norm specifies a coefficient of 2.2. This coefficient takes account that more fluid than solely the fluid in front of the front and back plate of the turbine casing need to accelerate upon sway accelerations. The fluid in front of the turbine is pushed to the sides upon accelerations. Hence, the fluid on the sides need to accelerate partly as well.

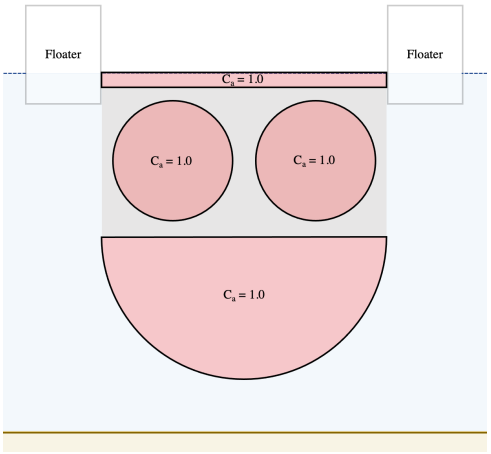

Figure 3.15 Front view of the added mass for the heave degree of freedom of the turbines

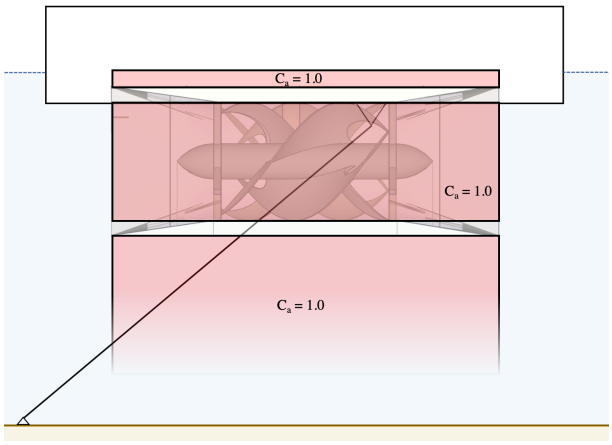

Figure 3.16 Side view of the added mass for the heave degree of freedom of the turbines

The fluid within the turbine is not included in the added mass contribution of the sway degree of freedom. The fluid within the turbine may move along with the impeller to some extent upon sway accelerations. Whelan, Graham, and Pierø (2009) concludes the article by stating that the added mass of horizontal axis tidal stream turbines has shown to be small. The effect is not taken into account as it is small and difficult to quantify.

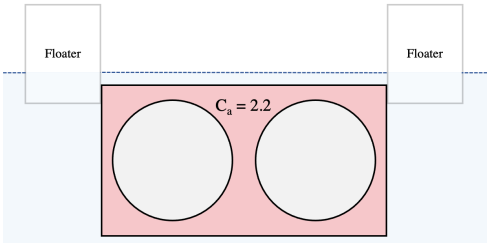

Figure 3.17 Front view of the added mass for the sway degree of freedom of the turbines

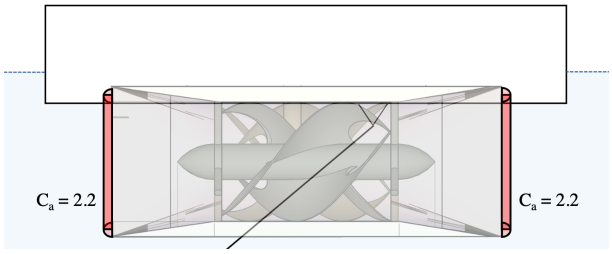

Figure 3.18 Side view of the added mass for the heave degree of freedom of the turbines

Roll The added mass found for the sway degree of freedom is used to calculate the added mass moment of inertia for roll degree of freedom. The added mass of the sway degree of freedom is multiplied by the lever arm squared from the centre of gravity of the Tidal Bridge to the middle of the turbine. The turbine added mass moment of inertia is the only relevant mass moment of inertia that should be taken into account for modelling the dynamic behaviour of the Tidal Bridge.

Qualitatively contemplating the interference effects

The choice to use the analytically determined formulas of the DNV design code has been made in Section 3.2.7. The small errors are introduced due to interference effects with the free surface or the bottom upon deciding to use these DNV formulas. This section qualitatively contemplates upon these interference effects to acquire an idea about the introduced errors.

Bottom effects The formulas of the DNV design code are flawless for a situation without interference effects of the free surface or the bottom. (Mutlu Sumer & Fredsoe, 2006) displayed a figure in his research about the added mass for a swaying cylinder near a wall. Figure 3.19 shows how the added mass increases upon getting closer to the wall. Within Figure 3.19 a smaller figure is sketched showing the added mass region for a swaying cylinder touches the wall. The added mass region for a cylinder which touches the wall is larger due to the fact that the water can only pass the cylinder on one side. This bottom effect takes a significant value for a distance to the wall of a quarter diameter or closer. This is not the case for the turbines.

Kolkman and Jongeling (2007) tries to quantify the proximity of the bottom for a heaving structure in formulas. Figure 3.14 shows a situation in which a heaving structure experiences bottom effects in the form of a larger added mass. The situation of Figure 3.14 can be approached as a symmetrical problem. The fluid that needs to 'get out of the way' has solely one exit. The structure experiences much resistance due to the energy needed to reach the immensely large flow velocity in order to discharge the volume through the only one gap. Hence, getting closer to the bottom, the experienced additional inertia of the water becomes larger. This effect starts to become significant as the 'cylinder' that circumferences the added mass region touches the bottom. This is not yet the case for the determination of the added mass region of the turbines. Both bottom effects are expected to be negligible and the formulas of the DNV can be safely used as regards of the bottom effects.

Free surface effects The determination of the added mass becomes dependent on the excitation frequency for a situation where the free surface effects the added mass (Kolkman & Jongeling, 2007). This frequency dependency increases as the distance to the free surface becomes smaller (DNV, 2010; Greenhow & Ahn, 1988). Figure 3.20 shows how the added mass changes depending on excitation frequency and depth. The sudden change from an enlarged added mass contribution for long excitation periods to a decreased added mass contribution for shorter excitation periods can physically be explained in terms of resonance. The free surface effects are then influencing mostly the fluid above the structure and not so much the fluid below the structure.

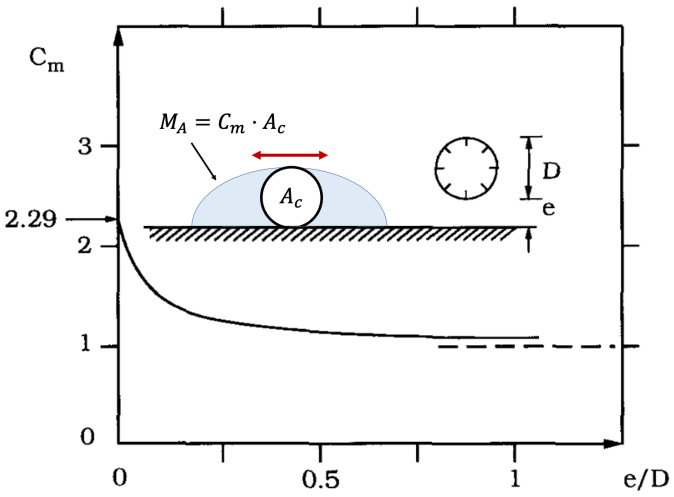

Figure 3.19 An increasing added mass upon a smaller distance to a wall for a swaying cylinder (Mutlu Sumer & Fredsoe, 2006)

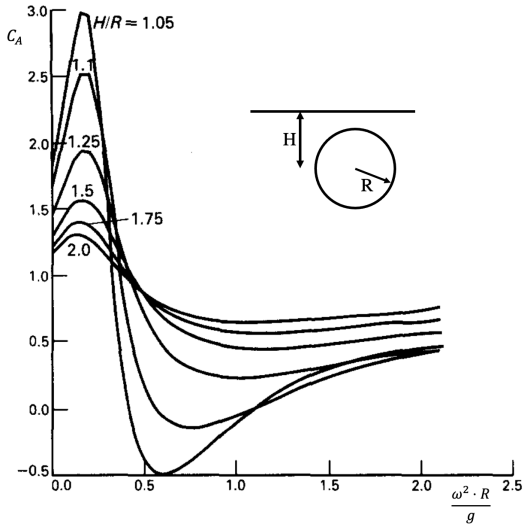

Figure 3.20 Depth and frequency dependency of the added mass (Greenhow & Ahn, 1988). A C_A equal to 1.0 means that the general added mass approximation like the one of the DNV code is valid.

Effect on the Tidal Bridge structure The studies of (Mutlu Sumer & Fredsoe, 2006) and (Greenhow & Ahn, 1988) showed the bottom and free surface effects. These effects are expected to be small for the Tidal Bridge. The bottom effects became significant for distance to the bottom of a quarter of the diameter of the object for the sway added mass, and a distance of half a diameter of the object for the heave added mass. The distance of the turbines to the bottom is about three quarters of the diameter of the added mass region. Hence, the effect of bottom influences are expected to be negligible.

The effects of the free surface on the added mass of the turbines or floaters is expected to be small as well. The effect of the free surface seems to be found mostly in the added mass region that touches the free surface. This is only the case for the added mass region above the turbines. Luckicly, this region is small and the effect on the dynamic response of the complete Tidal Bridge is therefore expected to be small as well.

3.2.8 Summarizing the relevant physical phenomena

The relevant physical phenomena have been sorted out by taking Equation 3.9 as a starting point. The equation shows all needed components of the structural dynamics model.

$$\boldsymbol{M\ddot{x}} + \boldsymbol{C\dot{x}} + \boldsymbol{Kx} = \boldsymbol{F} \tag{3.9}$$

The theory behind all the components has been sorted out. The list below summarizes the relevant physics of the specified unknown of Equation 3.9.

- $\boldsymbol{x}$ describes the displacement of the Tidal Bridge. The first derivative of the displacement $\dot{x}$ describes the velocity and the second derivative $\ddot{x}$ describes the acceleration.

- $\boldsymbol{M}$ describes the inertia of the Tidal Bridge element. The mass, mass moment of inertia, added mass and added mass moment of inertia all are added to this matrix.

- $\boldsymbol{C}$ describes the damping relative to the velocity of the Tidal Bridge. The components of the radiation damping described by the formula's of Vugts (1968) are included in this matrix.

- $\boldsymbol{K}$ describes the stiffness of the Tidal Bridge floating element. The stiffness matrix is composed of the hydraulic buoyancy stiffness and the pendulum stiffness.

- $\boldsymbol{F}$ describes the force vector. The force vector consists of the hydraulic loads of the waves and the current. The hydraulic load is described by the Morison equation. Important unknowns within the Morison equation are the drag coefficient C_d and the inertia coefficient C_m. The value for the drag coefficient is found within a table of DNV (2011) describing the drag coefficients for different geometries. The inertia coefficient depends on the submerged volume and the added mass. The latter is found by applying the suggested rules of DNV (2011).

3.3 Constructing the structural dynamics model

3.3.1 Introducing the structural dynamics model

The basis of the structural dynamics model is constructed by Dorgelo (2020), which was another student graduating from Delft University of Technology. He successfully modelled the dynamic response of the Tidal Bridge with his developed numerical model. He initially tried to simulate the four floating elements of the Tidal Bridge with six degrees of freedom. To reduce the complexity and the computation time, he chose to simplify the model to a 2D model that focuses on the dynamic behaviour of just one floating element. He successfully verified the model for forcing due to waves, currents, traffic (static load), and wind (static load). This model is used as a starting point for the structural dynamics model used in this design report.

The model has a two-dimensional approach to the dynamic problem. The significant degrees of freedom that define the dynamic behaviour of the Tidal Bridge fall within one 2D plane and are the sway, heave and roll degrees of freedom. The degrees of freedom yaw, pitch and surge may be present in reality with very minor magnitudes for the displacement and acceleration. Those small movements are not significant in the analysis to the serviceability limits of the Tidal Bridge.

3.3.2 The numeric model

There are three degrees of freedom in the 2D dynamic model. The horizontal movement, sway, occurs in the y-direction. The vertical movement, heave, occurs in the z-direction and the last degree of freedom, roll, occurs in the φ-direction as specified in Figure 3.1. A displacement can occur in the y, z or φ direction as it may all be called displacement. Therefore, these different types of displacement are bundled in the matrix notation which is specified in Equation 3.10.

$$\boldsymbol{x} = \begin{bmatrix} y \\ z \\ \varphi \end{bmatrix} \tag{3.10}$$

Where: $\boldsymbol{x}$ [m, m, rad] = displacement matrix
y [m] = sway translation
z [m] = heave translation
φ [rad] = roll rotation

The equation of motion for this dynamic model is found with help of the displacement method that finds its basis in Newton's second law. This classic formulation of the equation of motion is represented with Equation 3.11. Every component of this equation is in the matrix notation.

$$\boldsymbol{M\ddot{x} + C\dot{x} + Kx = f(t)} \tag{3.11}$$

Where: $\boldsymbol{x}$ [^{3}m] = displacement matrix
$\boldsymbol{\dot{x}}$ [m/s] = velocity matrix
$\boldsymbol{\ddot{x}}$ [m/s^2] = acceleration matrix
$\boldsymbol{M}$ [kg] = mass matrix
$\boldsymbol{C}$ [Ns/m] = damping matrix
$\boldsymbol{K}$ [N/m] = stiffness matrix

Using Modified Euler

The used model uses a numerical integration scheme to predict the dynamic response. Dorgelo (2020) used the Trapezoidal Method which is an implicit method. The model was made explicit by using the Forward Euler method. A more accurate way to do numerical integration is by making use of the Modified Euler integration scheme. The Modified Euler integration scheme is an explicit method. The Modified Euler method works with a predictor and a corrector to find a more accurate numerical integration scheme. The theoretical notation of the Modified Euler method may be found in Equation 3.12 as is drawn up by Vuik, Beek, Vermolen, and Kan (2004):

$$\begin{aligned} &\text{predictor:} \quad \bar{w}_{n+1} = w_n + hf(t_n, w_n) \\ &\text{corrector:} \quad w_{n+1} = w_n + \frac{h}{2}[f(t_n, w_n) + f(t_{n+1}, \bar{w}_{n+1}) \end{aligned} \tag{3.12}$$

Where: $\bar{w}_{n+1}$ [-] = numerical prediction on time step $n+1$
w_{n+1} [-] = numerical result on time step $n+1$
w_n [-] = numerical result on time step n
h [-] = time step length
$f(t_n, w_n)$ [-] = derivative at time step n
$f(t_{n+1}, \bar{w}_{n+1})$ [-] = predicted derivative at time step $n+1$

This Modified Euler method is adapted to the numerical scheme of the dynamic model takes into account the displacement, velocity and acceleration.

$$\begin{aligned} \bar{\boldsymbol{x}}_{n+1} &= \boldsymbol{x}_n + h \cdot \dot{\boldsymbol{x}}_n \\ \bar{\dot{\boldsymbol{x}}}_{n+1} &= \dot{\boldsymbol{x}}_n + h \cdot \ddot{\boldsymbol{x}}_n \end{aligned} \tag{3.13}$$

The corrector formulas need predicted derivatives of the displacement and the velocity. The predicted derivative of the displacement is the predicted value for the velocity as is found with Equation 3.13. However, the predicted derivative of the velocity is the acceleration component related to the predicted values for displacement and velocity. The predicted acceleration can be calculated by solving Equation 3.11.

The acceleration matrix of 3.11 is the unknown in the formula. The predicted values for the displacement- and velocity matrices are used to fill into 3.11. The M- and C-matrices are constant in the model. However, the matrix **K** is dependent on displacement due to the changing pendulum angle. The matrix **F** is dependent on time, displacement and velocity. Therefore, both matrices need to be updated before Equation 3.11 can be solved.

[3]The specified units do only apply for the translational degrees of freedom. The units are the same for the roll direction as long as the rad is replaced for m, kg·m^2 for kg and N·m instead of N.

$$\bar{\ddot{\boldsymbol{x}}}_{n+1} = \boldsymbol{M}^{-1}\left(\boldsymbol{f}(t_{n+1}, \bar{\boldsymbol{x}}_{n+1}, \bar{\dot{\boldsymbol{x}}}_{n+1}) - \boldsymbol{C}\bar{\dot{\boldsymbol{x}}}_{n+1} - \boldsymbol{K}(\bar{\boldsymbol{x}}_{n+1})\right) \tag{3.14}$$

The corrector formulas applied to the numerical problem of the python model is shown in Equation 3.15.

$$\begin{aligned} \boldsymbol{x}_{n+1} &= \boldsymbol{x}_n + \frac{h}{2}[\dot{\boldsymbol{x}}_n + \bar{\dot{\boldsymbol{x}}}_{n+1}] \\ \dot{\boldsymbol{x}}_{n+1} &= \dot{\boldsymbol{x}}_n + \frac{h}{2}[\ddot{\boldsymbol{x}}_n + \bar{\ddot{\boldsymbol{x}}}_{n+1}] \end{aligned} \tag{3.15}$$

The the newly determined values for the displacement and velocity, the matrices **K** and **F** can be updated again for the new displacement and velocity. With this updated values, the acceleration can be determined with Equation 3.16.

$$\ddot{\boldsymbol{x}}_{n+1} = \boldsymbol{M}^{-1}\left(\boldsymbol{f}(t_{n+1}, \boldsymbol{x}_{n+1}, \dot{\boldsymbol{x}}_{n+1}) - \boldsymbol{C}\dot{\boldsymbol{x}}_{n+1} - \boldsymbol{K}(\boldsymbol{x}_{n+1})\right) \tag{3.16}$$

The local truncation error of the Modified Euler method is $\mathcal{O}(h^2)$ which is better than the alternative of Forward Euler that has a local truncation error of $\mathcal{O}(h)$. Although two function evaluations are needed for the Modified Euler method per time step, the total function evaluations is still less due to the higher stability and convergence.

Time step size and stability

The chosen time step for the model is dependent on the smallest period when looking to the forcing period of the model and the natural periods of the model. The smallest natural period is about 0.97 seconds for the sway degree of freedom and this period is also smaller than the forcing period. The numerical model needs to have enough intervals to be able to describe this period of this signal well. There are at least 10 intervals needed to follow the curve of a sine wave to describe the period well. There are twice as many intervals needed to recognize such a signal. Therefore, the smallest natural period could be divided by 20 intervals to figure out the length of the time step.

$$h = \frac{min(T_{n_1}, T_{n_2}, T_{n_3})}{2 \cdot 10} \approx 0.05 \text{ seconds} \tag{3.17}$$

Verification of the Modified Euler scheme

The new Modified Euler scheme has been verified with success. The results of the simplified dynamic model have been checked to an equal model which made use of an truly existing solver of Matlab. The input of both models contained fixed matrices for the mass, damping, stiffness and forcing. Both models showed exactly the same results for the free vibrations that were activated by initial conditions. This verification shows that the enhanced numeric Modified Euler scheme works properly.

3.3.3 Modelling open boundaries

Experiments have been performed to find realistic boundary conditions that model the influence of the adjacent floating elements. The choices for boundary conditions could have a dependency to acceleration, velocity, displacement or a combination of the three types of kinematics with the kinematics of an additionally modelled floater.

Modelling the adjacent floating element with its own degrees of freedom became too complicated for the scope of the thesis. Modelling boundary conditions dependent to the acceleration or the velocity of the main structure would not approach the influence of the adjacent floating elements to the main structure realistically. Modelling a boundary that is dependent to the displacement approaches reality somewhat. Upon pushing down the main structure, the buoyancy force of the main structure pushes back, but also a part of the buoyancy force of both adjacent floating elements push back due to the restricted translations between elements due to the connections. This influence has been modelled as a boundary condition as additional stiffness.

This additional boundary condition mitigated the dynamic response. However, the adjacent floater may follow the same hydraulic loading and the additional modelled stiffness should be less than modelled. Therefore, open boundaries have been assumed to find a dynamic response which is not mitigated by a boundary condition as it is preferred to over-estimate the response instead of under-estimating the response.

3.3.4 Model input and output

The model takes as input the hydraulic conditions such as the wave height, wave length and current velocity. The complete design geometry and physical characteristics can be inputted in the parametric model by design parameters and model coefficients. The model calculates the dynamic response for the defined hydraulic conditions. Many tests with various hydraulic conditions lead to many results for the steady-state displacement, acceleration, etc. One type of the results, the steady-state displacement for example, can be displayed in a matrix that has a varying wave height on the x-axis and a varying wave length on the y-axis. These discrete results of the displacement can be made continuous with cubed interpolation.

The interpolated results can be displayed in many ways. The preferred way of displaying shows a simple line drawn in a figure. The figure shows an increasing wave height on the y-axis versus an increasing wave length on the x-axis. The line makes a distinction between the region in which the serviceability limit is not exceeded and a region in which the serviceability limit is exceeded. Such a type of plot can be observed in Figure 4.1 in the next chapter and is useful in determining the limiting wave characteristics.

3.3.5 Overview of additions and modifications to the original model

The original structural dynamics model of Dorgelo (2020) has been further improved as part of this design report. The model needed modifications to become usable for this design report and for the updated Tidal Bridge design with the FishFlow turbines. The most significant changes and additions to the model are presented below:

- **Numerical integration scheme:** The original model made use of a mix of the Trapezoidal numerical scheme and the Forward Euler numerical scheme. The Forward Euler method has a relatively high truncation error and is undesired for such applications. Furthermore, the Trapezoidal rule is implicit rule which cannot be used for this application either. The numerical scheme is adapted to a pure Modified Euler scheme. The Modified Euler rule is an explicit method that has a relatively small local truncation error.

- **Force vector variables:** The force vector was dependent to the acceleration vector of the structure. This is theoretically impossible as the acceleration vector of the structure is the unknown that should be solved by the numeric scheme. This dependence slipped in the force vector by the hydrodynamic force. The hydrodynamic force is dependent to the relative acceleration, and hence, dependent to the structure's acceleration vector. However, part of the hydrodynamic force dependent to the structure's accelerations is already accounted for by the added mass contribution in the mass matrix. The contribution related to the structure's accelerations can be taken out of the force vector as it is already accounted for in the mass matrix.

- **Integration of FishFlow turbines:** The original structural dynamics model took windmill shaped turbines structures into consideration. These types of turbines differed much from the FishFlow turbines which were part of the Tidal Bridge design. The FishFlow turbines are modelled with the Morison equation as well to define the hydraulic loads on the structure.

- **RAO plots:** The script has been adapted such that Response Amplitude Operator (RAO) plots can be constructed with the model. RAO's are commonly used for floating structures to describe the response to a regular wave with a unit height and a defined frequency. Such plots provide insight in the resonance frequencies. For this report, the plots can be used to observe dynamic optimizations as the response should become smaller with optimized designs. The RAO plots are more easy to read than the heatmap plots which were initially the main type of output.

- **Exceedance region plots:** An additional model output has been constructed. This model output shows on one plot, dependent to the wave height and the wave length, for which combinations the serviceability limit is exceeded or not. The advantage of this plot is that solely one plot defines whether a design leads to a reduction of the downtime or an increase of the downtime.

- **Variable time step:** Variable time steps have been integrated in the model to optimize the computation time.

- **Variable simulation time:** A variable simulation time has been introduced to optimize the computation time.

- **Optimization of the computation time:** A line by line analyzer found the time consuming steps of the model. Those time consuming lines have been optimized as much as possible.

3.3.6 Verification of the model

The model has been elaborately verified in the thesis of Dorgelo (2020). He verified the model to (experimental) literature that describes the same types of dynamic problems. He validated the model to some scale experiments that confirm the applied literature for added mass. He verified the model by performing simple computational tests to prove the effectiveness of the different model parts.

In this design report, the model has been thoroughly analyzed to check the correctness. The applied formulas of the model have been found in a separate literature study. The study confirms that all used equations are based on experimentally supported literature. Furthermore, changes in the input parameters lead to the expected changes in the model results, which is another argument for a well verified model.

The numeric integration scheme has been verified by comparing the results of a simplified dynamic problem to the results of a truly existing solver in Matlab.

3.3.7 Model structure

1. A parameter overview page makes it easy to change and add parameters to the model. The parameter overview page offers the ability to include or exclude some forcing mechanisms or change the output structure.
2. The matrices M, C, and K matrices are constructed.
3. The natural frequencies are calculated to determine the smallest possible step size. The step size is 20^{th} of the smallest natural period.
4. Then the numerical integration starts. Within every step, the following actions are taken:
   (a) For every time step predictor values for the displacement and the velocity are determined.
   (b) Based on the predicted values for the displacement and velocity, an update can be made for the angle of the pendulum; the drag force to the floater, turbine, and pendulum; the hydraulic inertia force to the floater and to the turbine; and the $\boldsymbol{K}$-matrix as the stiffness of the pendulum is dependent on the location of the floating element.
   (c) The updated $\boldsymbol{F}$-matrix and the $\boldsymbol{K}$-matrix helps to solve for $\ddot{\boldsymbol{x}}$. The displacement $\boldsymbol{x}$, the velocity $\dot{\boldsymbol{x}}$, the matrices $\boldsymbol{M}$, $\boldsymbol{C}$, $\boldsymbol{K}$, and $\boldsymbol{F}$ are known. Hence, the predicted $\ddot{\boldsymbol{x}}$ can be calculated.
   (d) With this predicted value for $\ddot{\boldsymbol{x}}$, the corrected values for $\boldsymbol{x}$, and $\dot{\boldsymbol{x}}$ can be calculated.
   (e) The matrices $\boldsymbol{K}$ and $\boldsymbol{F}$ are updated again with the corrected values for $\boldsymbol{x}$, and $\dot{\boldsymbol{x}}$.
   (f) The corrected value for $\ddot{\boldsymbol{x}}$ can be calculated which results in a new 'real
5. The maximum displacement, velocity, acceleration are calculated as well as the maximum and minimum pendulum force.
6. The generated data is stored in a plot and in a text file.

Chapter summary

This chapter developed, improved and described the structural dynamics model which is needed for the subsequent chapters to analyze the dynamic response of the original design and of the design optimizations. The original mechanical system of the Tidal Bridge was described as it serves as a basis for the model. Consequently, the relevant physical phenomena were gathered and explored.

Schrijven over de gekozen boundary conditions. Zie feedback hayo 22 juni in het word bestand Schrijven over de controle van het model.

4 | Narrowing the design space

This chapter uses the developed structural dynamics model of the previous chapter to analyze the dynamic behaviour of the original Tidal Bridge design. This analysis is needed to define the starting point for the design process later in the report. The downtime of the original Tidal Bridge design is determined by combining the results of the structural dynamics model and the results of the wave characteristics model. Consequently, the balance in mass and stiffness of the original design is explored by analyzing the sensitivity to the parameters and coefficients used in the structural dynamics model. The thesis scope is narrowed based on the chapter results.

4.1 Exploring the dynamic behaviour of the original design

4.1.1 The dynamic behaviour of the original Tidal Bridge design

The dynamic response of the original Tidal Bridge design can be calculated by making use of the structural dynamics model. The model calculates the maximum combined acceleration for 8 different wave periods and 6 different wave heights. This discrete data set of accelerations is made continuous with cubic interpolation. Consequently, a line is plotted that distincts the region where the serviceability limit of the floating element of the Tidal Bridge is exceeded. Figure 4.1 shows the result of the structural dynamics model for the base case, the original Tidal Bridge design. The red region above this line shows the region in which the combined acceleration is larger than 0.7 m/s^2.

The most probable wave characteristics are plotted in the Figure 4.1 as well. This data is obtained with the wave characteristics model as described in Chapter 2. The grey region shows all wave height and wave length combinations that fall within a 90% confidence interval. The wave height and wave length combination of the three wave characteristics lines all have a probability of exceedance which is displayed in Figure 4.2. The three wave heights defined the crossing of the serviceability limit line and the wave characteristics lines define the critical wave heights. The probability of exceedance of those critical wave heights can be found in Figure 4.2. These probabilities of exceedance can be multiplied by 365 days to know how many days per year the Tidal Bridge exceeds the serviceability limits. Table 4.1 shows an overview of the calculated yearly downtime for the base case, the original Tidal Bridge design.

	Probability		
	95%	**50%**	**5%**
Base case	31.6	23.4	16.3

Table 4.1 Yearly downtime in days for the base case

The critical wave height is 0.59 meters and the critical wave period is 4 seconds. The corresponding wave length is 24.8 meters. This wave length is about 70% of the floater length. The serviceability limit line of Figure 4.1 shows its minimum at a wave period of 4.9 seconds. The corresponding wave length is 37.4 meters. The floater length is 34 meters without the pointed tips and 39 meters including the pointed tips. The critical wave length has about the same length as the floaters. The critical response is found for the situation that the floater has interference with one trough and one crest at the same time.

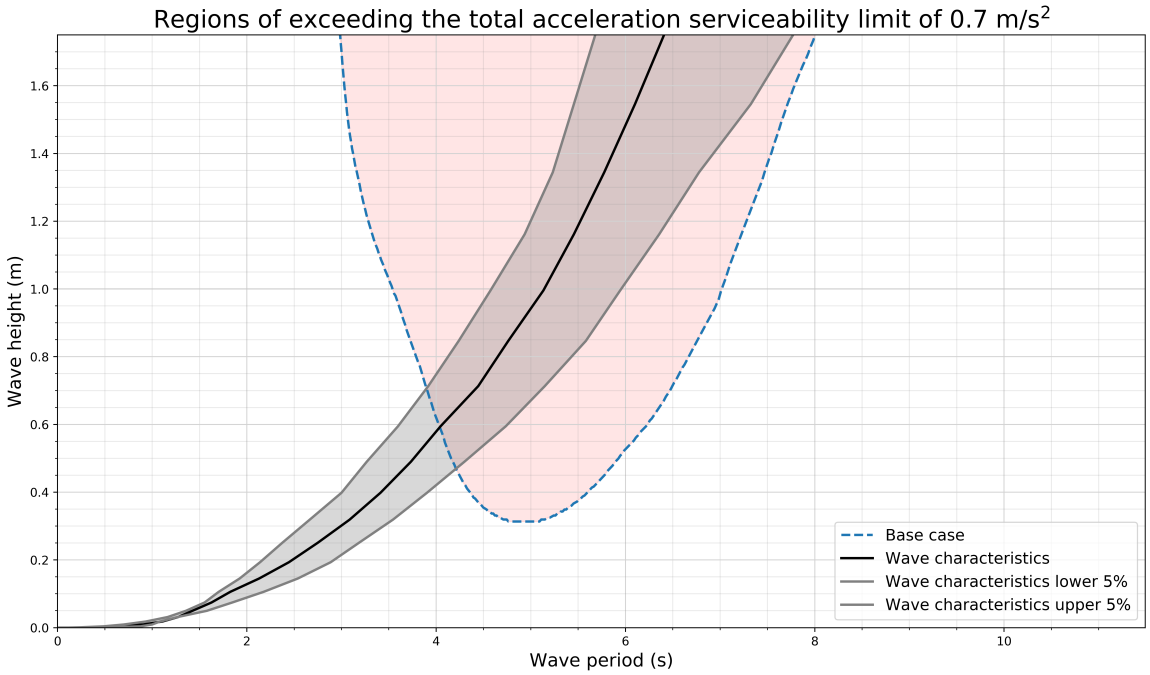

Figure 4.1 The figure shows the region where the combined acceleration serviceability limit is exceed for the original Tidal Bridge design.

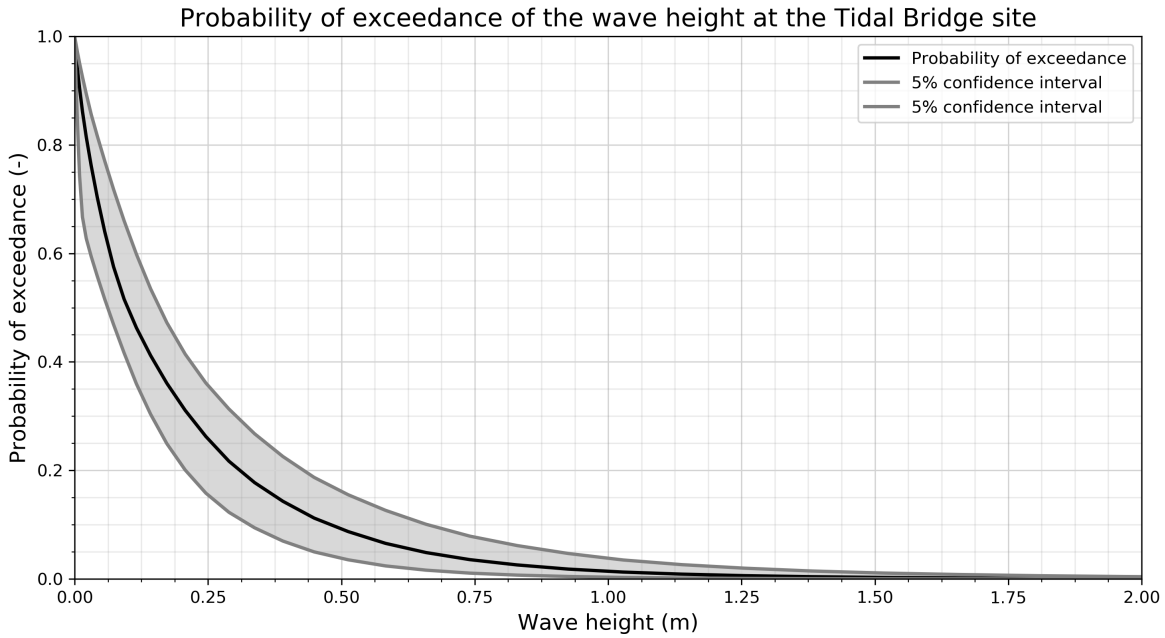

Figure 4.2 Probability of exceedance of the wave height at the Tidal Bridge location

4.1.2 Finding the governing serviceability limit

The serviceability limit is defined by a maximum combined acceleration limit of 0.7 m/s^2 and a maximum roll displacement of 0.06 rad. Results of several tests of different designs showed that the combined acceleration limit is always exceeded before the maximum roll displacement limit is exceeded. Proof of this statement for the original Tidal Bridge design can be found by comparing Figure 4.3 and 4.4 both show the line that defines the wave height and wave length combination of exceedance of the serviceability limit of the roll displacement

and the combined acceleration respectively. The region on the right side of the line marks the region where the serviceability limit is exceeded. The combined acceleration serviceability limit is always exceeded for lower wave heights compared to the roll displacement serviceability limit. This governing combined serviceability limit is therefore used in this report for determining the downtime.

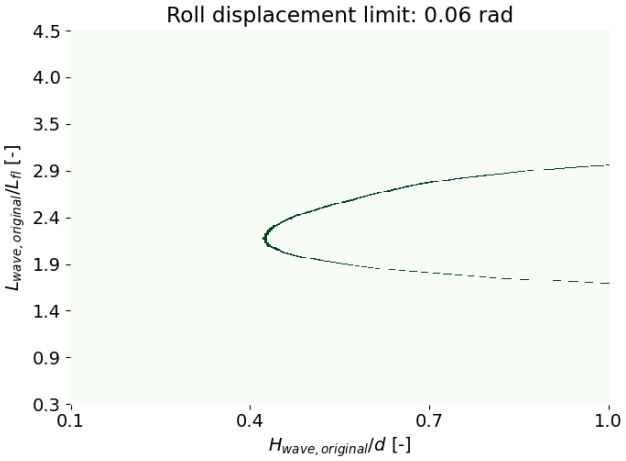

Figure 4.3 Line defining the exceedance of the roll displacement limit

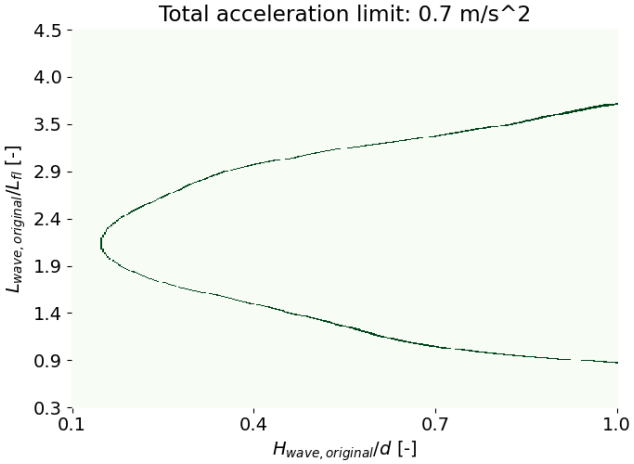

Figure 4.4 Line defining the exceedance of the combined acceleration limit

Where:

$L_{wave,original}$	[m]	=	wave length
L_{fl}	[m]	=	floater length
$H_{wave,original}$	[m]	=	regular wave height
d	[m]	=	draught

4.1.3 The effect of the chosen serviceability limit

The chosen combined serviceability limit of 0.7 m/s^2 for the Tidal Bridge has been found in literature. The chosen serviceability limit was not readily available for the situation of a floating bridge in Indonesia. The serviceability limit for floating bridges found in the Bridge Engineering Handbook has been used. The limits in Indonesia may be stricter or more tolerant compared to the limit specified by Lwin (2000). The effect of a stricter and more tolerant limit has been explored and the results have been presented in Table 4.2. The results of Table 4.2 are deduced from the Figure D.1 in Appendix D.1. Roughly speaking, a limit that tolerates a doubled acceleration limit has about half of the downtime of the original acceleration limit.

	Probability		
	95%	**50%**	**5%**
Serviceability limit of 0.5 m/s^2	39.9	29.9	20.8
Serviceability limit of 0.7 m/s^2	31.6	23.4	16.3
Serviceability limit of 1.0 m/s^2	25.8	18.4	11.7

Table 4.2 Yearly downtime in days for the original Tidal Bridge design for different serviceability limits.

4.1.4 Limiting degree of freedom

The acceleration serviceability limit that is governing over the roll displacement serviceability limit, is composed of the sway, heave and roll accelerations and combined by the Pythagorean theorem. The roll accelerations is decomposed in a sway acceleration and a heave acceleration before the combined acceleration is determined. The roll acceleration contributions to the sway and heave accelerations are found by multiplying the roll acceleration by the lever arm to the point of interest on the road deck.

Figure 4.5 shows the exceedance of the serviceability limit of the accelerations of the separate degrees of

freedom. The limit is exceed for the region on the right side of the dark green line as this is the region with the larger wave heights. The degree of freedom that exceeds its own acceleration limit for the lowest wave heights is assumed to be limiting in the determination of the combined acceleration as well. This assumption works fairly well as long as the differences between the exceedance of the acceleration limits between the degrees of freedom is large enough. The sway degree of freedom exceeds the serviceability limits for the smallest waves. This degree of freedom is therefore qualitatively determined to be limiting in the determination of the acceleration limit.

In other tests than the presented test of Figure 4.5, the sway degree of freedom stays clearly the limiting degree of freedom. The optimization solution could best be focusing on this degree of freedom in order to target the dynamic problem effectively.

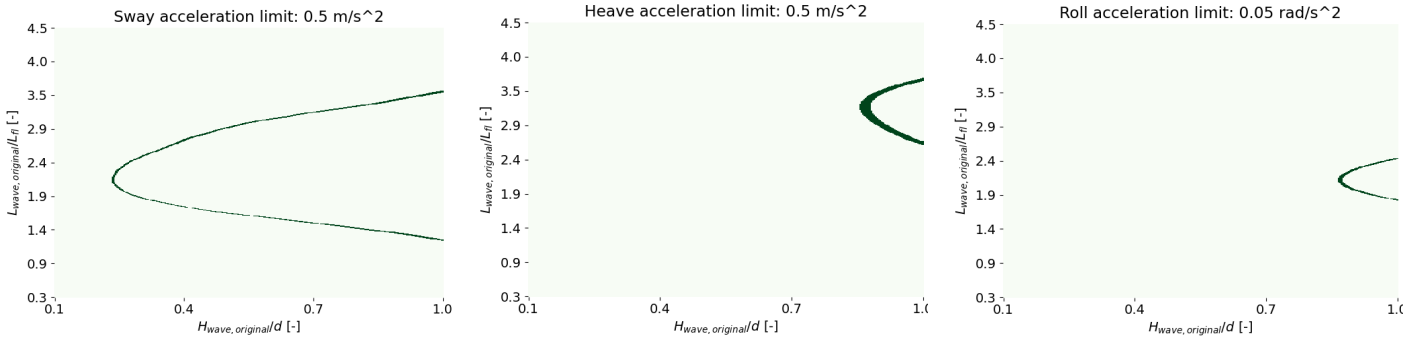

(a) Sway **(b)** Heave **(c)** Roll

Figure 4.5 The exceedance of the acceleration serviceability limit of the separate degrees of freedom

4.1.5 The resonance frequencies for the degrees of freedom

The degrees of freedom of the dynamic system is strongly coupled by the stiffness induced by the pendulum. Although a strong coupling is present in the dynamic system, the separate degrees of freedom all have their own gradient of responses to to a variable excitation frequency. Such dynamic response to a varying excitation frequency may be observed in Response Amplitude Operator (RAO) plots. Those plots show the dimensionless response to the waves for the various tested wave frequencies. The RAO plot for the original Tidal Bridge design may be observed in Figure 4.6.

The theoretical natural frequencies are calculated to be 6.5 rad/s, 0.44 rad/s, and 0.76 rad/s for the sway, heave and roll degrees of freedom respectively. These natural frequencies may be observed in a test with a free vibration. The response of Figure 4.6 is due to a forced vibration and some wave frequencies different from the natural frequencies show to become amplified more. The wave frequency of 1.25 rad/s and 0.75 rad/s lead to larger responses compared to other excitation wave frequencies. The wave frequency of 1.25 rad/s corresponds to a wave period of 5 seconds. This period shows to be leading to the exceedance of the serviceability limits for the lowest wave heights as is concluded in Section 4.1.1 before.

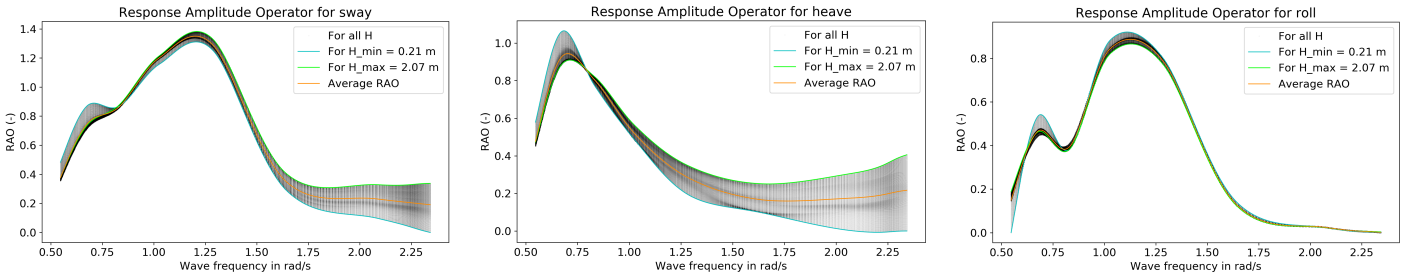

(a) Sway **(b)** Heave **(c)** Roll

Figure 4.6 The RAO plots of the three degrees of freedom for the original Tidal Bridge design

4.1.6 Analyzing the influence of turbines

Figure 4.7 shows the regions of exceeding the serviceability limit for the situation without the turbines compared to the base case that includes turbines. The figure shows that the serviceability limit is only exceeded for a small region with large wave heights and very short waves which is an unrealistic combination following the wave characteristics model. The structural dynamics model did not calculate the response for waves that have wave periods shorter than 2.7 seconds as such short waves have very small amplitudes as well. In short, the serviceability limits will not be exceeded for a Tidal Bridge design that does not have the FishFlow turbines connected.

Figure 4.7 clearly shows an enormous influence of the turbines to the dynamic behaviour of the Tidal Bridge. The turbines function as very large hard sails hanging below Tidal Bridge structure. These sails are very vulnerable to adopt the same kinematics of the waves around the sails. The additional inertia of the turbines is not counteracting this effect. This effect can also be explained by the used theory. The dominating inertia force is related to acceleration of the water multiplied by the additional mass. The added mass of the turbines is very large, and the acceleration of the fluid around this turbines is large as well due to the proximity to the free surface. This leads to a large additional forcing component that drives the dynamics of the Tidal Bridge. However, the additional mass and the additional added mass of the turbines lead to more inertia of the complete system. This inertia reduces the Tidal Bridge dynamics somewhat.

4.1.7 Analyzing the effect of the wave direction

Figure 4.8 shows the effect of the wave direction on the regions of exceeding the serviceability limits. The figure shows that negative directed waves lead to a slightly improved estimation of the yearly downtime as the wave characteristics line cross the serviceability limit line for higher wave heights. The different response for negative directed is due to the asymmetrical Tidal Bridge design. The hinge location and the pendulum orientation lead to a different transfer of forces and hence, a different dynamic response.

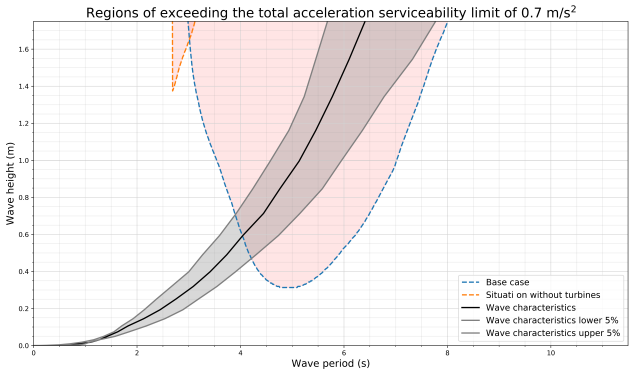

Figure 4.7 The region of exceeding the serviceability limit for the situation without the turbines compared to the base case

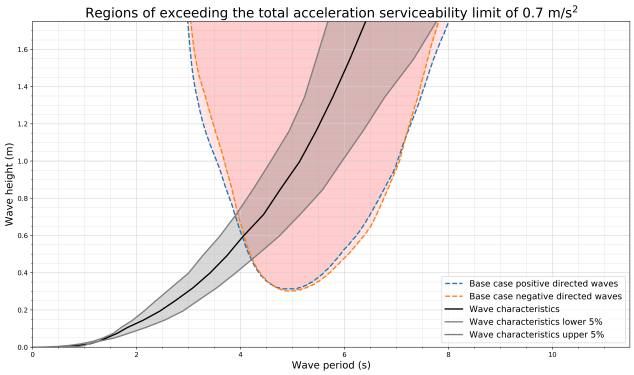

Figure 4.8 The region of exceeding the serviceability limit for the base case with positive and negative directed waves

4.1.8 Qualitative evaluation upon the influence of the currents

The influence of currents has not been modelled with the structural dynamics model. The verification of the model with currents has not been finished with success. However, the influence of the currents can qualitatively be considered. The tidal currents have an influence on the Keulegan-Carpenter (KC) number which adopts larger values. The structure becomes more drag dominant for larger KC numbers. The drag is quadratically related to the relative current velocity squared. With the influence of currents the drag forces increase quadratically. The drag forces have a damping effect to the structure due to the quadratic relation to the relative velocity squared. Hence, the structure is expected to be dynamically less active for a situation with the tidal currents.

The statement that the Tidal Bridge becomes dynamically less active for currents is only valid under the assumption that structure does not show dynamic instability. The system would surely show dynamic instability for an hypothetical situation with infinite drag forces due to the current. For both current directions the system

would not stay in its equilibrium position in that situation. Dorgelo (2020) concluded in his research that the Tidal Bridge system without the FishFlow turbines could not show dynamic instability due to the currents. However, the large FishFlow turbines contribute to much more drag in the system and it is unsure if the statement of Dorgelo (2020) is still valid.

4.2 Analyzing the balance in mass and stiffness

4.2.1 The Tidal Bridge as mass dominant structure

Figure 4.9 summarizes the content of this section by displaying the response of a simple mass-spring system with some damping. Although the response of the floating elements of the Tidal Bridge is more complicated that the figure, the basis of a dynamic response is similar. The response of a simple mass-spring system with some damping can be roughly categorized in either one of the three regions displayed in Figure 4.9: stiffness dominated, damping dominated, and mass dominated. The three regions determine which variable has relatively the largest influence in the dynamic response compared to the other variables.

An excitation due to very short period waves with short wave lengths falls in the mass dominated regime and the structure does practically not excite. However, a tidal wave which has a very low wave frequency leads to a response of the Tidal Bridge that follows the surface elevation within the strait. The hydraulic stiffness is responsible for following the tidal wave, and hence, the structure can be called stiffness dominated.

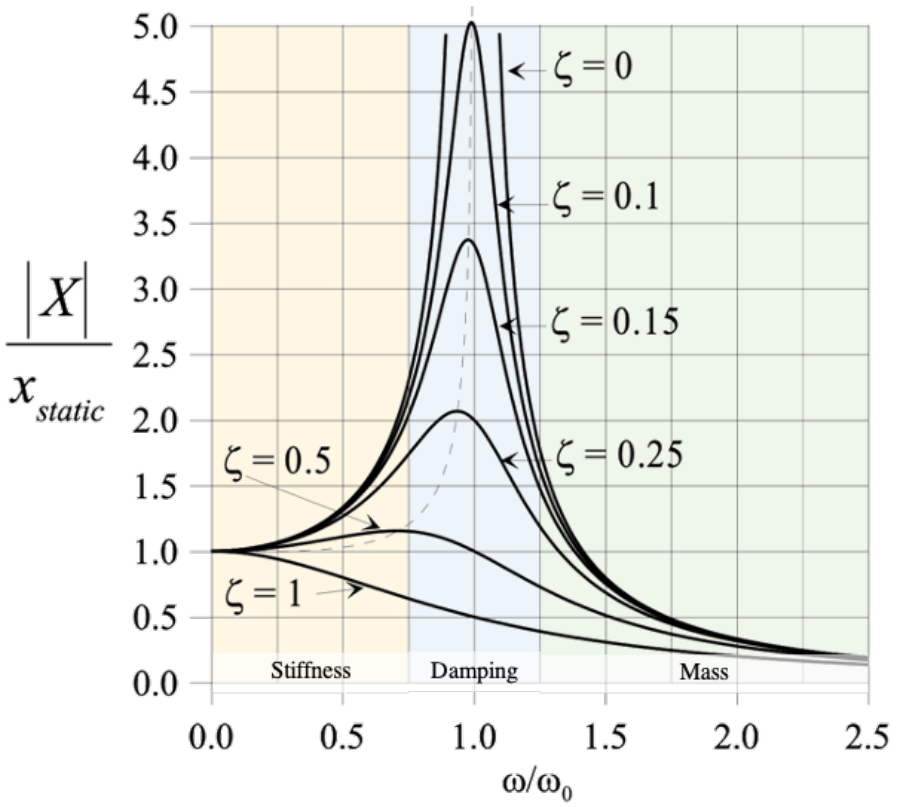

Figure 4.9 Dynamic amplification factor as a function of the relative radial frequency (Metrikine, 2015). Three distinct regions that specify stiffness, damping and mass dominance.

Where:	χ	[m]	=	dynamic response
	x_{static}	[m]	=	static response
	ω	[rad/s]	=	excitation frequency
	ω_0	[rad/s]	=	undamped natural frequency
	ζ	[-]	=	dimensionless amount of viscous damping

The RAO plots of Figure 4.10 show many similarities with Figure 4.9. The dimensions of the axis of the figures are similar and all RAO's show to have more or less a (clearly) defined peak. Estimates for the stiffness, damping, and mass controlled regions have been drawn in the RAO plots as well as the wave frequency that leads to the exceedance of the serviceability limits. Wave frequencies smaller than the specified wave frequencies lead to responses that exceed the serviceability limits. The red line is always situated in the mass dominated regimes. However, the larger wave periods would lead to an excitation which becomes more damping dominated.

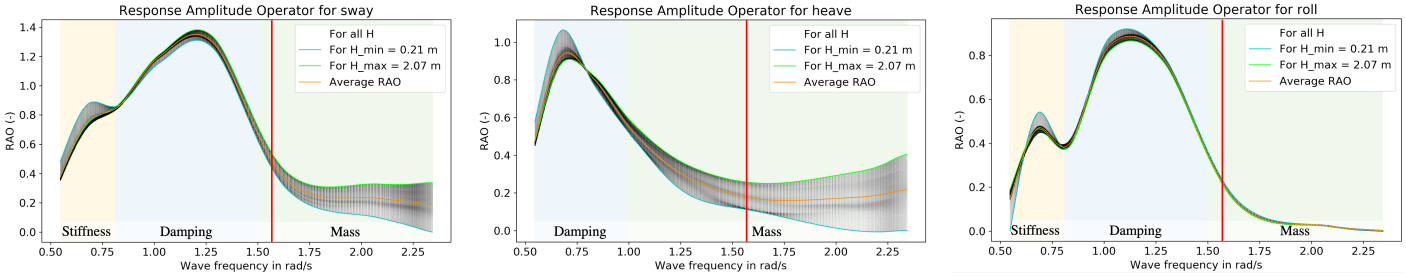

(a) Sway **(b)** Heave **(c)** Roll

Figure 4.10

This analysis shows that the dynamic response of the Tidal Bridge could best be mitigated by adapting the mass and damping. The effect of changing the stiffness is probably limited compared to the mass and damping variables. A changed stiffness may also have an effect as it shifts the resonance frequency towards the excitation frequency. However, this effect shall be limited compared to relative changes in the variables of damping and mass.

4.2.2 Analyzing the sensitivity to important design parameters

A sensitivity study has been executed to analyze the effect of changes in the important design parameters. 18 parameters have been analyzed in total. The complete list of parameters that have been analyzed may be found in Appendix D.2.

The results of the sensitivity analysis have been found by increasing or decreasing the concerned parameter by 10%. The relative response of the combined acceleration compared to the base case has been recorded in Table 4.3. Only the parameters which are noteworthy due to the large sensitivity or estimated sensitivity have been displayed. The sensitivity of the parameters has been analyzed for two different wave periods. The results show that the sensitivity of a parameter changes for the different wave periods.

	T = 4.0 s	**L = 24.8 m**		**T = 4.9 s**	**L = 37.4 m**	
Parameter	+10%		-10%	+10%		-10%
Mass	-1,9%		1,9%	0,0%		-0,6%
Mass moment of inertia	-4,0%		4,2%	-2,8%		2,5%
Floater length	47,0%		-42,2%	-3,0%		-14,4%
Floater width	6,4%		-6,1%	3,0%		-5,9%
Depth	0,0%		0,0%	0,1%		-0,2%
Pendulum angle	-0,8%		0,5%	-2,2%		1,6%
Pendulum stiffness	-0,1%		0,1%	0,1%		-0,1%
Drag coefficients	-0,1%		0,1%	-0,3%		0,3%
Radiation damping coefficient	-0,3%		0,3%	-1,5%		1,5%
Inertia coefficient	9,4%		-9,4%	10,9%		-11,2%
Wave height	9,6%		-9,7%	8,1%		-10,4%
Wave length	27,4%		-41,2%	-4,4%		-3,4%

Table 4.3 Results of the sensitivity study found for two different wave periods. The red bars indicate an increase of the combined acceleration and the green bars indicate an decrease of the combined acceleration.

Analyzing the sensitive parameters

The design parameters that have the largest influence to the dynamic response are listed in the order of importance: floater length, wave length, inertia coefficient and wave height. To begin with, the wave length and the wave height are parameters that cannot be influenced by changing the design and those parameters are not of relevance in the optimization analysis.

The most influential parameter is the floater length. An increment of 10% of the floater length showed to increase the combined acceleration with 47% for a wave period of 4.0 seconds. A decrease of the parameter of 10% showed to decrease the combined acceleration with 42%. This parameter may potentially be very effective to optimize the dynamic behaviour of the Tidal Bridge.

The inertia coefficient shows to be an effective parameter to use for optimizing the dynamic behaviour of the Tidal Bridge. An increment of 10% of this parameter leads to an increment of the combined acceleration of almost 10% as well. The opposite is valid for a decrease of the parameter.

4.2.3 Investigating optimizations with the sensitive design parameters

The floater length and the inertia coefficient both seemed to have a large sensitivity to the dynamic response of the Tidal Bridge. The sensitivity analysis of those two parameters has been pushed forward a little further. The response to various wave heights and wave lengths has been tested with the structural dynamics model for the potential optimized parameter values. The results of the tests may be observed in Figure 4.11a and 4.11b. The results in terms of downtime may be observed in 4.4.

	Probability		
	95%	**50%**	**5%**
Base case	31.6	23.4	16.3
Floater length 37.4 m	41.0	31.0	19.6
Floater length 30.6 m	28.8	21.7	15.4
Floater length 27.2 m	30.8	23.0	15.4
10% lower inertia coefficient	30.8	22.6	15.4

Table 4.4 Yearly downtime in days for the base case, one longer floater, two shorter floaters[1]and a design with a smaller inertia coefficient

The sensitivity analysis showed that the floater length parameter would be the most promising to structurally reduce the yearly downtime. The results of the structural dynamics model showed that the downtime reduced in the order of 1-2 days per year. The downtime of a floater that has a length 27.2 m does not show an improved downtime compared to the floater length of 30.6 meters. Hence, the optimization possibilities for the floater length are very limited.

The results of the reduced inertia coefficient showed that the downtime reduces for about a half day per year.

[1] A graphic representation of the region of exceedance of the serviceability limit is displayed in Appendix D.3 to avoid messy graphs.

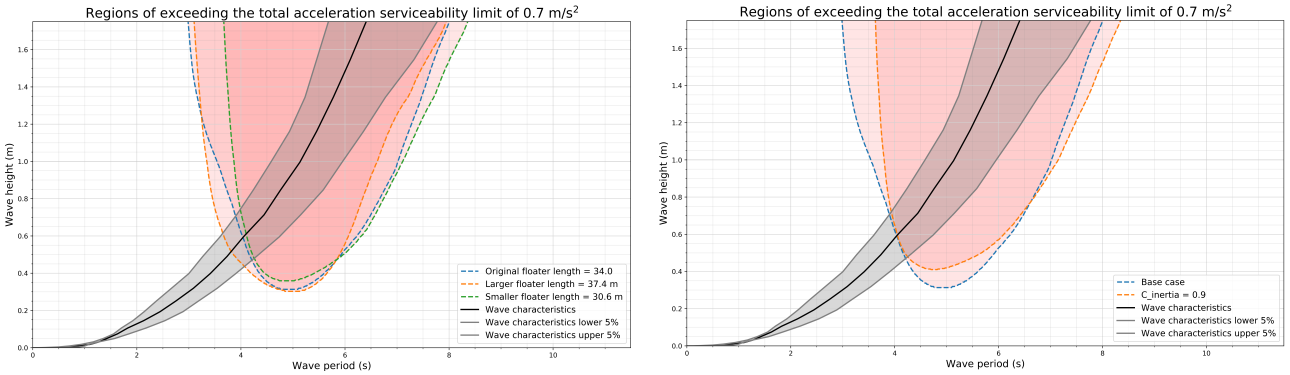

(a) For three different floater lengths

(b) For the reduced inertia coefficient

Figure 4.11 The regions of exceeding the serviceability limit

4.3 Refining the scope

The results of the sensitivity analysis suggested that optimizations in the floater length and inertia coefficient may lead to a significant reduction of the dynamic response. A more profound test to the performance of a Tidal Bridge design with a smaller floater length or a reduced inertia coefficient showed that such optimizations lead to a marginal reduction of the downtime. The other parameters of the sensitivity study did not show as much dynamic response dependency as the floater length and the inertia coefficient. These other parameters are not expected to lead to the objected reduction of the downtime either. Continuing optimizing the Tidal Bridge design in the mass and stiffness parameters would not lead to the objected reduction of the dynamic response, and hence, the objected reduction of the downtime.

The obtained knowledge about optimizations in mass and stiffness gives the possibility to refine the thesis scope. Initially, the thesis scope included additional structures or modifications to the original design as ways to achieve dynamic optimizations. Now it is known that an optimized balance between mass and stiffness does not lead to the objected performance, the design scope can be narrowed to look for additional structures that optimize the dynamic response of the Tidal Bridge.

Chapter summary

This chapter starts with an exploration of dynamic response of the original Tidal Bridge design. The original Tidal Bridge design has a downtime of 23.4 days based on a 50% confidence interval. The combined acceleration limit shows to be the governing limit over the maximum roll displacement limit. The sway accelerations have the largest contribution in the combined acceleration limit. The influence of the turbines is significant in the dynamic response and a Tidal Bridge design without turbines would have a downtime of 0 days per year. The wave direction is not relevant in the dynamic response of the Tidal Bridge. Furthermore, a qualitative analysis of the influence of the tidal currents suggests that the current related drag forces stabilize the dynamic response of the Tidal Bridge.

After the exploration of the dynamic response, the chapter continuous to analyze the balance in mass and stiffness and tries to find optimizations in the mass and stiffness parameters. The chapter shows that the Tidal Bridge structure is mass dominant. Consequently, the sensitivity analysis proved that the floater length is the most sensitive parameter in the structural dynamics model. An attempt to optimize this parameter showed that the downtime hardly reduces[2], and the conclusions is drawn that optimizations do not lead to the objected reduction of the downtime. The thesis scope excludes modifications to the original design as a way of reducing the downtime and the design should focus on an additional structure.

[2] A maximum reduction of the downtime was found in the order of 1-2 days.

5 | First design loop: qualitative design

This chapter follows upon the analysis to the dynamic response of the original Tidal Bridge design. This chapter starts the design process with the first of the three design loops. This chapter develops, verifies, evaluates and selects concepts. The concepts are found with a brainstorm process and describe a working principle that may eventually lead to a design after the two subsequent design loops. This chapter delivers three concepts that are developed into alternatives in the next chapter.

5.1 Developing the concepts

5.1.1 The starting point: the original design

Figure 5.1 shows the original two-dimensional design that forms the starting point for the creative process of the brainstorm. This design finds some source of dynamic mitigation in drag and radiation damping of the floater and the turbine. The concepts automatically benefit from this inherent type of dynamic reduction. The new ideas for the original design are represented with an orange colour in the upcoming figures.

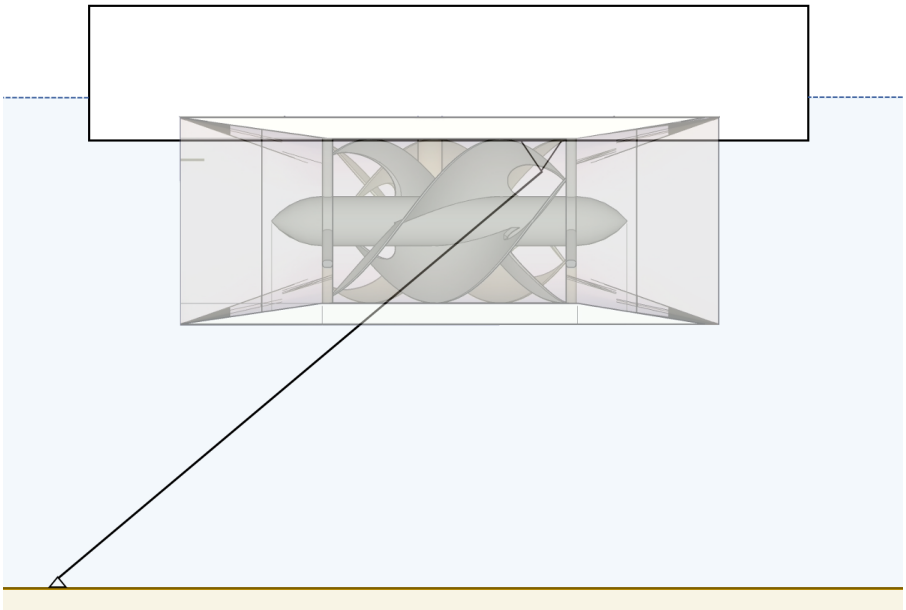

Figure 5.1 The original design without any damping measures

5.1.2 Defining the preferred working principle

The preferred working principle of the additional structure that mitigates the dynamic response may be found in either additional inertia or the dissipation of energy. The Tidal Bridge system shows to be mass dominant, which means that the driving forces are found in the inertia forces of the waves. Mitigation solutions that focus on this mass dominance, like additional weight, is expected to be an effective solutions. Another preferred

working principle is found in the dissipation of energy. A system which contains less energy is kinetically less active and has a smaller amplitude. Both solutions would be most effective if those are focused on the limiting degree of freedom of sway. However, a reduction of the dynamic behaviour of any degree of freedom is spread over the other degrees of freedom due to the strong coupling. Although the dynamic optimization is divided over all the degrees of freedom, the sway degree of freedom benefits somewhat from the dynamic reduction as well.

5.1.3 Brainstorming of concepts

The acquainted knowledge of the problem definition and the preferred working principle form the foundation of the creative process of exploring concepts ideas, which is also called the brainstorm phase. In this phase, concept ideas may lead to finding other and new concept ideas. Concepts that may be costly, sensitive to much maintenance, not durable or not satisfying any other requirements are presented below as well. Those may contribute and boost the creative process of finding new concept ideas that may be similar to the those concepts which are not feasible. Some concept ideas are based on reference projects that applied the same working principle. These reference projects are mentioned within the concept motivations.

The most interesting ideas have been worked out in a two dimensional sketch. The sketches give an idea of how the concept could be integrated within the original design and how the concept could be effective in mitigating the dynamics of the Tidal Bridge. A complete overview of the concept sketches is found in Appendix E. Some concepts have been presented below in Figure 5.2 to show how the concepts have been worked out in Appendix E.

Concept	Concept description	Concept	Concept description
1	Submerged spring-damper in pendulum	10	Wave energy air absorber
2	Emerged spring-damper in pendulum	11	Air cushion
3	Rotational damper at upper pendulum hinge	12	Rotating deck
4	Second pendulum and damper on same anchor	13	Translating deck
5	Two anchors, pendulums and dampers	14	Semi-submersible floater
6	Two anchors, two damped tethers	15	Bilge keel
7	Tuned mass damper	16	Heave plate
8	Slosh damper	17	Sway plate
9	Tuned liquid column damper		

Table 5.1 The selected concepts that have been worked out all in two dimensional sketches in Apppendix E.

5.2 Qualitatively verifying of the concepts

A qualitative verification to the requirements follows upon the brainstorm phase. This qualitative verification initially filters the concepts that do not fulfill the requirements specified in Section 2.1. Hereafter, the qualitative verification consists of a scoring process to the evaluation criteria of the realistic concepts that tries to select the concepts that have the most potential to become the final design.

The subsections below discuss requirements that the concepts should have in order to continue to the scoring process of the qualitative verification. The requirements used for the verification are: constructability, structural integrity, project scope, and computability.

5.2.1 Verifying to the constructability

The requirement of constructability verifies whether the concept is constructable with readily available machinery. Furthermore, it checks whether the needed construction parts are readily available by sub-contractors. Concepts that may be highly complicated to construct, should not be taken into consideration to keep the concept simple and risks far away.

Concept 3, 4 and 5 are not considered to be constructable. Concept 3, the rotational damper, needs a very high torque rotational damper which do not exists. Concept 4, second pendulum with damper on the same anchor, and concept 5, two additional pendulums with dampers with one additional anchor, need dampers that should adapt to the tidal difference of three meters. Those types of dampers do not exists either.

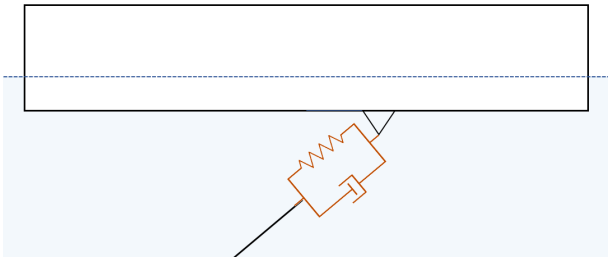

(a) [Concept 1] Submerged spring-damper combination engineered within the pendulum

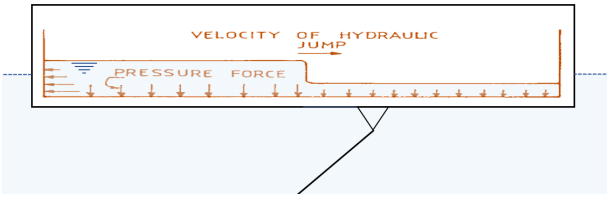

(b) [Concept 8] Slosh damper

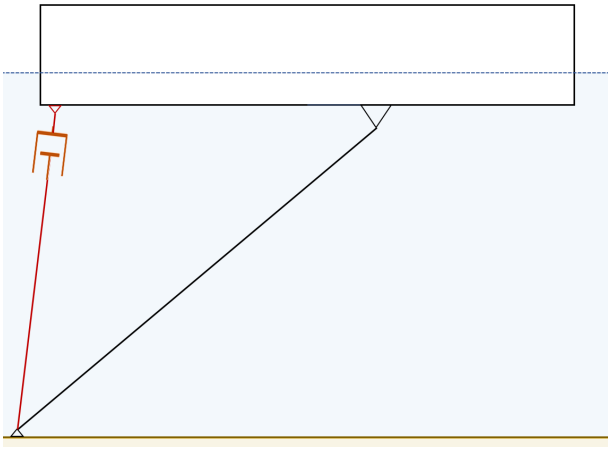

(c) [Concept 4] Second pendulum and damper on the same anchor

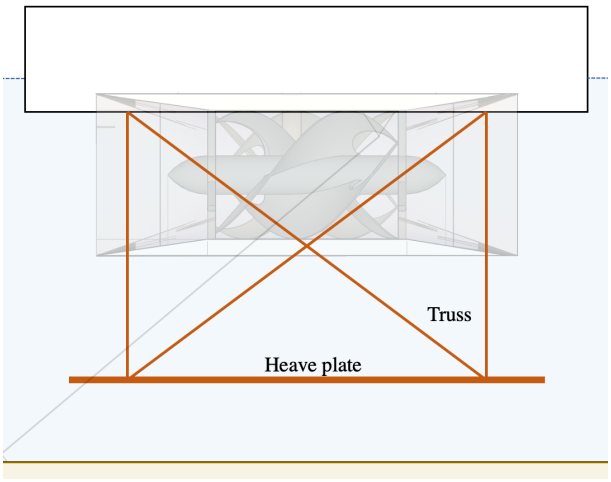

(d) [Concept 16] Heave plate

Figure 5.2 A selection of concept designs

5.2.2 Verifying to the structural integrity

The requirement of structural integrity checks whether a concept is inherently strong, stiff and stable enough. The strength and stiffness of a concept can in general be adapted by profile, material, or structural scheme modifications. However, stability problems are more complicated to overcome.

Concept 6 and 11 are considered to be unstable. The tethers of concept 6 are dynamically unstable in the tidal currents in the Strait of Larantuka. Flutter can happen and the generated dynamic movements could hinder comfortable usage. Concept 11 is considered to be unstable in the roll direction due to the air cushion that hinders pressure differences. A boat is stable in the roll direction due to changing pressures underneath the boat its bottom plate as a reactive force for roll movements. Parts of the boat that stick deeper in the water experience larger buoyancy forces. However, concept 11 does not generate a pressure difference upon rolling that counteracts the rolling motion by the air that evenly distributes the pressure at all times.

5.2.3 Verifying to the design scope

Concept 14 is considered to have a different solution strategy that does not comply with the project scope. Concept 14 may be an effective solution to mitigate the dynamics of the Tidal Bridge. However, this concept is an optimization within mass and stiffness of the system. The concept also affect the original Tidal Bridge design too much.

5.2.4 Verifying to the computability

The concept should be computable with the used structural dynamics model of this project in order to quantify the effectiveness. Concept 15, the bilge keel concept, is not considered to be computable with the available structural dynamics model. The working principle of the bilge keel concept is found in pressure differences below and above the bilge keel and dissipation of energy through the turbulence around the keel. The available structural dynamics model would not be able to compute accurately a solution to this problem.

5.3 Evaluating the concepts

The collection of the concepts has been refined by filtering out all concepts that do not satisfy the requirements of Section 2.1. An evaluation follows upon the verification. The evaluation is executed with a multi criteria analysis (MCA). This is a tool that can be used for the evaluation by scoring the concepts.

5.3.1 The relevant evaluation criteria

A MCA is a powerful analysis methodology that helps to evaluate the concepts. The MCA takes as input: the selection of concepts, the selection of evaluation criteria and a defined importance that relate to the evaluation criteria. The person using the MCA gives a score that varies between 0 and 5 for each concept and evaluation criteria combination. After multiplying the scores with the relative importance of the evaluation criteria, a total score can be calculated. The best concepts show up with the highest score. The importance have qualitatively been determined based on the relative importance of the evaluation criteria.

The evaluation criteria are derived from Section 2.2. The explanations of the used evaluation criteria are specified below and sorted on the given importance as well:

- **Sway effectiveness:** How well would the concept suppress sway motion?
- **Roll effectiveness:** How well would the concept suppress roll motion?
- **Heave effectiveness:** How well would the concept suppress heave motion?
- **Maintainability:** How well can the concept be maintained? How much maintenance is the concept going to need?
- **Simplicity**: Does the concept have mechanical parts? How complicated are the involved physics?
- **Forcing variability:** How well can the concept perform under different excitation frequencies and amplitudes?
- **Adaptability**: After the deployment, how well can the concept be adapted and improved to the situation of the project site or to the situation of changing environmental conditions?
- **Sustainability and durability**: How durable is the concept? How much materials are needed for the concept its lifetime and can the materials be recycled after usage?
- **Pendulum forces**: How are the pendulum forces be affected? Are the expected pendulum forces expected to become larger or smaller?
- **Aesthetics** How does the new concept influence the aesthetics of the Tidal Bridge?

5.3.2 Neglecting the cost in the evaluation

The cost have not been taken into account in the quantitative evaluation of the concepts. The cost are evaluated later in the process as those are of such significant importance to civil engineering projects. In general, the client is looking for a solution that scores best on the ratio that represents the most functionality per dollar. If a solution is more functional but proportionally less functionality per dollar, then this solution may be discarded in order to choose for the concept that has most functionality per dollar. Obviously, solutions that do not fulfill the minimum requirements are not considered by the client.

		Sway effectiveness	Roll effectiveness	Heave effectiveness	Maintainability	Simplicity	Forcing variability	Adaptability	Sustainability and durability	Pendulum forces	Aesthetics	Total
	Importance	22%	13%	13%	11%	11%	7%	7%	7%	7%	4%	**100%**
1	Submerged spring-damper in pendulum	4	4	4	0	1	5	1	1	5	5	**3,0**
2	Emerged spring-damper in pendulum	4	4	4	0	1	5	2	1	5	0	**2,9**
7	Tuned mass damper	5	2	0	3	4	0	3	2	3	5	**2,8**
8	Slosh damper	4	3	0	5	5	0	5	5	3	5	**3,4**
9	Tuned liquid column damper	4	2	0	4	4	0	4	4	3	5	**2,9**
10	Wave energy air absorber	0	2	2	4	2	3	4	4	3	2	**2,2**
12	Rotating deck	0	5	0	1	1	2	2	2	3	3	**1,6**
13	Translating deck	5	0	0	1	1	2	2	2	3	3	**2,0**
16	Heave plate	0	4	5	5	5	5	1	4	3	5	**3,3**
17	Sway plate	5	3	0	5	5	5	1	4	0	5	**3,4**

Table 5.2 Multi Criteria Analysis scoring sheet that suggest which concepts should be chosen as results for the first design loop.

5.3.3 The MCA results

The results of the multi criteria analysis can be observed in Table 5.2. The relative importance of the evaluation criteria is displaced right below the evaluation criteria. All concepts have a number which is complementary to the concept numbers that are specified right below the concept sketches. The weighted scores are given in the most rightward column. The table shows that the three concepts have a relatively high score. These concepts are the: slosh damper [8], heave plate [16] and sway plate [17]. These three concepts are chosen to be the result of the first design loop. The three concepts will be developed further into alternatives in the next design loop.

Summarizing the first design loop

Concepts have been developed in this chapter from (brainstorm) ideas and reference projects. The concepts have been verified to the requirements of constructability, structural integrity, design scope, and the computability. The concepts that passed this verification phase have been evaluated to the evaluation criteria. The evaluation has been executed with a multi criteria analysis. The results of the qualitative scoring showed that the three best concepts are the slosh damper concept, the heave plate concept and the sway plate concept. These concepts are chosen to be worked out quantitatively into alternatives in the second design loop of the next chapter.

6 | Second design loop: quantitative design

This chapter develops alternatives from the three chosen concepts in this second design loop. The chosen concepts are developed into alternatives which have geometry and mass such that those can be tested with the structural dynamics model. The results of the model is used to verify the dynamic response. The alternatives that perform well enough are selected to continue with in the third design loop.

6.1 Developing alternative 1: the slosh damper

The slosh damper is the first concept that if designed further into an alternative. The functionality of the slosh damper is to be found in the transfer of energy from the main structure into the mass of the water body of the slosh tank. The mass of the slosh water resonates upon the main structure's excitations and moves out of phase with a difference of 90 degrees. This out of phase movement of the slosh water mass counteracts the movements of the main structure. Furthermore, energy is dissipated from the slosh water mass by flow damping objects within the slosh damper.

A just tuning of the slosh damper is important to find the desired effect around the critical excitation period of the main structure. The tuning of the slosh damper can be controlled by: the slosh water mass, slosh tank geometry and the flow damping objects.

This section motivates the those chosen slosh damper tuning characteristics. The details of this section can be found in Appendix F.1.

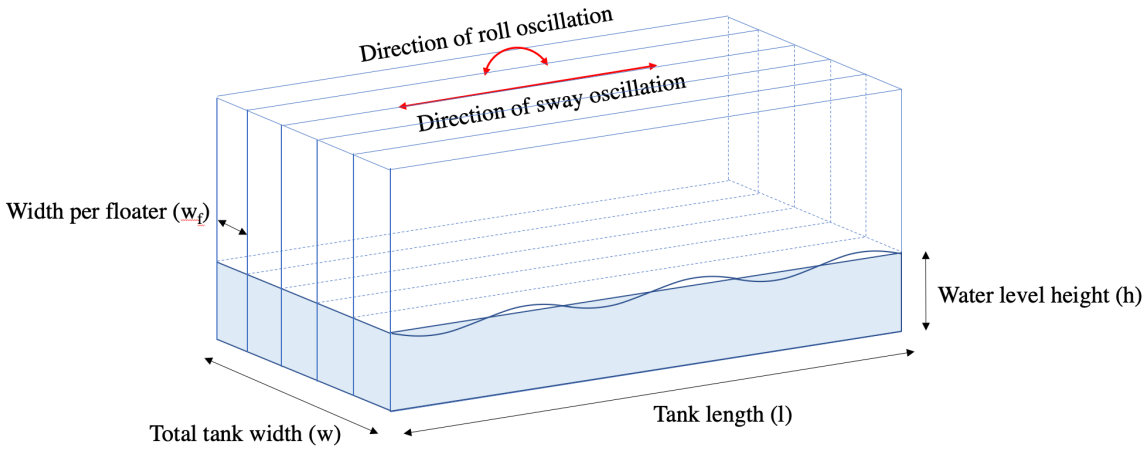

Figure 6.1 The slosh tank dimensions and its orientation relative to the sway and roll oscillations

6.1.1 Formulating additional requirements

The slosh damper tuning characteristics should be carefully chosen such that the effectivity of the slosh damper suits the needs of the Tidal Bridge. The slosh damper alternative starting points are defined as follows:

- The damper should have a natural sloshing period of 4.3 seconds as this period compromises with the critical period of Tidal Bridge structure for sway and roll.
- The slosh tank should fit in the floaters.
- The slosh tank length is preferably as long as possible to mitigate roll rotations better.

6.1.2 The chosen alternative variables

The motivation for the chosen slosh tank tuning characteristics is elaborately described in Appendix F.1. The most important conclusions of this Appendix is summarized below:

- **Subdivision over the floaters:** The total width of the slosh tank as specified in Figure 6.1 is split into five slices. Those slices are placed within the five floaters to distribute the damping forces equally over the Tidal Bridge floating elements.
- **Water mass:** The slosh tank water mass is determined to be 175.000 kg. This is about 5% of the total mass of the Tidal Bridge floating element together with the added mass in the sway direction.
- **Water level height:** The maximum water level height is determined to be 2 meters in order to avoid counteractive effects within the slosh tank upon large slosh water excitations.
- **Tank length:** The total tank length is determined to be 8.9 meters based on the preferred sloshing period of 4.3 seconds, the preferred water level height, and linear wave theory.
- **Flow damping objects:** Poles have been chosen as flow damping objects. The forces that the poles exert on the water mass can be evaluated well with Equation 3.2. A frontal surface area of the poles has been set to 15 m^2. This results in a reduction of the displacements by a factor two after five oscillations.

These slosh tank tuning characteristics form alternative 1. Figure 6.2 shows a top view of the slosh tank alternative integrated within the floaters.

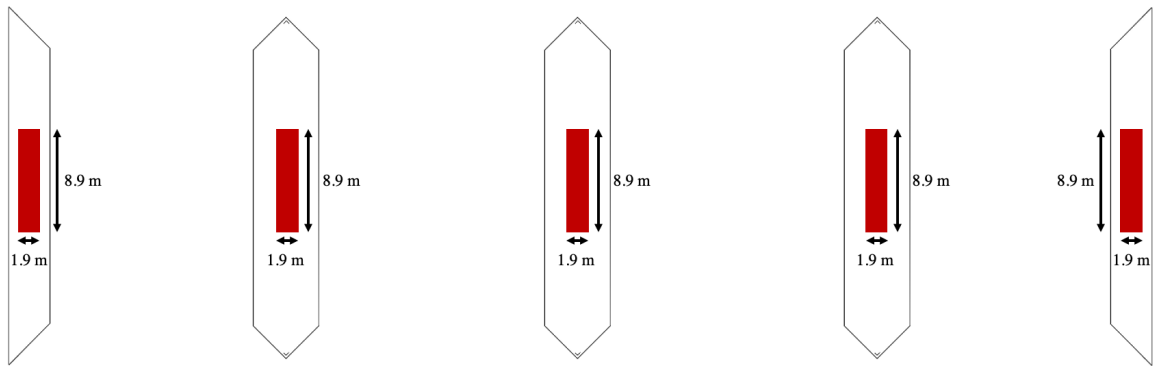

Figure 6.2 Top view of one Tidal Bridge element with five small slosh tanks of which each small slosh tank is placed within each floater.

6.1.3 Modelling the alternative with the structural dynamics model

An elaborate explanation of the used approach to model the slosh tank in the structural dynamics model has been explained in Appendix F.1.1. The movement of the water within the slosh tank has been simplified to a point mass that moves along a frictionless trajectory. This point mass is excited by the Tidal Bridge roll displacement, and the sway, heave and roll accelerations. This point mass starts to move and exerts forces on the Tidal Bridge structure as well. These forces mitigate the dynamic behaviour of the Tidal Bridge.

6.1.4 General characteristics of the slosh damper

- **Construction method:** The slosh tanks can be installed within the floaters while the floaters are constructed. The slosh tanks may be filled with water at any time in the construction process that suits the needs well as stability has not become endangered.

- **Adaptability:** The slosh tanks may be filled with more or less water to tune the sloshing period to the needed damping period.

- **Draught:** The draught of the Tidal Bridge design increases with about 20 centimetres to a draught of about 2.30 meters. This additional draught does not lead to problems in the construction method or stability of the Tidal Bridge structure.

- **Stability:** Appendix F.1 shows that the floating stability is reduced for the situation with the slosh damper. However, the GM distance still has a value of 39 meters which ensures much redundancy to eccentric forces.

- **Distribution of forces:** The division of the slosh damper in smaller slosh dampers over the floaters can result in three dimensional forces on the Tidal Bridge floating element. The slosh dampers may not excite in phase due to a three dimensional excitation of the Tidal Bridge. Due to the character of the slosh damper to follow the excitations, this is probably not going to lead to problems.

6.2 Developing alternative 2: the heave plate

The heave plate is the second concept that is designed further into alternative 2. The effectiveness, the material need and other evaluation criteria that may be decisive in the evaluation process of the heave plate are yet unknown. The second alternative becomes developed further in this section. The details of this section can be found in Appendix F.2

6.2.1 Heave plate characteristics

Main working principle

Appendix F.2 shows that the main working principle of the heave plate is to be found in the additional added mass that the plate generates. The other forcing type, the drag forces, do not significantly contribute to the mitigation of the dynamic characteristics. Therefore, the design of the heave plate should be focused on generating as much added mass as possible with taking the defined requirements, boundary conditions and evaluation criteria into account.

Wave influences

The heave plate has a forcing interaction with the waves induced by differences in the velocity or accelerations in the vertical plane. The velocities and accelerations of the water particles in the vertical plane due to waves reach zero at the bottom. A heave plate that is engineered as close as possible to the bottom is less subjected to the wave forcing.

Keel clearance

It has already been stated that the wave forcing becomes smaller closer to the bottom. However, the heave plate may not touch the bottom as this would lead to peak forces in the heave plate structure which it is undesirable. Therefore, the heave plate has a minimum keel clearance. This minimum keel clearance depends on the extreme heave and roll displacement, to the tidal difference and to a certain margin.

The maximum heave displacement is 1.3 meters and the maximum rotation is 0.19 rad for a loading condition that has a return period of once in 1000 years. The maximum tidal difference is 1.5 meters relative to MSL. An adequate added margin is estimated to be 1.5 meters. The minimum keel clearance should be 7 meters for a neutral tidal position. Appendix F.2 shows the order of reduction of a heave plate that takes values of 40%. The keel clearance may become less upon having smaller heave displacements and roll rotations. A safe minimum keel clearance could therefore be estimated to be 5 meters.

Proposed geometry

The alternative geometry consists of the plate dimensions and the vertical location of the plate with respect to the main structure. The heave plate is preferably constructed as close as possible to the bottom concerning the effectivity. From a structural and material need point of view, the heave plate is preferably constructed as close as possible to the floater. The heave plate alternative is constructed close to the bottom to find out the maximum potential effect since the effect of the plate increases closer to the bottom.

In line of finding the largest possible effect of the heave plate, the outer plate dimensions will also be given large values. The alternative heave plate will have a length of 98 meters and a width of 30 meters.

The proposed conceptual design dimensions and keel clearance can be observed in Figure 6.3 and 6.4.

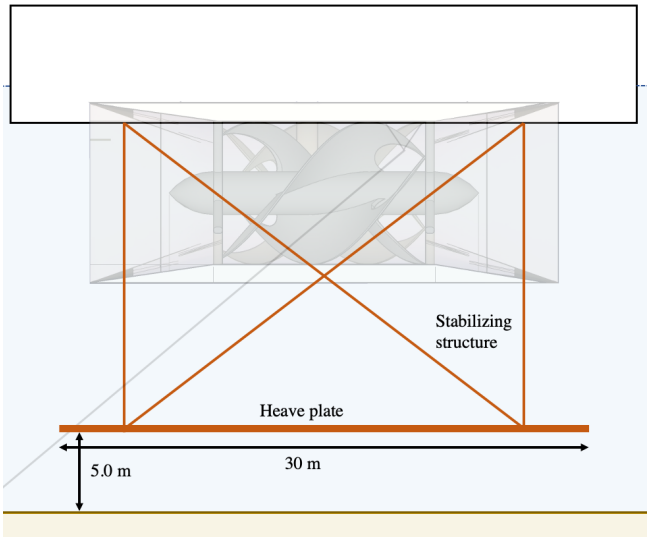

Figure 6.3 Visualization of the width and the height of the heave plate

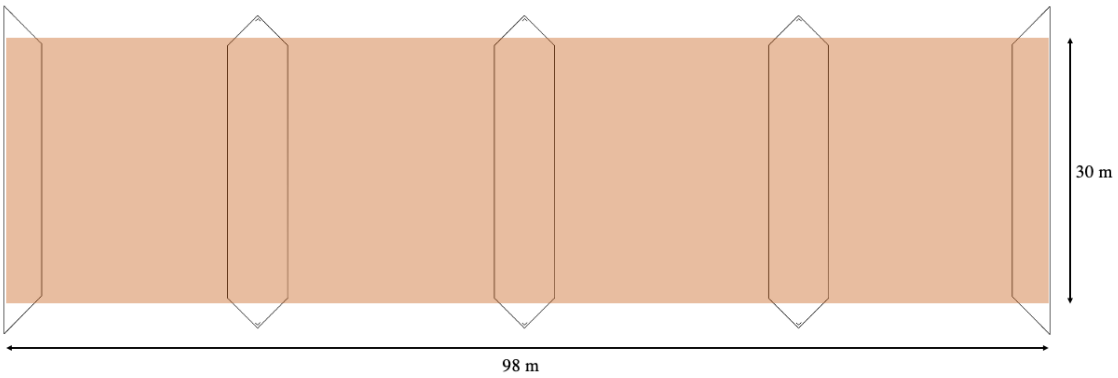

Figure 6.4 Visualization of the length and width of the heave plate

Modelling the heave plate in the structural dynamics model

The alternative of the heave plate may be programmed in the structural dynamics model by making use of the Morison Equation as specified with Equation 3.2 before. The heave plate surely has interference effects with the bottom as described in Section 3.2.7. The heave plate of this alternative will be modelled without the additional experienced added mass due to the bottom effects. The expected effectivity of the alternative may turn out lower than it should be. With such an approach, the effectivity could only turn out positively farther in the design process.

Considering porosity for the heave plate

For small KC numbers, the porosity of the heave plate may lead to an increased damping. However, the added mass coefficient may reduce with too much porosity, which makes the effect of pores in heave plates to become uncertain and therefore unattractive. There may be an optimal porosity of the heave plate to increase damping before the added mass coefficient significantly reduces (Tao & Dray, 2008). A research to the most optimal porosity is out of scope of this design report.

Evaluating of material need

The structure that mitigates the dynamic behaviour of the Tidal Bridge needs preferably as little material as possible as a steel need has an impact to the environment and to the project cost. The expected total cost of the solution with the least material need is generally also the smallest.

Structurally, the heave plate alternative is not optimized concerning the material need. The transfer of loads to the turbines is not possible following the requirements specified in Section 2.1. The forces of the heave plate alternative need to span the space between the floaters of at least 19 meters to transfer the heave plate forces to the main structure. Additional material is needed for the structural elements that transfer the forces over this distance.

A creative process may lead to heave plate designs that need less materials to ensure the structural integrity while generating a lot of added mass. Such creative designs lead to a comparable effectiveness and may reduce the material need of the structure. Such creative designs may be found in the next design loop only if the heave plate alternative shows enough effectivity in the verification phase of this design loop.

6.3 Developing alternative 3: the sway plate

The sway plate is the third concept that is designed further into alternative 3. The sway plate is an all new brainstorm design idea that has not been seen in reference projects yet. The sway plate combines the idea of a heave plate and a bilge keel. The sway plate brainstorm design consists of a plate below the Tidal Bridge structure that is directed perpendicular to the wave and current direction.

This section focuses on physical and theoretical characteristics of the sway plate to figure out the feasibility and the effectiveness of a sway plate alternative. The effectiveness of the sway plate alternative is researched with the structural dynamics model in latter sections.

The details of this section may be found in Appendix

6.3.1 Sway plate characteristics

Main working principle

The main working principle of the sway plate is closely related to the working principle of the heave plate. The added mass is mostly responsible for mitigating the dynamic behaviour as shown in Appendix F.3. The forces related to the additional added mass of the sway plate are much larger than the drag forces generated by the sway plate. Furthermore, the added mass is directly related to the combined acceleration limit of the Tidal Bridge, as more inertia leads to smaller accelerations. An effective sway plate alternative focuses on generating much added mass. The maximum sway plate dimensions are restricted by the available space between the minimum keel clearance, the turbines and the length of the floating element.

Minimum keel clearance

The keel clearance of the sway plate alternative is preferably as small as possible for several advantages. At first, a larger height leads to a larger added mass which forms the main working principle of the sway plate. The added mass scales quadratically with the height as this length is shorter than the width. Secondly, a lower placed sway plate results in a larger lever arm to the centre of gravity of the main structure. The sway plate can more effectively counteract roll rotations with this larger lever arm. Thirdly, the horizontal particle movements due to the wave excitations are smaller closer to the bottom. The sway plate is less probable to add energy to the system instead distribute the energy over more added mass.

The smallest keel clearance may be found for a sway plate placed in the middle of the structures to makes sure that roll rotations of the main structure do not push the sway plate closer to the bottom. The keel clearance is dependent on the maximum heave displacement (1.3 m), the maximum tidal amplitude (1.5 m),

and an additional margin (1.5 m). The recommended keel clearance is 4.3 meters by adding those contributions. An estimation of the reduced maximum heave displacement by the effect of the sway plate is not taken into account in this calculated minimum keel clearance. This reduced maximum heave displacement is unsure as this only happens by the coupling in the system.

Investigating the combination of sway and roll displacements

An unintentional dynamic mode of sway and roll displacements could lead to a net-displacement of the sway plate close to zero. Such a sway and roll displacement is displayed in Figure 6.5 and would not lead to a mitigation of the dynamic behaviour of the Tidal Bridge. The effectivity results of the sway plate alternative of the next section will show if this may happen to the sway plate alternative.

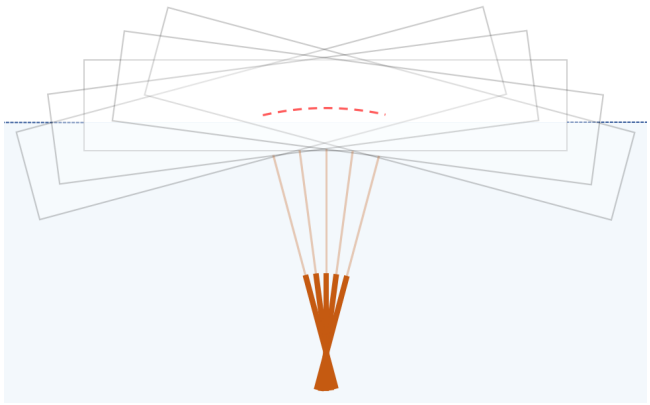

Figure 6.5 Awkward sway and roll displacement combination undoing the effectiveness of the sway plate

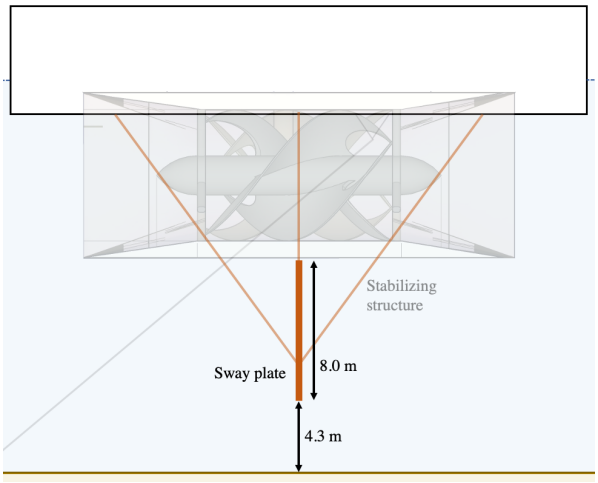

Figure 6.6 Side view of the sway plate concept design

Modelling the sway plate in the structural dynamics model

Integrating the sway plate within the structural dynamics model has many similarities with the integration process of the heave plate within the model. The Morison Equation, as specified in Equation 3.2, translates the waves into forces onto the sway plate.

Estimating the new pendulum hinge location

The sway plate gives the structure a permanent rotation by the current-related drag forces. The rotational equilibrium of forces is unbalanced upon adding or changing a structure which influences this balance. This permanent rotation due to the rotational imbalance of forces can be counteracted by moving the hinge location further away from the centre of the floaters.

6.3.2 Choosing the alternative dimensions

Realistically large dimensions are proposed for the sway plate alternative to anticipate to the working principle of the added mass. Also, a clear understanding of the order of magnitude of the maximum of effect of the sway plate may be obtained with large dimensions of the alternative. The length of the sway plate is restricted by the length of one Tidal Bridge floating element. The height of the sway plate is restricted by the keel clearance and the available space below the turbine. The the sway plate length and height are therefore respectively determined to be 98 meters and 8.0 meters. A visual representation of this sway plate alternative may be observed in Figure 6.6 and 6.7.

Evaluating the pendulum forces

The sway plates could be interpreted as larges sails hanging below the Tidal Bridge structure. These sails enlarge the blockage effect of the total Tidal Bridge structure such that the tidal currents become more hindered to freely flow through the Strait of Larantuka. This has two disadvantages and one advantage.

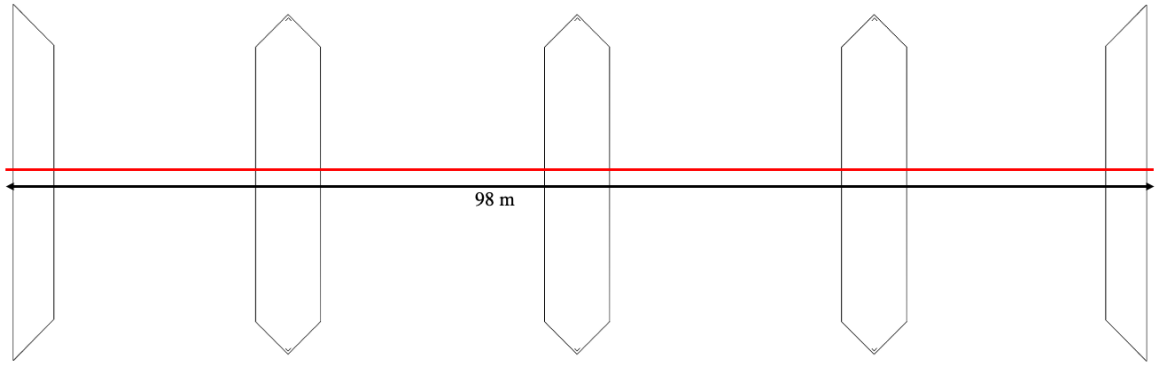

Figure 6.7 Top view of the sway plate alternative

The first disadvantage is that these sails lead to larger pendulum forces. Hence, the pendulums need more structural capacities and become more expensive to resist those additional horizontal forces. This additional force is calculated to be about 34% of the maximum calculated pendulum force following Appendix F.3.1. A pendulum force increment of 34% is a significant increase, but this increment is not insurmountable. The second disadvantage is that the tidal currents will find there way more around the floating part of the Tidal Bridge and look for ways with less resistance closer to the shore. The tidal currents closer to the shore become larger and shore erosion is more prone to happen. The advantage of those sails is that the energy yield of the turbines rises. With these sails, the working principle of the turbines become more driven by a head loss instead of harvesting energy from the momentum of the flow.

Evaluation the material need

Ideally, the alternative needs as little material as possible to reduce the impact to the environment, the material cost, and the construction cost as explained in Section 6.2.1. The alternative has not been optimized yet to reduce the material need. The sway plate alternative needs less material compared to the heave plate alternative. The material need of the plate of the sway plate alternative is just 27 % of steel need of the plate of the heave plate alternative.

6.4 Verification of the alternatives

6.4.1 Exploring the performance of the alternatives

The performance of the three alternatives is verified with the structural dynamics model as developed in Chapter 3. The performance of the alternatives needs to be sufficient enough to be developed further into specific variants in the third design loop. The performance is verified in the first part of this Section and a conclusion is drawn based on the reviewed dynamic performance.

Slosh damper alternative

Figure 6.8 shows the region in which the total serviceability limit of 0.7 m/s^2 is exceeded for two alternatives of the slosh damper alternative. The slosh damper alternative which has a mass of 10% relative to the structure mass showed very minor improvements of the dynamic behaviour of the Tidal Bridge. Therefore, a slosh damper alternative with a mass of 30% relative to the Tidal Bridge mass has been modelled in the structural dynamics model as well to find an improved effect. The effect of the slosh damper alternative with 30% mass shows a small improvement compared to the alternative with a relative mass of 10%.

Both slosh damper alternatives have been tuned to the critical period of 3.9 seconds. This critical period is defined by the wave period where the lines of the wave characteristics and the serviceability limit cross each other. An improvement of the dynamics around this period would directly lead to a reduction of the downtime. The results show that the largest effect of the slosh damper tuned to 3.9 seconds is found around 4.3 seconds. The expected corresponding downtime of the two slosh damper alternatives is displayed in Table 6.1.

The slosh damper should theoretically be effective for the modelled regular waves. Possible reasons that may have lead to the disappointing effectivity of the slosh damper:

- **Numerical problems:** The numerical integration of the slosh damper may have been dysfunctional for an unknown reason. The slosh damper did not reach the expected functionality, although positive checks have been performed to verify the correctness of the time step, the slosh water kinematics, and the corresponding forces on the structure.

- **Too much damping:** The relatively low horizontal amplitude of 1 meter diminishes by a factor two after five free oscillations due to the applied 'numeric' damping. This amount of damping may be too much for the water mass to start resonating with large amplitudes. Large sloshing amplitudes are needed to generate a significant damper force. However, these large sloshing amplitudes may lead to a counteractive effect as the slosh water touches the slosh tank ceiling.

- **Coupled degrees of freedom:** The sway degree of freedom is strongly coupled to the heave and roll degrees of freedom by the pendulum. This coupling may lead to a dynamic response which does not satisfy the regular sinusoidal response which is normally used to prove the slosh damping concept. Hence, the coupled dynamic response of the Tidal Bridge does not suit the needed response to 'activate' the slosh damper well.

These possible reasons have not been validated. The correct reason for the disappointing functionality of the slosh damper may not be listed in the itemization above.

Heave plate and sway plate alternative

Figure 6.8 shows the positive effect on the dynamic behaviour of the Tidal Bridge of the heave plate and sway plate alternatives. The serviceability limits are exceeded for larger wave heights compared to the base case result. Hence, the downtime is reduced and the alternatives show that variations may lead to fulfilling the design objective. Table 6.1 shows the number of days that the Tidal Bridge needs to be taken out of service with the alternative. The table shows that both alternatives do not realize enough effectivity to meet the design objective of a maximum downtime of five days. Variants of these alternatives may be promising in an enhanced effect.

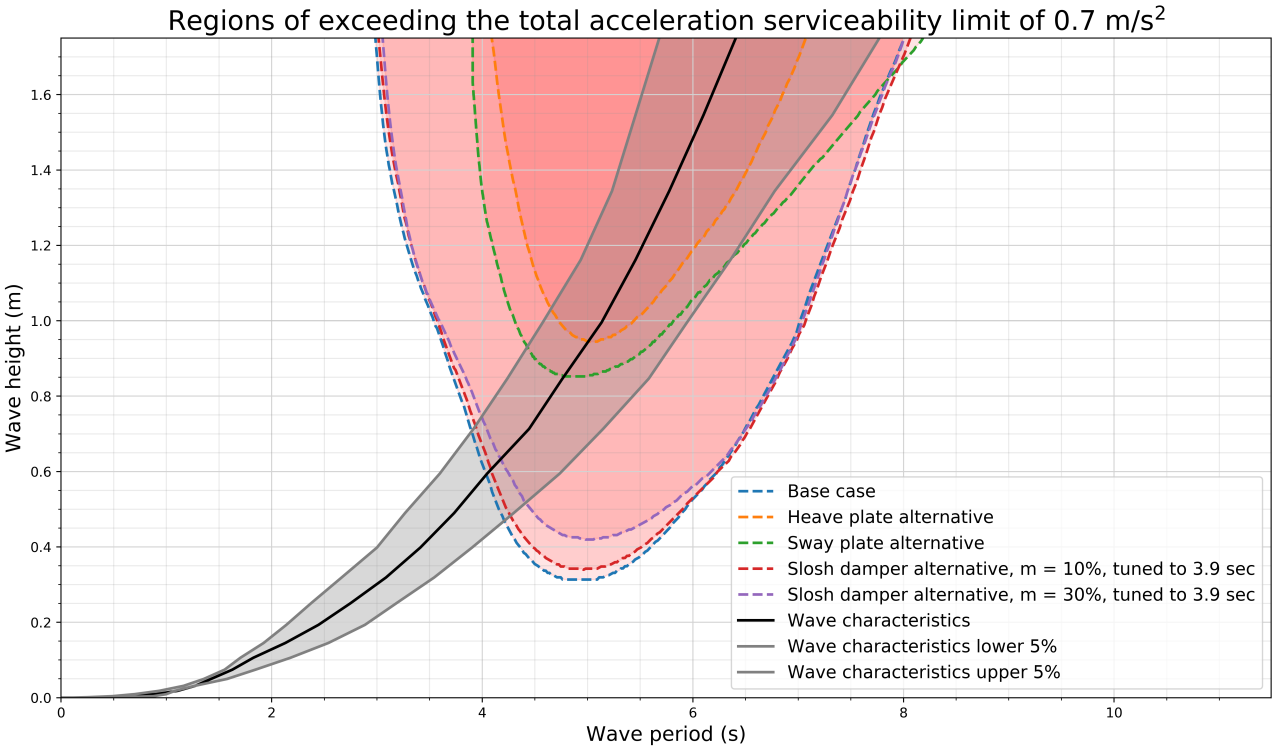

Figure 6.8 Regions of exceeding the serviceability limit for the three alternatives and the base case

	Probability		
	95%	**50%**	**5%**
Base case	31.6	23.4	16.3
Slosh damper alternative 10% mass	30.5	21.8	15.4
Slosh damper alternative 30% mass	28.5	19.5	12.2
Heave plate alternative	12.7	6.1	0
Sway plate alternative	16.7	8.7	0.5

Table 6.1 Yearly downtime in days for the three alternatives and the base case

6.4.2 Conclusion of the slosh damper alternative

The slosh damper does not prove to be a solution that could lead to the objected reduction of the downtime. The total reduction of both slosh damper alternatives do not show enough dynamic reduction such that an optimized slosh damper may lead to fulfilling the design objective. Optimizations to increase the effect of the slosh damper alternative have already been applied to find an increased effectivity. The slosh damper is tuned to the critical wave period, the mass of the slosh damper has been increased and a numerical computation with very small time steps has been executed. Neither of those optimization strategies showed that the slosh damper reaches significant optimizations in the downtime of the Tidal Bridge. The slosh damper will not further be taken into account as a potential solution for the design objective.

6.4.3 Conclusion of the heave plate and sway plate alternative

The heave plate and the sway plate alternatives show to have a promising performance. Developed variants in a new design loop may potentially lead to meet the design requirements. Optimizations that focus on performance and a reduced material need may lead to a variant that satisfies the design objective.

Summarizing the second design loop

This design loop developed the chosen concepts of the slosh damper, the heave plate and the sway plate further into three alternatives that have dimensions and mass. The slosh damper alternative should theoretically be functional for the modelled regular waves. However, the structural dynamics model did not succeed in modelling the alternative with a satisfactory optimization in dynamic response of the Tidal Bridge. The performance of the slosh damper alternative lead to a reduced downtime of about 1.5 days, whereas the objected order of magnitude of the optimization should take values of 18 days. The heave plate and sway plate alternatives both had promising performances. These two alternatives are selected in this design loop to be developed further into variants in the next design loop of the next chapter.

7 | Third design loop: detailing the designs

This chapter develops variants from the two selected alternatives of the heave plate and the sway plate. The level of designing is going up to the level of a structurally checked design. The optimized dynamic response of the variants is tested with the structural dynamics model and verified to the design objective. The variants that satisfy the design objective are evaluated to the evaluation criteria by an MCA The design which scores the best to the evaluation becomes the resulting design.

7.1 Developing the variants

Variants are developed in this section from the selected two alternatives of the heave plate and the sway plate. The knowledge obtained in Chapter 3, 4 and 6 form the theoretical basis for development of variants from the alternatives. Initially, variants for the heave plate alternative are developed and explained. Afterwards, the variants for the sway plate alternative are developed and explained. The variants are supported with one overview figure and a table that specifies the most important numbers about the variant. The variants are detailed further with more figures in Appendix G.1.

7.1.1 Developing the heave plate variants

Variant 1: Lower heave plates

The heave plate of the heave plate alternative spans the large distance between the floaters in order to transfer its forces to the floaters. This span of 19 meters in the heave plate alternative makes the structure in need for much steel in order to ensure enough strength and stiffness over the complete span. The environment and the construction cost would benefit from a variant with smaller spans. This variant focuses on a reduced steel need while maintaining as much added mass as possible. A summary of the most important numbers may be found in Table 7.1.

The lower heave plates variant has three heave plates placed below the floaters as may be seen in Figure 7.1. The *height* of the heave plates is placed such that the added mass region does not overlap with the added mass region of the turbines while keeping a safe distance from the bottom. The *length* of the heave plates is comparable to the floater length such that the transfer of forces to the floater does not need large spans. The *width* of the plates is tuned such that the added mass region does not overlap with the turbines or with the bottom. A graphical motivation for this dimensions and the added mass plans of this variant may be found in Figure G.5. More figures about the variant have been supplied in Appendix G.1.1.

The variant has a reduced the steel need. However, the reduction of the downtime is 12 days and this should be at least 18.4 in order to fulfill the design objective. Another variant with a greater effectivity should be found.

Reduction of the downtime	12.1 days
Steel needed for four floating elements	833 tons
Generated added mass sway per floating element	-
Generated added mass heave per floating element	8453 tons
Depth of COG of added mass	18.8 m

Table 7.1 Important numbers for the lower heave plates variant

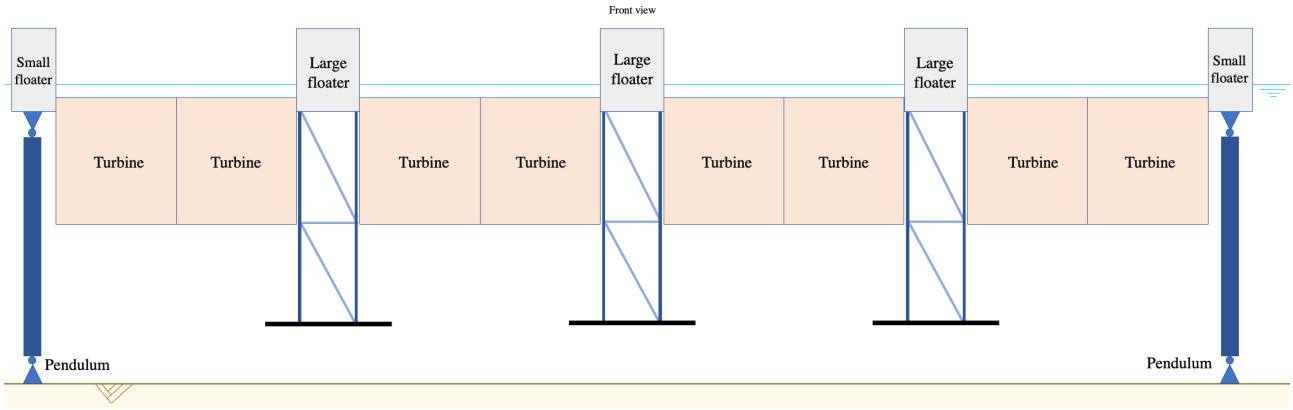

Figure 7.1 Front view of the lower heave plates variant

Variant 2: Upper heave plates

Figure 7.2 shows the upper heave plates variant. The upper heave plates variant tries to reduce the total material need like the lower heave plates variant. This variant makes use of the turbines to collaborate in generating the added mass. This variant also tries to trap the water between the upper heave plates and the floaters to generate added mass. Figure G.10 shows how the upper heave plates form one solid heave plate together with the turbines by a bottom view. The *height* of the variant is tuned to the bottom height of the turbines. The *width* and *length* of the upper heave plates is such that one large heave plate arises together with the bottom of the turbines. An added mass plan of this variant may be observed in Figure G.11. More figures about the variant have been supplied in Appendix G.1.2.

The upper heave plate variant does not need much steel. However, the effectivity is almost 12 days and this should be at least 18.4 days in order to reach the design objective. Another variant with a greater effectivity should be found.

Reduction of the downtime	11.9 days
Steel needed for four floating elements	426 tons
Generated added mass sway per floating element	-
Generated added mass heave per floating element	7907 tons
Depth of COG of added mass	11 m

Table 7.2 Important numbers for the upper heave plates variant

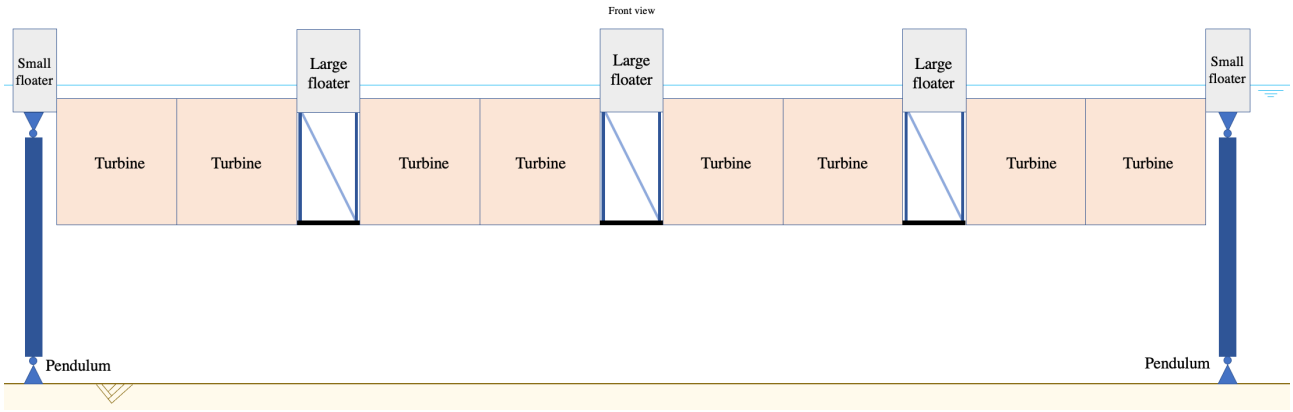

Figure 7.2 Front view of the upper heave plates variant

Variant 3: Heave plate 1 x 68 m

Figure 7.3 shows the heave plate 1 x 68 m variant. This variant shows much similarities with the original heave plate alternative. This variant is a bit shorter on both sides in order to free up space for the pendulums. This variant needs much more material compared to variant 1 and 2 as it spans the distance below the turbines like the original heave plate alternative. The advantage is that more added mass is generated with this variant compared to the other two preliminary heave plate variants.

The *height* of the plate is based on the minimum keel clearance of the heave plate. The length of the plate is the maximum *length* such that the point moment force below the main tubes is equal to the span moments between the main tubes below the turbines. The *width* is designed such that the plate would not touch the bottom with extreme heave and roll displacements.

The objected effectivity of 18.4 days less downtime is not reached by this variant that reaches a downtime reduction of 13.6 days. All preliminary heave plate variants did not show to be effective enough to reach the objected effectivity. More figures about the variant have been supplied in Appendix G.1.3.

Reduction of the downtime	13.6 days
Steel needed for four floating elements	1938 tons
Generated added mass sway	-
Generated added mass heave per floating element	16614 tons
Depth of COG of added mass per floating element	18.3 m

Table 7.3 Important numbers for the heave plate 1 x 68 m variant

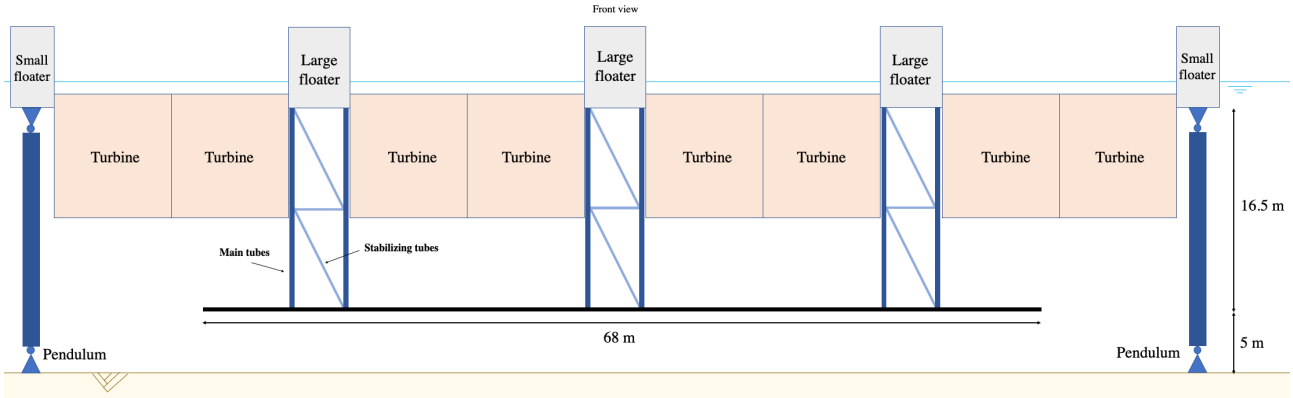

Figure 7.3 Front view of the heave plate 1 x 68 m variant

7.1.2 Developing the sway plate variants

Variant 4: Sway plate 3 x 17 m

Figure 7.4 shows the front view of variant 4. This variant is optimized for the material need. The spans below the turbines have been removed in order to avoid the large field moments within the structural elements below the turbines.

This variant tries to generate as much added mass as possible like the other variants. The added mass scales quadratically with the shortest length of the plate dimensions. The height of this sway plate is shorter than the width. Therefore, the *height* is tried to be kept as large as possible to lead to an increased effectivity. The *width* of the plate has been designed such that the point moment forces stay of acceptable values. The added mass in the sway direction of the turbines is not present below the turbines such that added mass region of the turbine and the sway plate do not overlap. An added mass plan for this variant may be observed in Figure G.22. More figures about the variant have been supplied in Appendix G.2.

The effectivity of this solution of 8.6 does not fulfill the optimistic objective of a downtime reduction of 18.4 days. However, this solution has the ability to be scaled up easily. The variants 5 and 6 are scaled up versions of this variant. The effectiveness of those variants grows with having more sway plates.

Reduction of the downtime	8.6 days
Steel needed for four floating elements	268 tons
Generated added mass sway	2576 tons
Generated added mass heave per floating element	-
Depth of COG of added mass per floating element	16.5 m

Table 7.4 Important numbers for the sway plate 3 x 17 m variant

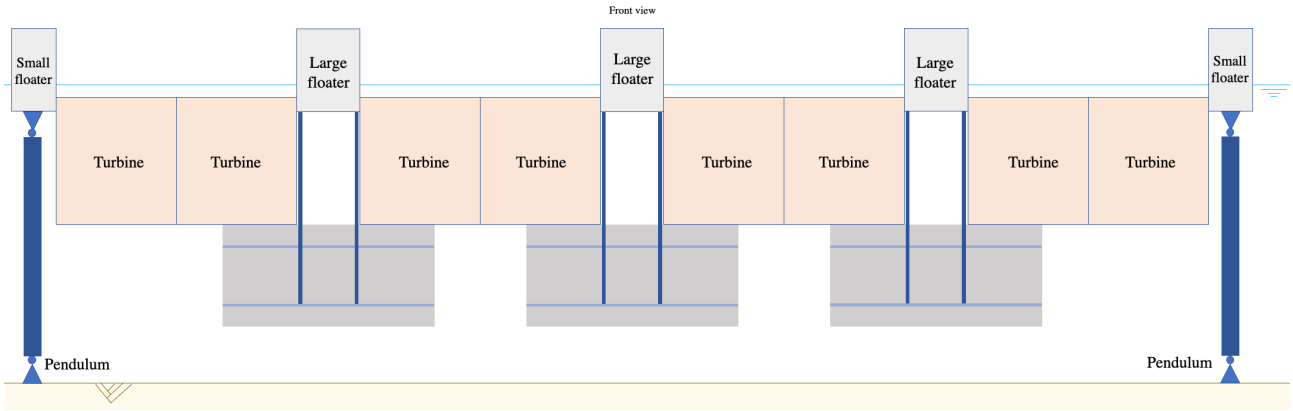

Figure 7.4 Front view of the sway plate 3 x 17 m variant

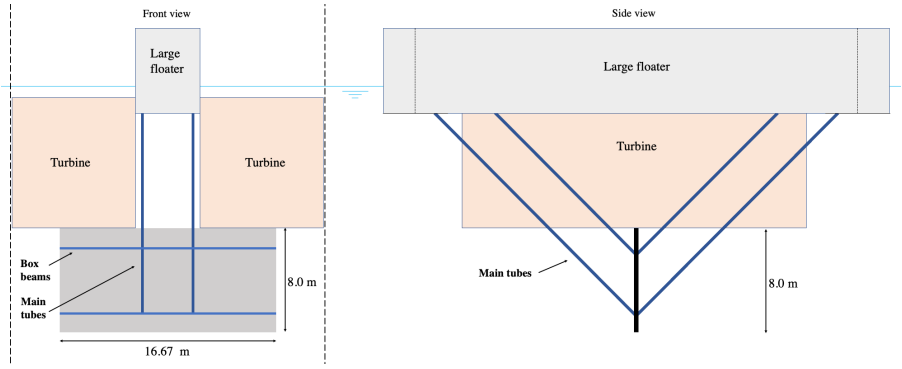

Figure 7.5 Side view of the sway plate 3 x 17 m variant

Variant 5: Sway plate 6 x 17 m

Figure 7.6 shows variant 5 and is almost identical to variant 4. Variant 5 has an additional row of sway plates placed behind the first row. The total added mass for the sway direction has been doubled. An added mass plan for this variant is to be observed in Figure G.26. The added rotational moment of inertia that prevents roll rotations is also doubled. More figures about the variant have been supplied in Appendix G.2.2.

The effectivity of 15.5 days comes close to the objected effectivity of 18.4 days. Another upgrade of this variant may lead to fulfilling the design objective.

Reduction of the downtime	15.5 days
Steel needed for four floating elements	497 tons
Generated added mass sway	5152 tons
Generated added mass heave per floating element	-
Depth of COG of added mass per floating element	16.5 m

Table 7.5 Important numbers for the sway plate 6 x 17 m variant

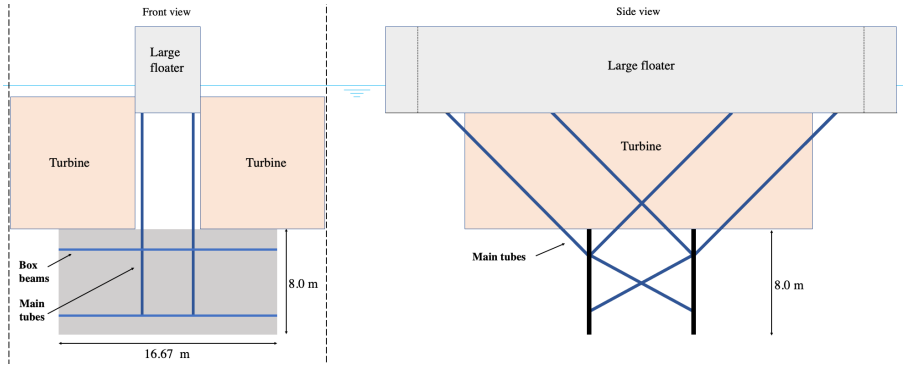

Figure 7.6 Front and side view of the sway plate 6 x 17 m variant

Variant 6: Sway plate 9 x 17 m

Figure 7.7 shows variant 6 and is almost identical to variants 4 and 5. Variant 6 has a third row of sway plates. The added mass is three times more the added mass of variant 4. More figures about the variant have been supplied in Appendix G.2.3.

The effectivity of this variant is 22.3 days and this variant fulfills the design objective of 18.4 days.

Reduction of the downtime	22.3 days
Steel needed for four floating elements	750 tons
Generated added mass sway	7728 tons
Generated added mass heave per floating element	-
Depth of COG of added mass per floating element	16.5 m

Table 7.6 Important numbers for the sway plate 9 x 17 m variant

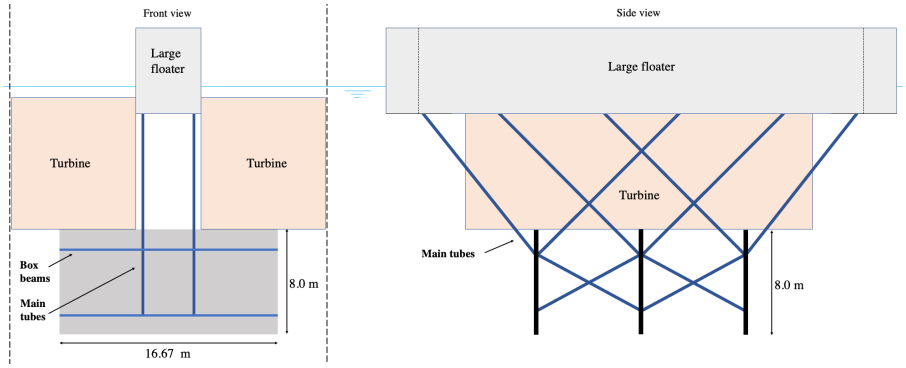

Figure 7.7 Front and side view of the sway plate 9 x 17 m variant

Variant 7: Sway plate 1 x 70 m

Figure 7.8 shows variant 7. The sway plate variants 4 and 5 with plates of 3 x 17 m and 6 x 17 m did not show to be effective enough. A variant that takes advantage of the possibility to generate added mass below the turbines may be able to generate more added mass. However, the span below the turbines asks for more structurally strong elements to ensure the strength and stiffness of the variant. The variant is therefore expected to be effective while more steel is needed.

The *height* is chosen such that the available space between the turbines and the keel clearance is respected with the same criteria of variant 4. The *width* of the variant is chosen such that the field moment below the turbines is as large as the peak moments at the supports of the plate at the main tubes on the sides. More figures about the variant have been supplied in Appendix G.2.4.

The effectivity of this variant is 11.9 days and the variant does not fulfill the design objective of a reduced downtime of 18.4 days. Variant 8 tries to increase the effectivity by doubling the added mass by an additional full span sway plate.

Reduction of the downtime	11.9 days
Steel needed for four floating elements	444 tons
Generated added mass sway	3607 tons
Generated added mass heave per floating element	-
Depth of COG of added mass per floating element	16.5 m

Table 7.7 Important numbers for the sway plate 1 x 70 m variant

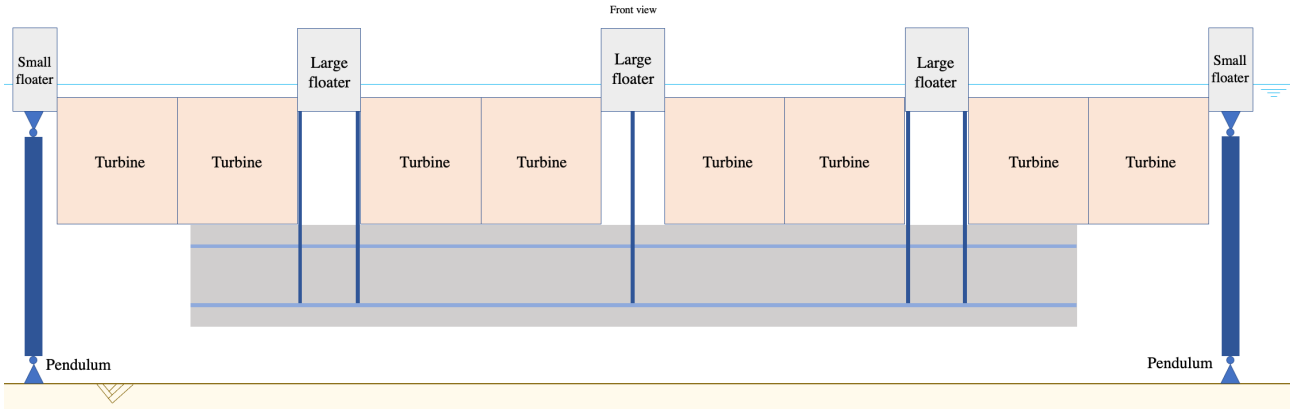

Figure 7.8 Front view of the sway plate 1 x 70 m variant

Variant 8: Sway plate 2 x 70 m

Figure 7.9 shows a figure of variant 8. This variant is almost identical to variant 7. This variant has an additional sway plate such that the added mass is doubled as well. Figure G.38 shows the added mass plan of this variant. More figures about the variant have been supplied in Appendix G.2.5.

The effectivity of this variant is 20.7 days. This effectivity fulfills the design objective of a downtime reduction of 18.4 days.

Reduction of the downtime	20.7 days
Steel needed for four floating elements	873 tons
Generated added mass sway	7214 tons
Generated added mass heave per floating element	-
Depth of COG of added mass per floating element	16.5 m

Table 7.8 Important numbers for the sway plate 2 x 70 m variant

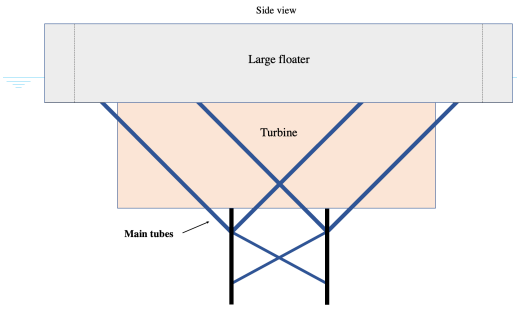

Figure 7.9 Side view of the sway plate 2 x 70 m variant

Variant 9: Sway plates between turbines

Figure 7.10 shows variant 9 which tries to generate the added mass closer to the floaters to save materials that transfer the forces of the sway plate to the floaters. Below the large floaters there is space to place sway plates that can be positioned very close to the floater. The advantage of this variant is found in the structural materials that transfer the sway of heave plate forces to the floater. This variant does not need much structural steel to transfer the sway plate loads to the floaters.

The height of the plate spans between the bottom of the floater and the bottom of the turbine. The width of the floater is equal to the width of the floater. Figure G.42 and G.43 in Appendix G.2.6 show the added mass plan for this solution. More figures about the variant have been supplied in Appendix G.2.6.

The effectivity of this solution is very low and only 5.9 days. This effectivity does not come close to the objected effectivity of 18.4 days. This effectivity is expected to be so low due to the wave forcing. The wave forcing onto objects becomes larger and larger for objects that are placed closer to the free surface. These sway plates are placed fairly close to the surface area and the plates function more like sails vulnerable for the wave forcing than that those plates mitigate the dynamics by the additional generated added mass.

Reduction of the downtime	5.9 days
Steel needed for four floating elements	327 tons
Generated added mass sway	4645 tons
Generated added mass heave per floating element	-
Depth of COG of added mass per floating element	8 m

Table 7.9 Important numbers for the sway plates between turbines variant

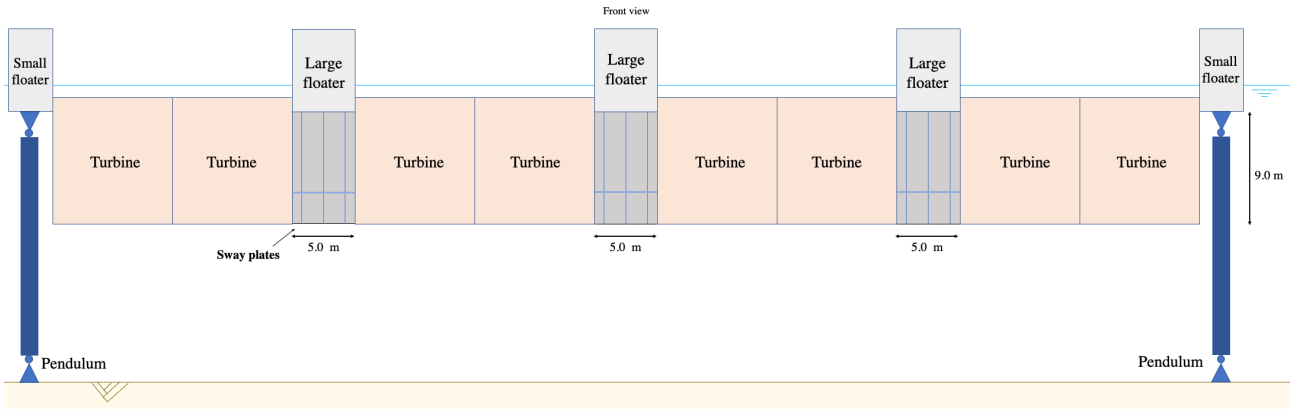

Figure 7.10 Front view of the sway plates between turbines variant

7.2 Testing the performance of the variants

The results of the variants have already been presented in the report just by a number of days that specifies the reduction of the downtime. These numbers have been deduced from the graph displaying the exceedance of the serviceability limit for wave height and wave length combinations. An example of such a graph can be observed in Figure 7.11. This section presents the results of the tested variants.

7.2.1 Heave plate variants

The variants of the heave plate alternative do not show very significant differences. The effectivity of the three variants varies between 11.9 and 13.6 days and the variants do not meet the design objective of an effectivity of 18.4 days. An interesting observation concerns the amount of added mass of variant 3. Variant 3 succeeds in generating almost twice as much added mass as variant 1 and 2. This additional added mass is not proportional to the effectivity as the effectivity is not risen with the same factor.

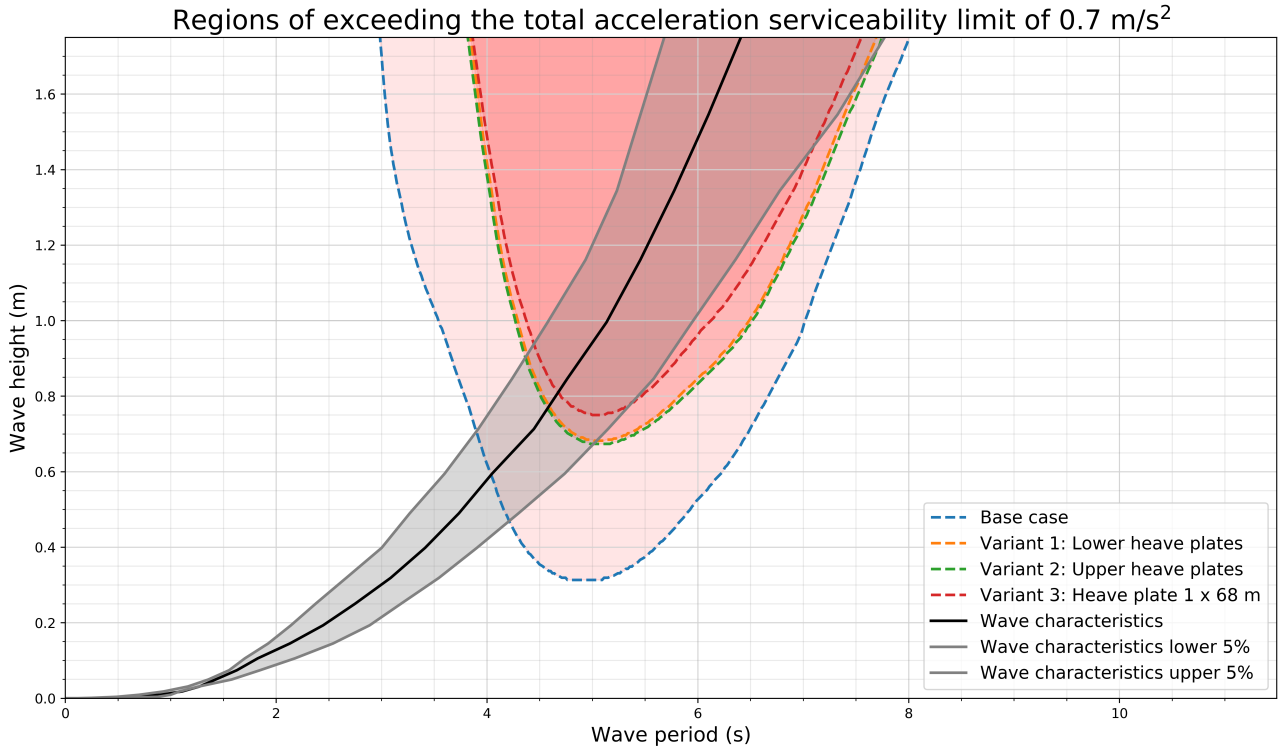

Figure 7.11 The exceedance of serviceability limits curves for variants 1, 2 and 3

7.2.2 Sway plate variants

Figure 7.12 shows the regions of exceeding the combined acceleration serviceability limits for the defined wave length and wave height combinations for the sway variants. All sway plates, except for the sway plate of variant 9, hang below the structure on the same height. For all those sway plates, one general conclusion can be drawn. Sway plates with a larger total width also have an improved result concerning the dynamic behaviour of the sway plate variant. The needed sway plate width can therefore be adapted such that the design objective is reached.

7.3 Performance observations

The sway plate distance to the surface elevation

Variant 5 and 9 both have almost the same amount of added mass, respectively 5152 and 4645 tons. Variant 5 has slightly more mass, but significantly more effectivity with 15.5 days instead of an effectivity of 5.9 days which can be observed graphically in Figure 7.12. The difference in effectivity may be found in either one of both of these suggested arguments.

1. **Higher sway plates are more prone to be excited by the wave forcing:** The dynamic behaviour of the Tidal Bridge is mostly due to the wave forcing on the turbines that hang below the Tidal Bridge. These turbines function as large sails and the waves have much grip on these sails. The sway plates of variant 9 hang between the turbines and are prone to be excited by this same wave forcing more than the sway plates of variant 5.

2. **Lower sway plates can reduce roll movements more effectively:** The lever arm from the COG[1] of the sway plate to the COG of the Tidal Bridge is larger for variant 5 compared to the lever arm of variant 9. The sway plate of variant 5 contributes to more added mass moment of inertia.

[1] Centre of gravity

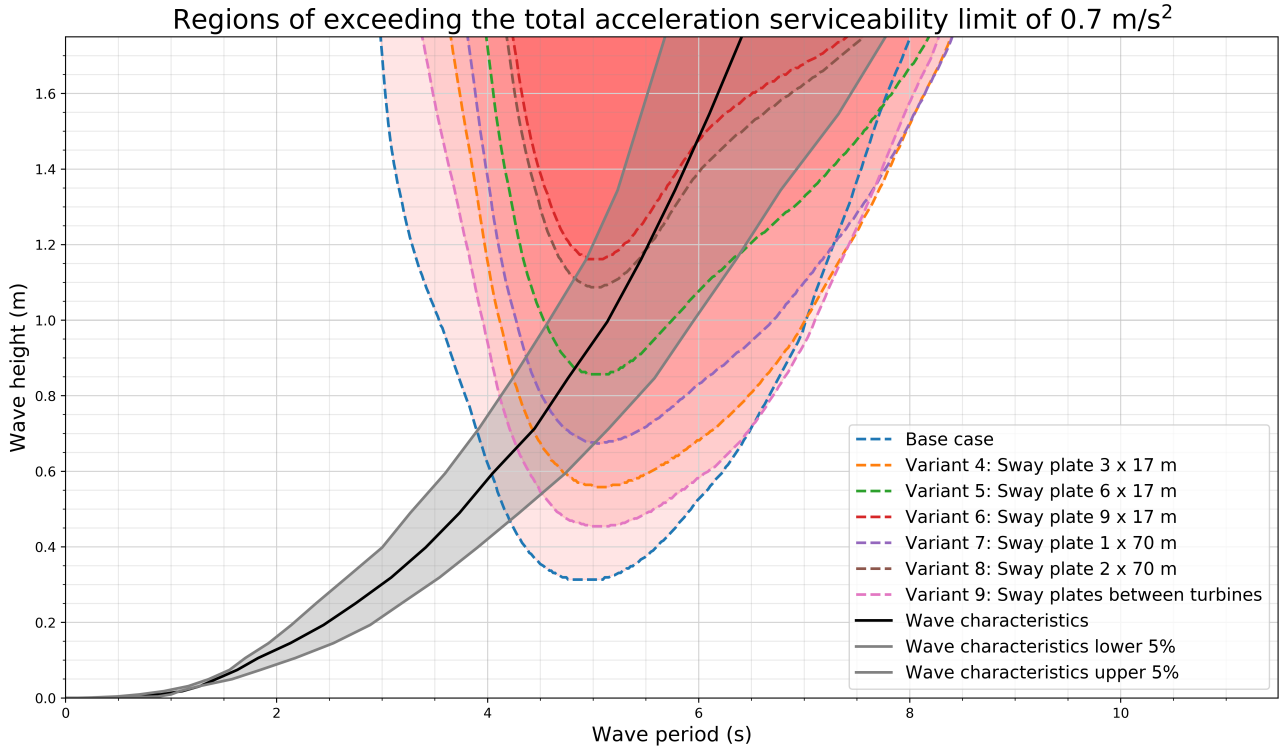

Figure 7.12 The exceedance of serviceability limits curves for variants 4, 5, 6, 7, 8, and 9

The effect of the structure mass to the dynamics

Figure 7.13 shows that the heave plate structure mass is beneficial to the dynamic behaviour of the Tidal Bridge. The heave plate structure mass adds up to the total inertia and the combined accelerations become less for all wave periods. The Tidal Bridge can withstand wave heights of about 5 centimetres upon including the variant structure mass to the structural dynamics model. Unfortunately, this increase of effectivity is insignificant in the determination of the downtime.

7.4 Verifying the variants

Table 7.10 shows the yearly downtime. The same results have been differently displayed in Appendix G.3 by showing the relative improvement compared to the base case.

	Probability		
	95%	**50%**	**5%**
Base case	31.6	23.4	16.3
Variant 1: Lower heave plates	17.7	11.3	5.3
Variant 2: Upper heave plates	18.1	11.5	3.4
Variant 3: Heave plate 1 x 68 m	16.4	9.8	3.2
Variant 4: Sway plate 3 x 17 m	21.1	14.8	8.4
Variant 5: Sway plate 6 x 17 m	14.3	7.9	0.5
Variant 6: Sway plate 9 x 17 m	9.1	1.1	0
Variant 7: Sway plate 1 x 70 m	18.1	11.5	3.4
Variant 8: Sway plate 2 x 70 m	10.1	2.7	0
Variant 9: Sway plates between turbines	24.2	17.5	10.8

Table 7.10 Yearly downtime in days for the base case and the variants

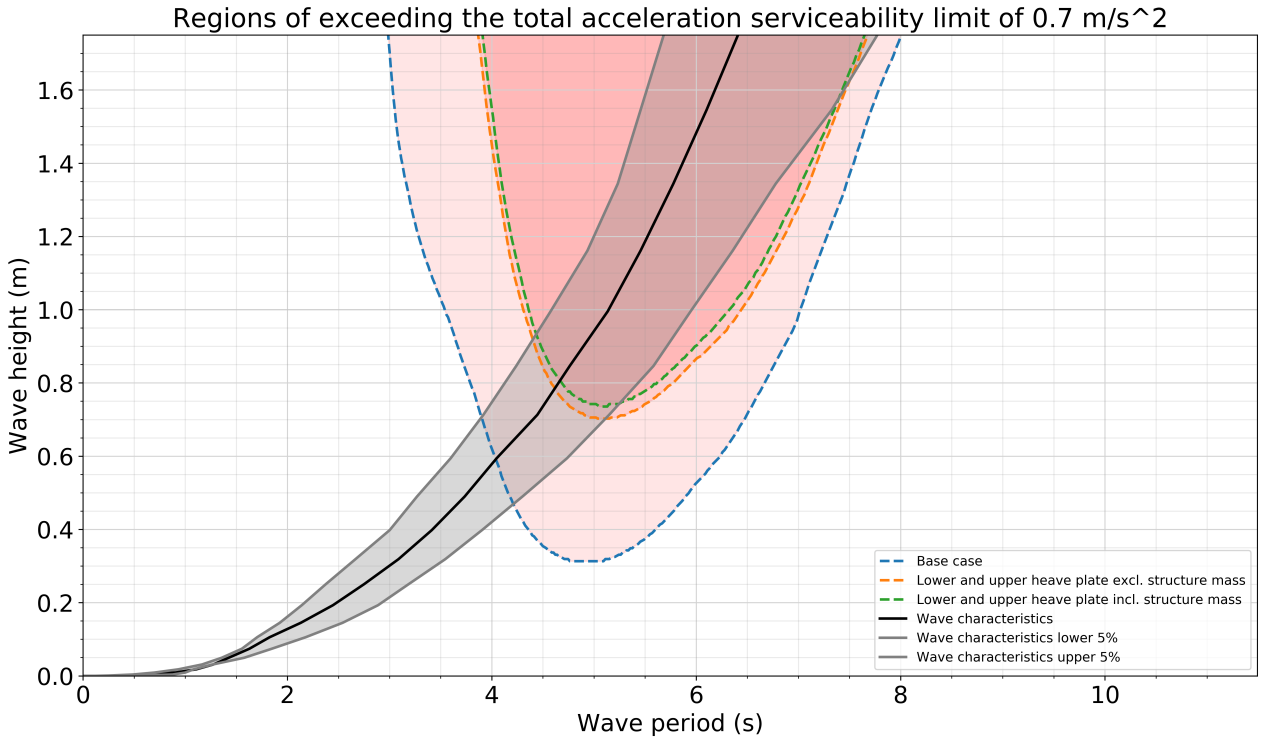

Figure 7.13 Figure showing a positive effect of the heave plate structure mass to the dynamic behaviour of the Tidal Bridge

The slosh damper alternative has not been included in the list of Table 7.10. The effect of this alternative was too small to lead to successful variants. An elaborate explanation of the slosh damper and its effectivity has been written in Section 6.1.

Variants that have a maximum downtime of more than five days per year do not satisfy the design objective. Those designs should not be taken into consideration in the selection procedure for the resulting design. This harsh norm results in filtering seven of the nine variants. The only two designs that meet the design objective are:

- Variant 6: Sway plate 9 x 17 m
- Variant 8: Sway plate 2 x 70 m

Those two designs will be taken in consideration for the qualitative selection to the evaluation criteria.

7.5 Evaluating the variants

The two designs that have not been filtered by the strict design objective show many similarities. Both designs would score equally on many evaluation criteria. Such evaluation criteria are not taken into account for this evaluation process. The relevant evaluation criteria for this design loop have already been stated in Section 2.2 and are described more in depth in the list below which starts with the most important evaluation criteria.

- **Material need per improved day:** Section 6.2.1 explains how the material need is strongly related to the total cost of the structure. The effectiveness of both designs is sufficient to fulfill the design objective and is therefore irrelevant as a single evaluation criterion. The evaluation criteria material need per improved day combines the material need and the effectiveness to find the most efficient solution concerning cost versus effect. Appendix G.4 writes about the steel need of the designs and visualizes this in Table G.11, Figure G.45, and Figure G.46.
- **Adjustability to depth:** One of the floating elements of the Tidal Bridge is situated in a more shallow area. This evaluation criteria tells how well the design can be adapted to this shallow area.

- **Energy yield:** Designs with a larger blockage effect lead to a larger energy yield and a lower investment cost on the long term.
- **Constructability and maintainability:** This evaluation criteria makes a distinction in constructability comfort and maintainability comfort. Designs which are easier to construct or easier to maintain receive higher scores.
- **Pendulum forces:** Pendulum forces may reduce as a result of the reduced dynamic behaviour of the Tidal Bridge. However, the increased blockage effect leads to larger pendulum compression and tension forces in due current-related drag forces. Pendulum forces stay preferably as low as possible.
- **Impact on coastal equilibrium:** The blockage effect leads to a disbalance in the coastal equilibrium. A larger blockage effect leads to larger currents closer to shores of the Strait of Larantuka increasing the coastal erosion.
- **Redundancy to unforeseen weather events:** The design which is the least prone to touch the bottom upon extreme displacements scores the best on this evaluation criterion.
- **Estimating pendulum hinge location:** Designs that disrupt the rotational balance around the centre of gravity need to compensate this by moving the hinge. Designs that have a large influence on the rotational balance introduce more uncertainty in defining this hing location.

The evaluation criteria of Section 7.5 are integrated in a multi criteria analysis with a well considered scoring importance. The first criterion, material need per improved day, is the most important criterion as this combines an estimation of design cost and effectiveness, which are both extremely important to the client of the design. Table 7.11 shows the scoring of the evaluation criteria by a multi criteria analysis. The analysis showed that the Sway plate 9 x 17 m is the solution that suits the considered evaluation criteria the best. Section 7.2 showed that the design already satisfies the requirements and boundary conditions. The high score of the Sway plate

	Material need per improved day	Adjustability to depth	Energy yield	Constructability and maintainability	Pendulum forces	Impact on coastal equilibrium	Redundancy to unforeseen weather events	Pendulum hinge location estimation	**Total**
Importance	36%	21%	14%	14%	4%	4%	4%	4%	**100%**
Sway plate 9 x 17 m	4	4	4	3	3	2	2	3	**3,6**
Sway plate 2 x 68 m	3	2	5	2	2	1	1	2	**2,7**

Table 7.11 Multi criteria analysis of the two variants that fulfill the design objective

9 x 17 m with respect to the Sway plate 2 x 70 m is mostly due to two factors. 1. The Sway plate 9 x 17 m is the most efficient solution concerning material need versus the effectiveness. 2. The structure of the Sway plate 9 x 17 m is split into three parts below the three floaters and can therefore be considered as a more modular solution. This means that such a module may be adapted specifically to the depth at location, be replaced more easily which comes in handy for construction or maintenance operations. Furthermore, the pendulum forces, the impact on the coastal equilibrium, and the estimation of the pendulum hinge location are expected to be lower or less complicated due to the smaller total current-related drag forces of the Sway plate 9 x 17 m.

Summarizing the third design loop

In this chapter, nine variants were developed from the two chosen alternatives of the heave plate and the sway plate. The verification of the nine variants with the structural dynamics model showed that the sway plate 9 x 17 m and the sway plate 2 x 70 m where the only two variants that satisfied the design objective. An evaluation with a multi criteria analysis of those two variants showed that the sway plate 9 x 17 m variant scored the best to the relevant evaluation criteria. This variant was chosen in this third design loop to be developed further as the resulting design in the next chapter.

8 | Resulting design

The previous chapter chose one specific variant to continue with in the design process. This chapter develops this chosen variant further into a resulting design. The structural design has been developed further and is structurally checked against combination of dynamic loads and current related drag loads. The implications to the original Tidal Bridge design are checked and a new hinge location for the pendulums is proposed. The chapter also elaborates upon some design characteristics such as the advantages, the construction method, the connections, the corrosion, the fatigue damage, the mass, the draught, the stability and the failure mechanisms.

8.1 Structural overview

8.1.1 Effectivity and geometry

The resulting design finds its effectivity mostly in additional added mass. The nine sway plates per floating element generate enough added mass to achieve the design objective. The *width* of the plates is chosen such that the moment forces in the box beams of the sway plates stay within acceptable values. The *height* of the plate is restricted by the available space between the turbines and the sea strait bottom. A safety margin of 4.3 meters has been included for the tidal differences in combination with extreme heave displacements. The sway plates are not placed between the turbines as the effectivity of the sway plate concept decreases if closer to the free surface.

Figure 8.1 and 8.2 give an impression of the dimensions of the sway plate compared to the Tidal Bridge structure. More figures of the resulting design may be found in Appendix H.2.

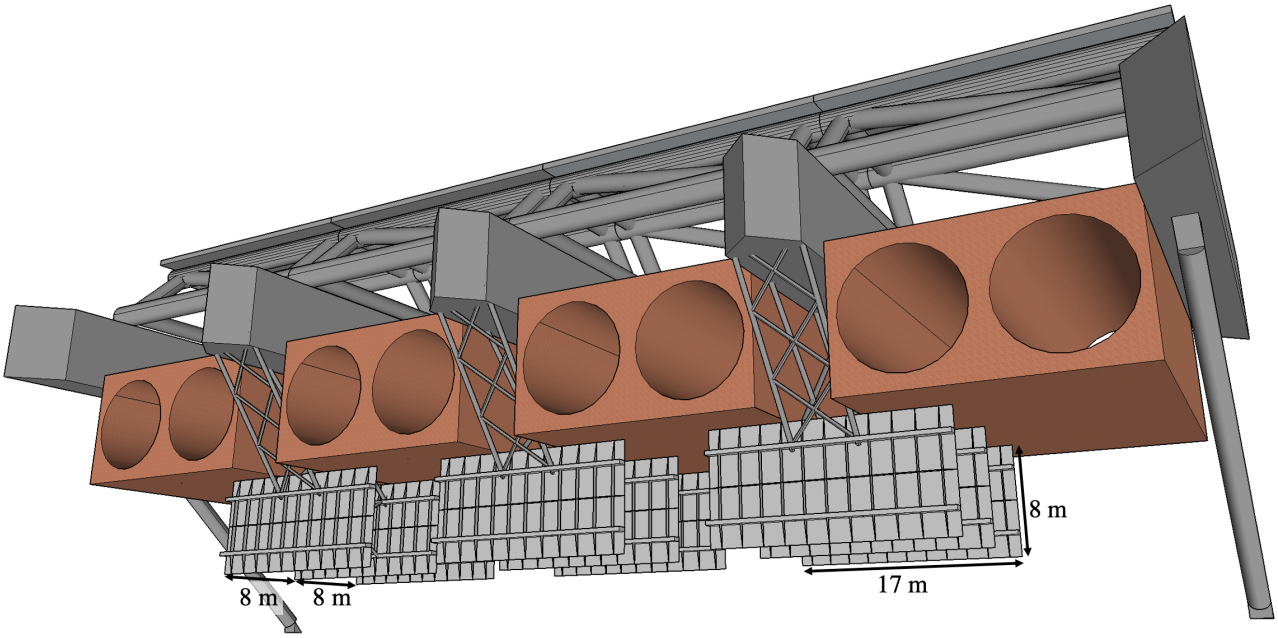

Figure 8.1 Perspective sketch of some basic measurements and the integration of the resulting design within the Tidal Bridge

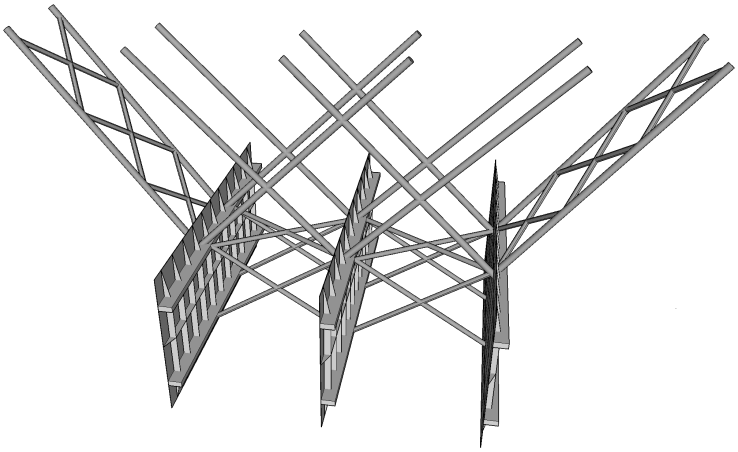

Figure 8.2 Perspective sketch of the resulting design

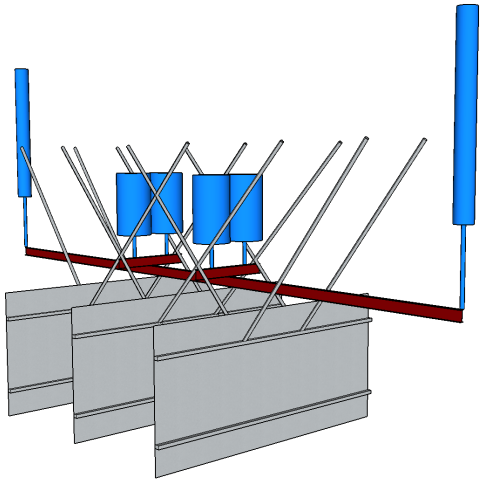

Figure 8.3 Perspective view of the sway plate structure hanging below the floaters of the auxiliary structure during the connection process of the sway plate to the Tidal Bridge

8.1.2 Structural components

The itemization below shows an overview of the used structural elements of the resulting design of which a complete overview of the material need is given in Table 8.1. Three of those structures are needed for one floating Tidal Bridge element and twelve of those sway plate structures are needed to equip the four floating Tidal Bridge elements with. The weight of one sway plate structure is expected to be around 124 tons.

- **Plate:** The sway plate itself is a steel plate with a thickness of 15 mm. Corrosion is the governing driver for the determination of the plate thickness.
- **Stiffeners:** The stiffeners transfer the forces of the plate to the box beams. The strength of the plate is governing in the stiffener centre to centre distance. The stiffeners have a height of 350 mm, a width of 15 mm, and a centre to centre distance of 1500 mm.
- **Box beam:** Box beams provide stiffness and strength to the sway plate to transfer the forces to the tubes. The moment forces in the box beams at the supports of the tubes are governing in determining the dimensions. The box beams have a height of 700 mm, a width of 300 mm, a flange width of 30 mm and a web with of 20 mm.
- **Tubes long:** The long tubes transfer the forces of the sway plate to the floaters. The buckling resistance is governing in determining the dimensions of the cross section of the tubes. The tubes have a length of 14.5 m, a diameter of 350 mm and a thickness of 15 mm.
- **Tubes short:** The shorter tubes support the lower part of the sway plates. The buckling resistance is governing in determining the dimensions of the cross section. The tubes have a length of 9.0 m, a diameter of 250 mm, and a thickness of 10 mm.
- **Stability tubes:** Stability tubes ensure that incidental side loads on the structure are transferred to the floaters. The stability tubes have a diameter of 200 mm and a thickness of 10 mm. The cross sectional area of the stability tubes is about 35% of the cross sectional area of the main tubes.

The structural elements of the box beam and the tubes deal well with corrosion. The cross sections can be closed of to prevent water to intrude into the elements and the inside plate skin stays protected for corrosion. Tubes are the favourable types of structural elements to transfer the forces from the plates to the floaters as those have a small drag force and the same hydraulic characteristics in all directions.

[1] There is not a defined force that should be accounted for by the stability tubes.
[2] Average length of stability tube

Type	UC 1 (-)	UC 2 (-)	Length (m)	Volume per meter (m^2)	Quantity (-)	Volume (m^3)
Plate	0.44	0.74	16.7	0.1200	3	6.00
stiffeners	0.56	0.70	8.0	0.00525	36	1.51
Box beam	0.79	0.85	16.7	0.0436	6	4.37
Tube long	0.58	0.67	14.5	0.0158	12	2.75
Tube short	0.64	0.79	9.0	0.0075	8	0.54
Stability tubes	-[1]	-	7.2 [2]	0.0060	16	0.68
					Total	**15.85**

Table 8.1 Overview of the structural elements needed for one set of sway plates hanging below 1 floater. UC 1 represents the unity check after construction. UC 2 represents the unity check after losing 1.75 mm of steel due to corrosion at the end of its lifetime of 50 years.

8.1.3 Structural load calculation

The following loads have been taken into account for the Ultimate Limit State calculation:

- **Inertia force:** Waves that have a return period of once in 1000 years have a height of 2 meters. The corresponding sway acceleration is 0.6 m/s^2 and the corresponding roll acceleration is 0.066 rad/s^2. Multiplying this rotational acceleration by the lever arm to the centre of gravity leads to an additional sway acceleration of 1.09 m/s^2 at the height of the centre of the sway plate. The total sway acceleration is 1.69 m/s^2. Multiplying this value by a partial factor for hydraulic loads[3]of 1.5, then a design acceleration of 2.53 m/s^2 is found (BSI, 2017). The pressure on the sway plate is found by multiplying the added mass per squared meter which gives a pressure of 16.6 kPa.
- **Drag force:** The maximum current velocity is 4 m/s. The current related pressure on the sway plate can be calculated by using Equation 3.2 and is 9.6 kPa. Using a partial factor for hydraulic loads[3] of 1.5 leads to a pressure of 14.4 kPa (BSI, 2017).

The combined pressure on the sway plates that should be taken into account for the structural calculation is 31 kPa. This value is used for calculating the dimensions of the structural elements. The chosen steel class is S355, which is commonly used offshore structures. The partial factor of $\gamma_{M0} = 1.00$ has been used to calculate the design resistance (Nederlands Normalisatie-instituut, 2020). The unity checks are mostly lower than 0.8 to have some redundancy to fatigue damage and weak welds.

The moment resisting stiffeners are protected to lateral buckling by a stability plate, which is placed in the middle of the sway plate perpendicular to the stiffeners. The sway plates need a good quality of the welds to resist for fatigue damage and to have a structural capacity which is larger than the capacity of the welded cross sections.

Some improvements to the resulting design for a next iteration step are suggested as well. The line of forces of the tubes is not crossing each other in the same virtual location which results in moment forces within the joints. This problem should be accounted for in the next design iteration. Furthermore, the design should be optimized to avoid fatigue damage by rounded shapes on the inward corners.

8.2 Investigation of the additional current related drag force

The resulting design leads to additional drag forces to the main Tidal Bridge structure due to the currents through the strait. The additional drag force is transferred through the truss structure to the pendulums and consequently to the foundation. The maximum horizontal drag force is calculated with Equation 3.2 and is 7.5 MN per Tidal Bridge element for both current directions. Figure 8.4 shows the direction and the attachment point of the drag force.

Torsional force in the truss

The horizontal drag force multiplied with the lever arm to the centre of the truss (23.8 meters) results in a torsion force within the truss structure of 178.5 MNm. The turbines hanging below the Tidal Bridge lead to an

[3]Independent to the Consequence Class

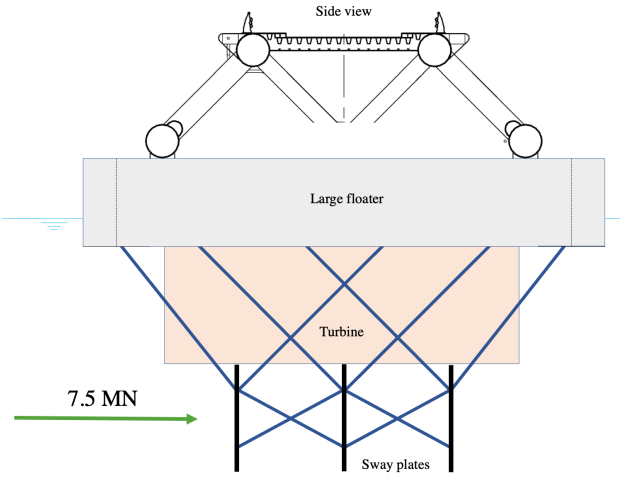

Figure 8.4 Maximum horizontal force on one floating element due to the drag forces on the sway plate

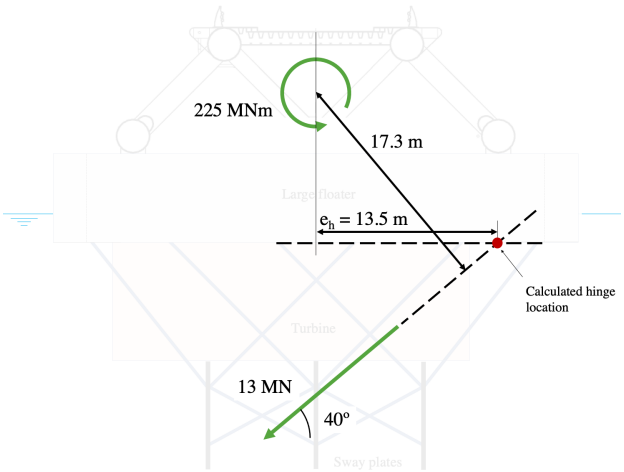

Figure 8.5 Hinge location estimation calculation

additional torsion force of about 25% of the torsion force of the sway plates leading to a total torsion force in the truss of 225 MNm. This torsional force can be divided over the two supports, the two pendulums, leading to a torsional load just before the supports of 112.5 MNm. The four slanting tubes within the truss need to transfer this force to the supports. The maximum compression force within these slanting tubes is estimated to be 25 MN. Upon multiplying this value with a characteristic value of 1.5 for hydraulic loads for a ULS calculation, then the design force within the tubes is estimated to be 37.5 MN. Figure 8.6 shows a diagram of the torsion forces within the truss structure and one of the slanting tubes.

With slanting tubes that have a diameter of 1500 mm and a thickness of 30 mm, then a design buckling resistance of 46.7 MN is found for the longer tubes of 22 meter. This would lead to a UC of 0.8. This is a very marginal unity check upon knowing that shear forces within the truss are not included in this calculation. The truss design can be easily improved by enlarging the angle of the slanting tubes. An example is drawn in Figure 8.6 on the left side of the truss structure. The normal forces within those slanting tubes on the left side are smaller than the normal forces within the slanting tubes of the right side of the figure due to the different angle of the slanting tube.

8.2.1 Normal force in the pendulum

The total horizontal drag force of the structure has the order of magnitude of 10 MN upon including the drag of the FishFlow turbines. This horizontal force, when divided over the two pendulums and compensated for the pendulum angle, leads to a pendulum force of 6.5 MN per pendulum and 13 MN for the two pendulums together. The dynamic load on the pendulum due to the waves has the order of 3.6 MN per pendulum. The total compression and tension characteristic force is 10 MN and the design force is 15 MN per pendulum[4]. This value is equal to the pendulum load that was accounted for in the feasibility studies of the Tidal Bridge. The design resistance of the feasibility design pendulum is 19.7 MN leading to a UC of 0.76.

8.2.2 Forces on the foundation

Each foundation gives support to two pendulums. The design forces on the foundation due to the pendulum forces are calculated to be 20 MN for the vertical direction and 23 MN for the horizontal direction. The foundation of the feasibility study has three steel vertical piles of a diameter of 1800 mm and a thickness of 40 mm and a length of 2 meter that are placed in bored holes in the bed rock. The piles are fixed to the bed with grout. Such a foundation is sketched in Figure C.3. It is calculated that the connection to the ground has a UC for the vertical forces of 0.4 and a UC for the horizontal forces of 0.11. The foundation is calculated to be large enough to resist for the additional drag forces.

[4]Due to the multiplication of the characteristic value for hydraulic loads of 1.5

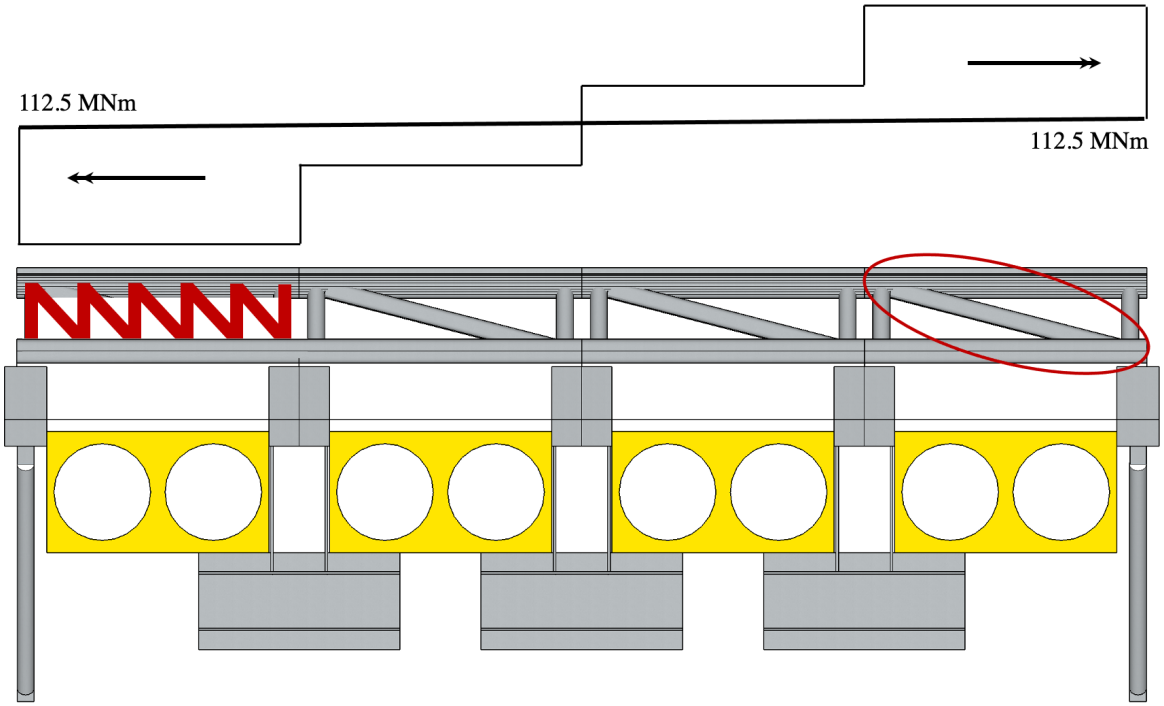

Figure 8.6 Diagram displaying the maximum torsion within the truss structure induced by the current through the strait. The red circle shows one of the slanting tubes providing torsional strength.

8.2.3 New hinge location

Estimation of the new hinge location

The additional drag forces need a shift of the pendulum hinge location to prevent for a permanent roll displacement. An initial estimation of the hinge location can be made by balancing the sum of moments as a result of the drag forces. A visualization of this balance of moment is given with Figure 8.5. The drag forces on the sway plates and the turbines lead to a maximum overturning moment of 225 MN. The reactive pendulum force due to these drag forces is 13 MN and leads to the restoring moment force. The needed lever arm to have a equilibrium of moments is 17.3 meter. This results in a pendulum hinge location of 13.5 meters away from the middle of the floater. This is 8.5 meters further away from the middle of the floater than the original pendulum hinge location. The new pendulum hinge location stays attached to the bottom plate of the floater.

Dynamic response with new hinge location

The new hinge location has a larger lever arm to the centre of gravity. This changed lever arm leads to a different dynamic response of the system. Figure 8.7 shows the dynamic response of the base case, the resulting design with the original hinge location of 5 m and the resulting design with the new location of 13.5 m. The design with the improved hinge location shows a smaller dynamic response which leads to a reduced downtime compared to the original resulting design. Table 8.2 provides an overview of the yearly downtime.

	Probability		
	95%	**50%**	**5%**
Base case	31.6	23.4	16.3
Resulting design original hinge location y = 4.5 m	9.1	1.1	0
Resulting design improved hinge location y = 13.5 m	3.1	0	0

Table 8.2 Yearly downtime in days showing that the changed hinge location has a beneficial effect to the dynamics.

The roll accelerations have been reduced with 43% compared to the resulting design test with the original hinge location. The larger lever arm to the centre of gravity leads to a more effective restriction of the

roll dynamics. The accelerations of the sway degree of freedom and the heave degree of freedom changed insignificantly to lead to the presented result of Table 8.2.

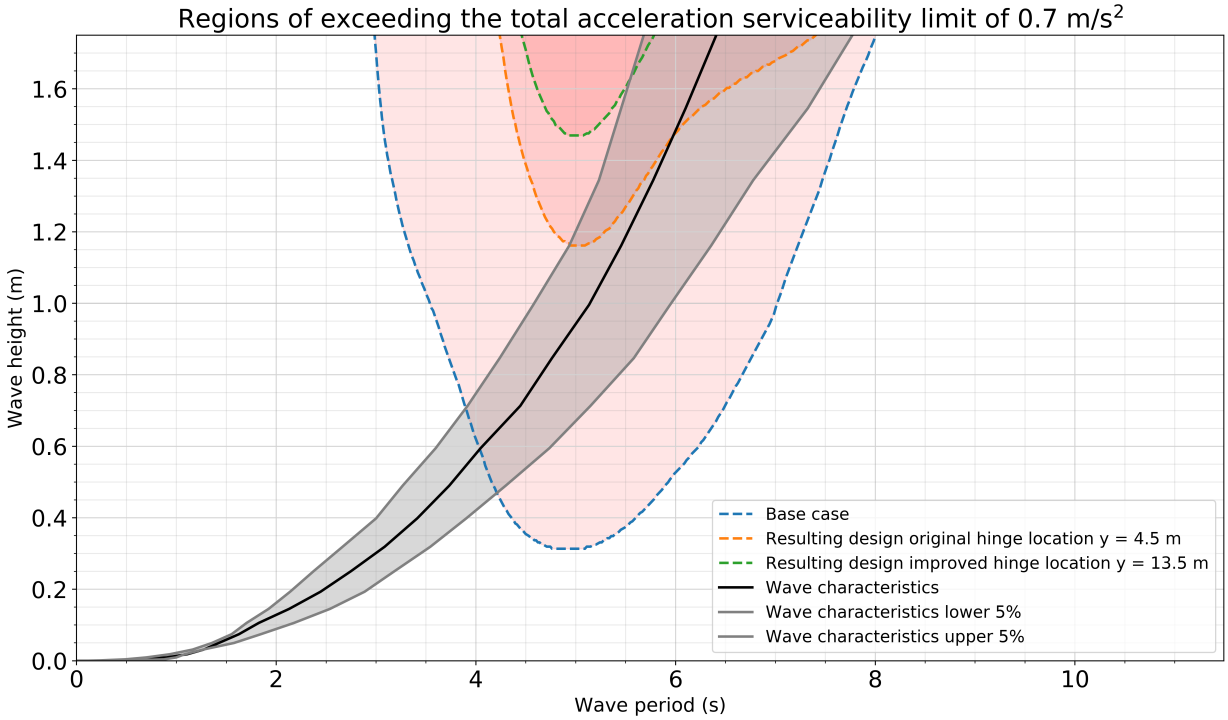

Figure 8.7 The region of exceeding the serviceability limit for the situation with the improved pendulum hinge location

Pendulum forces with the new hinge location

Section 8.2.1 showed that the normal force of the pendulum stayed within acceptable limits concerning the structural integrity for the resulting design. The maximum dynamic related force within the pendulum reduced with 12.5% for the resulting design compared to the base case. This reduction is further increased by the forced shift of the pendulum hinge location further away from the centre. The maximum dynamic related force within the pendulum is reduced by 25% compared to the base case.

8.3 Design characteristics

8.3.1 Advantages

The list below sums the significant advantages of the resulting design. The first two advantages are benefits over the other presented variants of Chapter 7. The last advantage describes an increased functional value to the original Tidal Bridge design.

1. **Relatively low steel need:** The resulting design needs less steel compared to the other variant which fulfills the design objective. A reduced steel need is beneficial for the cost and the impact to the environment.

2. **Modular approach:** The three different sway plate structures per floating element allow for a modular approach. The modules may need different dimensions depending on the depth and the desired amount of added mass. The pin connections provide convenient attaching and detaching. This allows for a comfortable constructability and maintainability, and adaptability to changing requirements after the construction phase.

3. **Increased energy yield:** The turbines have a higher efficiency due to the resulting design. Vennell (2013) states that the power output of a tidal turbine increases with an increasing blockage ratio. The

maximum power coefficient of tidal turbines in a free flow is defined by the Betz's limit and driven by a momentum loss, whereas tidal turbines dealing with a significant blockage ratio become more driven by a head loss. In those cases, the maximum power coefficient exceed the Betz's limit. The complete structure of the Tidal Bridge including the turbines leads to blockage of the strait, and hence, to an increased power coefficient (Vennell, 2013).

8.3.2 Construction method and connection to the floater

The construction method relevant for this report focuses mostly on the attachment of the sway plate structure to the Tidal Bridge design. A summary of the construction method is given in the steps below. See Appendix H.1 for an elaborate explanation all different steps in the construction method.

1. The complete sway plate steel structure is welded together and coated to prepare for submergence on the quay wall.
2. The auxiliary structure with its floaters is connected to the sway plate structure. The auxiliary structure ensures that the sway plate structure can float by itself at a regulated depth. This auxiliary structure with its floaters can be seen in Figure 8.3.
3. The sway plate structure including the auxiliary structure is launched to the water by two cranes.
4. The sway plate structure is positioned and fasted with the pin connections by divers.
5. The auxiliary structure is removed with the help of straps, floaters and divers.
6. The Tidal Bridge floating element together with the sway plate structure is towed into its position in the Strait of Larantuka. The turbines are connected to the Tidal Bridge consequently.

The resulting design has 12 long tubes that are connected to the floaters with pin connections on both sides of the tubes. The pin connections come in handy upon constructing or maintaining the additional structure. Figure 8.8 shows a perspective sketch of this pin connection. Two side views in parallel projection are added to Appendix H.3 to acquire a better understanding of the design detail.

The connection of the tube to the floater with the specified design of Figure 8.8 results in a point load to the plate material of the floater. The floater needs to be reinforced locally to distribute this point load over the surrounding plate material of the floater. Figure 8.9 shows a qualitative sketch of such a reinforcement. The reinforcement consist of plates welded to the inside of the floater.

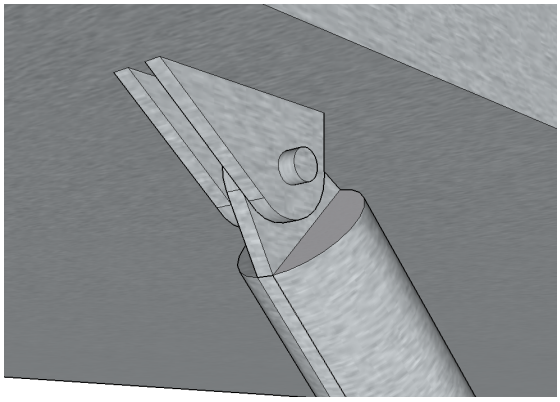

Figure 8.8 A perspective sketch of the connection between the floater and the tubes of the sway plate

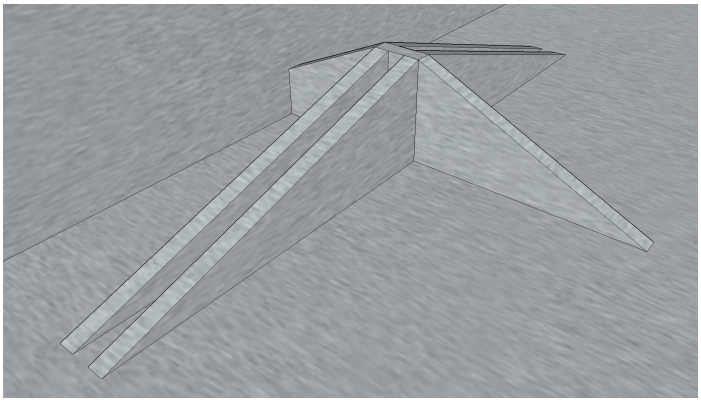

Figure 8.9 Local reinforcement to distribute the point load over the floater

8.3.3 Corrosion and fatigue damage

Corrosion takes place, despite the fact that the structure is submerged its whole lifetime. The prediction is that the structure would loose about 1.75 mm in the design lifetime of 50 years (BSI, 2009). There are two options to take account of this undesired effect.

1. The sway plate structures are dismounted from the floating element and maintained on a quay wall a few times in its lifetime. Dismounting and assembling the sway plate structures is a labour intensive and costly procedure as can be read in Section 8.3.2. The maintenance operation of the sway plate structures is costly as well.

2. The sway plate structures are equipped with heavier structural elements such that those have a redundancy capacity to loosing material due to corrosion over its lifetime. Equipping the structure with more material than needed is more costly and has an impact to the environment as well.

The exact total cost of both solutions are difficult to predict. The preference goes out to the seconds solution as this solution does not need any human intervention and, therefore, cannot fail by a lax maintenance attitude. All structural elements of the sway plate structure have been designed such that those can lose 1.75 mm to every side and still have enough structural capacities. Furthermore, corrosion is taken into account in the selection for the profile types. Tubes and box beams are both closed cross sections which only experience corrosion on the outer side of the cross section.

Fatigue damage is a relevant failure mechanism for the resulting design. Two factors are needed for fatigue failure to happen: 1. many repetitions, and 2. significant forces on the structure. The Tidal Bridge is moving all the time by the waves which result in many repetitions over its complete lifetime. The forces on the structure are generally very low and fatigue damage stays out. Extreme weather conditions lead to larger forces in the sway plate structure which leads to fatigue damage. It is yet unknown to what extent fatigue damage may play a significant factor in the failure tree of the complete Tidal Bridge structure. Additional research to this topic is recommended. In this state of the design, fatigue damage has been included in designing the structural elements of the sway plate structure. The unity checks of the chosen structural elements all stay well below 0.8 to include a redundancy capacity to fatigue damage.

8.3.4 Other design characteristics

Structure mass, draught, and stability

The structure mass for one Tidal Bridge element is expected to be 372 tons[5]. This additional structure mass leads to an increased draught of about 45 cm[6]. The centre of mass is moved downwards into the direction of the new sway plate structures by 12 cm. The stability of the total Tidal Bridge element including the resulting design has become larger.

Gathering possible failure mechanisms

The maximum expected accelerations for this structural check have been obtained from the structural dynamics model in collaboration with the probabilistic wave characteristics model. Other types of failures besides this loading condition have not been taken into account. An overview of possible failure mechanisms could provide more insights for loads to be taken into account in a next design loop. Possible other failure may be:

- **Corrosion, fatigue, exceeding maximum acceleration:** The loads of this category are already accounted for in the structural calculations. However, the impact of these characteristics may exceed the expected values which may result into failure.

- **External loss of integrity:** These types of failures may be a failure of the pin connection, a failure of the local reinforcements within the floater, or a failure of the floating element of the Tidal Bridge.

- **Dynamic instability:** Dynamic instability types like flutter may lead to an unforeseen forcing.

- **Touching bottom:** Touching the bottom could lead to a destructive point load. Touching the bottom can be induced by several reasons: a leak floater, a surveying fault, or a changing morphology.

- **Construction failures:** These types of failures may have the form of a weak weld seam, damage to the structure during construction, and wrongly installed profile dimensions.

[5]The original mass of one floating element was 3,000 tons
[6]The original draught was 2.1 meter

Chapter summary

This chapter developed the chosen variant of the previous chapter further into a resulting design. The design was structurally developed further and was checked to a combination of dynamic loads and current related drag loads. The foundations and the pendulums of the original design are capable of transferring the additional loads of the current relate drag forces. A small modification to the truss structure is proposed to resist for the additional current-related torsional load. The pendulum hinge location should move from 5 m to 13.5 m away from the middle of the floater to stabilize the structure due to the additional current-related drag forces and moments. The structural dynamics model showed that the downtime reduced from 1.1 days per year to 0 days per year based on a 50% confidence interval for the shifted pendulum hinge location design.

9 | Discussion

This section evaluates both the limitations and the capabilities of the report in order to be able to assess and value the outcome. It is argued that this report delivers a comprehensive and mutually well correlated set of results, being not only a design, but also the acquired knowledge about the dynamic response of the original Tidal Bridge design and the driving parameters in this dynamic response. The discussion concludes with a more zoomed out perspective, giving an objective evaluation of possible successive steps in the realization of a complete and firm Tidal Bridge design.

9.1 Evaluating the limitations of the report

The analysis used in this design report is a good approximation, but limitations of the analysis should be acknowledged. These limitations have to do with the physical phenomena that could not be modelled perfectly, which introduces uncertainties. A complete list of the limitations has been described in Appendix I. The most significant limitations has been specified below.

- **Unvalidated model:** The structural dynamics model is developed based on clear and experimentally confirmed theories. Consequently, the model is successfully and elaborately verified by checking the change in response induced by a change in the involved parameters and coefficients. As the model behaves robustly and reliably, it is applied with confidence for the investigations. However, as a final step, the model should be validated experimentally as well to assess its physical accuracy.

- **Excluded response to irregular waves:** The structural dynamics model only examines the response to regular waves and not to irregular waves. Theoretically, the response to irregular waves may accidentally lead to larger short peak accelerations in the deck than evaluated with the structural dynamics model. These short peak accelerations can only occur upon the combined coincidence of: a wave height larger than evaluated (significant) wave height, a wave having the critical wave period, and a leading dynamic response which is in phase with the critical wave. The probability of these short peak accelerations therefore is small. Furthermore, these may or may not become problematic depending on the user experience as the short duration is differently observed compared to a continuous exceedance of the limit.

- **Chosen serviceability limits:** The used serviceability limits have been found in literature which was scarcely available about the specific case of the Tidal Bridge. The serviceability limits for this design report have been deducted from an American author. Differently chosen serviceability limit may lead to a different determination of the downtime and a different geometry of the resulting design. Serviceability limits in Indonesia may be more tolerable and less risk averse, which could lead to less downtime and slightly smaller design dimensions.

Although the specified limitations may have an influence on the analysis of the design report, they do not impair the used analysis and the following results. If these limitations could have been tackled through the process, they would have had a limited impact and would have led to the same shape of the resulting design. Altogether, some numbers about the downtime or the dimensions of the resulting design may change upon precisely integrating and tackling the limitations. Most of the report stays unchanged and valid.

9.2 Evaluating the capabilities of the report

This design report provides both knowledge and an elaborate optimization solution in the study to dynamic response of the Tidal Bridge. The itemization below shortly discusses the significant contributions of the report:

- **Analysis of the involved parameters:** Many aspects of the dynamic response of the original Tidal Bridge design has been analyzed. The report expands on: the critical wave heights, the critical wave lengths, the limiting degree of freedom, the influence of the turbines and its shape, the influence of the serviceability limits, the wave direction, the current influence, and the sensitivity to the involved parameters and coefficients.

- **Quantification of the downtime:** The downtime of the Tidal Bridge has successfully been estimated, which provides valuable information about the usability of the Tidal Bridge.

- **Numerical laboratory:** The report also delivers a numerical laboratory to study the influence of the relevant Tidal Bridge parameters. This numerical model has been developed and can be used in further stages of the development of the Tidal Bridge concept.

- **Deliverance of a design:** The report delivers the resulting design which has carefully been found by using a systems engineering design methodology. The design is a result of assessing its pros against the cons of the rejected alternatives and variants.

- **Modular options:** The resulting design has modular options. It may be modified to a larger or smaller structure in case that the expected analysis about the dynamic response turns out to be different.

The capabilities of the report are only valuable as long as the used analysis has been performed in a scientific way. The summation below indicates some of the key features that characterize a scientifically well performed analysis:

- The used models have been functionally verified to check the dependency of the involved parameters to the model outcomes.

- The limitations have been kept in mind upon constructing and working with the models to keep the influence of those as small as possible.

- The sensitivity analysis showed that there are no too sensitive parameters in the model. The model outcomes therefore are not seriously influenced negatively by a faulty parameter.

- The used analysis has been the best that could be established in the available period of time, physical possibilities and computational possibilities.

9.3 Valuating the report

Section 9.1 shows how the results in this report are not perfectly accurate and the used analysis has some deficits. As discussed, the described limitations are not significant enough to reject the results of the report. The limitations introduce uncertainties that only lead to a little differently quantified downtime and resulting design dimensions. However, the reasoning that forms the basis for this resulting design stays firmly valid.

9.4 Evaluating the results within the overarching Tidal Bridge project

The report neatly finds an answer that meets the design objective and the straightforward project continuation includes the application of the resulting design in the subsequent Tidal Bridge design iterations. However, the additionally acquainted knowledge about the dynamic behaviour of the system does not validate the original Tidal Bridge design. The Tidal Bridge design could have been constructed differently taking the dynamic system in consideration from the start of the design process. The itemization below questions some fundamental design choices which are made earlier in the design process. The items below suggest a more integrated design approach:

- **The turbine design:** The intermediate report results showed that the large and heavy FishFlow turbines affect the total dynamic response tremendously. The large added mass of the turbines located close to the free surface leads to the disadvantageous dynamic behaviour. Why do the turbines need such long casings? Why are the turbines hanging so close to the free surface. Could the turbines contribute to the buoyancy capacity such that the floaters and the added mass of the floaters may be omitted?
- **The combined functionality:** The Tidal Bridge dynamic system becomes more complicated by the additional turbine functionality. What is the benefit of combining the functionality of the floating bridge and the tidal power plant? How can both functionalities benefit from separation into two independent structures?
- **The floating bridge design:** The original floating bridge design with the five boat like floaters is not the optimal solution for avoiding wave forces on the structure. Theory and the intermediate report results suggest that a semi-submersible floater design avoids wave forces. How does a floating bridge design look like that is optimized for the boundary conditions of the Strait of Larantuka?

The posed questions suggest three realistic options for the continuation of the Tidal Bridge project:

1. **Applying** the additional structure of the resulting design to mitigate the dynamic response.
2. **Redesigning** the Tidal Bridge with an integral design approach of the dual functionality and the challenging dynamic boundary conditions.
3. **Splitting** the two functionalities into two independent structures.

10 | Conclusions and recommendations

10.1 Conclusions

The design report looks into the dynamic problem of the Tidal Bridge, which is economically the preferred solution to cross the Larantuka Strait. The floating elements exceed the serviceability limit 23.4 days[1] per year which is undesirable. This design report quantified the downtime of the original Tidal Bridge structure and found an design improvement by making use of the system engineering design methodology. The objective of the design has been formulated as:

> *The objective of the thesis is to design an additional structure or modification to the Tidal Bridge that reduces the dynamic behaviour as a response of the wave forcing. The downtime must be reduced to a maximum of five days per year based on a 50% confidence interval. The design must respect the original Tidal Bridge design and follow the design requirements of the original design such as the lifetime, maintainability and constructability.*

The resulting design of the sway plates 9 x 17 m satisfies this design objective well. The design consist of nine sway plates with a width of 17 meters per floating bridge element. The plates hang in groups of three below the three middle floaters of each of the four floating elements of the Tidal Bridge. Figure 10.1 shows how those three groups of three plates hang below one floating element of the Tidal Bridge. The design has been structurally checked to an ultimate limit state forcing for a combined loading condition of current-related drag forces and the dynamic response due to waves with a return period of once in 1000 years.

The resulting design follows from one of the three alternatives of the slosh damper, the heave plate and the sway plate. The slosh damper should theoretically work, but the tested effectiveness showed to be marginal and a continuation of developing the slosh damper was stopped. Nine variants have been developed from the heave plate and sway plate alternatives. The variants that showed a sufficient dynamic optimization were taken into account for an evaluation. The sway plates 9 x 17 m scored the best to the evaluation criteria.

Improved downtime The first result of the design report is the determination of the downtime as this was unknown at the start of the process. The downtime of the original design is found to be 23.4 days per year and forms the base case for the design optimisations. Uncertainty introduced by the quantification of the near shore processes ensures that the downtime varies between 31.6 days and 16.3 days.

Table 10.1 shows the expected downtime for the base case and the resulting design determined with the probability of exceedance of the wave characteristics. The table shows that the resulting design leads to a downtime of 0 days per year based on a 50% confidence interval. Hence, the aims of the design objective concerning the functionality have been met very well.

	Probability		
	95%	**50%**	**5%**
Base case	31.6	23.4	16.3
Resulting design	3.1	0	0

Table 10.1 Yearly downtime in days for the base case and the resulting design

[1] based on a 50% confidence interval

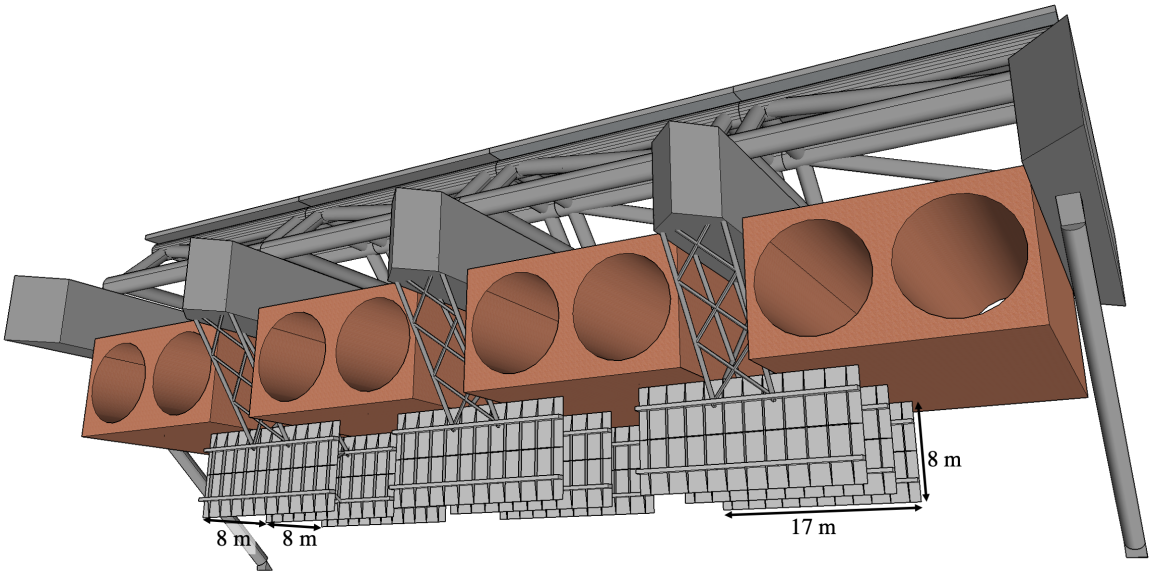

Figure 10.1 Perspective view with some provided measurements of the resulting design: the sway plate 9 x 17 m

Working principle The Tidal Bridge showed to be an inertia dominant system (Keulegan-Carpenter number $\approx 0.1 - 0.3$). Inertia based solutions to mitigate the dynamic behaviour are relatively most effective for small KC-values. The resulting design is an inertia based solution by generating much added mass in the critical degree of freedom of sway and the degree of freedom of roll. The additional inertia mitigate the dynamics as long as the driving wave forcing is not adapted. The wave related fluid particle accelerations are insignificant at the depth of the resulting design. Hence, the additional objects of the resulting design do not lead to additional driving wave forces.

Design geometry and additional current drag forces The sway plates are placed below the turbines to minimize the influence of wave forces. This works well as the forcing potential of the waves becomes significantly smaller farther away from the free surface. The added mass scales quadratically with the height of the sway plates. Therefore, the height of the plate is chosen as large as possible to lead to much effectivity. The height is restricted by the turbines and the minimum keel clearance. The width of the plate is set to 17 meter to avoid large moment forces within the sway plate structure. Multiple plates have been included in the design to generate enough added mass.

The large sway plates increase the current related drag forces. These additional drag forces lead to an increase of the torsion in the truss structure, the normal force in the pendulum, and the force on the pendulum foundation. The originally designed truss structure should be adapted somewhat to resist for the additional torsion force. The pendulums and foundations are able to resist for the additional loads without any modification.

The additional drag force leads to an unbalance in the rotational equilibrium. Moving the pendulum hinge location from 5 m to 13.5 m away from the middle of the floaters brings back the rotational equilibrium.

Advantages The list below sums the significant advantages of the resulting design. The first two advantages are benefits over the other presented variants of Chapter 7. The last advantage describes an increased functional value.

1. **Relatively low steel need:** The resulting design needs less steel than the other variant that fulfills the design objective. A reduced steel need is beneficial for the solution cost and the environmental impact.

2. **Modular approach:** The three different sway plate structures per floating element allow for a modular approach. The modules may need different dimensions depending on the depth and the desired effectivity. The pin connections provide convenient attaching and detaching. This allows for a comfortable constructability, maintainability, and adaptability to changing requirements after construction.

3. **Increased energy yield:** The turbines have a higher efficiency due to the additional blockage of the free flow of the resulting design.

10.2 Recommendations

This report provides a next step in the development of the Tidal Bridge concept. However, going forward it is recommended to assess a number of other topics before going to final conclusions regarding this design. The recommendations have been listed below and split into three groups, recommendations to improve: 1. the integral design, 2. the resulting design, and 3. the used analysis.

Recommendations to improve the integral design: The Tidal Bridge with its floating functionality, the turbines and the sway plate structure have all been designed separately one after another in the presented order. Preferably, such complex structures should be designed with an integral approach to avoid unnecessary complexity of additional structures. The findings of this report about the dynamic behaviour provide much input for an integrated design approach that may lead to a different Tidal Bridge design. Some ideas that could be part of a different design approach are:

- **Combining functionality:** The turbine casings may be developed such that they are able to carry both the bridge functionality and the turbine functionality. Floaters become unnecessary and their corresponding wave forces do not need to be taken into account anymore.

- **Splitting functionality:** The turbines make the system of the floating bridge dynamically complicated and more prone to be excited by wave forces. A split functionality leads to two less complicated systems, which may be cheaper to realize and to maintain.

- **Optimizing turbine casings:** The turbine casings can be further optimized such that they are less susceptible to the wave forcing.

Recommendations to improve the resulting design:

- **Using different types of materials:** About 50% of the needed steel of the resulting design is used for the plates and 50% is used for the supporting structure of the plates. The steel need of the plate is large to ensure structural integrity after loosing almost 2 millimetres on both sides due to corrosion. About 25% of the steel of the plate corrodes over its complete lifetime. Materials like recycled plastics or wood may be interesting solutions that lead to the same desired effectiveness while the material is more sustainable.

- **Introducing creative ideas to increase effectivity:** The original design may be further optimized with creative ideas that optimize the generation of added mass while the cost stay low. Interesting ideas may have the form of: 1. placing an additional plate below and above the sway plates encaging a larger volume of water, or 2. making use of water tanks instead of plates that encage water mass and have an optimized shape to reduce the current-related drag forces.

- **Integrating structural properties of turbines:** The turbines are avoided as structural supports in the designs as the capabilities for the transfer of forces are unknown of this third party product. Involving FishFlow Innovations, the turbine manufacture, in the design process of the sway plate may lead to a reduced need of structural elements to transfer the forces to the floaters.

- **Effectivity optimization:** The effectivity of the resulting design is much more than the objected effectivity. Cost for required material and cost for the construction phase could be saved by reducing the design dimensions such that objected effectivity is reached.

- **Porosity:** Porosity of the sway plate may lead to an increased drag force which results in more energy dissipation. The added mass is negatively effected by adding too much porosity and this optimization should be used with care.

Recommendations to improve the used analysis

- **Validation of the structural dynamics model:** A validation of the structural dynamics model with an experimental scale model to define the accuracy of the model is recommended. Simple experiments that simulate one complete floating element or solely a small cross section of the floating element may already lead to a successful initial validation.
- **Determination of the added mass:** Some uncertainty in the analysis relates back to the determination of the added mass. The added mass could be better determined with a computational fluid dynamics program to incorporate the effects of the complex geometry, the interference effects of the free surface and the bottom, and the dependency to excitation frequency.
- **Revision the serviceability limits:** A change in serviceability limits leads to a different understanding of the downtime and hence, to different dimensions of the resulting design. Research to the serviceability limits is recommended as the used research about the serviceability limits did not relate well to the situation of the Tidal Bridge. Preferably, practical tests to user safety and comfort are executed with conditions that correspond to the situation of the Tidal bridge. A barge or boat with a freely available deck that can be excited by waves already provides a satisfactory laboratory for testing the user comfort and safety.
- **Integration of irregular waves:** The integration of irregular waves in the structural dynamics model would contribute to making the numerical laboratory more complete. The duration and the magnitude of the short peak accelerations due to the irregular waves can be quantified with such an optimization.
- **Improving the wave characteristics model:** The wave characteristics model already neatly shows confidence intervals representing the uncertainty of the model. This uncertainty could be reduced by making use of hydrodynamic modelling software like Delft3D. Delft3D can model the process of wave generation by wind forces with the SWAN module taking depth, fetch and wind velocities into account. Delft3D also neatly incorporates the near shore processes by the usage of the WAVE module. A licence for the software of Delft3D and a bathymetry is needed to model the wave characteristics at the project site better.
- **Investigation of the drag related instabilities:** It has been assumed that drag related instabilities do not occur. The used analysis of this design report would be enriched by an investigation to the drag related instabilities that studies if those instabilities can occur and at which current velocity those instabilities become initiated.
- **Investigation of the slosh damper effectivity:** Theoretically, the slosh damper should be effective, especially for the used regular waves. Further research is recommended to study the effectiveness of the slosh damper for the situation of the Tidal Bridge as it might be an excellent solution to mitigate the dynamic response.
- **Investigation of the structural loads:** Hand calculations showed that the current-related torsional loads on the truss structure lead to reaching the maximum structural capacity. Further research is recommended to quantify the combination of the current-related torsion forces, the current-related shear forces, and the wave-related dynamic forces.

References

BSI. (2009). *UK National Annex to Eurocode 3: Design of steel structures – Part 5: Piling.* BSI Standards Limited.

BSI. (2017). *Maritime works – Part 1-2: General — Code of practice for assessment of actions.* BSI Standards Limited.

De Rijke, S., Koot, R., & Sengers, F. (2017). *Design report Palmerah bridge* (Tech. Rep.).

DNV. (2010). *Environmental Conditions and Environmental Loads.*

DNV. (2011). *Modelling and Analysis of Marine Operations.*

Dorgelo, G. (2020). *Optimising the dynamic response due to wind, waves and current.*

Drost, L. C. (2018). *An experimental study on the hydrodynamics and kinematics of a submerged rectangular cylinder in a wave-current environment.*

Faltinsen, O. M. (1990). *Sea loads on ships and offshore structures.* Cambridge University Press.

Gerritsma, J. (2015). *Hydromechanica 4 - Scheepsbewegingen, Sturen en Manoeuvreren.* Delft: Werktuigbouwkunde en Maritieme Techniek.

Greenhow, M., & Ahn, S. I. (1988). Added mass and damping of horizontal circular cylinder sections. *Ocean Engineering*, *15*(5), 495–504. doi: 10.1016/0029-8018(88)90012-1

Holthuijsen, L. H. (2007). *Waves in oceanic and coastal waters.* Cambridge University Press. Retrieved from www.cambridge.org/9780521860284

Hoogsteder, F. (2019). *An analysis of the dynamic response of the Palemerah Tidal Bridge.*

Journée, J. M. J., & Massie, W. W. (2008). *Offshore Hydromechanics* (Second ed.).

Kolkman, P. A., & Jongeling, T. H. G. (2007). *Dynamic behaviour of hydraulic structures - Part A: Structures in flowing fluid.*

Lwin, M. M. (2000). Floating Bridges. In W. Chen & L. Duan (Eds.), *Bridge engineering handbook* (pp. 549–571). CRC Press LLC. doi: 10.1201/b16523

Manshanden, G. (2020). *Dimensions FishFlow turbines* (Tech. Rep.). FishFlow Innovation Solutions.

MetOceanView. (2020). *Wind data at INDONESIA 0.2° 8S 123.2E.* Retrieved from https://app.metoceanview.com/hindcast/sites/indo/-8/123.2

Metrikine, A. V. (2015). *Dynamics, Slender Structures and an Introduction to Continuum Mechanics.*

Molenaar, W., & Voorendt, M. (2020). *Hydraulic Structures - General Lecture Notes* (2020th ed.).

Mutlu Sumer, B., & Fredsoe, J. (2006). *Hydrodynamics Around Cylindrical Strucures* (Revised ed.). World Scientific Publishing Co. Pte. Ltd.

Navionics. (2020). *Navionics Chart Viewer.* Retrieved from https://webapp.navionics.com/?lang=en#boating@14&key=d%60wq%40ec%7BmV

Nederlands Normalisatie-instituut. (1998). *NEN-ISO 2631-1:1997.* Nederlands Normalisatie-instituut.

Nederlands Normalisatie-instituut. (2019). *NEN-EN 1990+A1+A1/C2/NB.* Koninklijk Nederlands Normalisatie-instituut.

Nederlands Normalisatie-instituut. (2020). *Eurocode 3: Ontwerp en berekening van staalconstructies.* Koninklijk Nederlands Normalisatie-instituut.

Orhan, K., & Mayerle, R. (2020). Potential Hydrodynamic Impacts and Performances of Commercial-Scale Turbine Arrays in the Strait of Larantuka , Indonesia. *Journal of Marine Science and Engineering*, *8*(3).

Orhan, K., Mayerle, R., Narayanan, R., & Pandoe, W. W. (2016). Investigation of the energy potential from tidal stream currents in Indonesia. *Proceedings of the Coastal Engineering Conference*, *35*, 1–9. doi: 10.9753/icce.v35.management.10

Rijkswaterstaat. (2013). *Richtlijnen Ontwerp Hemelwaterafvoer van wegen en kunstwerken.* Rijkswaterstaat Dienst Infrastructuur.

Sadeghi, K., Dzayi, G. J., & Alothman, Z. (2017). An Overview of Generation, Theories, Formulas and Application of Sea Waves. *Academic Research International*, *8*(4), 57–67. Retrieved from www.savap.org.pk

Tao, L., & Dray, D. (2008). Hydrodynamic performance of solid and porous heave plates. *Ocean Engineering*, *35*(10), 1006–1014. doi: 10.1016/j.oceaneng.2008.03.003

Tidal Bridge. (2020). *The Larantuka Tidal Power Plant.*

Velicko, J., & Gaile, L. (2015). Overview of tuned liquid dampers and possible ways of oscillation damping properties improvement. *Environment. Technologies. Resources. Proceedings of the International Scientific and Practical Conference*, *1*, 233–238.

Vennell, R. (2013). Exceeding the Betz limit with tidal turbines. *Renewable Energy*, *55*, 277–285. Retrieved from http://dx.doi.org/10.1016/j.renene.2012.12.016 doi: 10.1016/j.renene.2012.12.016

Vos, R., Hoogeveen, A., & Van den Eijnden, E. (2017). *Deliverable 1 Management feasibility* (Tech. Rep.). Tidal Bridge.

Vos, R., Seinen, S., & Van den Eijnden, E. (2017). *Deliverable 2 Technical feasibility* (Tech. Rep.). Tidal Bridge.

Vugts, J. T. H. D. (1968). *The hydrodynamic coefficients for swaying, heaving and rolling cylinders in a free surface* (Tech. Rep.). Technische Hogeschool Delft.

Vuik, C., Beek, P. V., Vermolen, F., & Kan, J. V. (2004). *Numerieke Methoden voor Differentiaalvergelijkingen.*

Whelan, J., Graham, J., & Pierø, J. (2009). Inertia Effects on Horizontal Axis Tidal-Stream Turbines. *Proceedings of the 8th European Wave and Tidal Energy Conference, Uppsala, Sweden*, 586–591.

Zaaijer, M., & Viré, A. (2019). *Introduction to wind turbines : physics and technology.*

Appendices

A | Introduction

Contents of this appendix chapter

A.1 Geometry

All the four floating elements within the Tidal Bridge project have the same dimensions. The outer two floaters have a connection to a spud pole on the landfall side. The other side of this floater has a connection to the bed with a pendulum. The middle two floaters are both connected to the bed with two pendulums as is shown in Figure A.1. This study focuses on modelling one of those two middle floaters and the specified information later in this report reflects on one of those middle two floating elements.

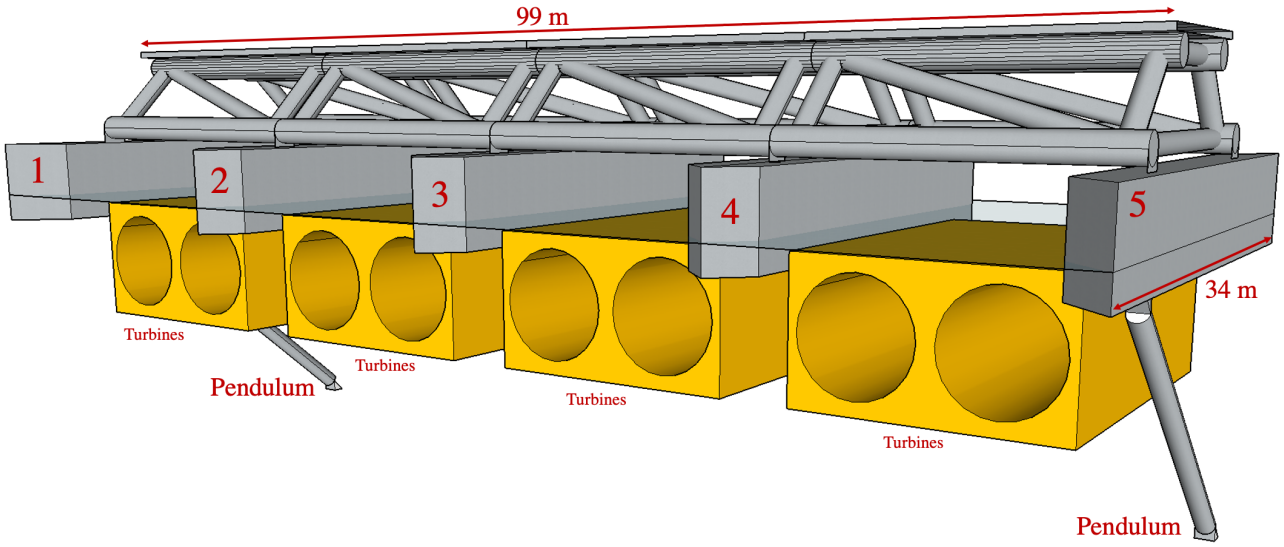

Figure A.1 Perspective sketch of one floating element with some dimensions

Figure A.2 displays the geometry of the floater. The geometry of the floater is relevant as the floaters interact with the water. Parameters such as the added mass, hydraulic stiffness and the inertia forces do all depend on the floater geometry.

The report from Antea (De Rijke et al., 2017) describes the dimensions and materials used for the floating elements of the Tidal Bridge. Dorgelo (2020) calculated the weight of the different parts of the structure and summarized the geometrical and mass data in Table A.1. Dorgelo (2020) calculated the mass moment of inertia around the origin for the three different axes. The parallel axes theorem is taken into account in these calculations. The masses and the moment of inertia is relevant for constructing the mass matrix.

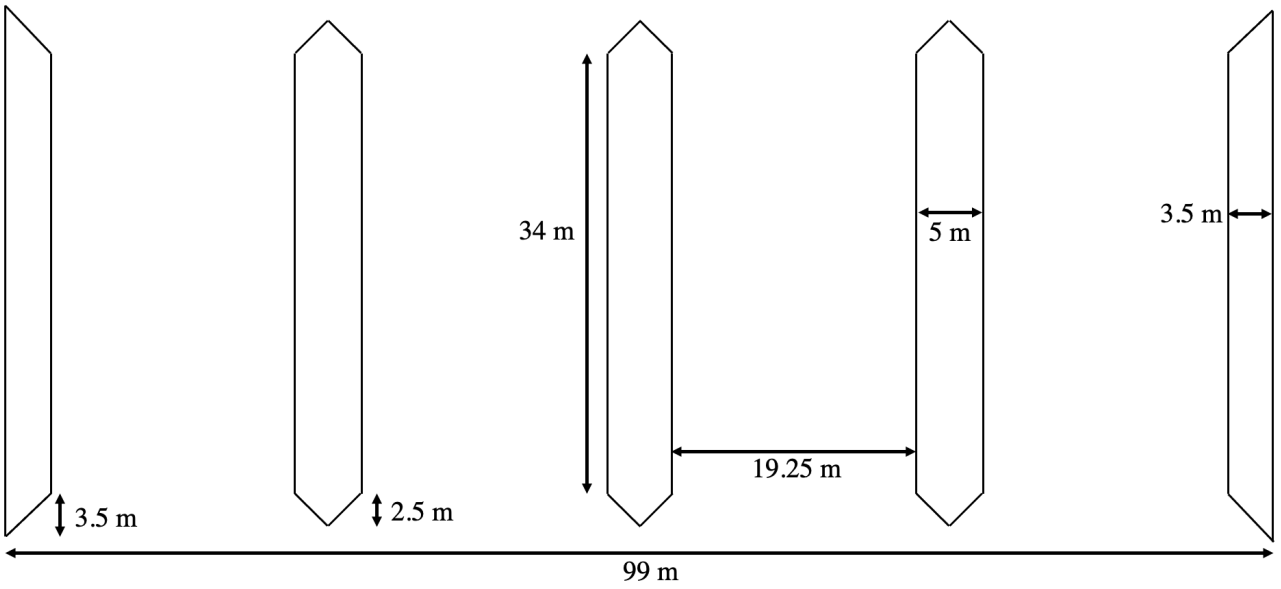

Figure A.2 Floater geometry part 1

A.2 Stakeholder analysis

This stakeholder analysis provides a short description of each stakeholder and a visual overview of all the stakeholder's power and interest in the project. This appendix should provide information about the interest of the stakeholders, their preferred solution and their importance for alternative solutions.

A.2.1 Stakeholder overview

The description of the stakeholders is given for the most powerful stakeholders first in the list below. The least powerful stakeholders are found at the bottom of this list.

PLN Perusahaan Listrik Negara (PLN) is the state owned electricity supplier in the region of the project. This company supplies electricity to most of the country. PLN is the client and project owner. The project procurement is in the hands of PLN as well. PLN contracts a loan from the Indonesian government to finance the project. The interest of PLN is very high as PLN tries to connect as many Indonesians as possible to the electricity grid. The power of PLN is very high as well as they are financing the project. Their preferred solution contains a power plant that continuously produces power to supply the people around the project area.

BAM BAM is a leading Dutch contractor that is directly contracted for the Tidal Bridge project. BAM owns the patent of the technical concept for the Tidal Bridge and the open tender requirements of PLN do not apply anymore. BAM will conduct the construction works following the EPC contract form. Project development, design, implementation, procurement of equipment and materials, construction, and some maintenance is all included in the contract. The high interest of BAM is to execute the project such that it can benefit economically from the project. Their preferred solution contains a connection that may be easy to construct and maintain over years with the least amount of risk. BAM has much power in the project due to patented idea of the Tidal Bridge.

FMO FMO is a Dutch state owned entrepreneurial development bank which provides loans for projects beyond the boarders of the Netherlands. The client PLN contracts a loan from the Indonesian government. The Indonesian government loans this money at the FMO. The FMO has interest in the project as this stakeholder could make a profit from loaning out the money. The stakeholder has some power as it could refuse to provide the loan as the project contains too much risk. Finding a different bank that loans out to the Indonesian government with such low interest rates could be complicated.

Table A.1 Geometry, mass and mass moment of inertia in SI-units (Dorgelo, 2020)

Component	**Size [x,y,z] (m)**	**Centre of mass [x,y,z] (m)**	**Mass (kg)**	**Mass moment of inertia [x,y,z] (10^6 kg·m^2)**
Road	[100, 11, 2]	[0, 0, 10.5]	400,000	[48 , 378 , 337]
Truss	[100, 22, 5.5]	[0, 0, 7.3]	900,000	[87, 800, 786]
Small floater 1	[3.5, 34, 6.6]	[-47.8, 0, 0]	48,000	[5, 110, 114]
Small floater 5	[3.5, 34, 6.6]	[47.8, 0, 0]	48,000	[5, 110, 114]
Large floater 2	[5, 34, 6.6]	[-23.9, 0, 0]	68,000	[7, 39, 46]
Large floater 3	[5, 34, 6.6]	[0, 0, 0]	68,000	[7, 0, 7]
Large floater 4	[5, 34, 6.6]	[23.9, 0, 0]	68,000	[7, 39, 46]
Turbines 1, 2	[19, 43.5, 13]	[-37.5, 0, -7.5]	320,000	[73, 482, 510]
Turbines 3, 4	[19, 43.5, 13]	[-12.5, 0, -7.5]	320,000	[73, 82, 110]
Turbines 5, 6	[19, 43.5, 13]	[12.5, 0, -7.5]	320,000	[73, 82, 110]
Turbines 7, 8	[19, 43.5, 13]	[37.5, 0, -7.5]	320,000	[73, 482, 510]
Equipment	[2.3, 12, 3]	[0, 0, 4.4]	120,000	[4, 2, 1]
Total		**[0, 0, 0**	**3,000,000**	**[461, 2608, 2692]**

Indonesian Government The Tidal Bridge project is part of the development strategies of the government to develop a prosperous Indonesia. The client of the Tidal Bridge project is a state-owned company. The client is not creditable enough. The Indonesian governments is willing to take a financial responsibility in the project. The Indonesian government is more creditable and the Dutch companies in construction and financials agree upon collaborating with the Indonesian government. The Indonesian government has a large interest in the project. The project contributes to a prosperous Indonesia clearly by the electricity yield and the connection between the two islands. The Indonesian government is taking responsibility and, therefore, can enforce ideas or changes to the design or the financials.

Atradius Dutch State Business Atradius is a Dutch state owned insurance company for export contracts. Atradius provides the insurance for the situation that the client refuses to pay or is not able to pay back its debt. The client directly pays to Atradius for providing its service. Atradius has some interest in the project as this stakeholder could find profit in the project as well. Atradius has some power as this stakeholder is one of the links that form the contract between the contractor and the client. Not informing or managing this stakeholder could delay the project.

Nusa Tenggara Timur (NTT) government This local government is the land owner of the landing locations. Furthermore, this local government is responsible for engaging the local community in the project to make the project a success. The local government should also take lead in the regional competitiveness of which the Tidal Bridge is a perfect example (Vos, Hoogeveen, & Van den Eijnden, 2017). The NTT could benefit very much from the Tidal Bridge and its interest is large. The power of the NTT is found in owning the land of the landing locations.

FishFlow Innovations FishFlow Innovations is a small Dutch company specialized in fish friendly pump and turbine solutions. FishFlow Innovations is providing the turbines for Tidal Bridge project in the original design. The developed turbines have not been tested yet on large scale. There are advanced plans to start large scale model test in the region of Bordeaux, France. The interest of the company is mostly driven by finding profit from the project. The company has some power as the FishFlow Innovations concept is unique. However, there are several other manufactures constructing turbines to yield tidal energy.

Witteveen+Bos Witteveen+Bos is a Dutch engineering consultancy firm providing the AMDAL and ESIA studies. These studies investigate the potential environmental and social impacts of the project. The AMDAL is conducted following Indonesian EIA regulations in collaboration with the Indonesian firm BITA. The ESIA is conducted following the IFC performance standards. Witteveen+Bos is interested in the project as it could make profit from performing the AMDAL and ESIA studies. The consultancy firm has not much power as there are many consultancy firms that could perform these types of studies.

Residents of the Flores and Adonara region The area may receive much economical and social benefits from the bridge. The area becomes interesting to develop tourism and companies in the region due to the enhanced connectivity. The Tidal Bridge stimulates the economy locally which is in favour of the people living around the bridge. The residents do not have much power in the project as those are not providing any service to the project.

Fischer men Fishermen experience hinder from the bridge as they cannot navigate freely through the strait anymore. Most local ships will be able to pass the Tidal Bridge by using the special ship passage close to one of the landfalls. The fisherman have interest in the bridge as it could potentially lead to economic benefits and hinder. The fisherman do not have much power in the project as they are not providing any service to the project.

Traffic The traffic between Flores and Adonara experience much interest in the enhanced connection. The traffic would benefit from a save and reliable passage. The traffic does not have much power in the project as it does not provide a service in the financials or the construction.

Large vessels Large vessels navigation cannot use the strait anymore and need to take a detour of about 80 kilometres. However, the Strait of Larantuka has not been a main route for large vessels (Vos, Seinen, & Van den Eijnden, 2017). Large ships do not have much power or interest in the project.

Dutch Government The Dutch government has great interest in the project as well. The realization of the project would offer economically much. The Dutch government would indirectly benefit from having the project to proceed. The Dutch government has not much power in the project. The Dutch government helps in the contract phase with the contact between the Indonesian and the Dutch stakeholders.

A.2.2 Stakeholder classification

A power interest grid is a visualizing tool that helps to organize the stakeholders of a project. The power interest grid for the Tidal Bridge project is visualized with Figure A.3. The grid helps in prioritizing the stakeholders concerning their power and interest in the project.

A.3 Analyzing previous theses

A.3.1 Overview of earlier work

Hoogsteder (2019) and Dorgelo (2020) both performed research to the dynamic characteristics of the Tidal Bridge. Their theses focused on describing the dynamic behaviour of the Tidal Bride design. This design report continues their theses by designing a solution that optimizes the dynamic behaviour. The results of Hoogsteder and Dorgelo form the basis for this design report. This appendix section summarizes the conclusions of Hoogsteder and Dorgelo to have a seamless connection between the previous report and this report. The chapter below initially explains the work done by Hoogsteder and secondly the work done by Dorgelo.

Hoogsteder performed a general study to the complete dynamical system of the floating elements of the Tidal Bridge. She looked into the dynamic response to the current and wave forces and whether these would not make that traffic serviceability limits to be exceeded. She concluded that the serviceability limits are exceeded. However, the models used showed awkward results and the verification of the models have not successfully been completed. Hoogsteder laid the basis for studying the dynamics and she gave an initial insights needed for further research.

Dorgelo continued to study the dynamics of the Tidal Bridge as many questions were left unanswered concerning the topic. Dorgelo's approach focuses on just one single floating element as a dynamic object. He tried to model the dynamic behaviour of one floating element with a numerical model which he succeeded to do. He demonstrated the sensitivity to the design parameters. He suggested design optimization strategies which have not been tested by him.

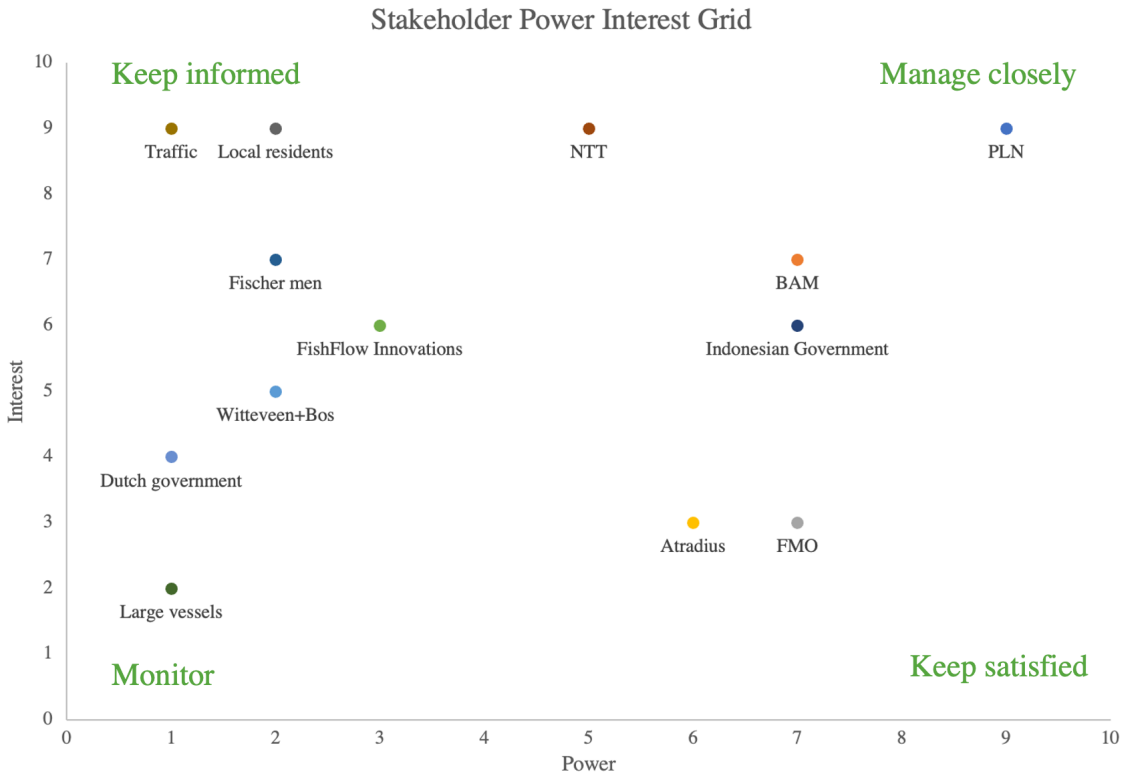

Figure A.3 Power Interest Grid for the Tidal Bridge project

A.3.2 Hoogsteder's thesis

Motivation for the study Hoogsteder started to research the dynamic behaviour of the Tidal Bridge. The contractor BAM possesses the initial design of the Tidal Bridge project, but the technical feasibility concerning the dynamic behaviour of the project has not been proven yet. Hoogsteder formulated here the major research question as: "Is the dynamic response of the present design of the Palmerah Tidal Bridge induced by waves and currents of an acceptable magnitude regarding traffic serviceability?" With this question she tried to "create insight in the behaviour of the coupled floating bridge structure" (Hoogsteder, 2019). In here research she also tried to obtain information about the most sensitive structural parameters in order to be able to improve the dynamic behaviour by tweaking those sensitive structural parameters.

Results Hoogsteder concluded that the floating elements experience severe motions due to the current and wave forcing and the dynamic response was not of an acceptable magnitude regarding traffic serviceability. She also proposed design optimizations which could improve the dynamic behaviour of the bridge. She introduced to rotate the Tidal Bridge elements and pendulums around the z-axis such that the pendulum orientation is dynamically more favourable to the normative wave and current loads. Here analysis proved this solution to have favourable effects on the dynamic behaviour.

Furthermore, she introduced an improved spud pole design. With this improved spud pole design, she tried to increase the tension in the x-axes in order relieve compression in the pendulums. The compression forces in the pendulums made here model unstable. This design improvement worked for her model. This design optimization assumes that the transfer of forces due to the currents is conveyed by a catenary system with four catenary elements (the four floating elements). This assumption is not valid as the pendulums are responsible for the transfer of the horizontal drag and wave inertia forces due to the current.

Drawbacks in modelling Her analysis results seemed to be off for several reasons. With a negative current direction, the floating element started to hoover as a kite above the water line due to the drag forces. This special outcome resulted from a simplification in here model. The simplification needed to be applied as the

model was not able to process the current forces. Furthermore, modelled acceleration magnitudes did not satisfy modelled displacement magnitudes. The ratio of the displacement over the acceleration magnitudes differed in her study from a factor 0.75 up to a factor 100. Normally, those ratios do not differ that much and are more in the order or 1 to 5 depending on the excitation frequency.

Flaws in the thesis There were a some flaws in the work of Hoogsteder that affects the credibility of the thesis. Initially, Hoogsteder tried to model the complete system which is very expanded and complex. She needed to make simplifications which resulted in a model that could not be verified. Unfortunately, the outcomes resulted to be unrealistic and unusable. Secondly, she looked into the significant wave period and the largest significant wave heights to find out what forcing characteristics were normative. However, wave periods that are close to the eigenperiods of the system may have a more significant effect to the structure, than the significant wave period or wave height. Thirdly, here assumption that a catenary system was responsible for transferring the current forces to the sides, lead to positive effect in here model. However, this assumption is not physically realistic and brings difficulties in the construction phase. Finally, the stabilizing effect of the turbines were not taken into account in here dynamic model.

Conclusion The work of Hoogsteder gives good insight in factors that may influence the dynamic behaviour of the Tidal Bridge. She tried to model the complete system which lead to problems with the verification. Here conclusion that states that the serviceability limits of the Tidal Bridge are exceeded, may not be valid. Further research with a different approach is needed to define the problems concerning the dynamic behaviour of the Tidal Bridge.

A.3.3 Dorgelo's thesis

As Hoogsteder's thesis focused on the complete dynamic system of the Tidal Bridge floating elements, Dorgelo's thesis focused on modelling one single floating element of 100 meters of the Tidal Bridge. On a fundamental level, Dorgelo tried to find parameters that drive the dynamic behaviour of one floating element as modelling the complete system did not work out well with Hoogsteder's research. He constructed a numeric python model to model one element. He did scale experiments to find the relations in the added mass and radiation damping formulas to enhance his model.

Motivation for the study Dorgelo tried to find answers to two questions: "1. How can the dynamic response due to a two-dimensional forcing of a Tidal Bridge be determined? 2. What design choices can further optimize the dynamic behaviour of a Tidal Bridge?" (Dorgelo, 2020). Answers to these questions were not studied yet. The questions were interesting as the answers provided possibilities to optimize the current Tidal Bridge design. The questions were also interesting as the answers showed the relation between the wave heights and the complementary accelerations and displacements.

Method Dorgelo constructed a numerical python model in which he included all relevant processes that drove the dynamic behaviour of one single floating element. He did not include the boundary condition that the floating element is connected to the other floating elements on the sides and he assumed open boundaries on the sides. Dorgelo conducted scale experiments with a model to determine relations for geometry with added mass and geometry with radiation damping. He consequently added those relations in his model as well. He was not able to find relations for the radiation damping and used simple existing formulas to model the radiation damping. After verifying his model, he performed a sensitivity analyses to identify the sensitivity of the included parameters.

The constructed model did not take into account that the waves transform while propagating from open sea into the strait. The model looked into the dynamic response of the waves that are present exactly on the spot of the tidal bridge. However, models that predict wave heights and wave lengths are constructed to open ocean circumstances. The model does not take the near shore processes and wave-current interactions into account. Therefore, the results of the model may not be directly compared to open ocean waves. Furthermore, the model can only process regular waves.

Results A result of his modelling was that traffic and wind have negligible effects on the dynamics. Dorgelo did also research the effects of an approaching wave field. With such an approaching wave field he showed

that accelerations may adopt values of 200% of the constant wave fields. A very important result from Dorgelo is that the maximum accelerations for the three degrees of freedom happened under three different loading combinations. The dynamic behaviour of the elements differed upon the changing wave direction. Hence, there were six conditions that realized six different maximum accelerations. A positive or negative current did only lead to a constant rise or decrease in draught. He did not combine the accelerations for the different degrees of freedom into a combined acceleration term.

Dorgelo also performed a sensitivity study to the most important parameters that define the dynamic behaviour. He concluded that the mass of the segment, the added mass, the floater length, the design turbine force and the pendulum angle are the most significant parameters in finding design optimizations. Another result of Dorgelo is that he discovered that the dynamic properties improved with a decreasing pendulum angle. The downside of this adaptation is that the buckling length increases. An increased buckling length results in a need for a structurally more strong and stiff pendulum design.

Missing results Dorgelo's research has been very complete and many results about the dynamic behaviour and the sensitivity to the important parameters have been presented. After reading this research, there is still much to be researched and Dorgelo's research introduces new questions. At first, the sensitivity to the most important parameters has been described and a corresponding design optimization has been qualitatively been proposed. The effect of those proposed optimizations is not known yet. Secondly, Dorgelo paid much attention to making the structure stiffer, but making the structure softer could also improve the dynamic behaviour. Thirdly, Dorgelo wrote initially about serviceability limits, but did not use those limits in his conclusions. Dorgelo's research does not show how much time the Tidal Bridge may be out of service. Fourthly, all results of the research of Dorgelo have been found under regular waves. Irregular waves may provide different results. Last of all, he did not look into researching damping strategies for the Tidal Bridge as there are many possible ideas concerning damping that could enhance the bridge dynamics.

Conclusion Dorgelo conducted elaborate research on the dynamic behaviour of the Tidal Bridge. He constructed an in depth numerical model with which he neatly researched the significant parameters of the Tidal Bridge design that influence the dynamic behaviour the most. He took a highly scientific approach for his research and his conclusions were well considered. A study to the downtime of the Tidal Bridge is lacking and strategies to optimize the dynamic behaviour have not been tested yet.

Seamless continuation of research The thesis of Hoogsteder gave the initial insights in the complete system of the Tidal Bridge and how those exceed the serviceability limits. The thesis of Dorgelo provide much more specific information on the dynamic behaviour of one floating element. An evident continuation of these theses focuses on improving developments and evaluating those developments. Dorgelo's numerical model forms a computational laboratory in which these new developments may be tested. This project seamlessly continues the previous theses by using Dorgelo's numerical model to design improvements such that the serviceability limits of the Tidal Bridge will not be exceeded.

B | The basis of the design

Contents of this appendix chapter

B.1 Defining the serviceability limits

The serviceability limits define the tolerable movements of the floating element that ensures people to pass the structure safely and comfortably. These limits are leading in defining the maximum tolerable dynamic behaviour of the Tidal Bridge. These defined serviceability limits within this appendix are used in the itemization of functional requirements in Section 2.1.

Expressing serviceability limits

Serviceability limits are expressed in maximum accelerations. Acceleration is the only kinematic characteristic that can be perceived by a user if displacement, velocity and accelerations are the concerned kinematics. A user cannot perceive its displacement nor its velocity. However, accelerations of the Tidal Bridge translate into forces through Newton's second law and those may be perceived by its users.

Therefore, Tidal Bridge serviceability limits are expressed in maximum accelerations for either the sway, heave and roll degrees of freedom separately. The serviceability limit can also be expressed in solely one maximum combined accelerations value, which combines the three degrees of freedom into one value.

There is one exception to the stated information. The roll displacement are perceived by users as well. A bridge deck with a rotation leads to a different user experience than a regular flat deck. Therefore, the Tidal Bridge serviceability limits are also expressed in maximum roll displacements, also known as rotations.

Specified serviceability limits

The Indonesian government does not specify any serviceability limits for floating structures. Norms and studies addressing Tidal Bridge like structure will therefore be values as leading to determine the serviceability limits. Dutch norms composed by the Nederlands Normalisatie-instituut (1998) presents results from research conducted in public transport that may serve as serviceability limits. The research shows that people in public transport experience: "no uncomfortable movements" with accelerations smaller than 0.315 m/s^2, a "little uncomfortable movements" with accelerations between 0.315 m/s^2 and 0.63 m/s^2, and "fairly uncomfortable movements" for accelerations between 0.5 m/s^2 and 1 m/s^2 (Nederlands Normalisatie-instituut, 1998). Those serviceability limits are adopted as combined acceleration limits in this report as split out serviceability limits are lacking.

Research to experienced comfort on board of ships may be summarized by Figure B.1 which is specified in the coarse reader MT3408 of the bachelor of maritime structures at Delft University of Technology (Gerritsma, 2015). The figure shows that passengers do not perceive any accelerations as long as those are smaller than 0.3 m/s^2. The ship's movements become uncomfortable as the accelerations take larger values than 1.1 m/s^2 (Gerritsma, 2015).

The handbook of floating bridges specifies serviceability limits for the sway, heave and roll directions separately to be 0.5 m/s^2, 0.5 m/s^2 and 0.05 m/s^2 for sway, heave and roll respectively (Lwin, 2000). A dutch manual describing norms for constructing roads specifies a norm for the maximum slope roads to be 0.06

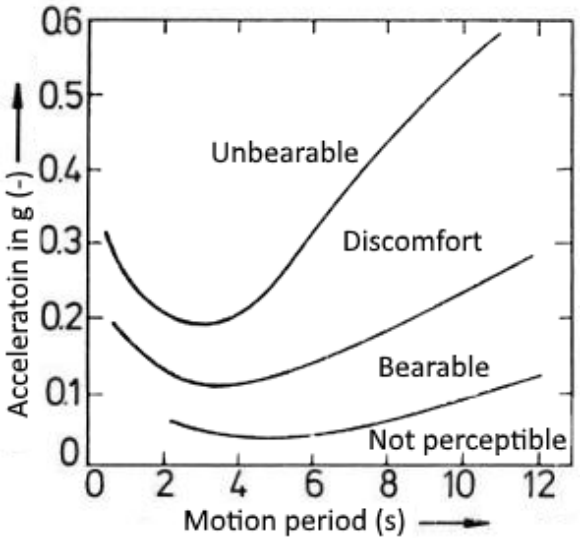

Figure B.1 Ship acceleration perceptions as a function of the specific excitation period (Gerritsma, 2015)

radians.

Overview of the found serviceability limits

Table B.1 shows an overview of the found serviceability limits. The results of Table B.1 shows that the user comfort enhances with smaller accelerations and roll displacements. Accelerations below 0.3 m/s^2 can be considered as not perceptible. Accelerations up to 0.5 m/s^2 may be well acceptable by users. Accelerations between 0.5 and 1.0 m/s^2 may be bearable and most users may be able to use the bridge. However, safety can not be be guaranteed by authorities anymore for accelerations that would are not acceptable for all users. Accelerations of the bridge deck over 1.0 m/s^2 are uncomfortable and may be highly unsafe for all type of users.

Table B.1 Heave, sway, roll and total serviceability limits as defined by different sources (Nederlands Normalisatie-instituut, 1998; Gerritsma, 2015; Lwin, 2000; Rijkswaterstaat, 2013)

Source	**Sway**		**Heave**		**Roll**		**Total**		
	(m)	(m/s^2)	(m)	(m/s^2)	(rad)	(rad/s^2)	(m)	(m/s^2)	
NEN-ISO 2631-1:1997	-	-	-	-	-	-	-	0 - 0.32	(not perceptible)
	-	-	-	-	-	-	-	0.32 - 0.63	(a little uncomfortable)
Reader MT 3408	-	-	-	-	-	-	-	0 - 0.3	(not perceptible)
	-	-	-	-	-	-	-	0.3 - 1.1	(bearable)
Handbook Floating Bridges	0.3	0.5	0.3	0.5	0.009	0.05	-		
Precipitation guidelines	-	-	-	-	0.06	-	-	-	

Chosen serviceability limits

The chosen serviceability limits follow the guidelines of the Handbook Floating Bridge by Lwin (2000) as this Handbook is specifically written for floating structures. The serviceability limits for sway, heave and roll are 0.5 m/s^2, 0.5 m/s^2 and 0.05 m/s^2 respectively. Furthermore, the maximum rotation is set to be 0.06 radians.

Accelerations of one degree of freedom may stay within its limits. However, the perceived acceleration becomes larger whenever an acceleration of a different degree of freedom arises as well. The user experiences the combined combined acceleration. A limit for this combined acceleration is defined as well and is set to be 0.7 m/s^2 based on the results of Table B.1. Chapter 3 shows that the limits of the separate degrees of freedom and the maximum rotations are automatically respected as long as the combined acceleration serviceability limit is not exceeded. The only one important serviceability limit is therefore the combined acceleration limit of 0.7 m/s^2. A summary of the formally chosen serviceability limits for the different degrees of freedom may

be found in Table B.2. In the course of this report, the combined acceleration limit is the only serviceability limit that is tested to the results of the dynamic model since the other accelerations of the separate degrees of freedom automatically fulfill the chosen serviceability limits upon fulfilling the combined acceleration limit. These defined serviceability limits are used in the summation of functional requirements in Section 2.1.

Table B.2 Acceptable accelerations for heave, sway, and roll for the Tidal Bridge

Source	**Sway**		**Heave**		**Roll**		**Total**	
	(m)	(m/s^2)	(m)	(m/s^2)	(rad)	(rad/s^2)	(m)	(m/s^2)
Total	**-**	**0.5**	**-**	**0.5**	**0.06**	**0.05**	**-**	**0.7**

B.2 Developing the wave characteristics model

Data of field experiments to wave characteristics at the project site are not existing. The missing wave data is greatly unfortunate as the waves are governing in the dynamic behaviour of the Tidal Bridge. Probabilistic wave data is needed to know how many days per year the Tidal Bridge need to be shut of due to exceeding the serviceability limits. This section shows how data about the wave probabilistics of the project site is estimated.

B.2.1 Initial estimation of the extreme wave height

The orientating studies about the Tidal Bridge of Antea and Tidal Bridge BV experienced the same problem that field experiment data about the wave probabilistics is lacking. Vos, Hoogeveen, and Van den Eijnden (2017) opted to make an estimation of the wave climate around the project site by transforming wind data into wave data. He used the formulas of Bretschneider, wind probabilistic data, average depth and fetch to calculate the maximum wave heights, wave lengths and wave periods that occur once per year and once in 100 years. The maximum wave heights that occur once per year are about 65% to 75% the wave height that occur once in 100 years. These estimated wave heights occur on open sea in deep water conditions. Near shore processes have not been taken into account in this estimation. The wave height at the Tidal Bridge location may differ from the findings of Vos, Hoogeveen, and Van den Eijnden (2017) due to the near shore processes. The results of Vos, Hoogeveen, and Van den Eijnden (2017) have been summarized in a radar plot in Figure B.2. Also, wave data of the maximum wave height of either one of the directions have been presented in Table B.3.

	210-230°	**030-050°**
Fetch	32,000 m	660,000 m
Average water depth	18 m	2,000 m
Wind velocity	8.5 m/s	11.9 m/s
Significant wave height	0.8 m	3.3 m
Significant wave period	3.4 s	7.4 s
Significant wave length	18.5 m	85.6 m

Table B.3 The approached significant wave height, period and length that may occur once in one hundred year on open sea for the two orientations of the strait calculated with the Bretschneider formulas by Vos, Hoogeveen, and Van den Eijnden (2017).

Conclusion

The analysis of Vos, Hoogeveen, and Van den Eijnden (2017) provides a good initial estimation for wave characteristics that could occur on open sea close to the Larantuka Strait. However, the wave heights at the Tidal Bridge project site may be different due to near shore processes. These near shore processes are not included in the estimation. Furthermore, this wave data is only provided for the return period of once per year and once per 100 years.

B.2.2 Calculating the wave probabilistics at site

This design report tries to find design optimizations that lead to less downtime yearly. The structural dynamics model developed for this report can determine with which wave height the serviceability limit is

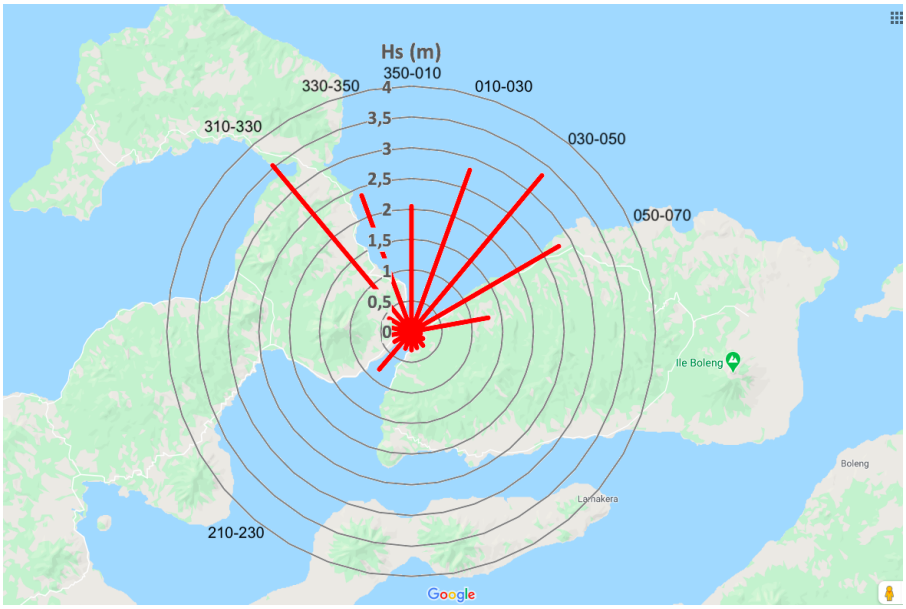

Figure B.2 A directional plot of estimated significant wave heights that have a probability of occurrence of once in one hundred years (Vos, Hoogeveen, & Van den Eijnden, 2017)

exceeded. The downtime can be determined by finding the probability of exceedance of this found wave height by the structural dynamics model. A tool that can calculate the probability of exceedance for every wave height at the project location is needed to determine the yearly downtime of the Tidal Bridge or a possible design optimization of the Tidal Bridge.

A tool is developed by python programming that can determine the probability of exceedance of a defined wave height at the project site of the Tidal Bridge. This tool finds this probability of exceedance by performing four steps that can be observed in Figure B.3. The tool takes as input a wave height at the project site of which the probability of exceedance is unknown. Step 1 takes near shore processes into account to account to transform the wave height of the project site into a wave height offshore. This wave offshore has been generated by wind that may come from eight different directions. Step 2 calculates these winds speeds from eight different directions and takes the offshore wave height, fetch and average depth per direction as input. In step 3, the probability of the wind speeds is calculated by making use of wind data and Weibull distributions. Step 4 combines the eight probability of occurrences of the wind speed into one probability of exceedance. The computations of every steps have been explained within smaller paragraphs.

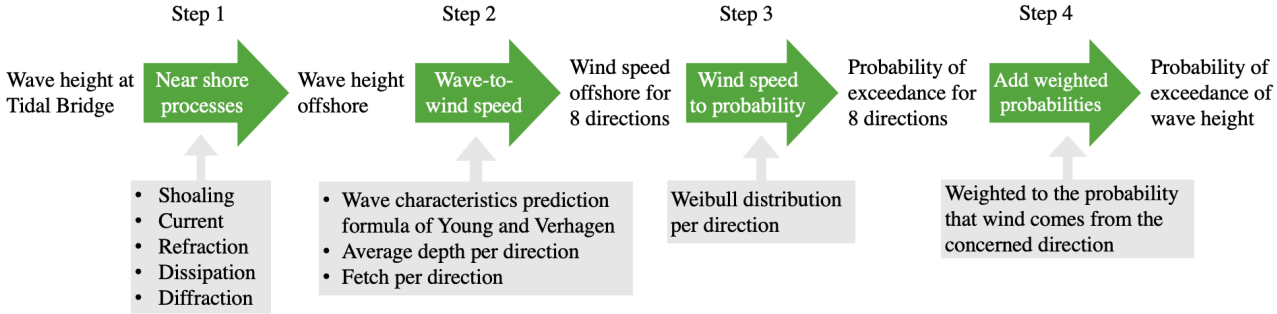

Figure B.3 Flow chart of the steps executed by a programmed tool to find the probability of exceedance of a defined wave height at the project site

Step 1: Transforming near shore wave heights to offshore wave heights

Waves come from offshore and the wave probabilistics are known offshore. Therefore, waves heights at the project site need to be transformed into wave heights offshore. This transformation can be done by including near shore processes into account. The near shore processes that are taken into account, are:

1. **Shoaling:** The depth at the project site is smaller than offshore. Wave heights becomes slightly larger as waves propagate from deep water into the transitional water depth of the project site.
2. **Current:** Strong tidal currents are present at the project site, while this current does not exist offshore. Waves become larger as those travel in the opposite direction of the current. Waves become smaller as those travel parallel to the current direction.
3. **Refraction:** Refraction describes the phenomenon that waves bend upon travelling over different depths. This effect can be observed in Figure B.4 Effectively, this results in two effects that should taken into account for the situation of the Tidal Bridge. The first effect is that wave heights are smaller within bays due to the waves that refract to the shore. The waves that "feel" the bottom also refract to the shores of the Strait partly and the wave height at the project location is smaller than offshore. The second effect happens to waves that come from a different direction than the directions parallel to the orientation of the strait. These waves need to make a turn into the strait. If this turn happens by refraction, than those waves loose energy and height.
4. **Dissipation:** Waves that travel into shallower areas, like the project site, are more prone to show white capping and energy dissipation. The significant wave height becomes smaller due to this phenomenon.
5. **Diffraction:** This effect describes the occurrence of waves in sheltered zones. Waves bend into sheltered zones and have smaller wave heights in the sheltered zone. The project site is sheltered from six directions. Waves that reach the project site from either one of those six directions have been reduced a lot by diffraction.

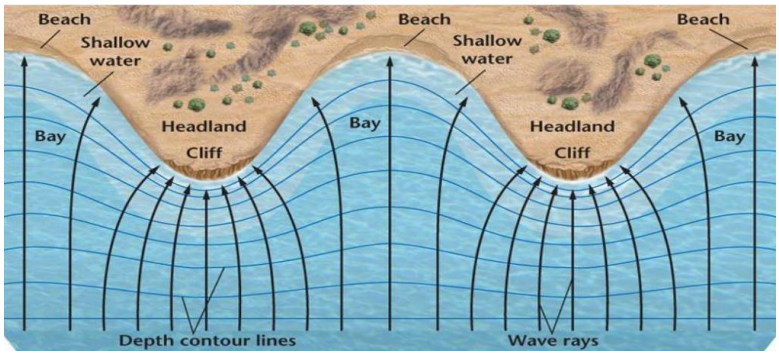

Figure B.4 Refraction of ocean waves

Almost all the near shore processes reduce the wave heights at the project site compared to offshore. Only the effects of shoaling and the wave-current interaction lead to an increase of the wave height at the project site compared to offshore. The next step can be started n the wave height at the project site has been transformed to a wave height offshore.

Step 2: Transforming offshore wave heights into wind speeds

This step transforms the offshore wave height into wind speeds from eight different directions. Bretschneider was the first who combined wind speed, fetch and average depth in a formula to calculate the wave height and the wave period. Bretschneider formulas have later been improved by Young and Verhagen in 1996 and by Breugem and Holthuijsen in 2006 (TU Delft lecture notes Hydraulic Structures, 2020). These improved equations may be found in Equation B.1 and Equation B.2.

$$\tilde{H} = \tilde{H}_{\infty} \left\{ \tanh\left(0.343 \cdot \tilde{d}^{1.14}\right) \cdot \tanh\left(\frac{4.41 \cdot 10^{-4} \cdot \tilde{F}^{0.79}}{\tanh\left(0.343 \cdot \tilde{d}^{1,14}\right)}\right) \right\}^{0.572} \tag{B.1}$$

$$\tilde{T} = \tilde{T}_{\infty} \left\{ \tanh\left(0.10 \cdot \tilde{d}^{2,01}\right) \cdot \tanh\left(\frac{2.77 \cdot 10^{-7} \cdot \tilde{F}^{1.45}}{\tanh\left(0.10 \cdot \tilde{d}^{2.01}\right)}\right) \right\}^{0.187} \tag{B.2}$$

Where:

$\tilde{H}$	[-]	=	$\frac{g \cdot H_{m0}}{U_{10}^2}$
$\tilde{T}$	[-]	=	$\frac{g \cdot T_p}{U_{10}}$
$\tilde{F}$	[-]	=	$\frac{g \cdot F}{U_{10}^2}$
$\tilde{d}$	[-]	=	$\frac{g \cdot d}{U_{10}^2}$
H_m0	[m]	=	significant wave height ($H_{m0} \approx H_s$)
T_p	[s]	=	peak wave period
U_{10}	[m/s]	=	wind speed at 10 meters height
g	[m/s^2]	=	gravitational acceleration (9.8 m/s^2
d	[m]	=	average water depth over the fetch
F	[m]	=	fetch
$\tilde{H_{\infty}}$	[-]	=	dimensionless wave height at deep water $\tilde{H_{\infty}} = 0.24$
$\tilde{T_{\infty}}$	[-]	=	dimensionless wave period at deep water $\tilde{T_{\infty}} = 7.69$

Normally, Equation B.1 is used to calculate the significant wave height and the peak period. The wind velocity at an altitude of 10 meters can be calculated with a solver upon inputting a wave height, fetch and average depth. The used fetch and average depth per wind direction are displayed in Figure B.4. Eight wind velocities can be calculated for the eight wind directions by using Equation B.1 in which the same wave height is inputted and the corresponding fetch and average depth per wind direction. The next step can be executed now the wind speeds of the eight different directions have been found.

Direction	Depth (m)	Fetch (km)
N	2000	270
NE	2000	600
E	2000	300
SE	200	8
S	200	6
SW	200	25
W	200	500
NW	200	450

Table B.4 Used depths and fetches to calculate the wind speeds from wave heights

Step 3: Transforming wind speeds into probabilities

This step transforms the found eight winds speeds into eight independent probabilities. This transformation is based on wind probabilistic data. Wind data has been retrieved from MetOceanView (MetOceanView, 2020). This web page provides data generated by the NOAA CFSR. This is a numeric model from the National Centers for Environmental Prediction taking the interaction between the oceans, land and atmosphere into account. Figure B.5 shows the location that has been used to retrieve wind data from. This location is chosen because it is relatively close to the project site while it is far enough from the land to make sure that disturbances of the land in the wind data are unlikely. The probability of occurrence of the different wind speeds for the eight directions is expressed in percentages and may be viewed in a radar plot of Figure B.6. The probability of occurrence of wind speeds follows a Weibull distribution. Weibull distributions have been plotted through the wind speed data of the eight wind directions in order to make the discrete data continuous. An example of such a continuous Weibull fit through the discrete wind probabilistics data can be found in Figure B.7.

The probability of occurrence of a wind speed of a defined direction can be calculated with the the continuous functions of the Weibull fit of the same direction. Eight probabilities of occurrences may be calculated by using the eight Weibull fits and the eight wind speeds. The next step can be executed now wind speeds have been transformed into probabilities.

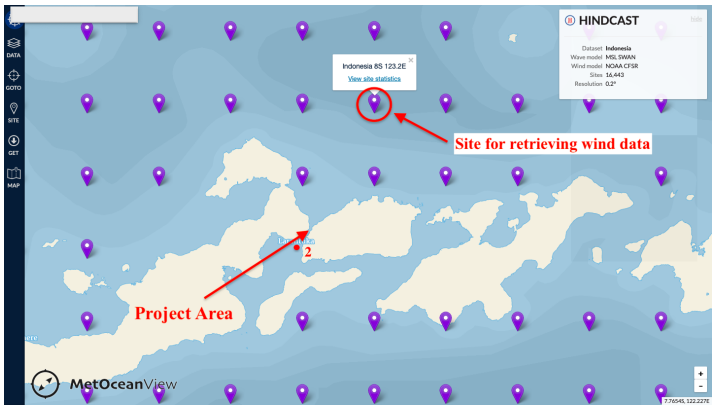

Figure B.5 The location used for retrieving the wind data (MetOceanView, 2020)

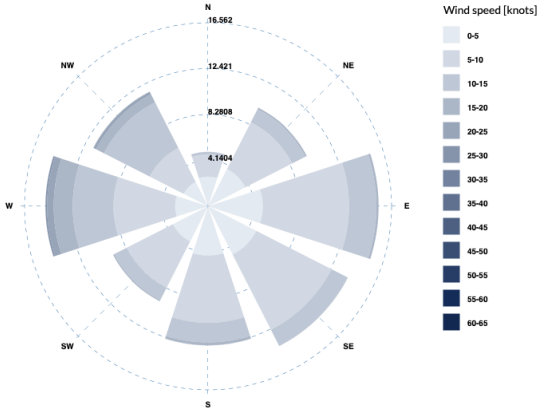

Figure B.6 The distribution of the wind speeds at the selected location in the form of a wind rose expressed in percentages (MetOceanView, 2020)

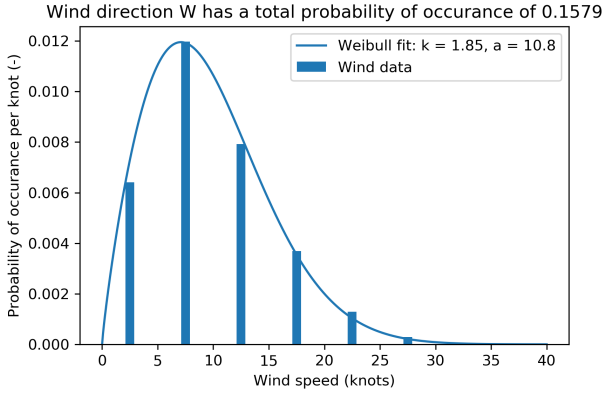

(a) Wind directed from West

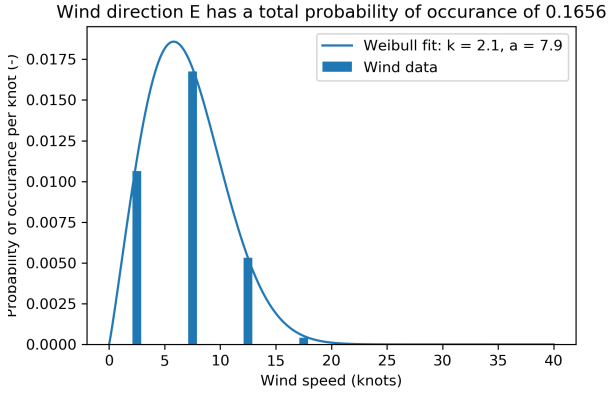

(b) Wind directed from East

Figure B.7 Weibull distributions fitted through the probabilistic wind data

Step 4: Combining the probabilities

This step is about combining the probability of occurrence of the eight wind speeds into one probability of exceedance. Wind can originate from only one direction at the same time. The wind data from MetOceanView (2020) also provides the probability of occurrence that wind originates form the defined directions. Upon multiplying the calculated probability of occurrence of a defined wind direction by the probability of occurrence that the wind originates from that corresponding direction, then the weighted probability is found. By adding all those probabilities, the final probability of exceedance is found. The probability that a wave height occurs is also the probability of exceedance. Equation B.3 displays the previous set of words in the form of an equation.

$$P_{tot} = \sum_{n=1}^{8} P_{1,n} \cdot P_{2,n} \tag{B.3}$$

Where: P_{tot} [-] = probability of exceedance of wave heights at the project location.
$P_{1,n}$ [-] = probability of occurrence of the defined wind speed from direction n
$P_{2,n}$ [-] = probability that the wind originates from direction n

Presenting the wave characteristics model results

Probability of exceedance The results of the wave characteristics model can be summarized in a graph that shows the probability of exceedance plotted to the concerned wave heights. This plot may be observed in Figure B.8. Three lines may be observed within Figure B.8. The middle line with the label "Probability

of exceedance" shows the result that expected probability of exceedance for the defined wave height at the Tidal Bridge location. The two lines around the middle line noted with the labels "5% confidence" define the confidence interval boundaries of the presented result.

These confidence interval lines have been obtained by differently chosen near shore processes coefficients in Step 1: transforming near shore wave heights into offshore wave heights. The near shore processes have been estimated by best guesses upon a good engineering understanding. Mistakes may have been introduced due to this estimation of the near shore processes coefficients. A best case and worst case estimate have been made for each near shore process. A model computation with all the best case coefficients and a computation with all the worst case coefficients lead to the presented confidence intervals

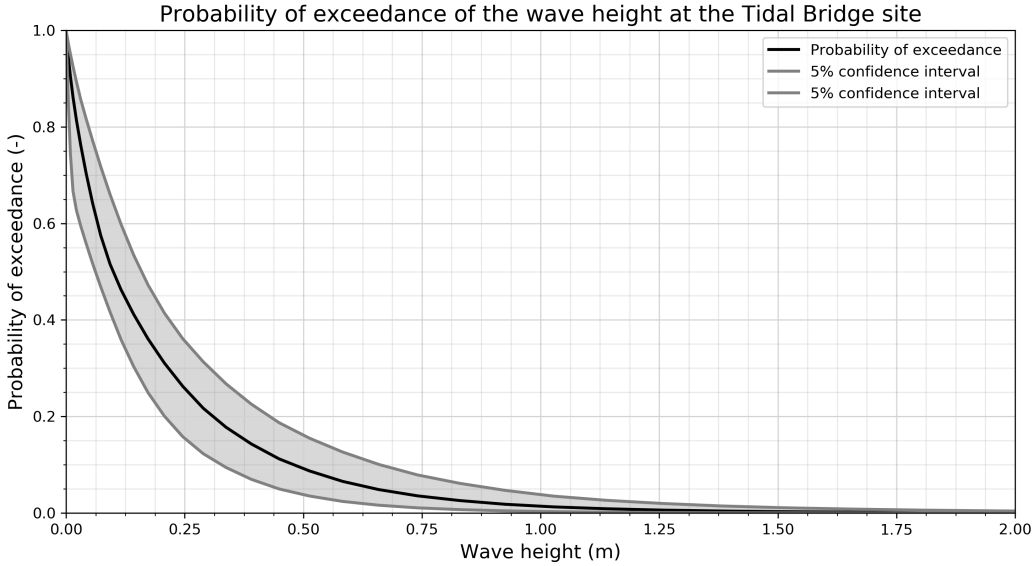

Figure B.8 Probability of exceedance of a significant wave height at the Tidal Bridge location

Wave characteristics at the project site The wave characteristics model can also be used to define the most probable wave characteristics at the Tidal Bridge project site. The most probable wave periods are coupled to the wave heights through Equation B.1 and B.2. Upon inputting a wave height in Equation B.1, then the wind velocity can be calculated as the fetch and average depth are constant. With this wind velocity, the wave period can be calculated with Equation B.2. The results of the most probable wave height as a relation of the wave period can be found in Figure B.9. The confidence intervals are introduced by uncertainty in the the near shore processes that are needed to construct this graph.

Figure B.9 is used in this design report to find the wave height and wave height at which the serviceability limits are exceeded. Consequently, the plot of Figure B.8 defines the probability of this wave height. The probability of the wave height can be calculated in the a defined downtime.

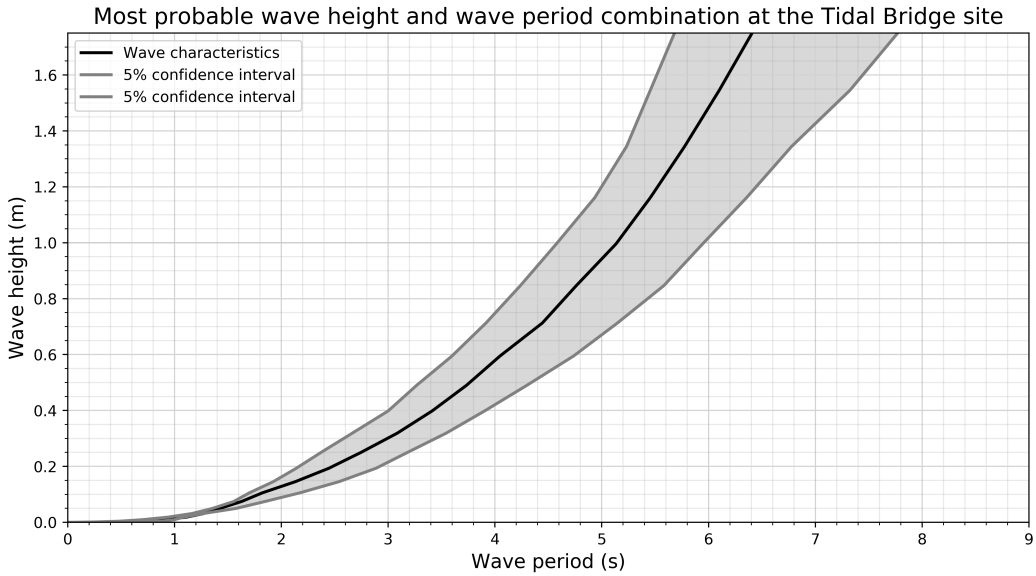

Figure B.9 Most probable wave height and wave period combination at the Tidal Bridge project site

B.3 Other boundary conditions

The physical characteristics of the project site provide the boundary conditions for the design report. The physical conditions assessed in are the bathymetry,tides, currents, and waves. The waves are expected to be governing in the dynamic behaviour of the Tidal Bridge. A more profound research to this boundary condition is presented that also includes the wave probabilistics.

B.3.1 Bathymetry

A British company named Aquatera performed on site research to acquire bathymetry data. Figure B.10 shows a plot of the bathymetry of the area around the objected project site. The Tidal Bridge is constructed around the triangled lines in the shallow area of the strait. The encircled areas are avoided for the Tidal Bridge location as these areas may have unfavourable effects to the bridge like obstacles, difficult bed profile or standing wave patterns. Figure B.11 shows a sonar chart of the Strait of Larantuka (Navionics, 2020). The edges of the strait start very shallow after which a sudden drop in the depth occurs. The floating part of the Tidal Bridge is placed in this deeper area.

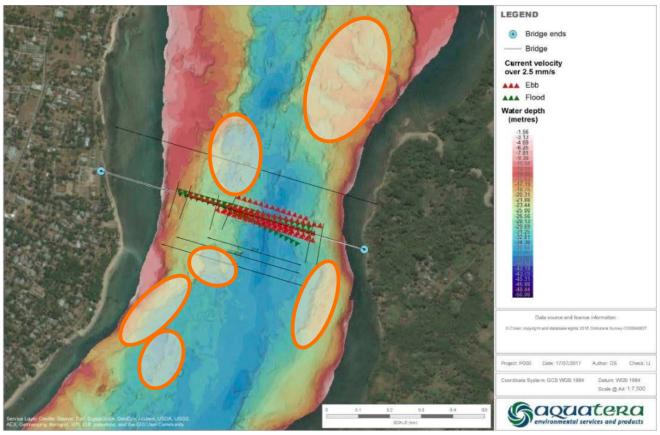

Figure B.10 Surveyed bathymetry by British company Aquatera (Vos, Hoogeveen, & Van den Eijnden, 2017)

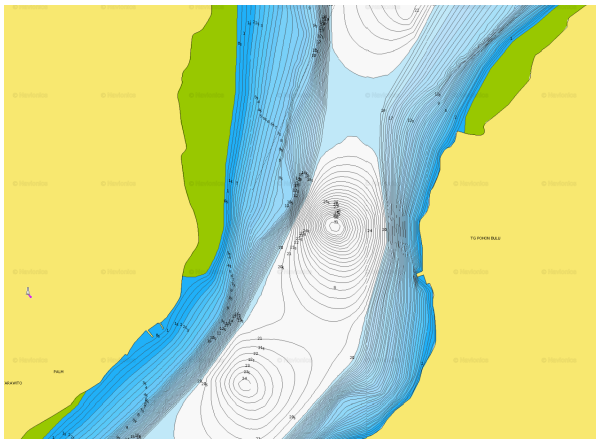

Figure B.11 Sonar chart of the Strait of Larantuka (Navionics, 2020)

Depth

The cross section of the floating part of the Tidal Bridge and its corresponding depths at the chosen location is represented with Figure B.12. The minimum keel clearance is 15 meters and the maximum keel clearance is 28.6 meters. A margin for the low tide and inaccuracies in the surveying are taken into account in these specified minimum keel clearances.

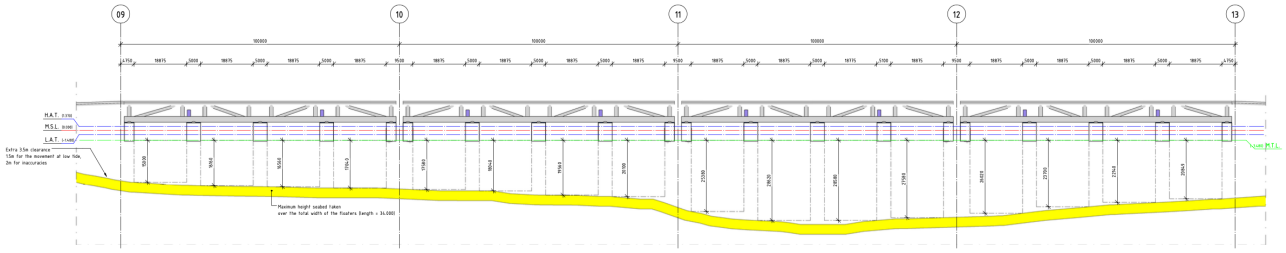

Figure B.12 The depths below the floating parts of the Tidal Bridge (De Rijke et al., 2017)

Squad

Dorgelo (2020) has calculated that the squad can be neglected. Squad is the principle that results from Bernoulli's equation. The flow locally takes higher velocities due to the reduced effective cross sectional area. The water level will drop by definition as the same discharge is valid while the current velocity is larger. However, this principle may be neglected due to the small reduced effective cross section relative to the total cross section.

B.3.2 Tides

Field research to the tides is conducted by Aquatera as well of which the most important results are showed in Table B.5. The reference point used for measuring the tides has been the same as for the measurements of the bathymetry specified in Section B.3.1.

		Tidal Level (m)	
		Relative to MSL	Relative to LAT
Highest Astronomical Tide	(HAT)	1.58	3.09
Mean High Water Spring	(MHWS)	1.11	2.62
Mean High Water Neap	(MHWN)	0.43	1.94
Mean Sea Level	(MSL)	0.00	1.51
Mean Low Water Neap	(MLWN)	-0.41	1.10
Mean Low Water Spring	(MLWS)	-1.09	0.42
Lowest Astronomical Tide	(LAT)	-1.51	0.00

Table B.5 Tidal data retrieved with a tidal gauge at the project location by Aquatera (Vos, Hoogeveen, & Van den Eijnden, 2017).

Figure B.13 shows a measurement of tidal data conducted by Aquatera. The tidal constituents can be calculated from this measured data. The calculated dominant tidal constituents have been displayed in Table B.6. The form factor corresponding to these calculated tidal constituents is $F = 0.454$. The corresponding tidal climate of this location is a mixed, mainly semi-diurnal tidal climate. The significant tidal constituent is the M_2 tide which has an amplitude of 0.76 m (De Rijke et al., 2017). The tidal signal can be predicted by using the calculated tidal constituents. A prediction of the tidal signal that should correspond to the measured tidal signal is displayed with the blue curve in Figure B.13. The measured data is displayed with the green curve.

The dominating tidal constituent in the Strait of Larantuka is the M_2-tide. A plot of the phase lag of this tidal constituent is displayed in Figure B.14. The figure is composed with the use of a nonlinear hydrodynamic model which included ten year of satellite altimetry data as input. This figure is very help full in explaining the strong tidal currents through the strait. The figure shows a difference in tidal phase of the M_2-tide in the order of 45°between the ocean above and below the strait. This phase lag is accompanied in a difference in the surface

Constituents	Amplitude	Phase
M_2	0.762 m	314.4°
S_2	0.340 m	22.2°
K_1	0.317 m	311.5°
O_1	0.183 m	277.4°

Table B.6 The relevant tidal constituencies in the Larantuka Strait following the transformed measured data (De Rijke et al., 2017)

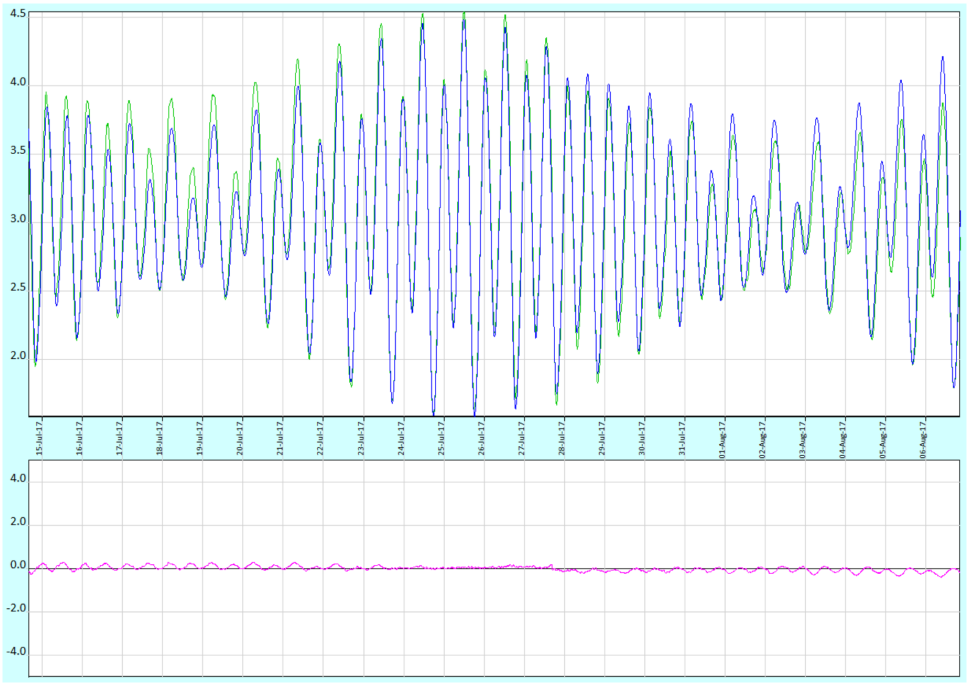

Figure B.13 Observed tidal data, predicted tidal data and the difference between the measured and predicted tidal data. The difference plot has an purple colour (De Rijke et al., 2017).

elevation between the upper and lower part. This water level difference forces the water to move through the straight with high currents.

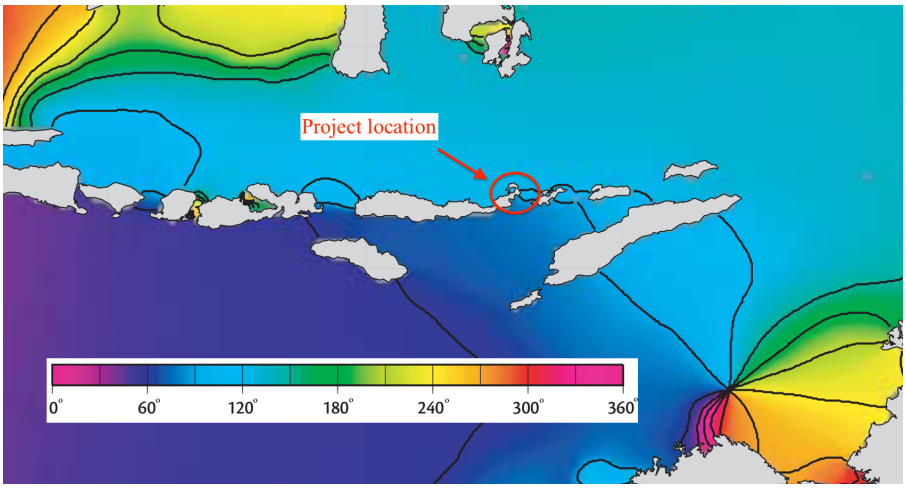

Figure B.14 Phase lag of the M_2-tidal constituent around the project location

This phase lag of the M_2-tide is driven by the special topography and the bathymetry of the Indonesian archipelago. The belt of islands and shallow straits between the islands from east to west around the project location hinders interaction of the northern and southern sea basin. The two sea basins function like physically independent basins due to the this island barrier. The tidal forcing of the two sea basins is not identical which results in a phase lag in the tidal surface elevation around the islands.

B.3.3 Currents

Interest of research

Foreign institution have paid much interest in trying to make use of the large current velocities in the Strait of Larantuka (Orhan & Mayerle, 2020). Orhan, Mayerle, Narayanan, and Pandoe (2016) studied different locations within the Indonesian archipelago and concludes that the Larantuka Strait is the most favourable locations to harvest tidal energy. This conclusions is purely based on the high current velocity. Other site specific characteristics have been left out of the research

Calculated current velocity

A calculated current velocity profile is displayed in Figure B.15 for a location in the middle of the Larantuka Strait (Orhan & Mayerle, 2020). The mixed, mainly semi-diurnal tidal characteristics becomes visible by the tidal current velocity inequality within the days and within the lunar cycle. The lower graph of Figure B.15 magnifies the highlighted part of the upper graph. The maximum calculated current velocity is a bit over 3.5 m/s.

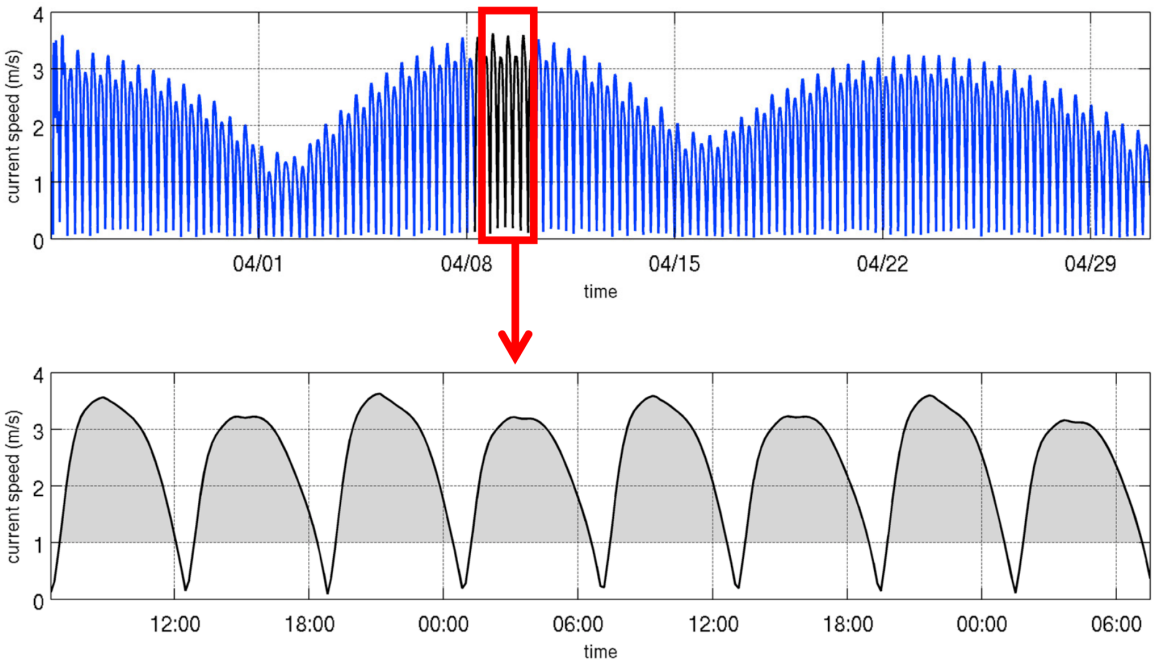

Figure B.15 Modelled depth averaged current velocity magnitudes in the middle of the Larantuka Strait (Orhan & Mayerle, 2020)

Measured current velocity

Aquatera has performed field research to the current velocities in the Strait of Larantuka (Vos, Hoogeveen, & Van den Eijnden, 2017), of which the results can be observed in Figure B.15. The results show that the current velocity may differ greatly depending on the location and the largest current velocities have been observed in the middle of the strait. Outliers of these measurements may take values of almost 4.5 m/s. In general, the measured maximum current takes a value varying between the 3.5 an 4 m/s. A maximum current of 4 m/s is taken into account for this design report.

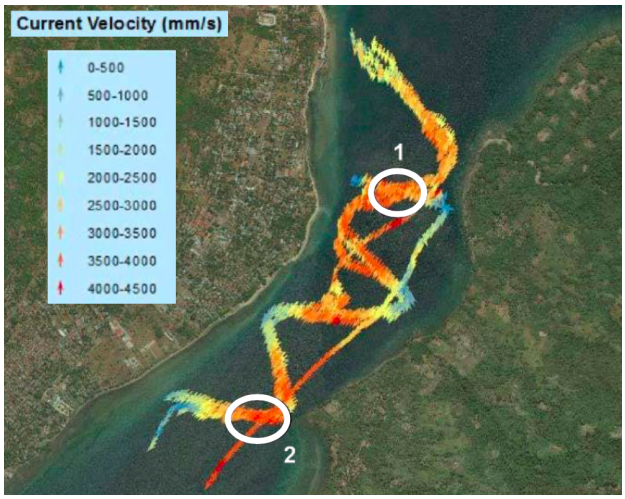

Figure B.16 Measured current velocity in the strait of Larantuka by Aquatera (Vos, Hoogeveen, & Van den Eijnden, 2017)

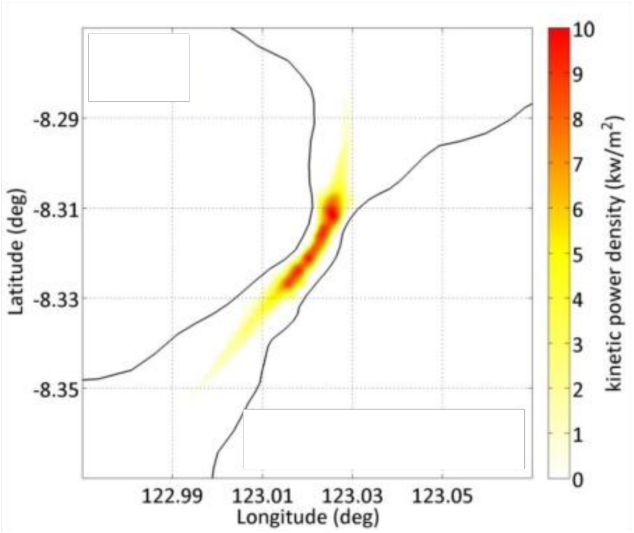

Figure B.17 The kinetic power density per squared meter (Orhan et al., 2016)

Blockage effect

The turbines have a blockage effect in the strait (Orhan & Mayerle, 2020). The turbines contribute an increased total drag of the strait and the averaged current velocities in the strait become a little smaller. Hence, the energy yield is expected to be a little less compared to a situations without the turbines.

The turbines also disturb the natural flow through the strait and the current starts to look for a routes with less drag. The tidal current looks for a route around the turbines closer to the shore (Orhan & Mayerle, 2020). The increased flow velocities on the sides of the strait should be taken into account as those could highly contribute to erosion of the shores around the Tidal Bridge. The eroding shores may cause hinder for people that live close to the shore or have economical benefit of the current shore location.

Potential energy yield

The tidal stream power per unit of area of flow is specified with Formula B.4. This formula specifies the theoretical energy yield for a specified current velocity and turbine efficiency. The formula shows that suitable areas for tidal energy harvesting have large current velocity magnitudes as the current velocity has a cubed relation to the generated power. With a current velocity of 3.5 m/s and a turbine efficiency of $\eta_{turbine} = 0.45$, then the maximum power per unit of area in the strait takes values in the order of magnitude of 10 kW/m^2. In other words, as the turbine rotor covers an area of 10 m^2, then the turbine may generate for 100 kW.

$$P = 1/2 \cdot \rho \cdot u^3 \cdot \eta_{turbine} \tag{B.4}$$

Where:	P	[W]	=	power
	ρ	[kg/m^3]	=	water density
	u	[m/s]	=	current velocity
	$\eta_{turbine}$	[-]	=	efficiency factor of the turbine

The distribution of this power per unit area around the Larantuka Strait is numerically modelled by Orhan et al. (2016) and may be observed in Figure B.17. The Figure shows that only a small part of the strait has large power densities. Due to the cubed relation to the current velocity, only a small part of the cross section of the strait that has large current velocities, yields much energy.

The energy yield changes much through one period of a lunar cycle. The energy yield in the Larantuka Strait is mostly provided by the spring tides. Figure B.16 shows that the current velocities may adopt values which are twice as large with spring tides compared to current velocities with neap tides. The energy yield is related to the current velocity cubed (Equation B.4). Hence, the energy yield is about eight times more with spring tides compared to neap tides.

C | Developing the structural dynamics model

Contents of this appendix chapter

C.1 The Tidal Bridge mechanical system

C.1.1 Geometry, mass and mass moment of inertia

The report from Antea (De Rijke et al., 2017) describes the dimensions and materials used for the Tidal Bridge floating element. Dorgelo (2020) calculated the mass and the mass moment of inertia of the different parts of the structure of which table C.1 shows improvements of his results. The table takes the FishFlow turbines into account which resulted in a lowered centre of gravity and an increased mass moment of inertia compared to the results of Dorgelo (2020).

Component	**Size** [x,y,z] (m)	**Centre of mass** [x,y,z] (m)	**Mass** (kg)	**Mass moment of inertia** [x,y,z] (10^6 kg·m^2)
Road	[99, 11, 2]	[0, 0, 10.5]	400,000	[48, 378, 337]
Truss	[99, 22, 5.5]	[0, 0, 7.3]	900,000	[87, 800, 786]
Small floater 1	[3.5, 34, 6.55]	[-47.8, 0, 0]	48,000	[5, 110, 114]
Small floater 5	[3.5, 34, 6.55]	[47.8, 0, 0]	48,000	[5, 110, 114]
Large floater 2	[5, 34, 6.55]	[-23.9, 0, 0]	68,000	[7, 39, 46]
Large floater 3	[5, 34, 6.55]	[0, 0, 0]	68,000	[7, 0, 7]
Large floater 4	[5, 34, 6.55]	[23.9, 0, 0]	68,000	[7, 39, 46]
Turbine 1, 2	[19, 43.5, 10]	[-37.5, 0, -7.5]	320,000	[73, 482, 510]
Turbine 3, 4	[19, 43.5, 10]	[-12.5, 0, -7.5]	320,000	[73, 821, 110]
Turbine 5, 6	[19, 43.5, 10]	[12.5.5, 0, -7.5]	320,000	[73, 821, 110]
Turbine 7, 8	[19, 43.5, 10]	[37.5, 0, -7.5]	320,000	[73, 482, 510]
Equipment	[2.3, 12, 3]	[0, 0, 4.4]	120,000	[4, 2, 1]
Total		**[0.0, 0.0, 0.0]**	**3,000,000**	**[461, 2586, 2670]**

Table C.1 Complete overview of the geometry, mass and mass moment of inertia of the most significant objects within one Tidal Bridge floating element.

Turbines

The turbines are developed by FishFlow innovations for turbulent free flow conditions. Figures C.1a, C.1b, and C.2 give an impression of the scale and the construction method. The large casings stabilize the very turbulent flow through the strait somewhat. The height of the impeller is 8 meters and the length of the casing without the floater bodies at the top of the turbine is 26.5 meters.

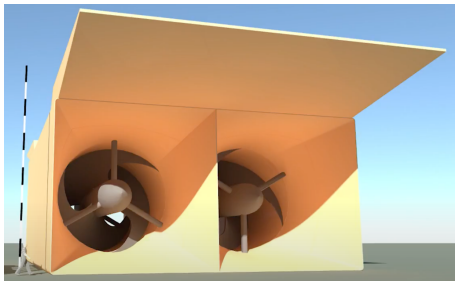

(a) Perspective sketch of the FishFlow turbine including the flotation compartment at the top of the turbine

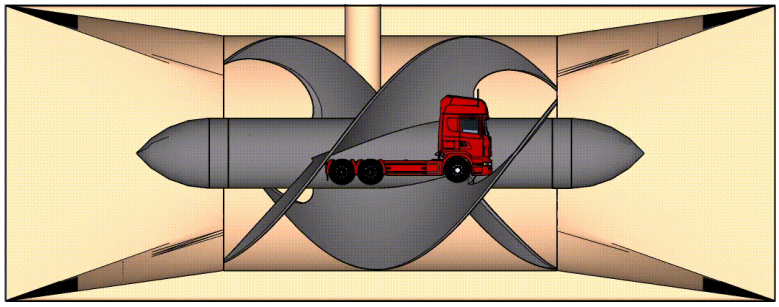

(b) The truck gives an idea of the size of the FishFlow turbine.

Figure C.2 shows an idea of FishFlow Innovations about the construction of the turbines to the floating bridge.

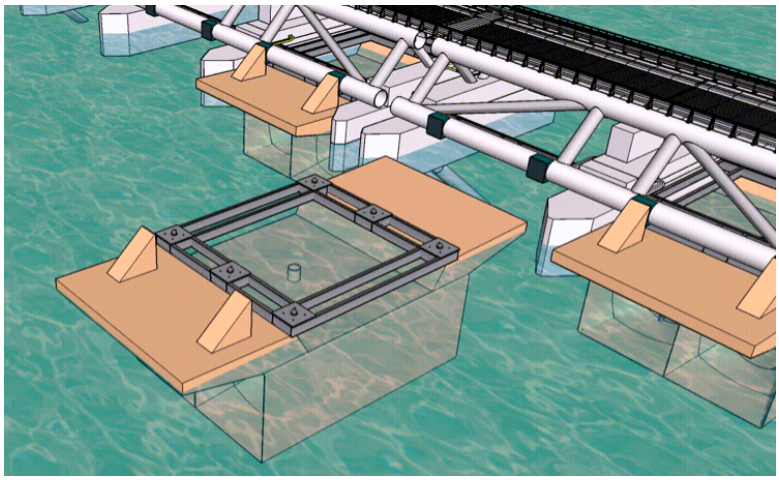

Figure C.2 The turbines float into their positions after installing the Tidal Bridge at its location.

Foundation

Figure C.3 shows a sketch of the foundation of the pendulums on the bed of the strait. The foundation structures consist of three poles with a diameter of 1800 mm which are grouted in the bed. The tree poles are connected to each other by a stability frame of smaller tubes that vary from a diameter of 500 mm to a diameter of 914 mm. The foundations can be constructed with jack up barges that drill wholes in the bed. Consequently, the foundation structures are lowered in the wholes and attached to the bed with grouting.

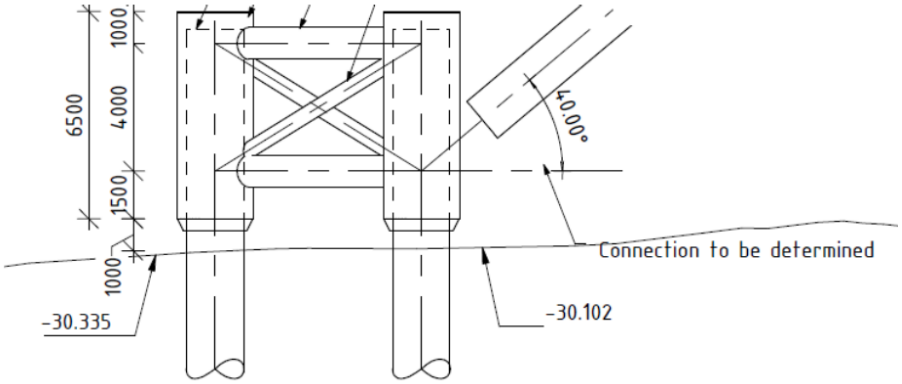

Figure C.3 Sketch and dimensions of the foundation giving support to two pendulums (De Rijke et al., 2017)

Stability of the floating Tidal Bridge element

Figure C.4 defines the relevant locations used in a stability calculation of a floating object (Molenaar & Voorendt, 2020). The distance GM needs to be positive and the object becomes more stable with a larger positive GM. A hand calculation helps to determine the distance GM:

$$\begin{aligned} BM &= \frac{I_{yy}}{V_w} \\ &= \frac{\frac{1}{12} \cdot b \cdot l^3}{A_w \cdot d} \\ &= \frac{\frac{1}{12} \cdot (3 \cdot 5 + 2 \cdot 3.5 \cdot 34^3}{809 \cdot 2.07} \\ &\approx 43 \; meter \end{aligned} \tag{C.1}$$

Where:				
	BM	[m]	=	distance from the centre of buoyancy to the meta centre
	I_{yy}	[m^4]	=	Area moment of inertia
	V_w	[m^3]	=	Volume of the displaced water
	b	[m]	=	total width of the five floaters together
	l	[m]	=	length of one of the floaters

For the case of the Tidal Bridge, the distance GB is determined to be about half of the draught and determined to be approximately 1 meter. This results in a GM of approximately 42 meters which defines a very stable structure. This stability value suggest that the rotational stiffness is very large as well which has a major influence to the Tidal Bridge dynamic behaviour. However, the rotational stiffness should be compared to the mass moment of inertia in order to evaluate the stiffness compared to the mass.

C.2 Gathering the relevant physical phenomena

This appendix section is complementary to the identically named section in the main report. This appendix contains the additional information needed to define the structural dynamics model with.

C.2.1 Drag coefficients

Figure C.2 shows drag coefficients as specified by (DNV, 2011). These situations are used for determining the needed drag coefficients for the structural dynamics model.

C.2.2 Definition of the turbine induction factor

The turbine induction factor is an important characteristic of the turbine impeller that is needed to define the thrust force and the power. Figure C.5 specifies the expected power that the turbine generates for a defined flow. The graph helps to determine the induction factor with help of Equation C.2 as described by Zaaijer and

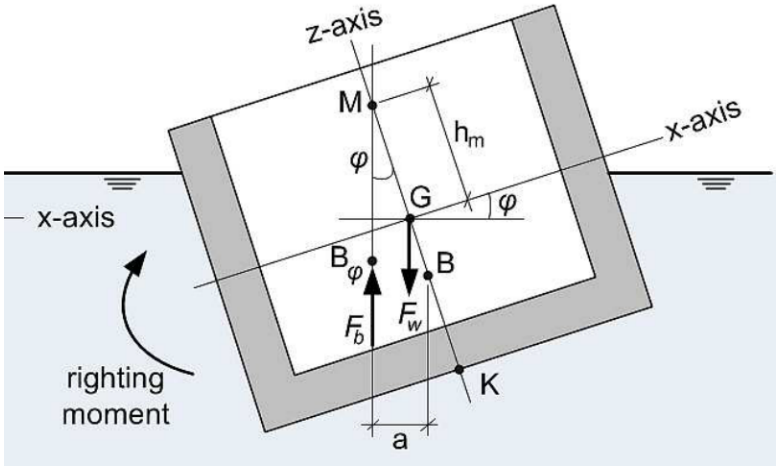

Figure C.4 Floating object with the relevant locations that help to define the stability of the object (Molenaar & Voorendt, 2020)

Viré (2019). The density of the water, the impeller frontal area are fixed constants. The electric power and the relative flow velocity can both be deducted from Figure C.5. The induction factor is determined to be 0.188 by making use of the specified variables and Equation C.2.

$$P = \frac{1}{2} \cdot \rho \cdot A \cdot u^3 \cdot 4 \cdot a \cdot (1 - a)^2 \tag{C.2}$$

Where:	P	[W]	=	electric power
	ρ	[kg/m^3]	=	density
	A	[m^2]	=	impeller frontal area
	u	[m/s]	=	relative flow velocity
	a	[-]	=	induction factor

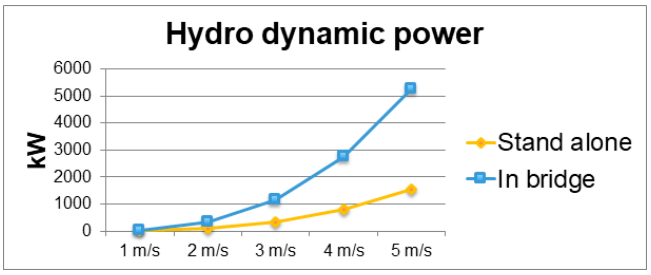

Figure C.5 The electric power plotted to the flow velocity through the turbines of the Tidal Bridge as specified by (Manshanden, 2020)

Table B-1
Drag coefficient on non-circular cross-sections for steady flow C_{DS}.
Drag force per unit length of slender element is $f = ½\rho C_{DS} D u^2$.

D = characteristic width [m].
R_e = uD/ν = Reynolds number.

Adopted from Blevins, R.D. (1984) *Applied Fluid Dynamics Handbook*. Krieger Publishing Co.

Geometry	*Drag coefficient, C_{DS}*	
15. Ellipse	D/L	C_{DS} (R_e ~10^5)
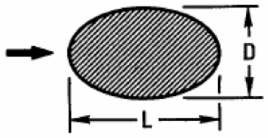	0.125 0.25 0.50 1.00 2.0	0.22 0.3 0.6 1.0 1.6

Table B-2
Drag coefficient on three-dimensional objects for steady flow C_{DS}.
Drag force is defined as $F_D = ½\rho C_{DS} S u^2$.

S = projected area normal to flow direction [m^2].
R_e = uD/ν = Reynolds number where D = characteristic dimension.

Geometry	*Dimensions*	*C_{DS}*
Rectangular plate normal to flow direction	B/H	
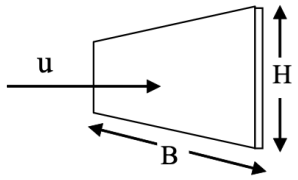	1 5 10 ∞	1.16 1.20 1.50 1.90 $R_e > 10^3$
Square rod parallel to flow	L/D	
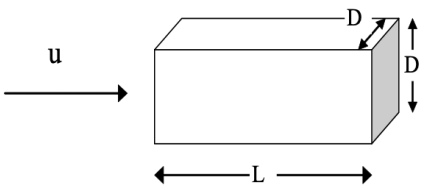	1.0 1.5 2.0 2.5 3.0 4.0 5.0	1.15 0.97 0.87 0.90 0.93 0.95 0.95 $R_e = 1.7 \cdot 10^5$

Table C.2 Table with drag coefficients for different shapes (DNV, 2011)

Where:	f *or* F_D	[N]	=	drag force
	ρ	[kg/m^3]	=	water density
	C_{DS}	[-]	=	drag coefficient dependent on length versus width ratio
	u	[m/s]	=	flow velocity
	ν	[m/s^2]	=	kinematic viscosity of water

C.2.3 Wave theory kinematic formulas

This appendix corresponds to Section 3.2.6 that elaborates upon the used wave theory in the structural dynamics model. The formulas below describe the surface elevation, the pressure, the velocity and the acceleration following Stoke's wave theory. Second order effects are included in the formulas as well. The effect of the current is integrated in the formulas. The formulas are all found in the works of Holthuijsen (2007).

Surface elevation

Equation C.3 provides the formula for the surface elevation as used in the structural dynamics model. This formula is used to define at which locations along the structure water is present.

$$\eta(y,t) = a\cos\left(utk - ky + \omega t\right) + ka^2\frac{\cosh(kd)}{4\sinh^3(kd)}\left(2+\cosh(2kd)\right)\cos\left(2(utk - ky + \omega t\right) \tag{C.3}$$

Where:

$\eta(y,t)$	[m]	=	surface elevation of second-order Stoke's waves dependent on position (y) and time (t)
a	[m]	=	regular wave amplitude
ω	[rad/s$^-$1]	=	wave frequency
k	[rad/m]	=	wave number
ε	[m^2/rad]	=	wave steepness
d	[m]	=	depth
u	[m/s]	=	current velocity

Pressure

Equation C.4 displays the formula for the wave pressure within a second-order Stoke's wave. The pressure is dependent on the position (y,z) and the time (t). This formula is used to calculate the pressures below the floaters. The variable pressures below the floaters lead to a variable buoyancy force.

$$\begin{aligned} p(y,z,t) = &-\rho g z + \rho g a\frac{\cosh\left(k\left(d+z\right)\right)}{\cosh\left(kd\right)}\cos\left(utk - ky + \omega t\right) \\ &+ \frac{3}{4}\rho g a^2 k\frac{\tanh\left(kd\right)}{\left(\sinh\left(kd\right)\right)^3}\left(\frac{\left(\cosh\left(2k\left(d+z\right)\right)\right)}{\left(\sinh\left(kd\right)\right)^3} - \frac{1}{3}\right)\sin\left(2(utk - ky + \omega t\right) \\ &- \frac{1}{4}\rho g a^2 k\frac{\tanh\left(kd\right)}{\left(\sinh\left(kd\right)\right)^2}\left(\cosh\left(2k\left(d+z\right)\right) - 1\right) \end{aligned} \tag{C.4}$$

Where: $p(y,z,t)$ [N/m^2] = pressure of second-order Stoke's waves dependent on position (y, z) and time (t)

Particle velocity

Equation C.5 describe the particle velocities within the waves in the sway (y) and heave (z) directions due to second-order stokes waves. The equations are dependent to the position (y, z) and time (t). These equations are used in the structural dynamics model to calculate the drag which is dependent to the velocity squared. This type of drag is included in the structural dynamics model for the pendulums, the floaters and the turbines.

$$\begin{aligned} u_y(y,z,t) &= \omega a\frac{\cosh\left(k\left(z+d\right)\right)}{\sinh\left(kd\right)}\cos\left(utk + \omega t - ky\right) + \frac{3}{4}\omega a^2 k\frac{\cosh\left(2k\left(z+d\right)\right)}{\left(\cosh\left(kd\right)\right)^3\sinh\left(kd\right)}\cos\left(2\left(utk + \omega t - ky\right)\right) \\ u_z(y,z,t) &= \omega a\frac{\sinh\left(k\left(z+d\right)\right)}{\sinh\left(kd\right)}\sin\left(utk + \omega t - ky\right) + \frac{3}{4}\omega a^2 k\frac{\sinh\left(2k\left(z+d\right)\right)}{\left(\cosh\left(kd\right)\right)^3\sinh\left(kd\right)}\sin\left(2\left(utk + \omega t - ky\right)\right) \end{aligned} \tag{C.5}$$

Particle acceleration

Equation C.6 describes the particle acceleration within the second-order Stoke's waves. The equations are dependent to the position (y, z) and time (t). These equations are used in the structural dynamics model to calculate the wave inertia forces which is dependent to the acceleration. The wave inertia forces are calculated

for the floaters and the turbines.

$$
\begin{aligned}
a_y(y,z,t) = &- \frac{(uk+\omega)\omega a \cosh(k(z+d))}{\sinh(kd)} \sin\left(utk+\omega t-ky\right) \\
&- \frac{3(uk+\omega)\omega a^2 k \cosh(2k(z+d))}{2\cosh^3(kd)\sinh(kd)} \sin\left(2(utk+\omega t-ky)\right) \\
a_z(y,z,t) = &- \frac{(ku+\omega)\omega a \sinh(k(z+d))}{\sinh(kd)} \cos\left(utk+\omega t-ky\right) \\
&- \frac{3(ku+\omega)\omega a^2 k \sinh(2k(z+d))}{2\cosh^3(kd)\sinh(kd)} \cos\left(2(utk+\omega t-ky)\right)
\end{aligned}
\tag{C.6}
$$

C.3 Constructing the structural dynamics model

The process of constructing the structural dynamics model is mostly explained in the main report in Section 3.3. One detail about constructing the model has been specified in this appendix section.

C.3.1 Radiation damping

The radiation damping, as applied in the structural dynamics model, has been made dependent to the excitation frequency. This dependency has been included as the large variations in the excitation frequency can lead to completely different radiation damping coefficients. The used relations between the radiation damping coefficient and the excitation frequency have been presented in Figure C.6. These relations have been deduced from the work of Vugts (1968).

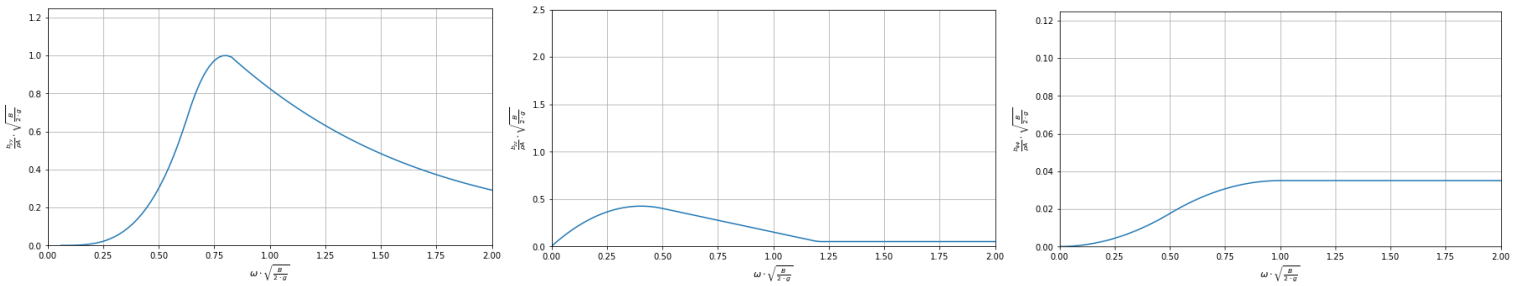

(a) Sway **(b)** Heave **(c)** Roll

Figure C.6 Used relations in the structural dynamics model for the radiation damping coefficient following the experimentally determined results of Vugts (1968)

Where:

b_{yy}	$[\frac{kg}{m \cdot s}]$	=	radiation damping per unit strip width for the sway degree of freedom
b_{zz}	$[\frac{kg}{m \cdot s}]$	=	radiation damping per unit strip width for the heave degree of freedom
$b_{\phi\phi}$	$[\frac{kg}{s}]$	=	radiation damping per unit strip width for the roll degree of freedom
B	[m]	=	breadth
T	[m]	=	draught
A	[m^2]	=	cross sectional area of the submerged part of the strip
ω	[rad/s]	=	wave frequency
ρ	[kg/m^3]	=	density of the water
g	[m/s^2]	=	gravitational acceleration

C.4 Link to structural dynamics model

The structural dynamics model used for this design report has been uploaded to the 4TU Data Repository. The structural dynamics model can be downloaded with either a direct link or the DOI link. The data becomes available after it has been reviewed by the 4TU Data Repository organization.

D | Narrowing the design space

Contents of this appendix chapter

D.1 The effect of the chosen combined serviceability limit

Figure D.1 shows the regions of exceeding the serviceability limit for different serviceability limit values. This figure helps to evaluate the relative importance of the choice for the serviceability limit magnitude. The figure shows that larger limit values lead to crossings at with larger wave characteristics. This leads to less yearly downtime. The downtime can be calculated by finding the wave height of the crossing of the limit line and the wave characteristics line. The downtime of the different limit values has been summed in the Table 4.2 in the main report.

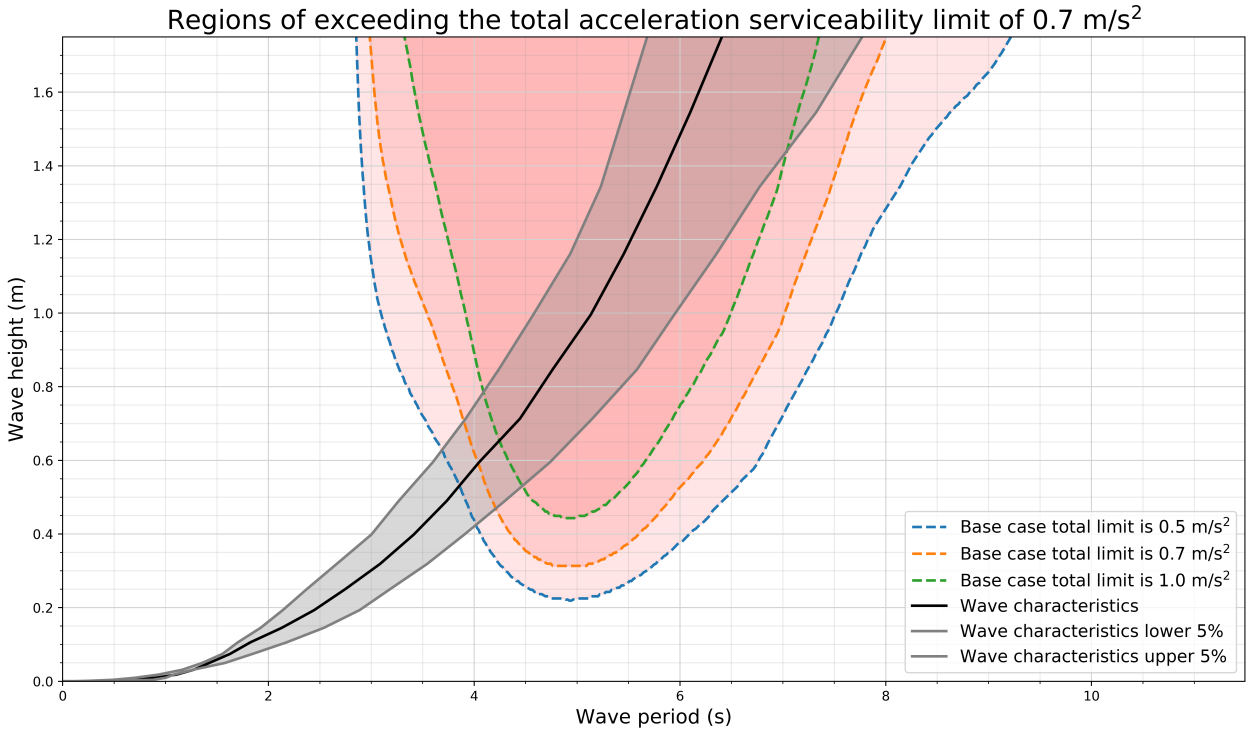

Figure D.1 Exceeding the serviceability limit for different limit values for the original Tidal Bridge design

D.2 Sensitivity analysis

Table D.1 shows all the parameters and coefficients of the structural dynamics model that have been included in the sensitivity analysis.

Model parameters	Model coefficients
– Mass	– Drag coefficient: pointed floater shape
– Mass moment of inertia	– Drag coefficient: floater bottom shape
– Floater length	– Drag coefficient: turbine shape
– Floater width	– Drag coefficient: turbine induction factor
– Depth	– Radiation damping coefficient: pointed floater shape
– Pendulum angle	– Radiation damping coefficient: turbine shape
– Pendulum length	– Added mass coefficient: pointed floater shape
– Pendulum stiffness	– Added mass coefficient: floater width
	– Added mass coefficient: marine growth
	– Inertia coefficient

Table D.1 All parameters and coefficients included in the sensitivity study

D.3 Influence of floater length

The floater length showed to be the most sensitive parameter following the sensitivity analysis. Promising optimizations of the dynamic response could potentially be found in this parameter. Figure D.2 shows the dynamic response for designs that have been optimized with different floater lengths. Table D.2 shows the yearly downtime of those test results. The design with a floater length of 30.6 meter shows a small improvement of the downtime compared to the base case. However, a floater length of 27.2 meter which is 80% of the original floater length does not have an improved yearly downtime compared to the floater of 30.6 meters which is 90% of the original floater length. The optimum floater length is somewhere around this 30.6 m for this Tidal Bridge design. However, the optimizations found in the floater length do not have the objected optimizations of this design report. Solutions in the form of an additional structure now become more important in the design scope.

	Probability		
	95%	**50%**	**5%**
Base case	31.6	23.4	16.3
Floater length is 37.4 m	41.0	31.0	19.6
Floater length is 30.6 m	28.8	21.7	15.4
Floater length is 27.2 m	30.8	23.0	15.4

Table D.2 Yearly downtime in days for the base case, and designs with a various floater length

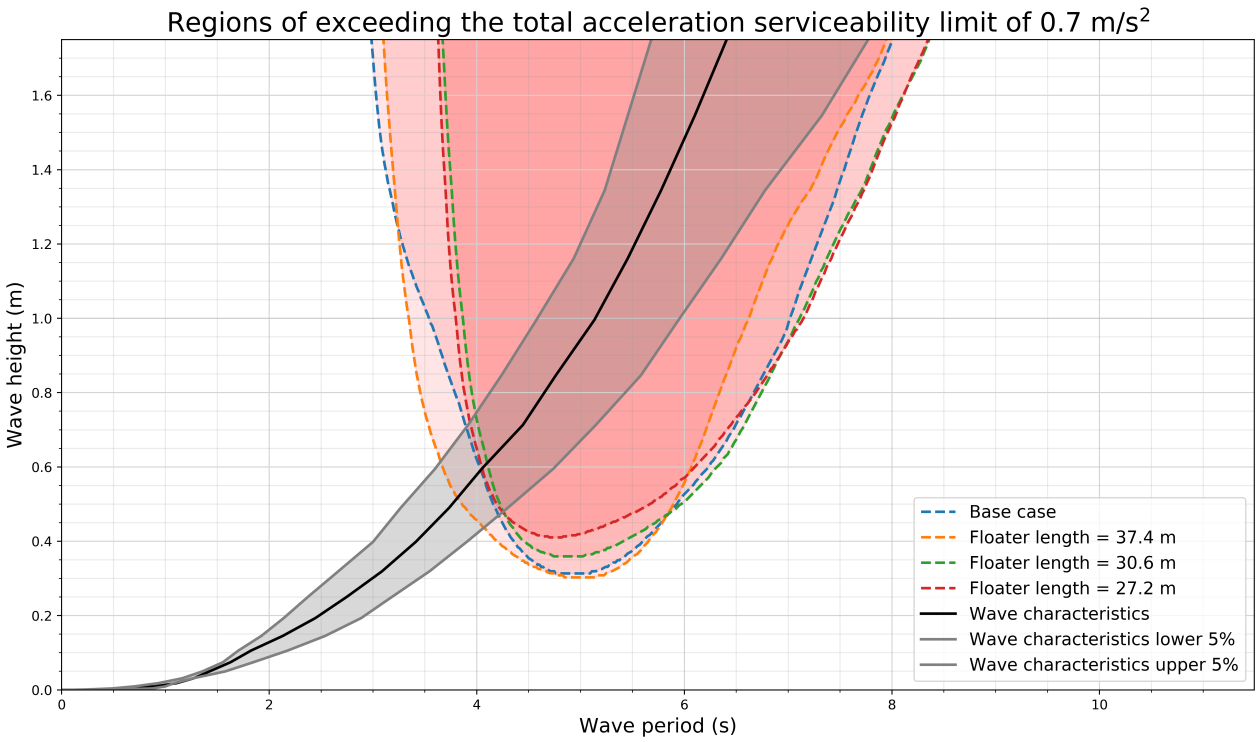

Figure D.2 The regions of exceeding the serviceability limit for various floater lengths

E | First design loop: qualitative design

Contents of this appendix chapter

This section sums the brainstorm designs that have been worked out with a two dimensional sketch. The sketches give an idea how the brainstorm design could be integrated within the original design and how the design could be effective in mitigating the dynamics of the Tidal Bridge. The brain storm designs have been sorted within five categories:

1. Concepts integrating viscous dampers
2. Tethered concepts
3. Tuned mass concepts
4. Out of the box concepts
5. Offshore inspired concepts

E.1 Concepts integrating viscous dampers

Figure E.1 shows a solution with a submerged spring-damper combination within the pendulum. The total length of the pendulum including the spring-damper combination is the same as the original design. The solution is effective in every degree of freedom.

Figure E.2 shows a solution with an emerged spring-damper combination in the pendulum. The total length of the pendulum including the spring-damper combination is longer than the original design which leads to a larger buckling length. The lever arm to the centre of gravity stays the same in this design to prevent for permanent roll rotations under the wave or current forcing. The solution is effective in every degree of freedom.

Figure E.3 shows a solution with a submerged rotational damper between the floater and the pendulum. The pendulum length stays the same. The rotational damper restricts the rotational movement of the floater and pushes moment forces into the pendulum. The solution is most effective for the roll rotations.

Figure E.4 shows a solution with an extra pendulum between the original anchor and the side of the floater. The pendulum has a special damper with an adaptive length such that the total length of the pendulum damper combination can adapt for the tidal surface elevation changes of almost three meters in total. The damper is most effective for the roll movements of the floater.

Figure E.5 shows a solution that has two additional pendulums that both have an integrated damper. An additional anchor is introduced in this solution. The dampers within these pendulums need to be adaptive to the tidal difference in the surface elevation like the solution of Figure E.4. The damper is most effective for the roll and heave movements.

E.2 Tethered concepts

Figure E.6 shows a solution that has two tethers on both sides of the floating structure. An additional anchor is introduced in this solution to connect the rightward tether to. The leftward tether connects to the original anchor for the pendulum. The tethers are kept under tension by the springs. The dampers on top

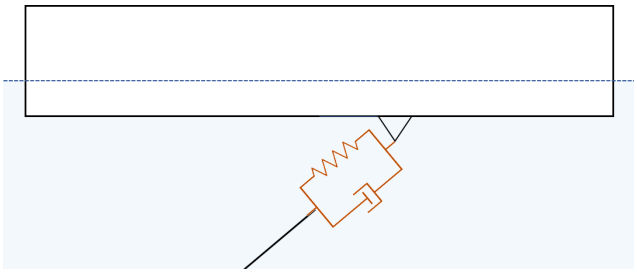

Figure E.1 [Concept 1] Submerged spring-damper combination engineered within the pendulum

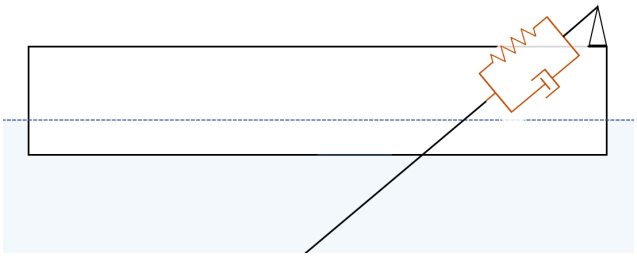

Figure E.2 [Concept 2] Emerged spring-damper combination engineered within the pendulum

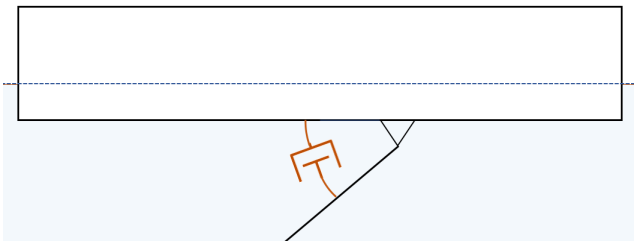

Figure E.3 [Concept 3] Rotational damper

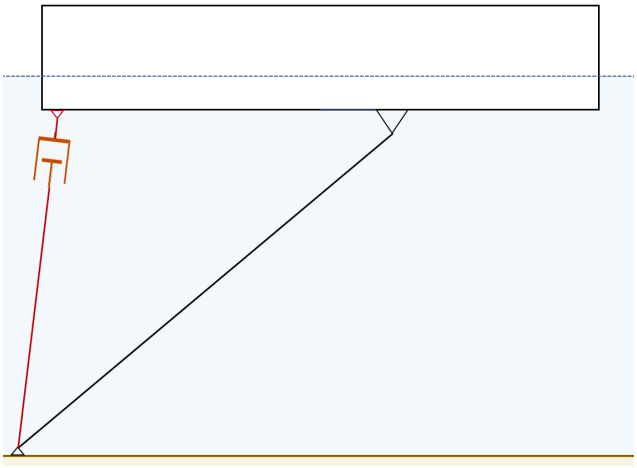

Figure E.4 [Concept 4] Second pendulum and damper on the same anchor

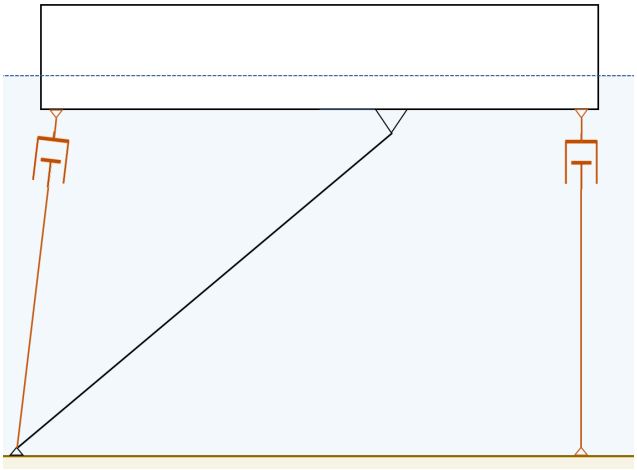

Figure E.5 [Concept 5] Two additional pendulums with integrated dampers on separate anchors

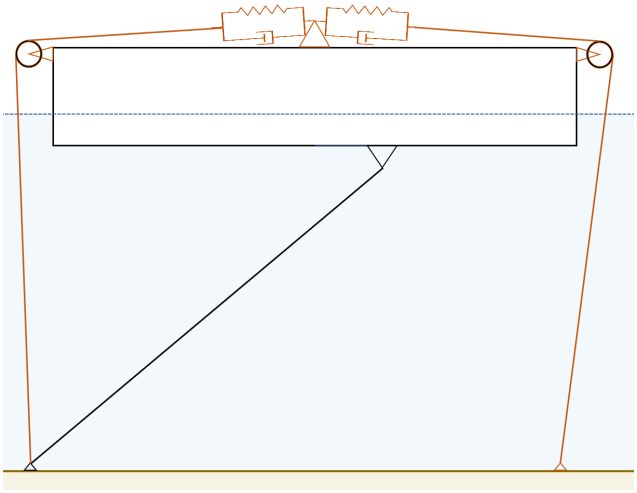

Figure E.6 [Concept 6] Damped tethers mounted on separate anchors

of the floaters dissipate energy from the system whenever the system starts to heave or to roll. The viscous dampers contain one way valves such that damping is functioning upon elongating and hardly giving resistance

upon shortening. This solution is most effective in the roll and heave movements.

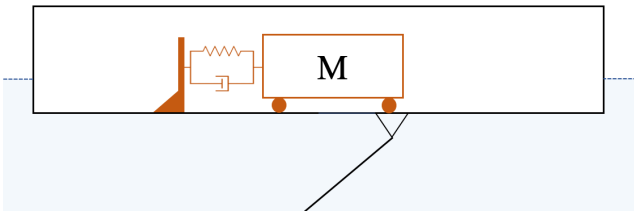

Figure E.7 [Concept 7] Tuned mass damper

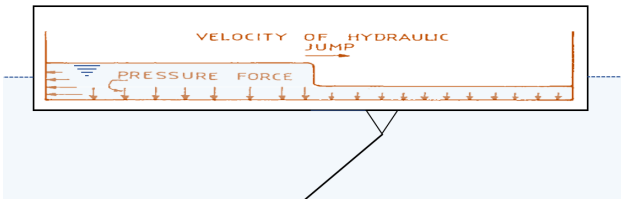

Figure E.8 [Concept 8] Slosh damper

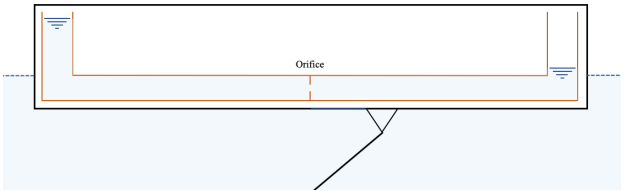

Figure E.9 [Concept 9] Tuned liquid column damper

E.3 Tuned mass concepts

Figure E.7 shows a solution with a tuned mass damper. The tuned mass damper can be adapted such that it is a very effective damping method around a specific excitation frequency. The damper is most effective in the sway direction. The design of this damper is integrated in the space within the floater. The effectiveness of the damper in the different degrees of freedom depends on the excitation amplitude of the mass. The damper is effective in the sway direction, but becomes more effective in the roll direction as well for the situation that the mass excites further away from its neutral position.

Figure E.8 shows a solution with a slosh damper. This solution dissipates energy due to the formation of a hydraulic jump within the slosh tank. The roll motion of the floater forces the water to move back and forth upon one roll period. The slosh damper can be tuned by adapting the width of the tank versus the height of the surface elevation of the water. This solution is most effective in the sway direction and may work well in the roll direction as the width of the tank is long enough.

Figure E.9 shows a solution with a tuned liquid column damper. The tuned liquid column damper mostly dissipates energy through the vortex shedding around the orifice. The natural frequency of the damper can be regulated by adapting the dimensions of the container and the orifice. The damper is most effective in the sway direction and works to some extent also in the roll direction.

E.4 Out of the box concepts

Figure E.10 shows a solution with wave energy absorbers in front and behind the floaters. The wave energy absorbers are spaces filled with air that have an open bottom. The waves generate pressure differences within those spaces. Air can flow in and out of the spaces through valves having much resistance. The energy dissipation happens around those air valves. The wave energy absorbers are effective to dampen the roll rotations.

Figure E.11 shows a solution of a floater that floats on a cushion of air. The cushion of air consist of a high air pressure space below the floater. This solution is not dissipating energy from the system, but it should make the structure less sensitive to wave forcing. The sides of the floater are made longer to make sure that the high pressure air may not escape from the floater.

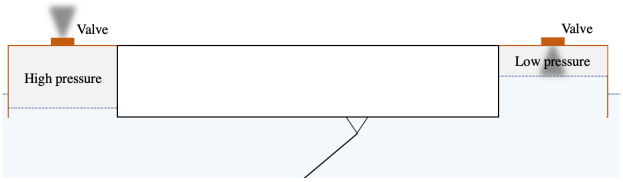

Figure E.10 [Concept 10] Wave energy air adsorbers

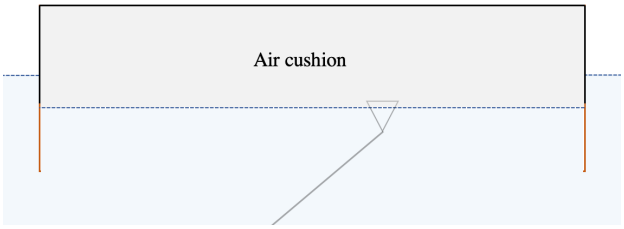

Figure E.11 [Concept 11] Air cushion

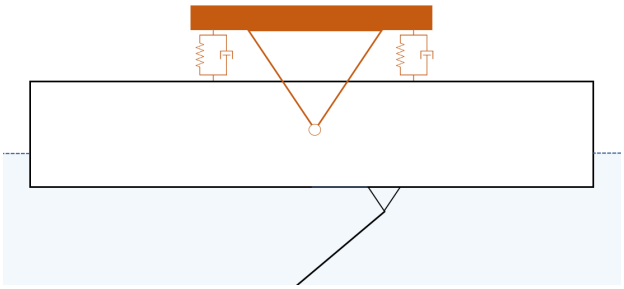

Figure E.12 [Concept 12] Rotating deck

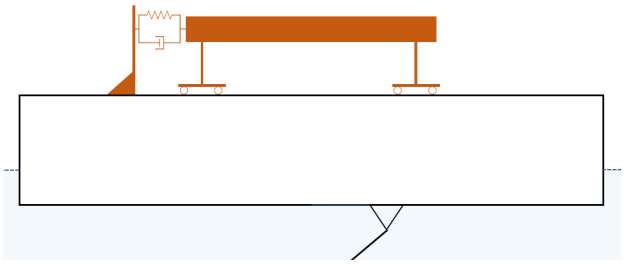

Figure E.13 [Concept 13] Translating deck

Figure E.12 shows a solution of a system with a floater and a bridge deck that are connected to each other with a hinge. The idea of this solution is that the floater may roll underneath the bridge deck which is opted for to keep stable. This solution has springs to bring the deck back in equilibrium position and dampers to make sure that the deck does not stay dynamically active after an oscillation.

Figure E.13 shows a solution in which the deck can translate with respect to the floater. With this solution the floater can sway underneath the deck while the deck stays less active and comfortable for its users. This solution has springs to bring the deck back to equilibrium position and the solution has a damper to make sure that the deck does not stay dynamically active after an oscillation.

E.5 Offshore inspired concepts

Figure E.14 shows a solution of a floater that is mostly submerged. This solution is not in line with the preferred concept working principle that a design should dissipate energy, but this solution tries to avoid its sensitivity to the wave forcing. The principle of this solution can be found in the reduced water plane area of the floater. The water plane area of this new design is smaller than the water plane area of the original design which results in a smaller hydraulic stiffness for heave and roll. This solution opts to steer into the mass dominance region of Figure 4.9.

Figure E.15 shows a solution that adopts a form of damping that is used with bilge keel damping as well. The presented solution dissipates mostly roll energy, but they could also dissipate some heave energy.

Figure E.16 shows a solution of a heave plate. A heave plate is a horizontal steel sheet rigidly connected to the structure to generate drag forces as the structure excites up and down. The drag of the sheet through the water is causing dissipation of energy. The structure does not have any moving objects with respect to the original Tidal Bridge design. The heave plate becomes more effective closer to the bottom as the wave particle accelerations in the z-axis become smaller closer to the bottom. Also, the added mass of the heave plate closer to the bottom becomes larger as it becomes harder and harder to squeeze the water out or suck it back into the space between the bed and the heave plate.

Figure E.17 shows a solution for a sway plate. The sway plate works with the same physical principle of the heave plate. However, the added mass of the sway plate takes a more constant value as it gets closer to the bottom than the heave plate. A constant current in combination with a sway plate gives the floater a fixed roll rotation. This rotation can be adapted for by replacing the hinge location farther from the centre of gravity. The sway plate works well in the sway and roll degree of freedom. The sway plate generates extra tension or compression in the pendulum.

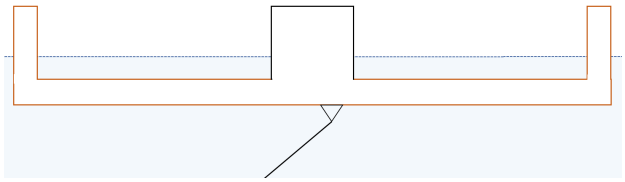

Figure E.14 [Concept 14] Semi-submersible floater

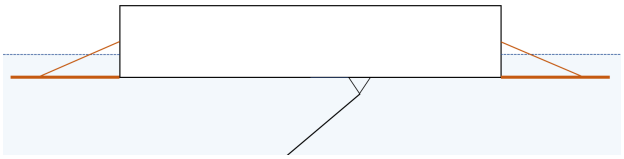

Figure E.15 [Concept 15] Bilge keel

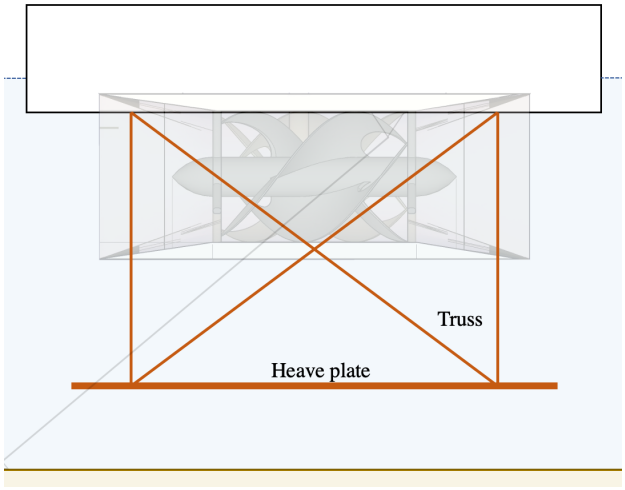

Figure E.16 [Concept 16] Heave plate

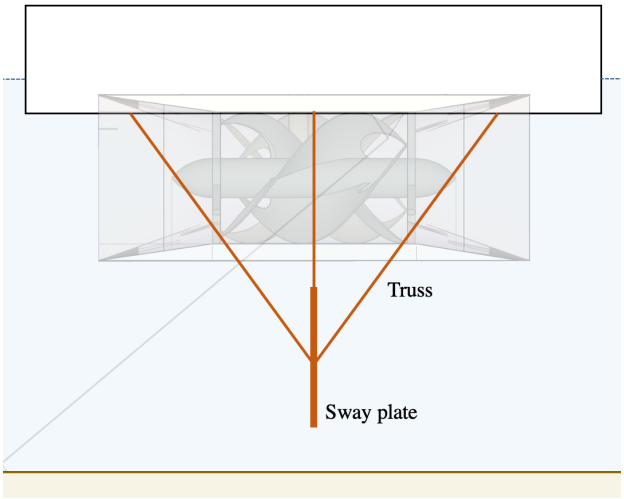

Figure E.17 [Concept 17] Sway plate

F | Second design loop: quantitative design

Contents of this appendix chapter

F.1 Developing the slosh damper alternative

Subdivision of the slosh damper over the floaters

The slosh damper can be constructed within the middle floater or it can be subdivided into smaller slosh dampers that are distributed over the other floaters of the Tidal Bridge element. Both solutions would dissipate energy and the solutions would not differ from each other concerning the structural dynamics model. However, the forces within the structure of the Tidal Bridge would be more equally divided over the complete structure if the complete slosh damper would be subdivided in smaller slosh dampers around the five floaters.

Total mass of the slosh damper water body

The mass of the slosh damper has, in general, a magnitude of about 3-5 % of the mass that needs to be damped. The added mass is moving along with the dynamics of the Tidal Bridge and this needs to be taken into account upon evaluating the slosh damper mass. The mass of the structure in sway direction including the added mass takes a value of $3.5 \cdot 10^6$ kg. Hence, the mass of the water in the slosh tank should have a value of about 175.000 kg in order to be 5% of the total mass in the sway direction.

Two slosh damper working principles

The slosh damper may dissipate energy by either of two different types of working principles to dissipate energy. The first working principle assumes that the water in the slosh damper is dynamically active following linear wave theory. The dissipation takes place by vortex shedding around objects placed within the slosh damper. The second working principle assumes that a hydraulic jump forms within the slosh damper that dissipates energy. The kinematics of the water particles are approached by different theories depending on this slosh damper working principle. Hence, the theoretical optimized dimensions differ between the two types of working principles. However, the difference between the calculated slosh damper dimensions do not differ radically between the two working principles.

Slosh tank natural frequency

The first formula within Equation F.1 provides the relation between the height of the water within the slosh tank, the length of the tank and the sloshing period for a working principle that follows linear wave theory (Velicko & Gaile, 2015). The presented relation is valid for a situation: 1. without objects within the slosh damper that provide resistance during the sloshing, and 2. without the formation of a hydraulic jump. A situation that includes objects providing resistance to the sloshing influences the angular frequency a little bit and this influence may be neglected.

The second working principle of the slosh tank targets a hydraulic jump that lead to energy dissipation. The relation between the water level height in the slosh tank, the tank length and the angular frequency can

be determined by using the travelling velocity of a hydraulic jump $c = \sqrt{gh}$. The hydraulic jump should travel twice the length of the slosh tank for one sloshing period. The result of the latter facts have been combined into the second formula of Equation F.1.

$$\omega_s = \sqrt{\frac{\pi g}{l} \cdot \tanh\left(\frac{\pi \cdot h_{linear}}{l}\right)}$$
$$\omega_s = 2\pi \cdot \frac{\sqrt{g \cdot h_{jump}}}{2 \cdot l} \tag{F.1}$$

Where:				
	ω_s	[rad/s]	=	angular frequency (1.45 rad/s)
	g	[m^2]	=	gravitational acceleration (9.81 m/s^2)
	l	[m]	=	slosh tank length
	h_{linear}	[m]	=	slosh tank water level height following linear wave theory
	h_{jump}	[m]	=	slosh tank water level height following the propagation speed of a hydraulic jump

The formulas within Equation F.1 can each be rewritten such that water level height can be plotted versus the water tank length as displayed in Figure F.1.

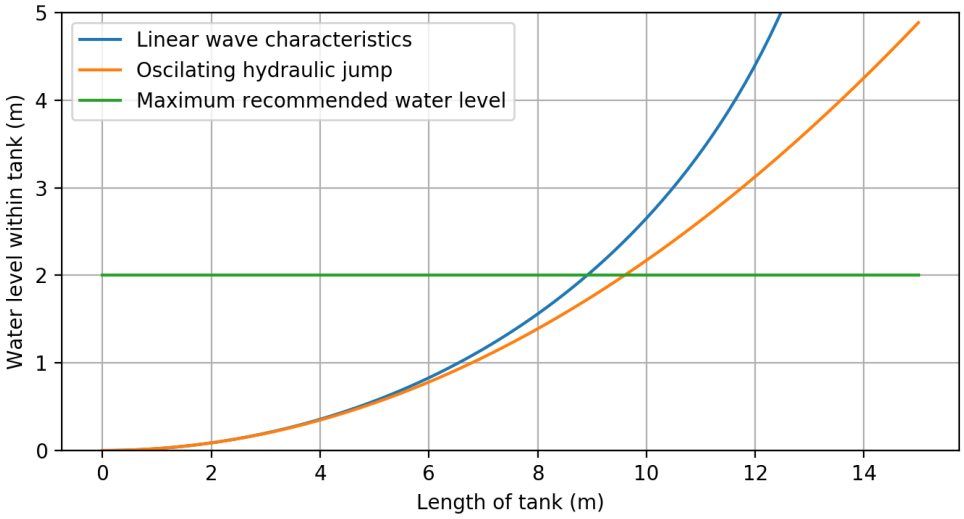

Figure F.1 The height of the water level in the slosh tank with respect to the length of the tank with a fixed value for $\omega_s = 1.45\ rad/s$ for a calculation based on linear wave theory and a calculation based on the velocity of a hydraulic jump. The crossing between the green and blue curve is at 8.9 m.

Chosen slosh tank dimensions

The slosh tank length is preferably as long as possible to achieve the largest lever arm of the slosh water mass with respect to the COG to counteract rotations. The tank lengths specified in Figure F.1 could all be potential slosh damper tanks as the floater length is larger than 15 meters. The slosh tank dimensions are therefore limited by the maximum height of the water level within the tank. A maximum recommended water level in the slosh tank is specified to be two meters. This maximum recommended water level is determined to avoid the phenomenon of saturation. The phenomenon of saturation means that the water hits the top of the slosh tank. This phenomenon does negatively influence the damper characteristics of the slosh tank (Faltinsen, 1990). Figure F.1 shows that a slosh tank with a length of 8.9 meters and water level height of 2 meters will result in a angular frequency of 1.45 rad/s. In case that only one slosh tank would be placed, then the width of this tank is:

$$width = \frac{m}{l_s \cdot h_{linear} \cdot \rho} = 9.35\ m \tag{F.2}$$

Where:	m	[kg]	=	mass
	l_s	[m]	=	slosh tank length
	h_{linear}	[m]	=	height of water level within the slosh tank
	ρ	[kg/m^3]	=	density of the water within the slosh tank

This calculated width of the slosh tank is split over five parts to distribute evenly the effect of the damping over the complete floating element of 100 meters in length. Figure 6.1 shows how the calculated width of the tank is divided in five equal parts. Every part has a width of 1.87 meter. This set up of five small slosh tanks divided over the five floaters is to be viewed within Figure 6.2 that is showing a top view of the slosh damper set up.

Slosh tank damping

The slosh tank damping devices are one of the tuning characteristics of the slosh damper. The slosh tank damping devices are objects that dissipate energy from the slosh water mass. The dissipation is important to avoid undesired extreme dynamics of the slosh water mass that lead to the counteractive effect. The damping devices could have the form of poles, nets, screens, baffles, or floating objects. Poles are suitable damping devices as the effectivity of those can be approached well with the Morison Equation as specified in Equation 3.2.

Floating stability

The stability of the Tidal Bridge floating element becomes affected by adding a water mass that may freely move through the Tidal Bridge. Figure C.4 shows some relevant locations that help to define the stability of the object (Molenaar & Voorendt, 2020). The distance GM needs to be positive and the object becomes more stable with a larger GM. A hand calculation helps to determine the distance GM:

$$\begin{aligned} BM &= \frac{I_{yy}}{V_w} \\ &= \frac{\frac{1}{12} \cdot b \cdot l^3}{A_w \cdot d} \\ &= \frac{\frac{1}{12} \cdot (3 \cdot 5 + 2 \cdot 3.5 \cdot 34^3}{809 \cdot 2.07} \\ &= 43 \; meter \end{aligned} \tag{F.3}$$

Where:	BM	[m]	=	distance from the centre of buoyancy to the meta centre
	I_{yy}	[m^4]	=	Area moment of inertia
	V_w	[m^3]	=	Volume of the displaced water
	b	[m]	=	total width of the five floaters together
	l	[m]	=	length of one of the floaters

The distance GB is about half of the draught and determined to be approximately 1 meter. This results in a GM of 42 meters. Upon adding the weight of the slosh damper, the stability reduces and the distance GM becomes 39 meters. This is still a very stable structure and the slosh damper does not endanger the structure stability.

F.1.1 Modelling the slosh damper in the structural dynamics model

The interaction of water particles of the slosh damper with the actual Tidal Bridge structure is complicated to describe and can only be achieved with an actual computational fluid dynamics program. The following simplifications are taken to make the modelling of the slosh damper possible in the structural dynamics model:

- The water mass of the slosh damper is simplified to a point mass following a predefined frictionless trajectory;
- The surface elevation is simplified by a strait line;
- The hydraulic dissipation of energy by the flow damping poles is integrated in the model by a dependency of the squared velocity of the point mass.

Description of the point mass trajectory

Figure F.2 shows how the first two simplification are included in a geometric model describing the trajectory of the point mass of the water of the slosh damper. The trajectory of the point mass of the water of the slosh damper is analytically described by Equation F.4 and F.5:

For $-\frac{b}{6} \leq y \leq \frac{b}{6}$:

$$z = \frac{3 \cdot h \cdot y^2}{b^2} \tag{F.4}$$

For $y \leq -\frac{b}{6} \text{and} y \geq \frac{b}{6}$:

$$z = -\frac{h}{4} - \frac{b \cdot h}{9 \cdot \left(y - \frac{b}{2}\right)} \tag{F.5}$$

The slope of the trajectory is equal to the slope that the water would adopt for the specified location of the point mass. The slope of the trajectory is driving the restoring force that brings the point mass back in its equilibrium position. This represents reality well as the slope of the water surface elevation is the restoring force that brings the water mass back in the equilibrium position. This restoring force driven by the water surface elevation slope has exactly the same magnitude as the restoring force that the point mass experiences from the trajectory slope.

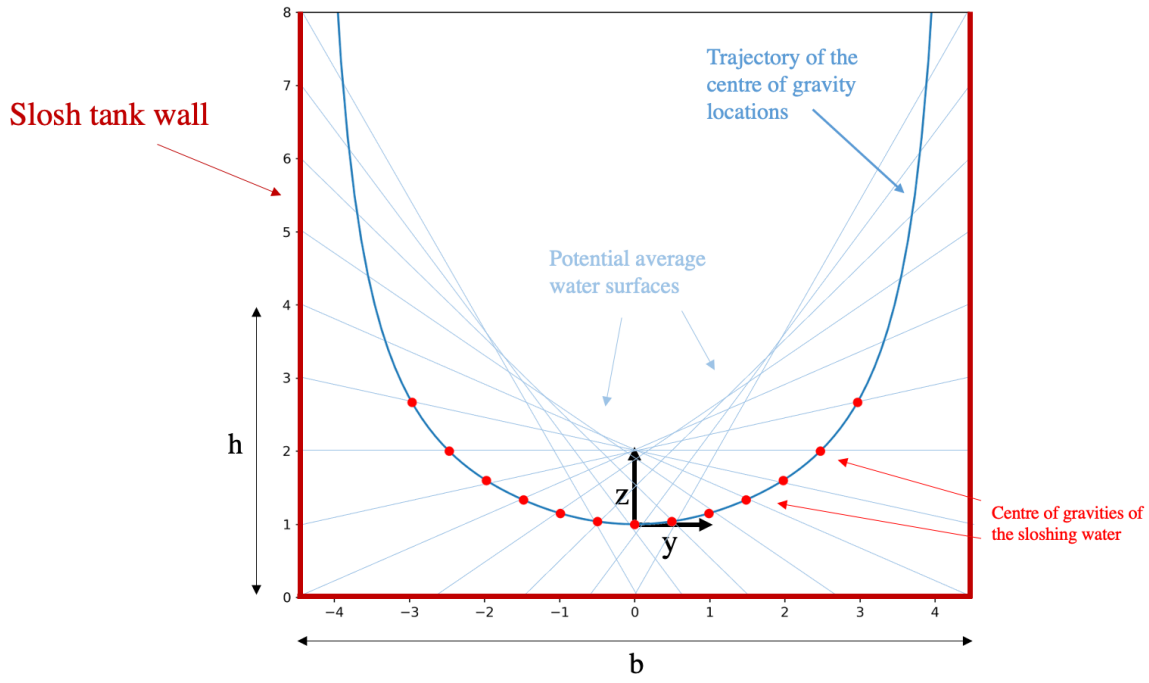

Figure F.2 Figure showing the trajectory of the locations of the centre of gravity of the slosh damper point mass within the slosh damper.

Where: h [m] = two times the slosh damper water level in rest
b [m] = slosh damper length

Free body diagram

An additional degree of freedom is introduced that describes the movement of the point mass over the described trajectory of Figure F.2. The location of the point mass within the described trajectory, the roll rotation of the Tidal Bridge and the sway, heave and roll accelerations lead to a resultant force of the point mass exerted onto the Tidal Bridge. This resultant force is split out into a sway, heave and roll forcing. The free body diagram of these forces that relate to each other is to be viewed in Figure F.3

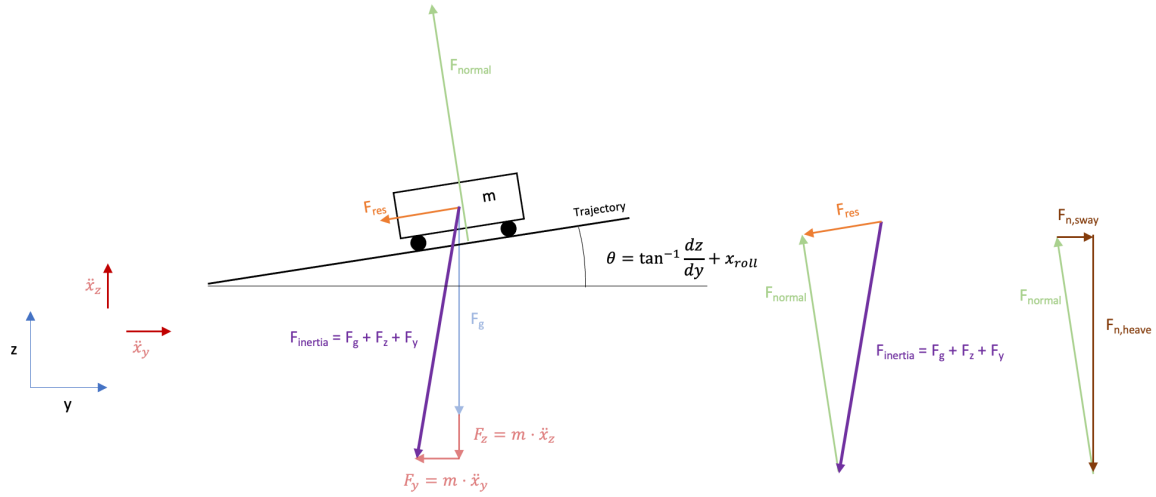

Figure F.3 Figure showing the free body diagram of the point mass representing the water body of the slosh damper

Where:	m	[kg]	=	mass of the point mass
	F_g	[N]	=	gravity force
	$\dot{x}_z$	[m/s^2]	=	heave acceleration of the Tidal Bridge
	$\dot{x}_y$	[m/s^2]	=	sway acceleration of the Tidal Bridge
	$\tan^{-1}\left(\frac{dz}{dy}\right)$	[rad]	=	angle of slope
	x_{roll}	[rad]	=	angle of roll rotation of the Tidal Bridge
	$F_{n,sway}$	[N]	=	sway force of slosh damper onto the Tidal Bridge
	$F_{n,heave}$	[N]	=	heave force of slosh damper onto the Tidal Bridge

Numerical scheme

The slosh damper force is added to the other forcing vectors and integrated in the numerical scheme describing the dynamics of the Tidal Bridge as described by Equation F.6.

$$\boldsymbol{M} \cdot \ddot{\boldsymbol{x}}_1 = \boldsymbol{K} \cdot \boldsymbol{x}_0 + \boldsymbol{C} \cdot \dot{\boldsymbol{x}}_0 + \boldsymbol{F}_{other} + \boldsymbol{F}_{slosh}(x_0, \ddot{x}_0) \tag{F.6}$$

Where:	$\boldsymbol{M}$	[kg]	=	mass matrix Tidal Bridge
	$\boldsymbol{C}$	[Ns/m]	=	damping matrix Tidal Bridge
	$\boldsymbol{K}$	[N/m]	=	stiffness matrix Tidal Bridge
	$\ddot{\boldsymbol{x}}_1$	[m/s^2]	=	acceleration of the Tidal Bridge at time step 1
	$\dot{\boldsymbol{x}}_0$	[m/s^2]	=	velocity of the Tidal Bridge at time step 0
	$\boldsymbol{x}_0$	[m]	=	displacement of the Tidal Bridge at time step 0
	$\boldsymbol{F}_{other}$	[N]	=	Other forcing vectors acting on the Tidal Bridge

This integration scheme assumes $\ddot{\boldsymbol{x}}_1 = \ddot{\boldsymbol{x}}_0$ which is not valid. For small time steps ($t \leq 0.02\ s$) $\ddot{\boldsymbol{x}}_1 \approx \ddot{\boldsymbol{x}}_0$ and the integration scheme represents reality well. A more accurate description of the numerical scheme would be:

$$\boldsymbol{M} \cdot \ddot{\boldsymbol{x}}_1 = \boldsymbol{K} \cdot \boldsymbol{x}_0 + \boldsymbol{C} \cdot \dot{\boldsymbol{x}}_0 + \boldsymbol{F}_{other} + \boldsymbol{E} \cdot \ddot{\boldsymbol{x}}_1 \tag{F.7}$$

In which $\boldsymbol{E}$ is the matrix describing the inertia of the slosh damper that moves counteractive and reduces the Tidal Bridge accelerations. This numerical scheme of Equation F.7 appeared to be very complicated to apply with straight forward algebra. Vector calculus would probably be more effective to obtain the $\boldsymbol{E}$. Rewriting the equations that follow from Figure F.3 into a physically correct model in the vector notation would take much efforts and would not surely lead to more accurate answers.

Modified Euler integration scheme

The point mass translates over its trajectory upon every time step within the numerical model. A modified Euler integration scheme has been used to describe these translations accurately. The Modified Euler numerical

integration scheme has been explained before in Section 3.3.2. Forward Euler was taken as the initial integration scheme to describe the movements of the point mass of the slosh damper. The Forward Euler integration scheme introduced to much error with the desired longer time step. The Modified Euler integration scheme showed to be an outcome in having a strong integration scheme that can deal with a relatively large time step without introducing errors. Figure F.4 proofs that the Modified Euler integration scheme is correctly applied. The slosh point mass moves freely without resistance or any other forcing from outside the point mass its normal trajectory. The point mass shows to keep its energy by returning to exact the same location after every period.

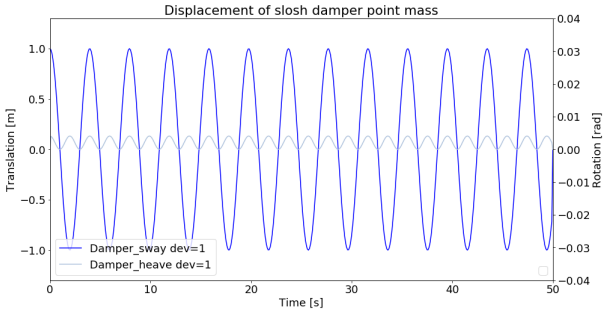

Figure F.4 Figure proofing the Modified Euler integration scheme to work with a relatively large time step of $t = 0.1$.

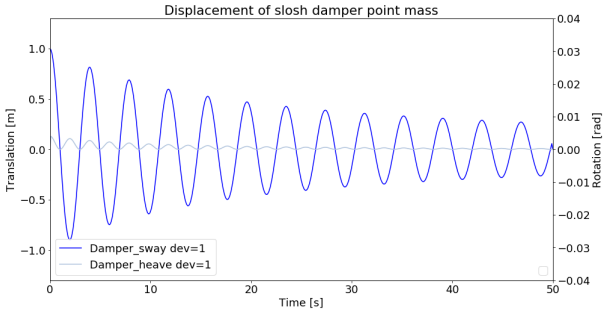

Figure F.5 Figure showing a free decay test of the slosh damper point mass

Free decay test

Poles have been placed in the slosh damper to dissipate energy from the slosh damper water mass. The frontal surface of the poles has been chosen such that the displacements reduce by a factor two after five oscillations following a free decay test. This amount of damping has been the initial guess for the slosh damper. This amount of damping may be adapted in later stages of optimization.

Discussion of the simplifications

The simplifications have been very effective in modelling the slosh damper in the structural dynamics model. However, these simplifications showed that the sloshing period of the numerical damper did not match the sloshing period of the linear wave theory precisely. The sloshing period of the slosh damper of the numerical scheme was off by about 10%. This may prove that the simplifications did not represent reality perfect. However, the utmost goal of integrating the slosh damper in the structural dynamics model was to find out whether the slosh damper is an effective damping solution. This goal could still be achieved by adapting the sloshing period to the desired sloshing period such that the effect of the simplifications does not influence reaching the goal.

F.2 Developing the heave plate alternative

Finding the effectiveness of drag forces

Hand calculations of Equation F.8 show that the drag forces lead to a reduction of the dynamic behaviour in the order of 0.05 m/s^2 or smaller. This reduction is insignificant as a main optimization strategy, but the reduction should not be neglected. Another disadvantage of a drag based solution may be found in the phase difference of the maximum velocity compared to the maximum accelerations. The moment within the oscillation that the the velocity is maximum and hence the drag forces are maximum, the acceleration is close to zero. The effectiveness would be larger upon having a drag force that would be in phase with the maximum acceleration.

Unfortunately, this is physically not possible.

$$\begin{aligned} {F_{d,heave}}^1 &= \frac{1}{2} \cdot \rho \cdot C_d \cdot A_{plate} \cdot \dot{x}^2 \\ &= \frac{1}{2} \cdot 1000 \cdot 1.9 \cdot (30 \cdot 98) \cdot 1^2 \\ &= 2.8 \cdot 10^6 \ N \\ a_d &\approx \frac{F_{d,heave}}{m_{heave}} \\ &\approx \frac{2.8 \cdot 10^6}{44.7 \cdot 10^6} \\ &\approx 0.06 \ m/s^2 \end{aligned} \tag{F.8}$$

Where:

$F_{d,heave}$	[N]	=	Drag force
ρ	[kg/m^3]	=	Density of the water
C_d	[-]	=	Drag coefficient
A_{plate}	[m^2]	=	Surface area of the heave plate
$\dot{x}$	[m/s]	=	Heave velocity of Tidal Bridge floating element
a_d	[m/s^2]	=	Reduced acceleration due to drag of the heave plate
m_{heave}	[kg]	=	Mass in the heave direction of Tidal Bridge element including the added mass

Finding the effectiveness of inertia forces

Equation F.9 shows the effect of the added mass to the total dynamics. Upon taking the volume situated within the limits of five meters above and below the heave plate, then the expected reduction in the dynamics is in the order of 40%. This effect may become slightly larger upon integrating the self weight of heave plate.

$$\begin{aligned} m_{added,heave} &= V_{added} \cdot \rho \\ &= 10 \cdot 30 \cdot 98 \cdot 1000 \\ &= 29 \cdot 10^6 \ kg \\ \frac{m_{added,heave}}{m_{added,heave} + m_{heave}} &= 0.40 \ [-] \end{aligned} \tag{F.9}$$

F.3 Developing the sway plate alternative

F.3.1 Finding the increased pendulum forces

The force on the sway plate can be calculated for the situation with a large tidal current with the formula for drag forces to objects within a flow. The largest tidal current at the depth of the sway plate is estimated to be around 2.5 m/s. The drag coefficient C_d for a plate in a flow is 1.9 (DNV, 2011). The maximum drag force of the sway plate is calculated to be:

$$\begin{aligned} F_d &= \frac{1}{2} \cdot \rho \cdot C_d \cdot A_p \cdot \dot{x}^2 \\ &= \frac{1}{2} \cdot 1000 \cdot 1.9 \cdot (8 \cdot 98) \cdot 2.5^2 \\ &= 4.7 \cdot 10^6 \ N \end{aligned} \tag{F.10}$$

This force is about 34% of the maximum pendulum force. In this stage of the design process, the pendulum force has not been an important design parameter. A pendulum force increment of 34% is a significant increase, but this increment is not insurmountable.

G | Third design loop: detailing the designs

Contents of this appendix chapter

G.1 Details and visualizations of the heave plate variants

G.1.1 Variant 1: Lower heave plates

Profiles	Dimensions (mm)	Unity Checks
Plate	t = 15	0.41
Stiffeners	h = 350	0.48
	t = 15	
Box beam	h = 450	0.67
	w = 250	
	t = 12	
Main tubes	d = 250	0.53
	t = 8	
Stability tubes	d = 200	0.50
	t = 6	

Effectivity	12.1 days
Steel needed	833 tons
Generated added mass sway	-
Generated added mass heave	8453 tons
Depth of COG of added mass	18.8 m

Table G.1 Specifications variant 1

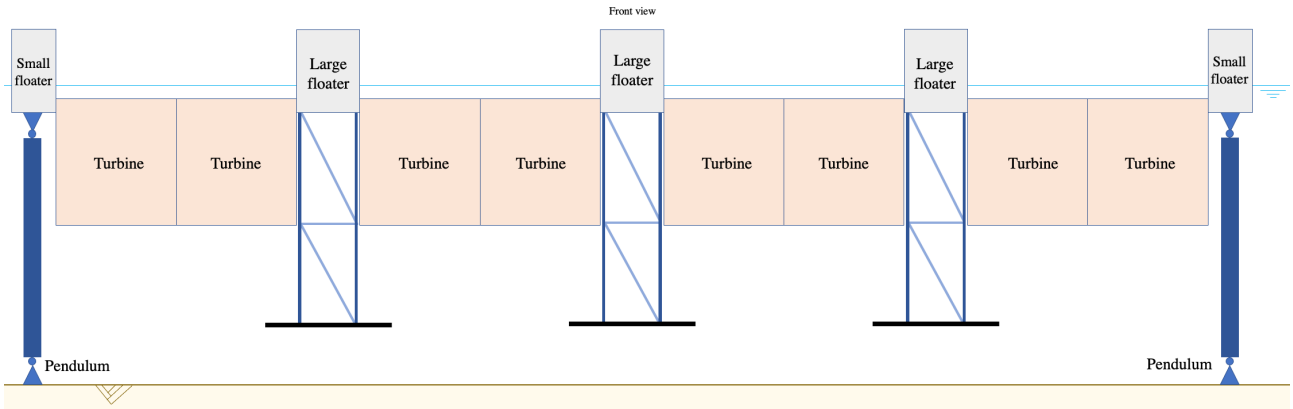

Figure G.1 Front view lower heave plates

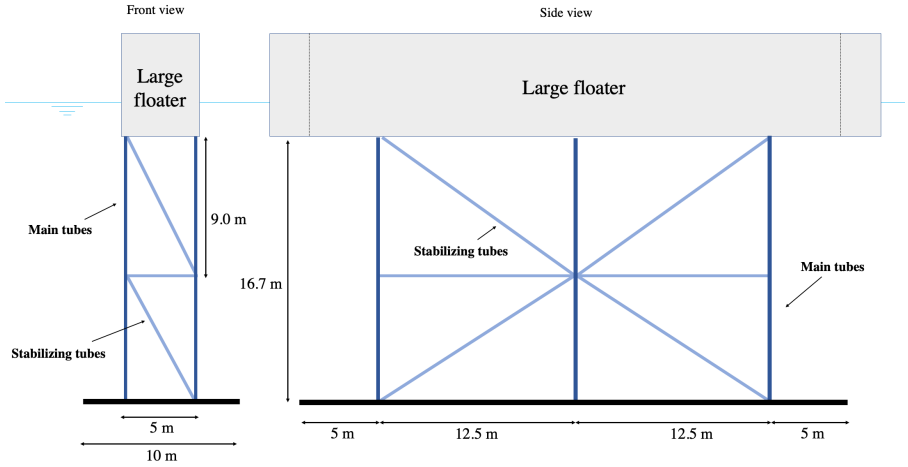

Figure G.2 Side view lower heave plates

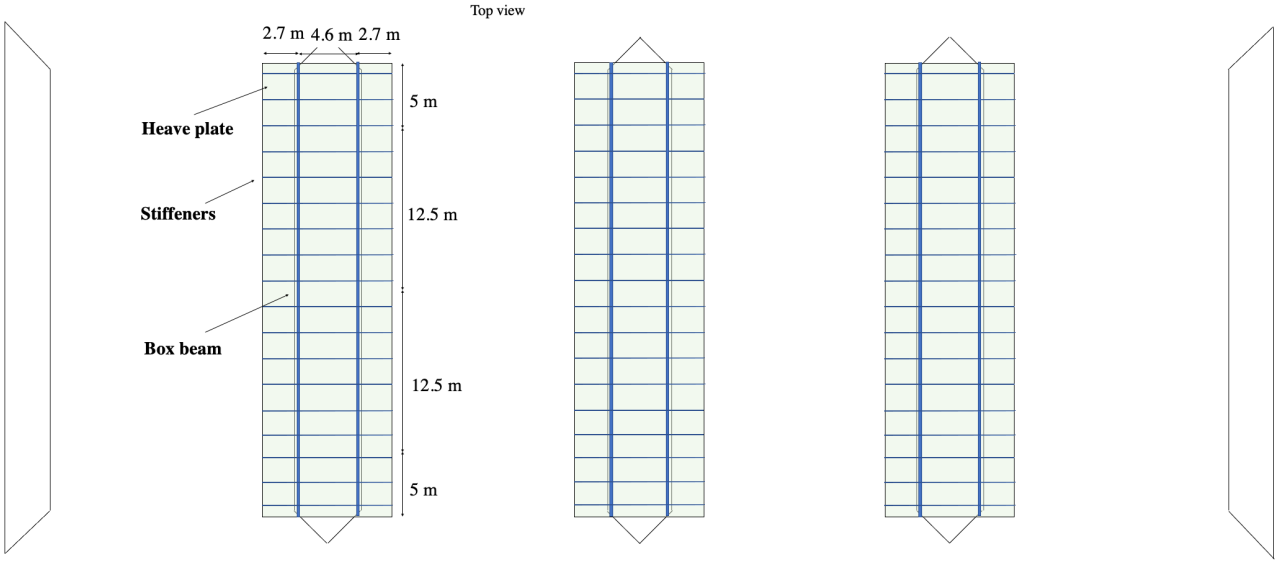

Figure G.3 Top view lower heave plates

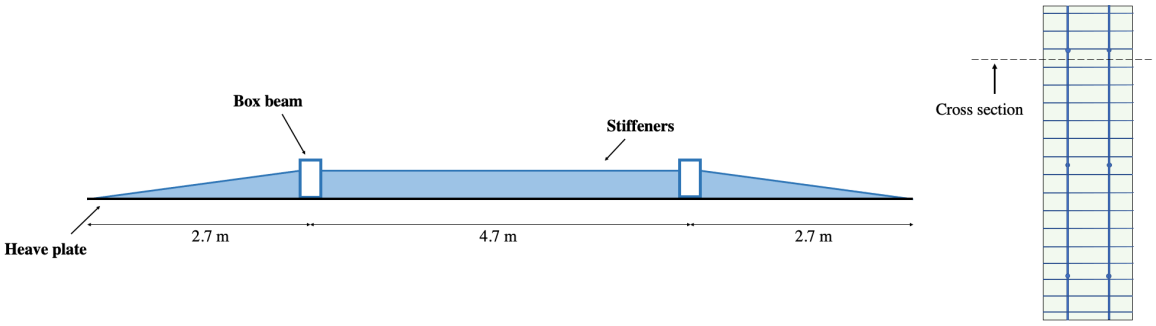

Figure G.4 Cross section of the heave plate of the lower heave plates

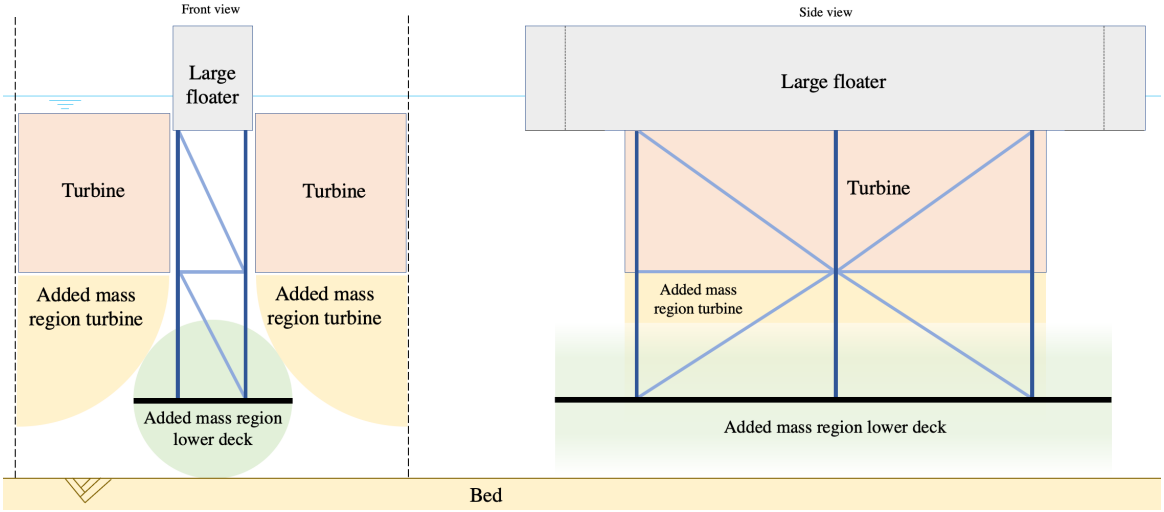

Figure G.5 Added mass plan of the lower heave plates

G.1.2 Variant 2: Upper heave plates

Profiles	Dimensions (mm)	Unity Checks
Plate	t = 15	0.41
Stiffeners	h = 300	0.49
	t = 15	
Box beam	h = 450	0.59
	w = 250	
	t = 12	
Main tubes	d = 250	0.53
	t = 8	
Stability tubes	d = 200	0.50
	t = 6	

Effectivity	11.9 days
Steel needed	426 tons
Generated added mass sway	-
Generated added mass heave	7907 tons
Depth of COG of added mass	11 m

Table G.2 Specifications variant 2

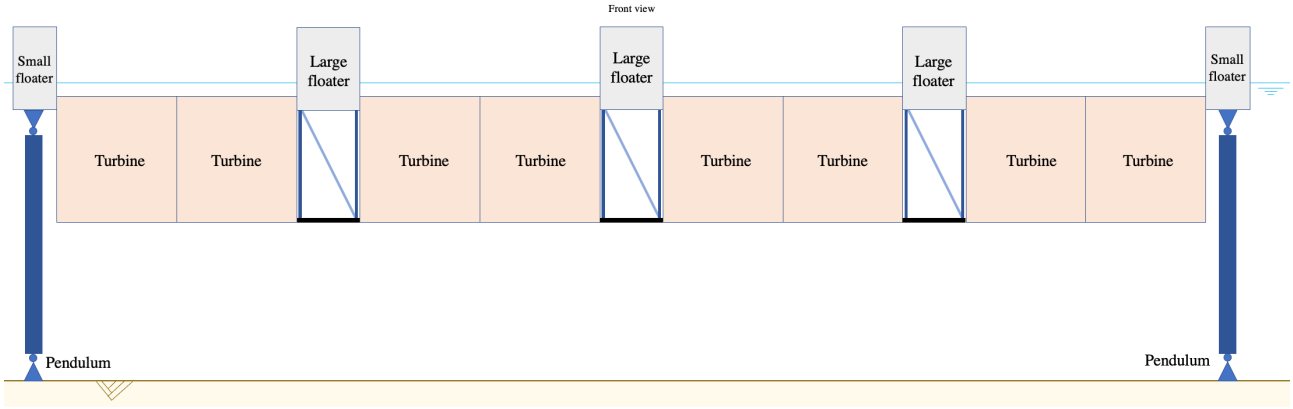

Figure G.6 Front view of the upper heave plates

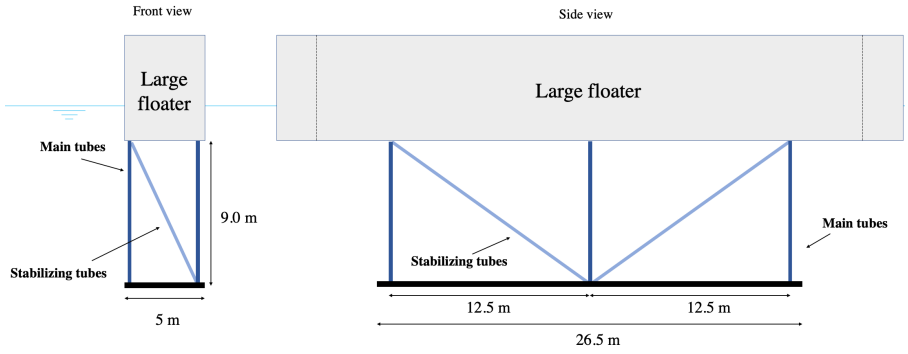

Figure G.7 Front and side view of the upper heave plates

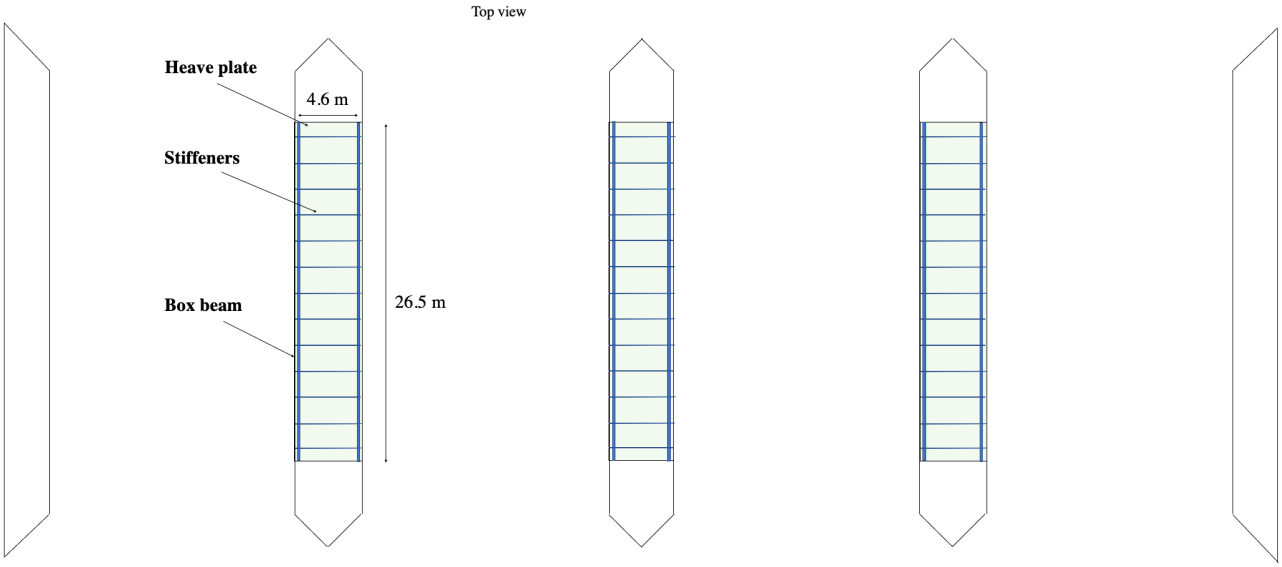

Figure G.8 Top view of the upper heave plates

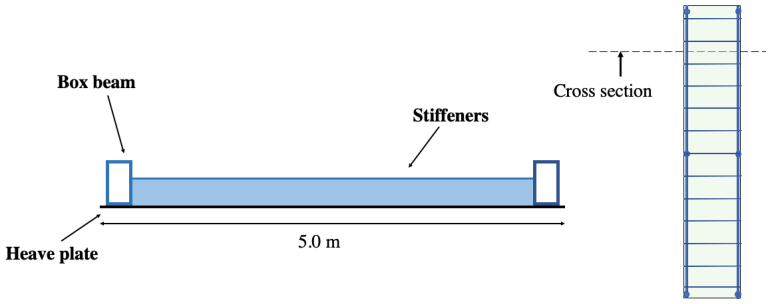

Figure G.9 Cross section of the heave plate of the upper heave plates

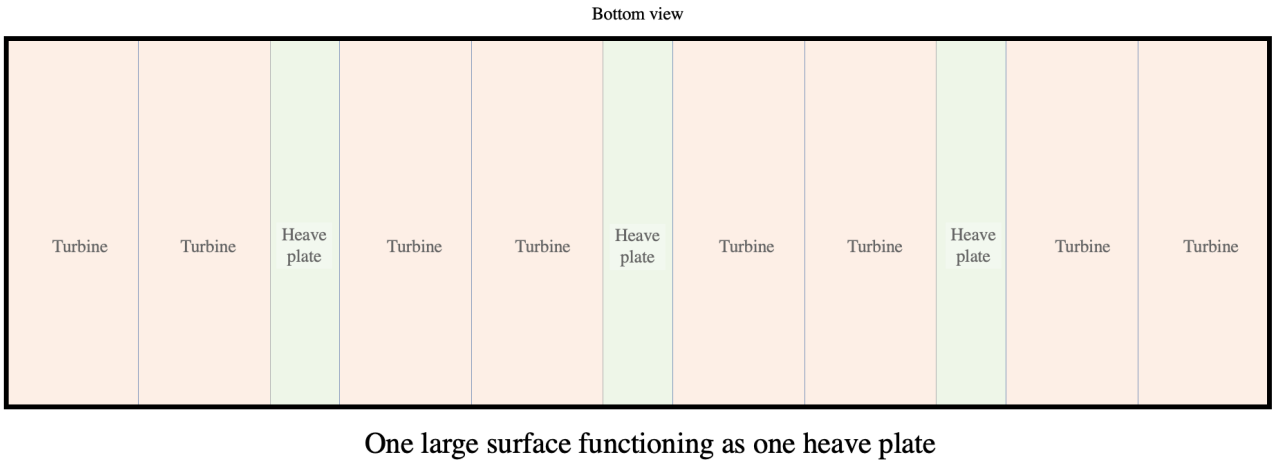

Figure G.10 Bottom view of the upper heave plates showing how the turbines and upper heave plates form one large slab generating added mass

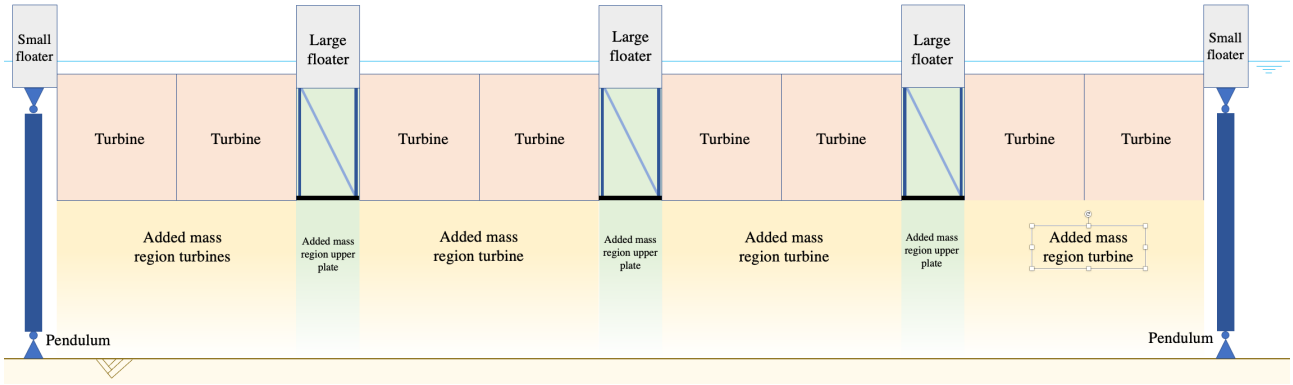

Figure G.11 Front view of the added mass plan of the upper heave plates

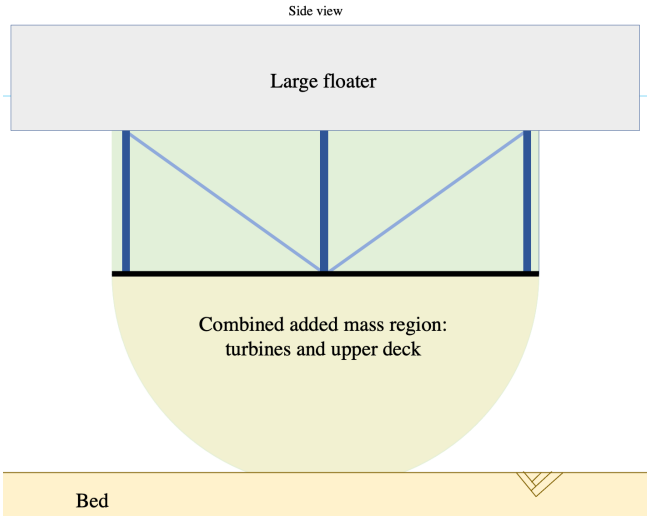

Figure G.12 Side view of the added mass plan of the upper heave plates

G.1.3 Variant 3: Heave plate 1 x 68 m

Profiles	Dimensions (mm)	Unity Checks		
Plate	t = 15	0.41	Effectivity	13.6 days
Box beam stiffeners	h = 200	0.60	Steel needed	1938 tons
	t = 10		Generated added mass sway	-
Box beam	h = 700	0.59	Generated added mass heave	16614 tons
	w = 400		Depth of COG of added mass	18.3 m
	t = 30			
Main tubes	d = 400	0.51		
	t = 10			
Stability tubes	d = 200	0.50		
	t = 6			

Table G.3 Specifications variant 3

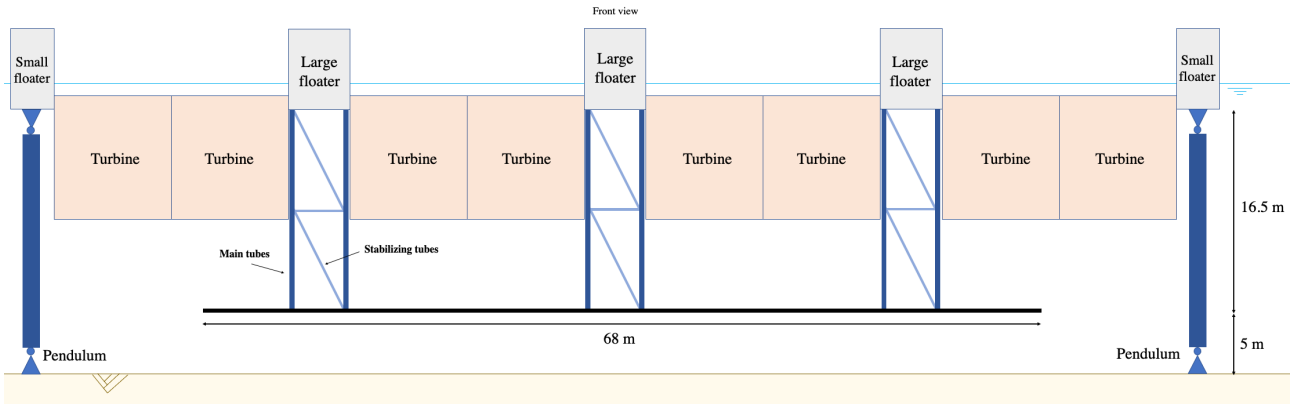

Figure G.13 Front view of the 1 x 68 m heave plate

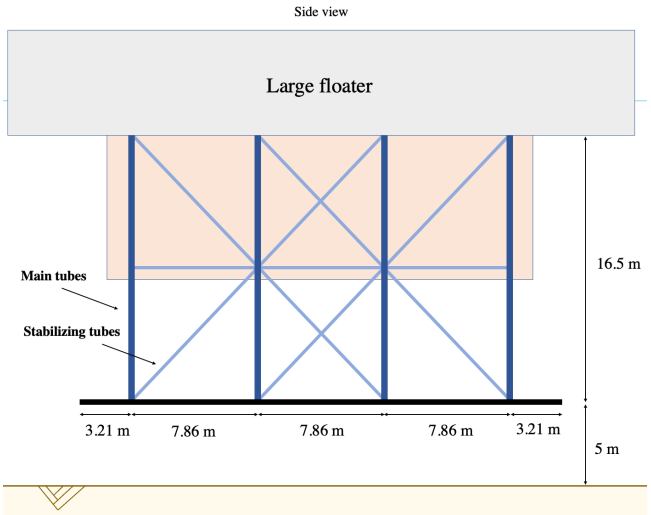

Figure G.14 Side view of the 1 x 68 m heave plate

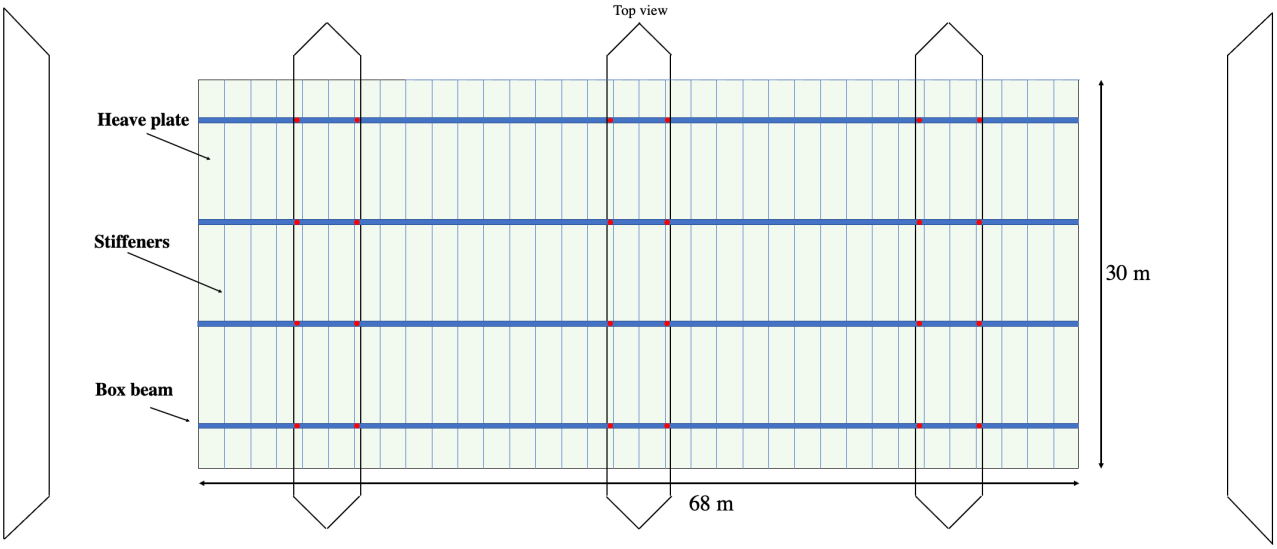

Figure G.15 Top view of the 1 x 68 m heave plate

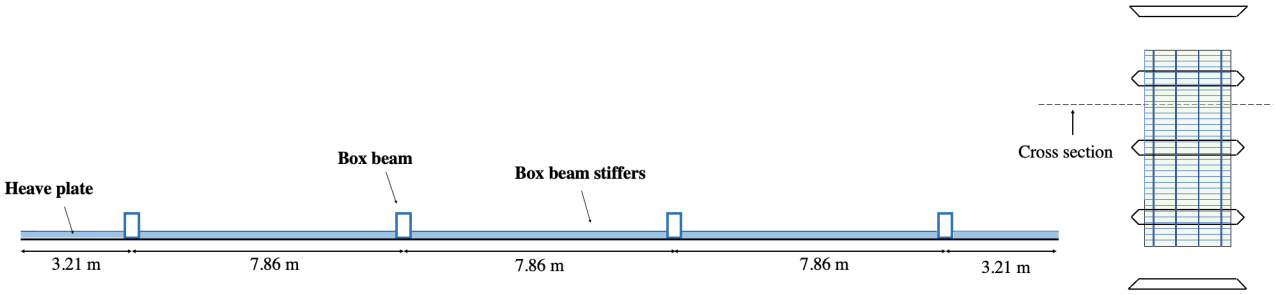

Figure G.16 A cross section of the plate of the 1 x 68 m heave plate

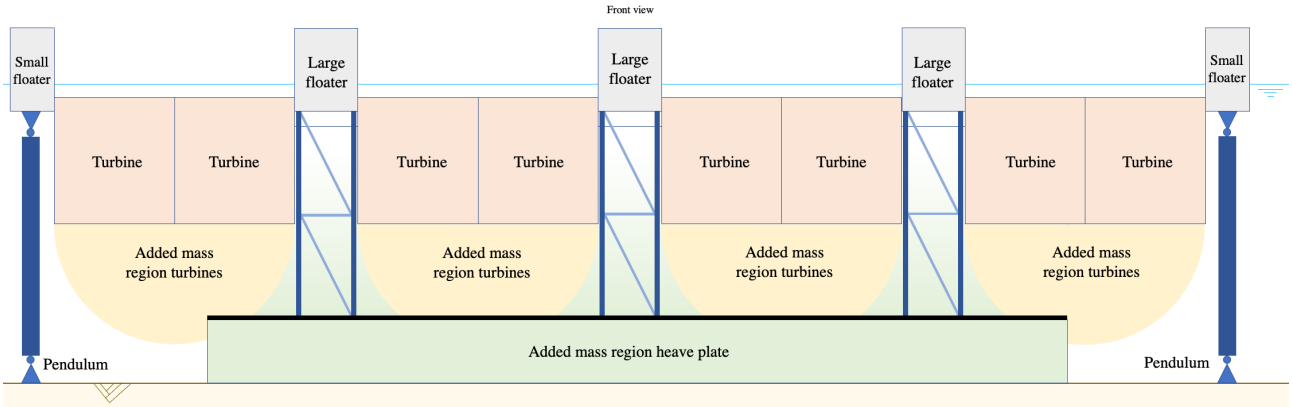

Figure G.17 Front view of the added mass plan of the 1 x 68 m heave plate

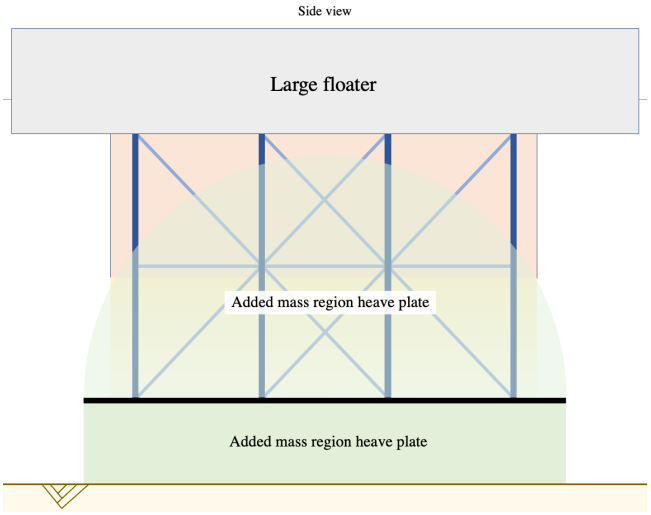

Figure G.18 Side view of the added mass plan of the 1 x 68 m heave plate

G.2 Details and visualizations of the sway plate variants

G.2.1 Variant 4: Sway plate 3 x 17 m

Profiles	Dimensions (mm)	Unity Checks
Plate	t = 15	0.20
Box beam	h = 300	0.51
	w = 200	
	t = 12.5	
Main tubes	d = 200	0.57
	t = 6	

Effectivity	8.6 days
Steel needed	268 tons
Generated added mass sway	2576 tons
Generated added mass heave	-
Depth of COG of added mass	16.5 m

Table G.4 Specifications variant 4

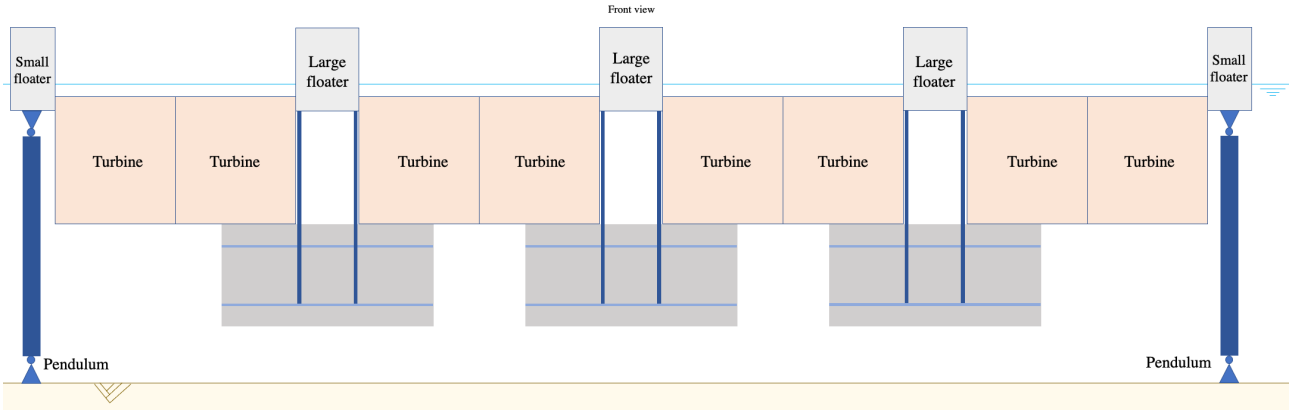

Figure G.19 Front view of the sway plate 3 x 17 m

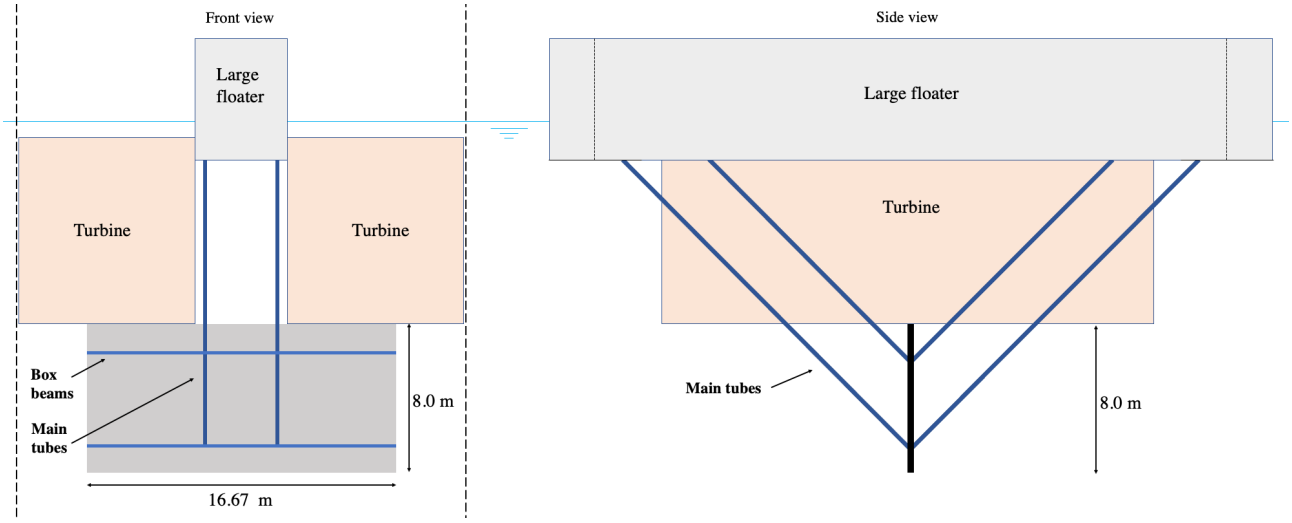

Figure G.20 Front and side view of the sway plate 3 x 17 m

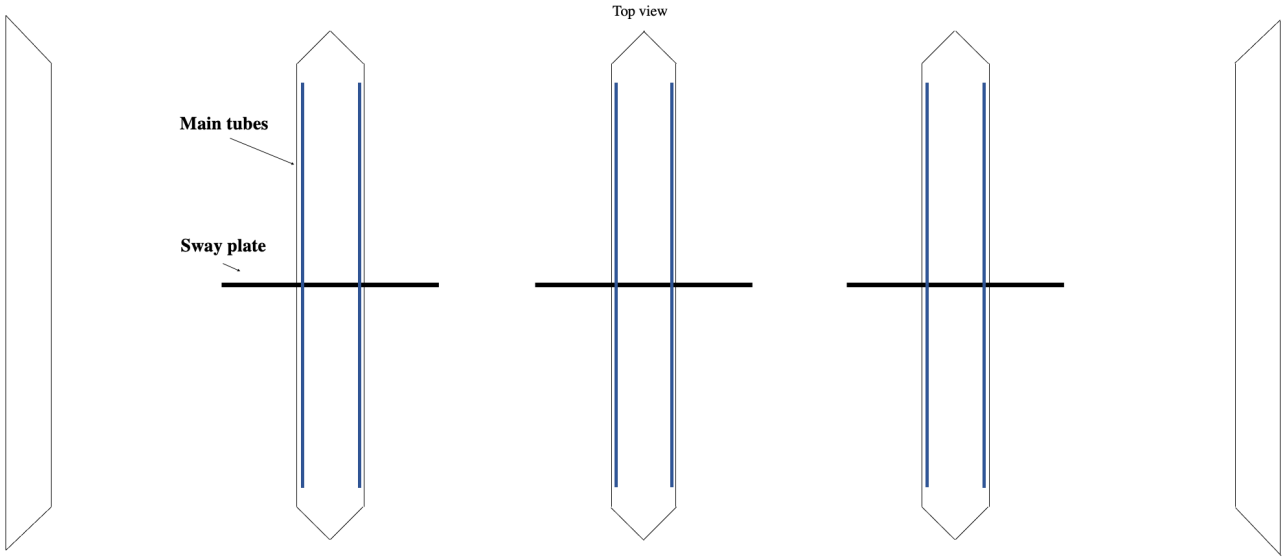

Figure G.21 Top view of the sway plate 3 x 17 m

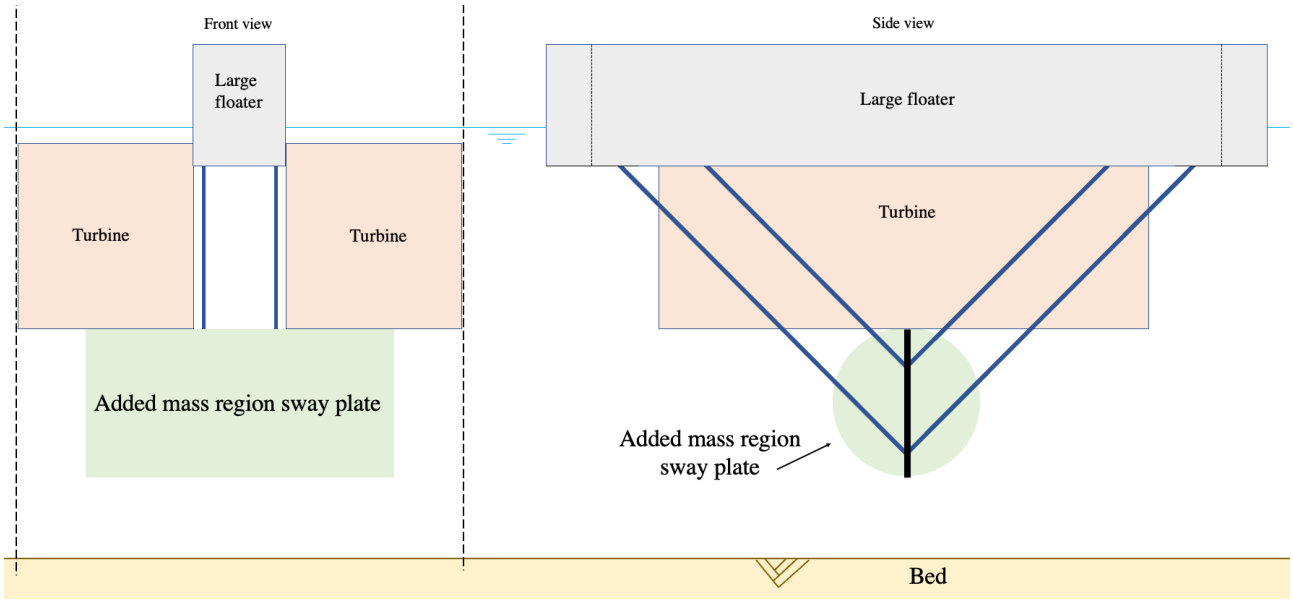

Figure G.22 Added mass plan of the sway plate 3 x 17 m

G.2.2 Variant 5: Sway plate 6 x 17 m

Profiles	Dimensions (mm)	Unity Checks
Plate	t = 15	0.20
Box beam	h = 300	0.51
	w = 200	
	t = 12.5	
Main tubes long	d = 200	0.57
	t = 7	
Main tubes short	d = 150	0.61
	t = 9	

Effectivity	15.5 days
Steel needed	497 tons
Generated added mass sway	5152 tons
Generated added mass heave	-
Depth of COG of added mass	16.5 m

Table G.5 Specifications variant 5

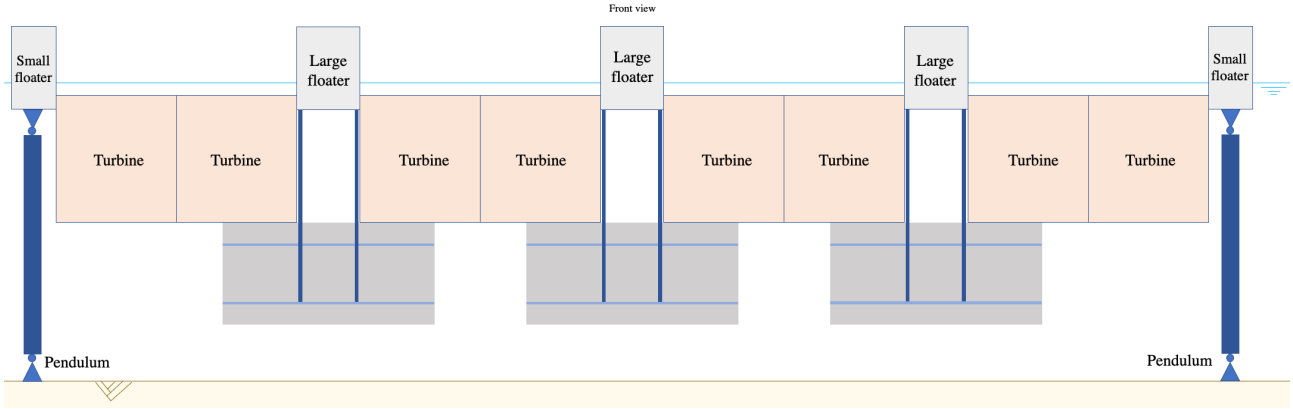

Figure G.23 Front view of the sway plate 6 x 17 m

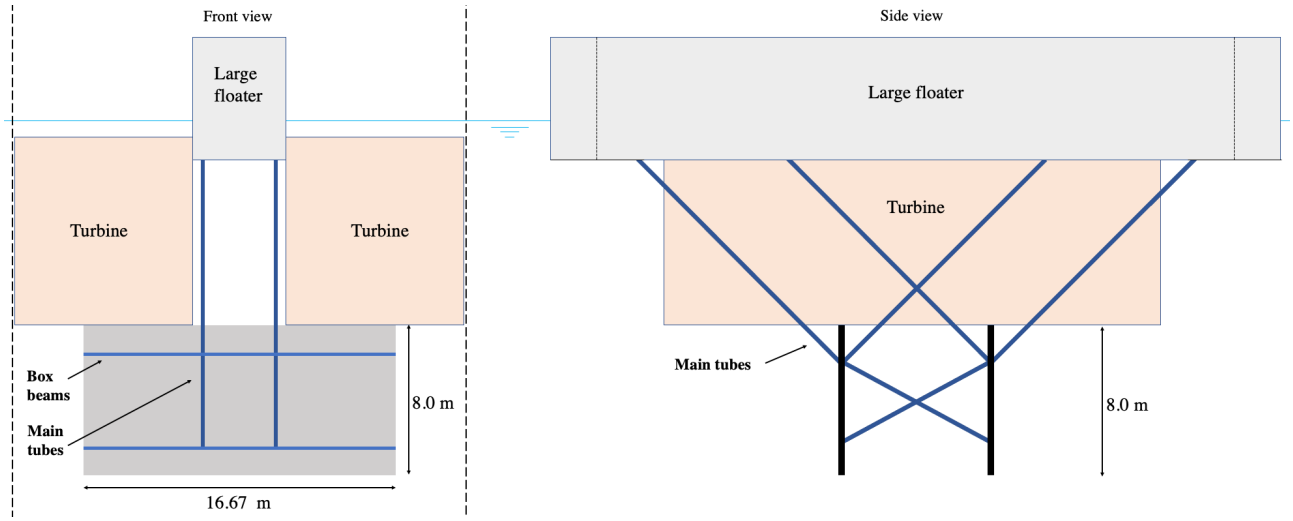

Figure G.24 Front and side view of the sway plate 6 x 17 m

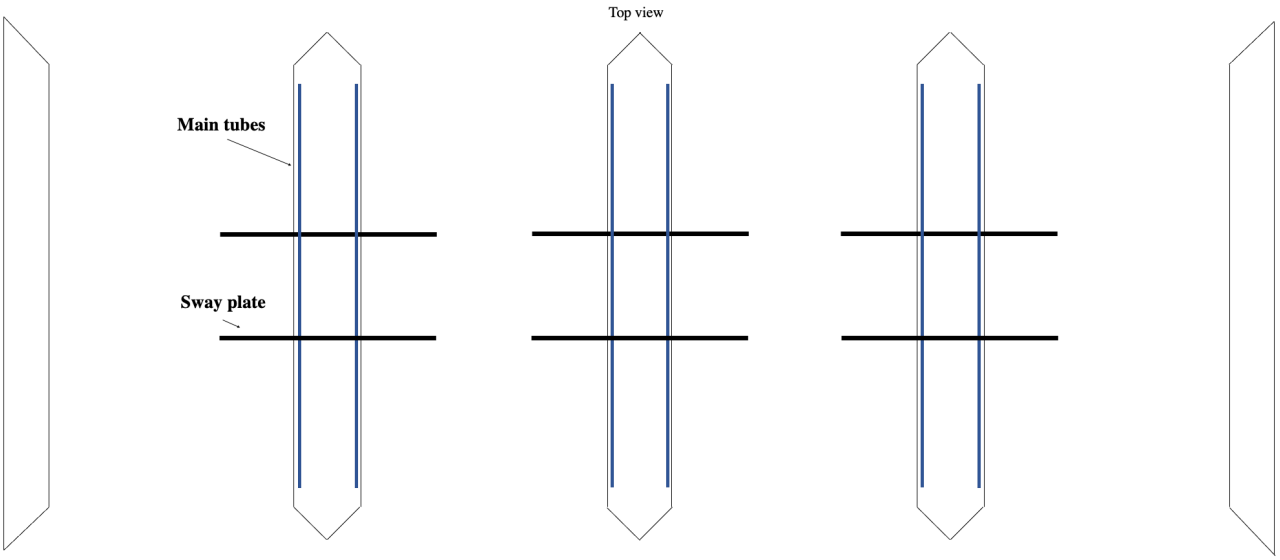

Figure G.25 Top view of the sway plate 6 x 17 m

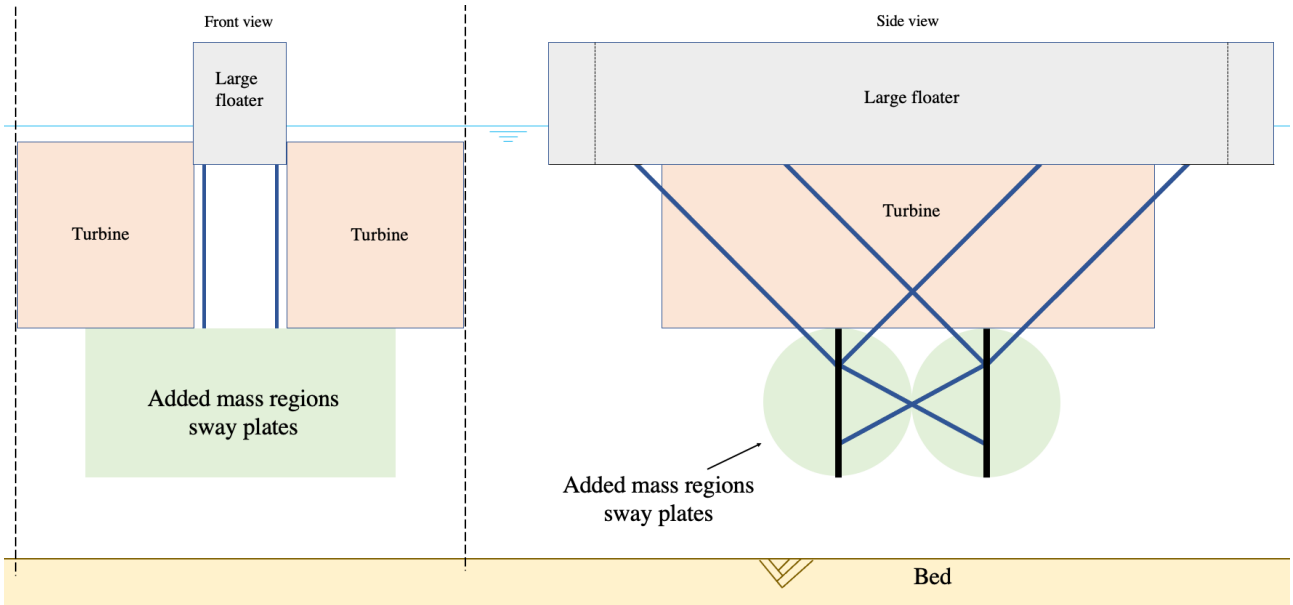

Figure G.26 Added mass plan of the sway plate 6 x 17 m

G.2.3 Variant 6: Sway plate 9 x 17 m

Profiles	Dimensions (mm)	Unity Checks
Plate	t = 15	0.20
Box beam	h = 300	0.51
	w = 200	
	t = 12.5	
Main tubes long	d = 200	0.57
	t = 7	
Main tubes short	d = 150	0.61
	t = 9	

Effectivity	22.3 days
Steel needed	750 tons
Generated added mass sway	7728 tons
Generated added mass heave	-
Depth of COG of added mass	16.5 m

Table G.6 Specifications variant 6

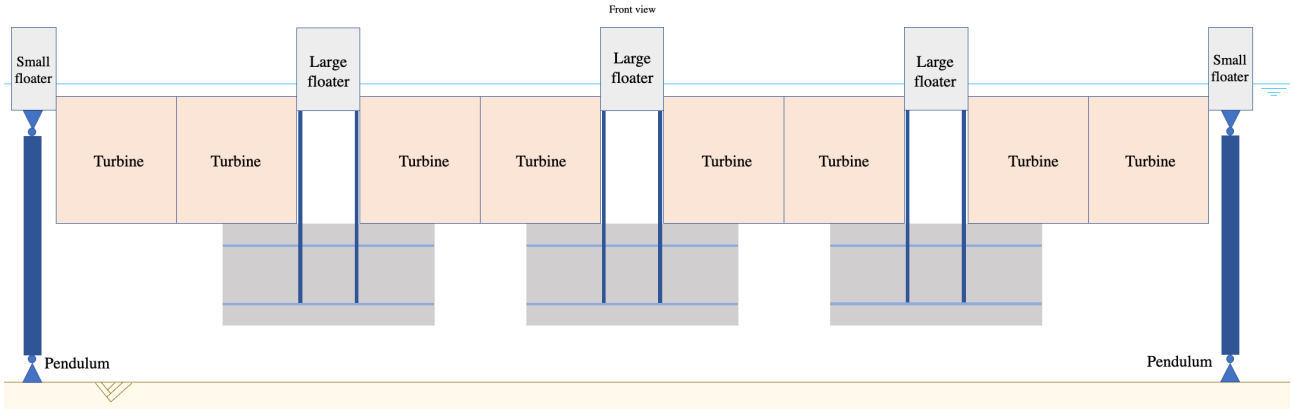

Figure G.27 Front view of the sway plate 9 x 17 m

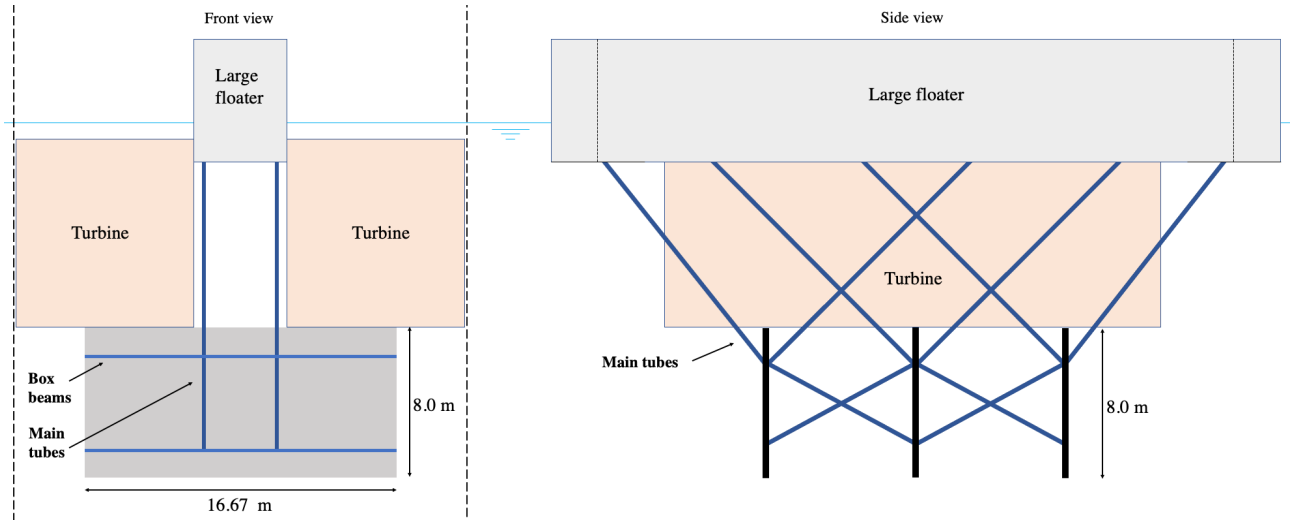

Figure G.28 Front and side view of the sway plate 9 x 17 m

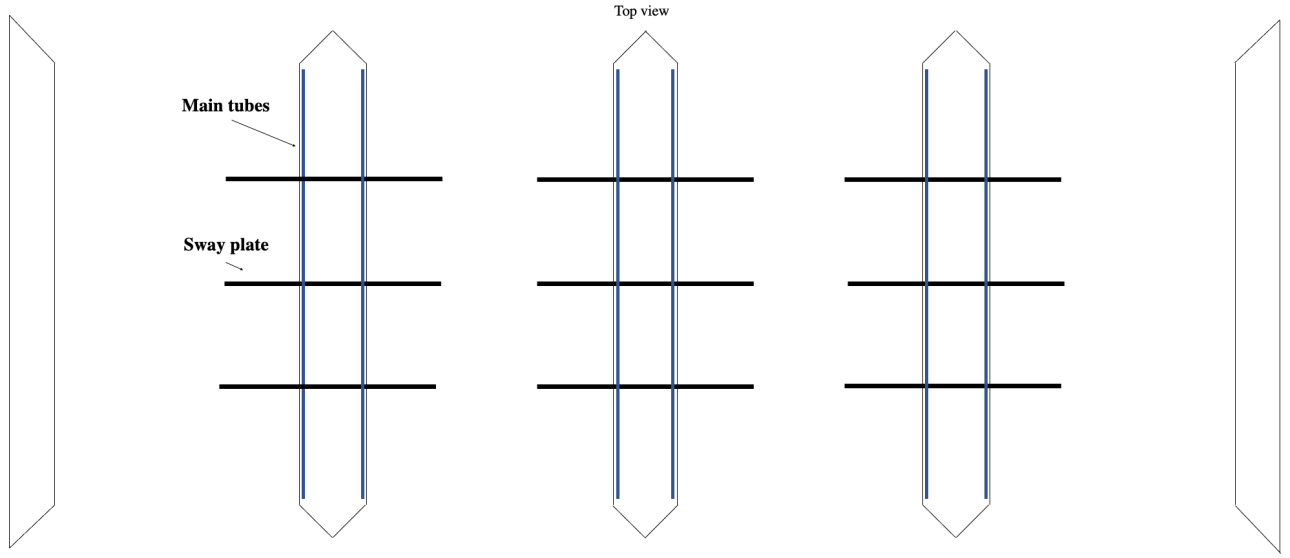

Figure G.29 Top view of the sway plate 9 x 17 m

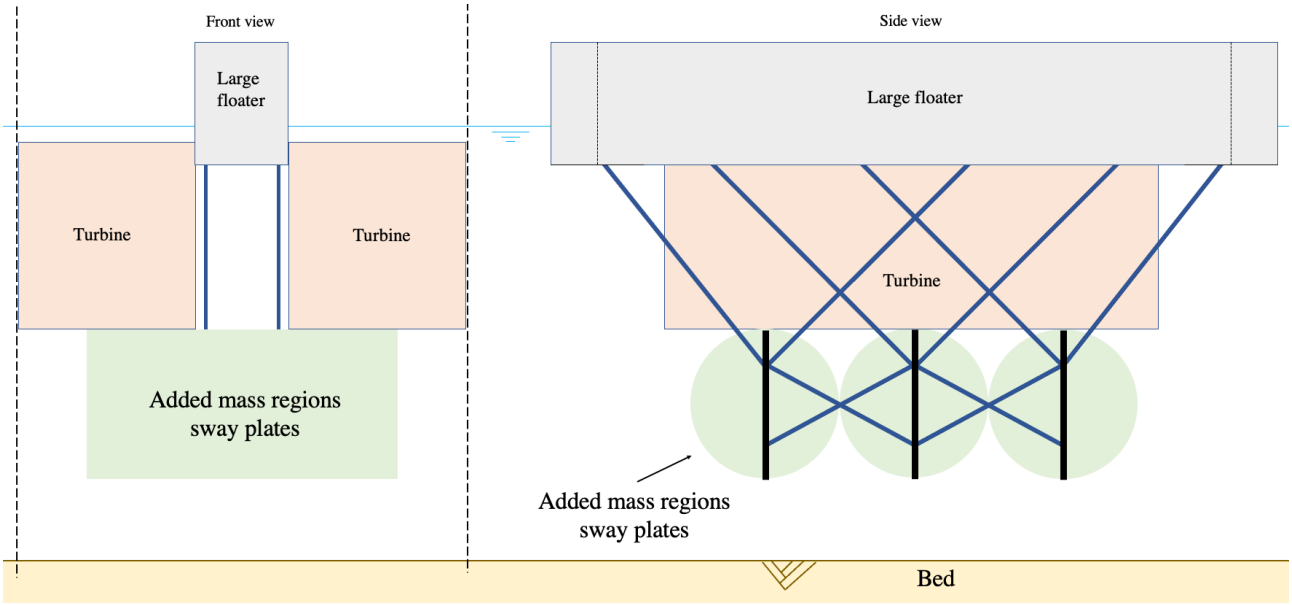

Figure G.30 Added mass plan for the sway plate 9 x 17 m

G.2.4 Variant 7: Sway plate 1 x 70 m

Profiles	Dimensions (mm)	Unity Checks
Plate	t = 15	0.20
Box beam	h = 500	0.48
	w = 300	
	t = 16	
Main tubes	d = 300	0.53
	t = 7	

Effectivity	11.9 days
Steel needed	444 tons
Generated added mass sway	3607 tons
Generated added mass heave	-
Depth of COG of added mass	16.5 m

Table G.7 Specifications variant 7

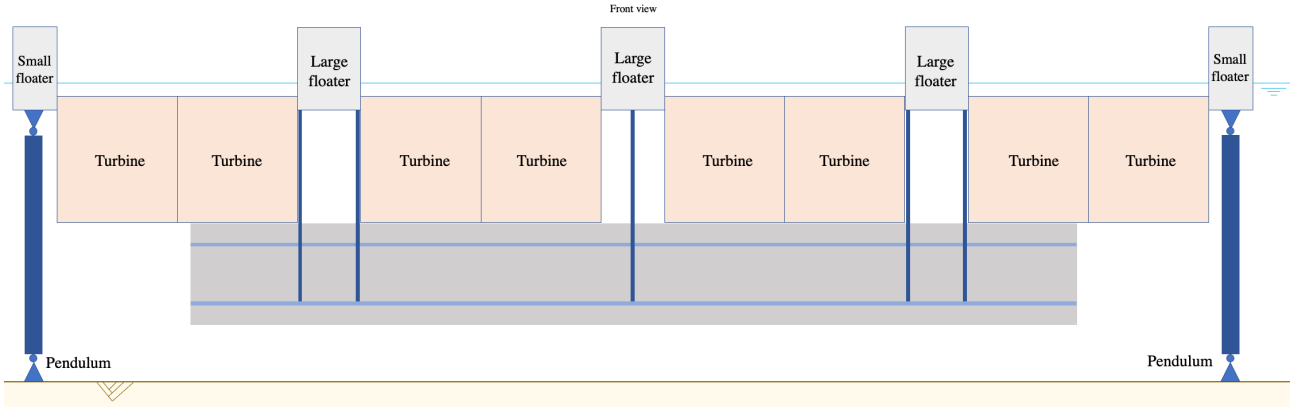

Figure G.31 Front view of the sway plate 1 x 70 m

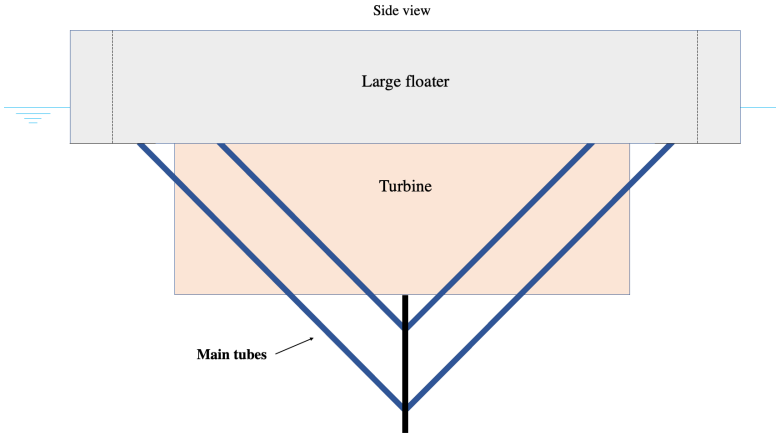

Figure G.32 Side view of the sway plate 1 x 70 m

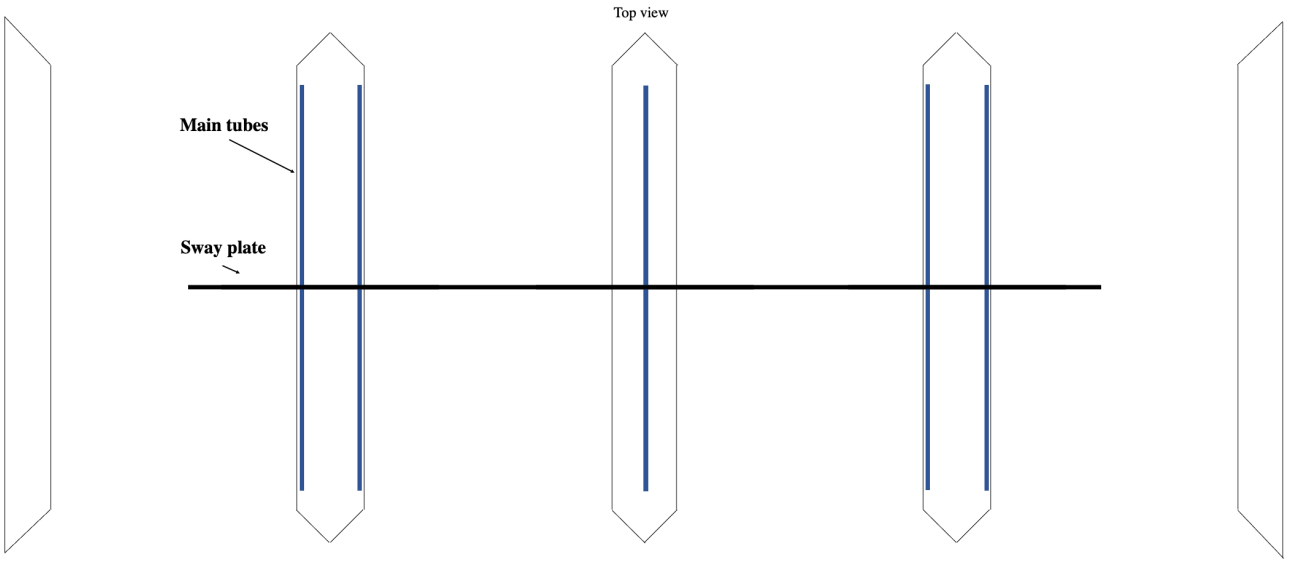

Figure G.33 Top view of the sway plate 1 x 70 m

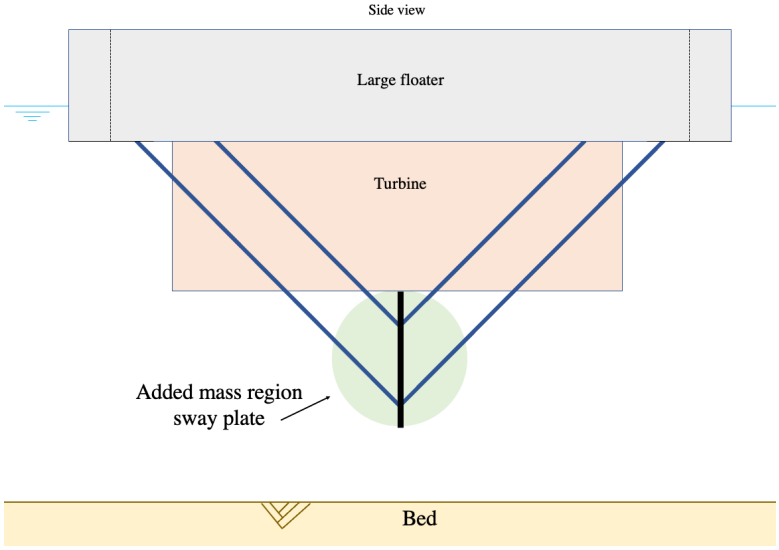

Figure G.34 Added mass plan of the sway plate 1 x 70 m

G.2.5 Variant 8: Sway plate 2 x 70 m

Profiles	Dimensions (mm)	Unity Checks
Plate	t = 15	0.20
Box beam	h = 500	0.48
	w = 300	
	t = 16	
Main tubes long	d = 300	0.62
	t = 12	
Main tubes short	d = 300	0.51
	t = 12	

Effectivity	20.7 days
Steel needed	873 tons
Generated added mass sway	7214 tons
Generated added mass heave	-
Depth of COG of added mass	16.5 m

Table G.8 Specifications variant 8

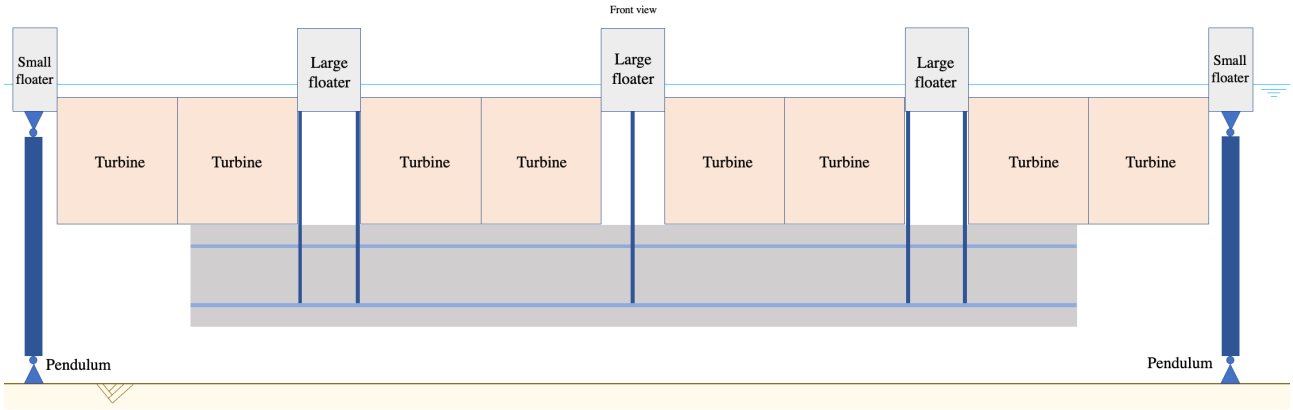

Figure G.35 Front view of the sway plate 2 x 70 m

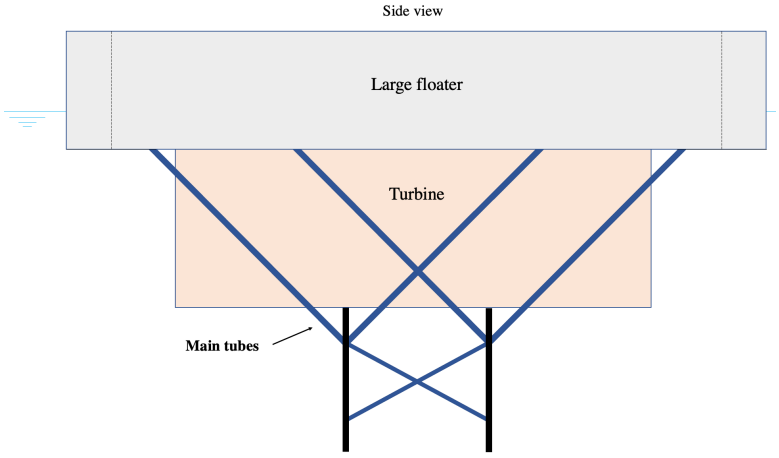

Figure G.36 Side view of the sway plate 2 x 70 m

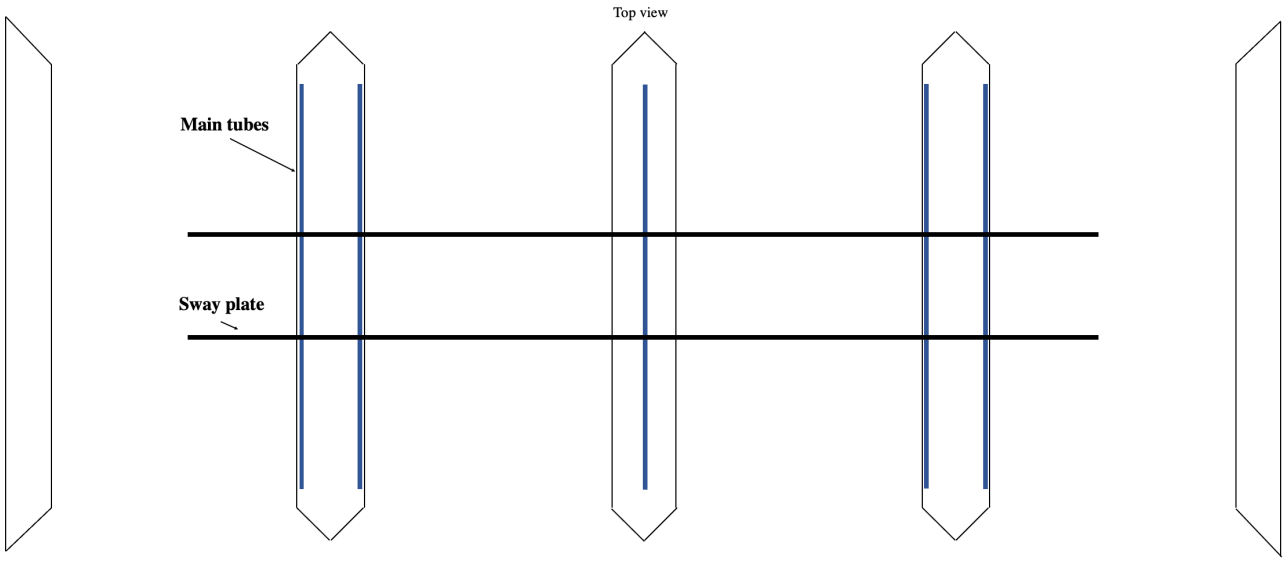

Figure G.37 Top view of the sway plate 2 x 70 m

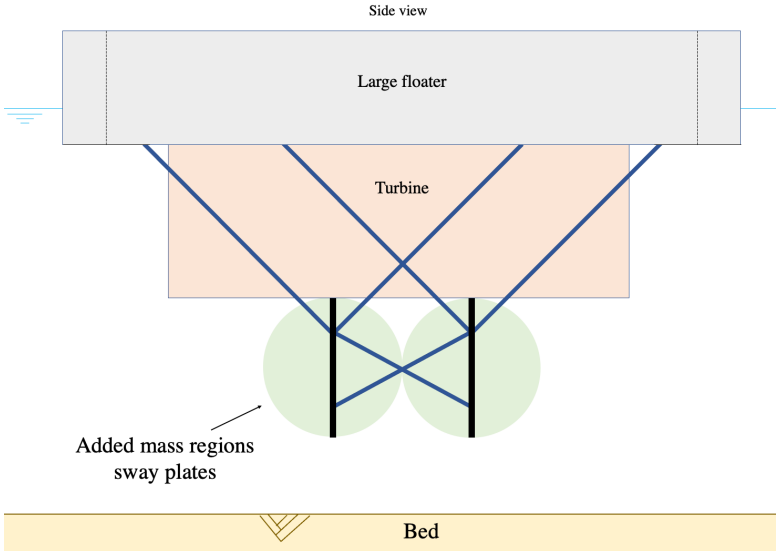

Figure G.38 Added mass plan of the sway plate 2 x 70 m

G.2.6 Variant 9: Sway plates between turbines

Profiles	Dimensions (mm)	Unity Checks
Plate	t = 15	0.20
Stiffeners	h = 200	0.60
	t = 15	
Box beam	h = 80	0.54
	w = 80	
	t = 9	
Main tubes long	d = 200	0.41
	t = 6	

Effectivity	5.9 days
Steel needed	327 tons
Generated added mass sway	4645 tons
Generated added mass heave	-
Depth of COG of added mass	8 m

Table G.9 Specifications variant 9

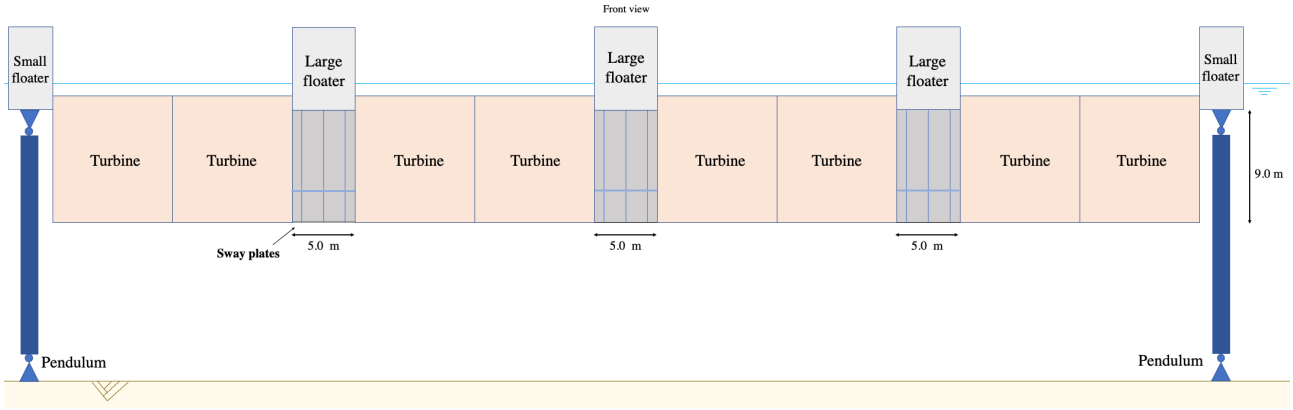

Figure G.39 Front view of the sway plates between turbines

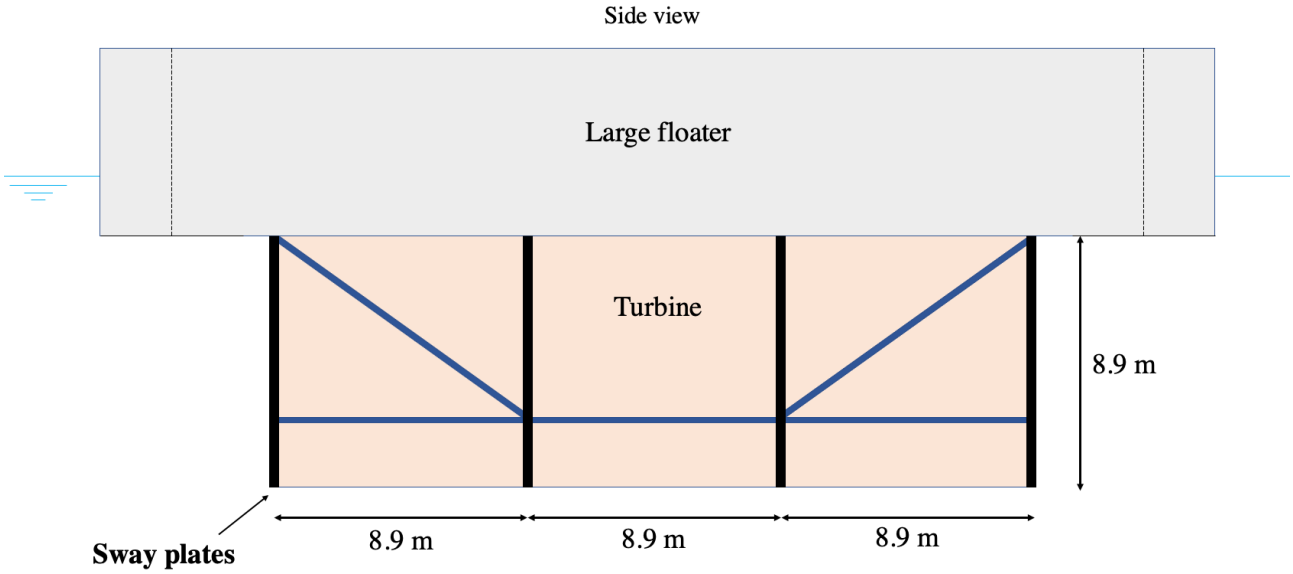

Figure G.40 Side view of the sway plates between turbines

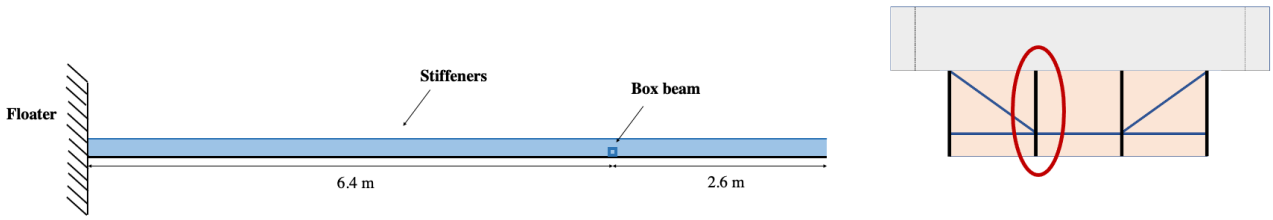

Figure G.41 Cross section of the plate of the sway plates between turbines

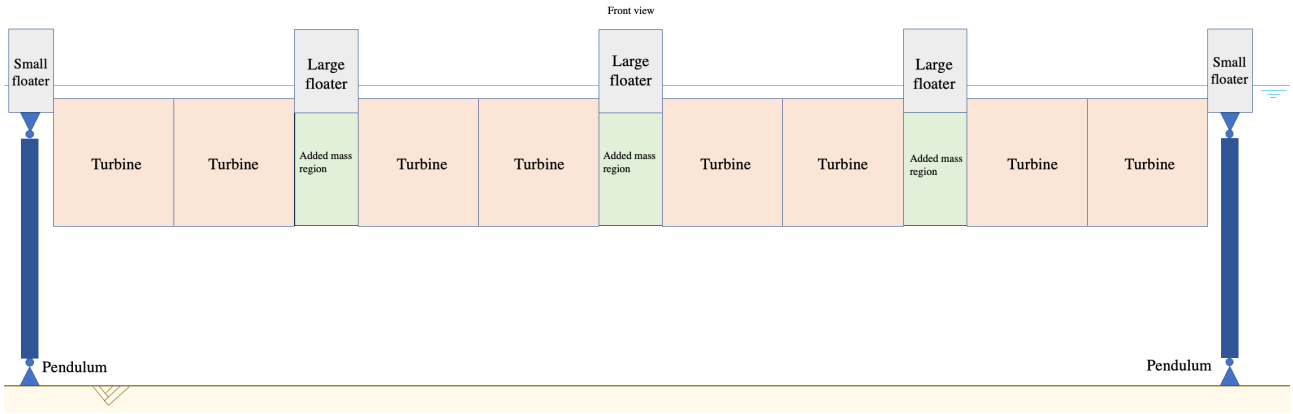

Figure G.42 Front view of the added mass plan of the sway plates between turbines

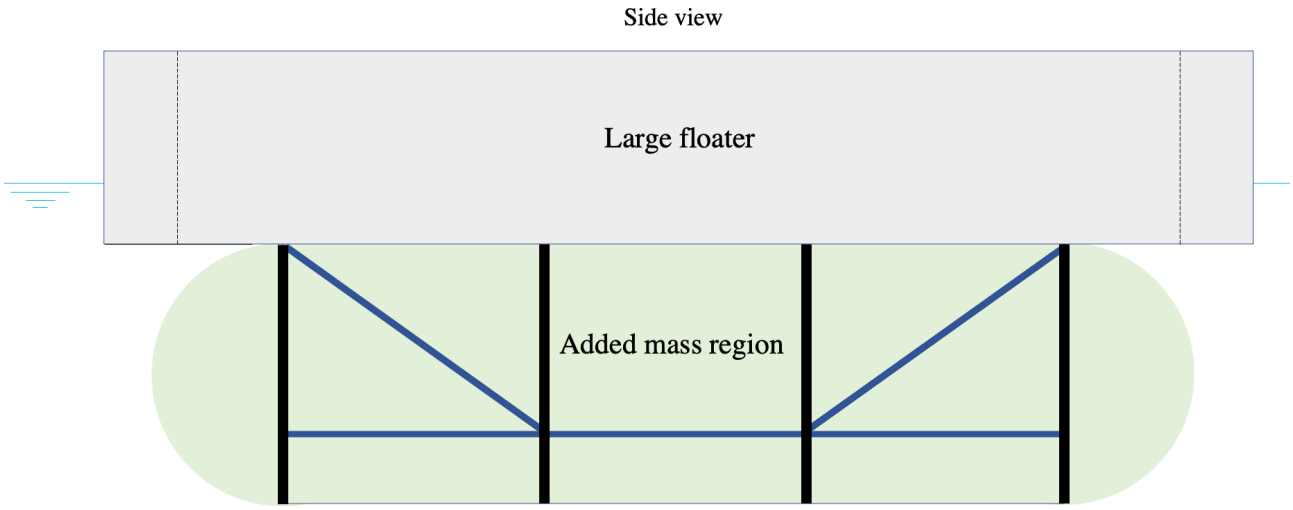

Figure G.43 Side view of the added mass plan of the sway plates between turbines

G.2.7 General figures about the sway plates

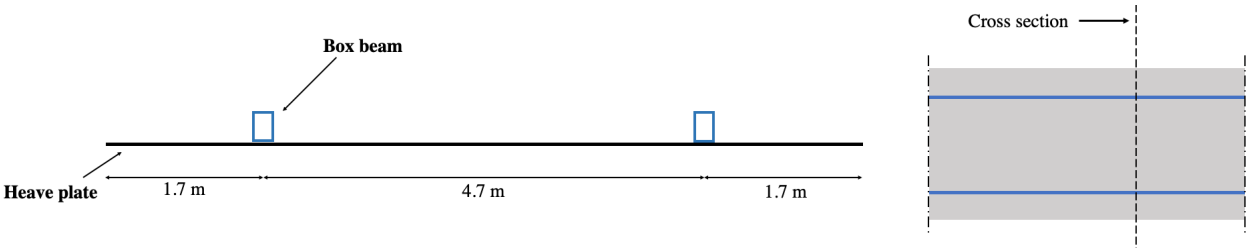

Figure G.44 Cross section of the plate of the sway plates hanging below the turbines

G.3 Presenting the downtime per variant

Table G.10 gives an overview of the yearly downtime per variant and its corresponding improvement relative to the base case. Conditional formatting in the column of "Days of downtime yearly" shows which variant has the least downtime yearly to the best improvement. Conditional formatting in the column of "Improvement" shows which variant fulfill the design objective.

	Days of downtime yearly			Improvement		
Probability	95%	50%	5%	95%	50%	5%
Design	(days)			(days)		
Base case	32	23	16			
Lower heave plates	18	11	5	14	12	11
Upper heave plates	18	12	3	14	12	13
Heave plate 1 x 68 m	16	10	3	15	14	13
Sway plate 3 x 17 m	21	15	8	11	9	8
Sway plate 6 x 17 m	14	8	1	17	16	16
Sway plate 9 x 17 m	9	1	0	23	22	16
Sway plate 1 x 70 m	18	12	3	14	12	13
Sway plate 2 x 70 m	10	3	0	22	21	16
Sway plates between turbines	24	18	11	7	6	6

Table G.10 Table displaying the yearly downtime per variant and its corresponding improvement relative to the base case. The given probabilities are introduced by the uncertainty in the wave characteristics.

G.4 Presenting the steel need per variant

The steel need is an important characteristic as this scales well with the total cost of the variant solution. The steel need can therefore help in determine which variant is probably going to be the cheapest. For every variant the steel need is calculated based on the used plate thickness, and the types and length of the concerned structural elements. Table G.11 shows a summary of the steel need of every variant to implement the variant in the total Tidal Bridge. The table also shows the steel needed per improved day. This second column shows which variant can achieve the most performance with the least amount of steel. Conditional formatting helps in finding the most efficient solution.

The results of Table G.11 are visualized in a Figure G.45 as well. The graph shows the steel needed to implement the variant for the four floating elements of the Tidal Bridge plotted to the corresponding improvement in days of downtime.

Figure G.46 shows the steel needed per improved day plotted to the total improved days. Variants that have a low need of steel per improved days show to be interesting and probably relatively cheap solutions. The variants that have a large improvement of the downtime may be found on the right side. The most optimal solutions, which are selected in Chapter 7, can be found in the lower right corner.

Design	Steel needed (tons)	Steel needed per improved day (tons/day) Probability 95%	50%	5%
Lower heave plates	833	60	69	76
Upper heave plates	426	32	36	33
Heave plate 1 x 68 m	1938	127	142	148
Sway plate 3 x 17 m	268	26	31	34
Sway plate 6 x 17 m	497	29	32	31
Sway plate 9 x 17 m	750	33	34	46
Sway plate 1 x 70 m	444	33	37	34
Sway plate 2 x 70 m	873	41	42	54
Sway plates between turbines	327	44	55	60

Table G.11 Table displaying the steel need to implement the variant for the complete Tidal Bridge project. The table also shows the steel need per improved day of less downtime. The given probabilities are introduced by the uncertainty in the wave characteristics.

Figure G.45 The total steel needed to implement the variant to the four floating elements plotted to the improved days. The number one shows two results that achieved their maximum improvement of 16.3 days. This 16.3 is found in the base case result of which is expected that there is a probability of 5% that the variant may have less downtime.

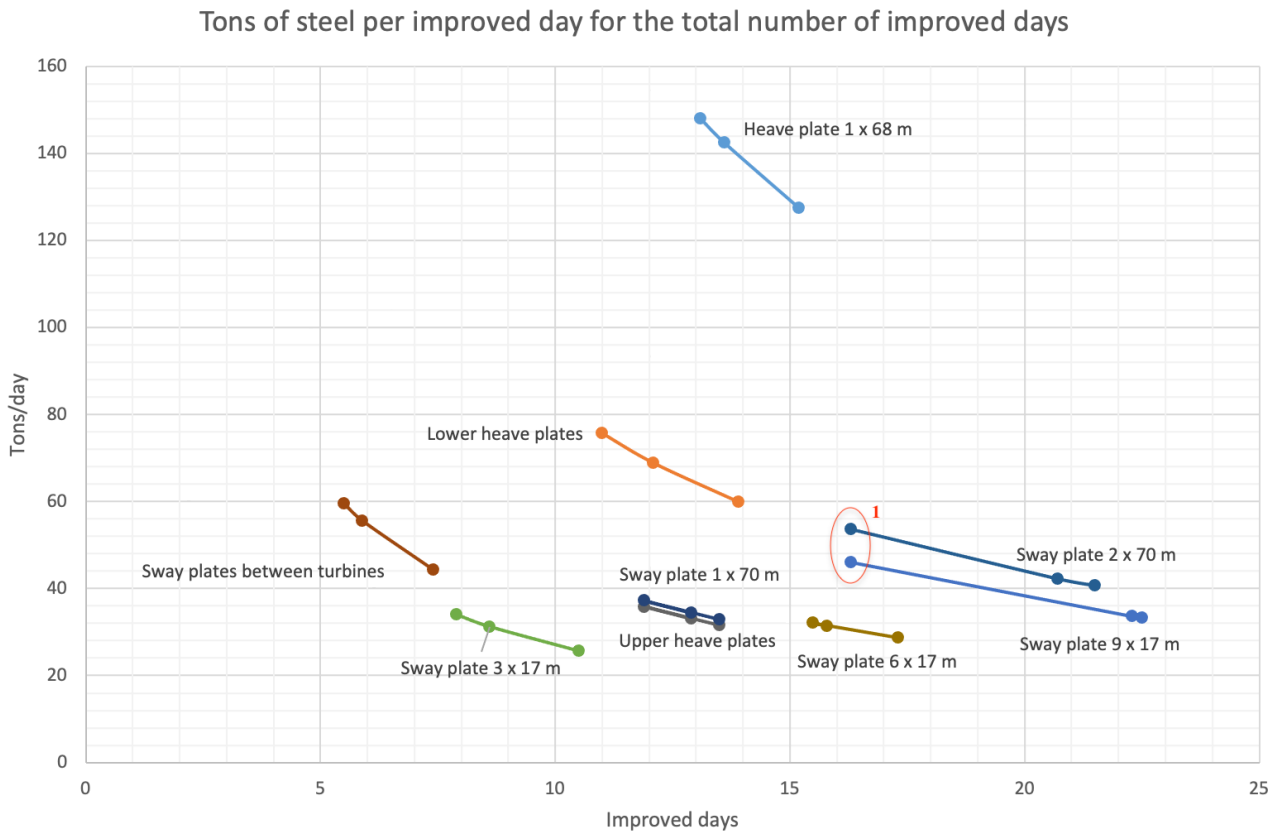

Figure G.46 Graph showing the steel needed per improved day plotted to the total improved days. An explanation for the number one may be found in the caption of Figure G.45.

H | Resulting Design

Contents of this appendix chapter

H.1 Construction method

This section sketches an idea about a possible construction method as there may be different ways to construct the resulting design. This described construction method is all about attaching the sway plate safely to the floating structure of the Tidal Bridge. This construction method is executed after the construction of the Tidal Bridge floating elements. The sway plates are attached to the floating Tidal Bridge elements before the turbines are attached to the Tidal Bridge floating elements.

1. **Construction of the complete steel structure:** The complete sway plate steel structure is welded together on an available quay wall. The box beams, the smaller tubes and the longer tubes are all welded together and are made ready for submergence. The complete structure is coated to avoid corrosion as much as possible.

2. **Attachment of the auxiliary structure and the floaters:** An auxiliary structure of IPE600 beams is welded together. The structure consist of an extra long beam of 42 meters. Shorter beams of five meter are connected perpendicular to the long beam on each side of the middle on a distance of four meters. These beams have a dark red colour in Figure H.1. Four cylindrical floaters with a diameter of 2.2 meter and a length of 4 meter are connected to the points of the smaller beams. These floaters together have exactly the needed floating capacity to carry the sway plate structure as it is submerged. Long floaters with a diameter of 1 meter and a length of 10 meters are attached to the end of the long IPE600 beam. These floater can inflate or shrink to increase or decrease the floating capacity. These floater are used to regulate the draught when the steel sway plate structure is brought into the water.

3. **Launching the structure to the water:** Two large cranes lift the sway plate structure including the auxiliary structure with the floaters and launch the structure to the water. The two long floaters are regulated such that the structure floats independently at the desired height. This desired height is a little lower than the height at which the structure is going to hang permanently.

4. **Positioning and fastening the sway plate structure:** The sway plate structure is towed into its final position underneath the Tidal Bridge floater. The long floaters are regulated such that the sway plate structure is lifted into the objected place. Divers secure the structure to the floaters with the twelve pin connections.

5. **Removing the auxiliary structure and floaters:** The long beam of the auxiliary structure becomes supported to floaters of the Tidal Bridge by 6 large straps. The four main floaters and the long floaters on the end are removed by the divers such that the IPE600 beams are only supported by the straps. Two of the main floaters are connected to both ends of the long beam. The floaters are inflated such that the beam mostly floats. The beam is towed out of its position through the available space between the sway plate, the tubes and the floater of the Tidal Bridge. The beam is carried by the floaters and stabilized by the straps the hanging to the Tidal Bridge floaters.

6. **Finishing:** After hanging the three sway plate structures below the three floaters of the Tidal Bridge, the Tidal Bridge can be towed into its position in the Larantuka Strait. The website Navioncs shows that there are not shallow parts present in the region around project area of the Tidal Bridge. The total draught of the towing process of the Tidal Bridge is not an issue. The turbines are installed after the complete installation of the Tidal Bridge.

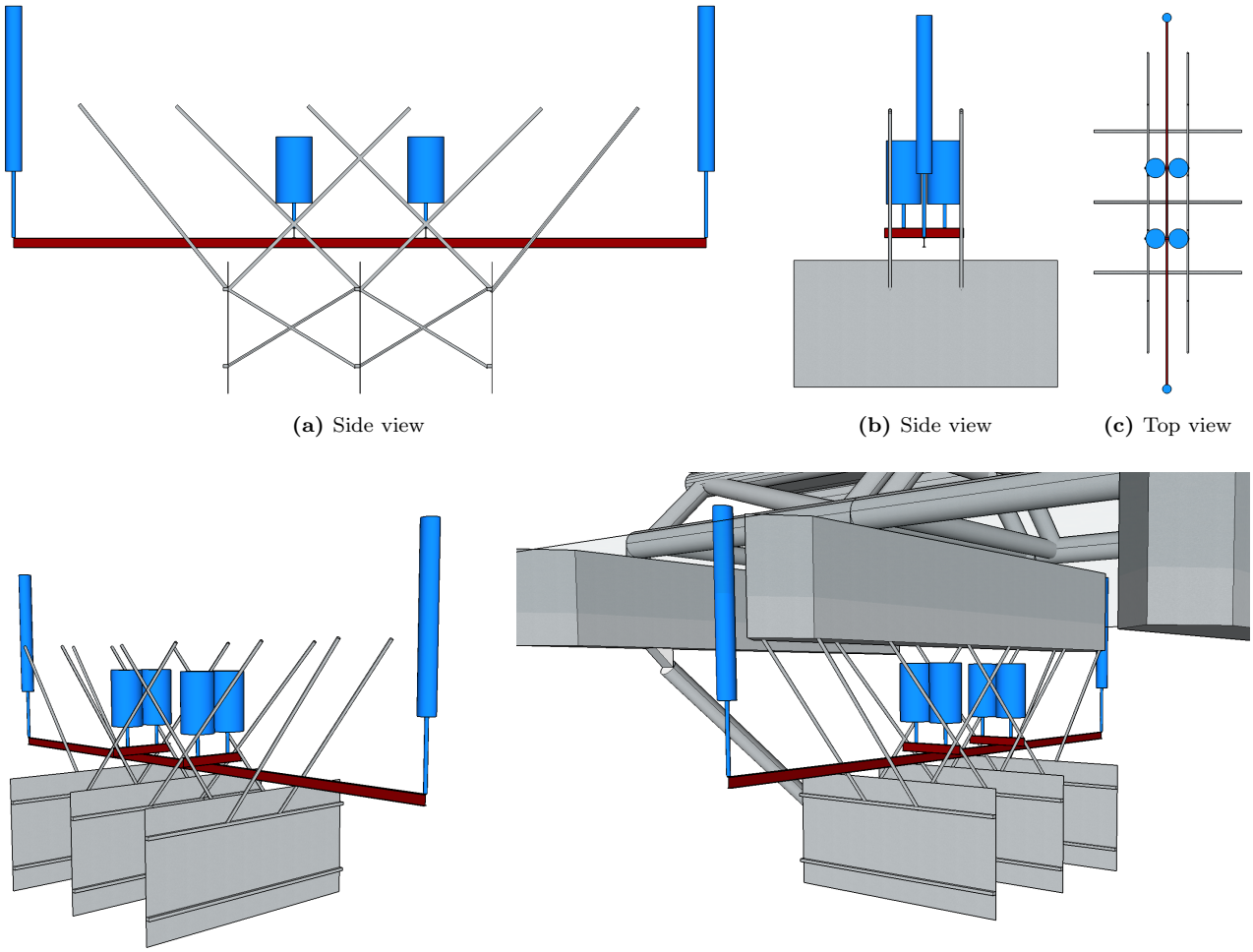

(a) Side view **(b)** Side view **(c)** Top view

(d) Perspective view **(e)** Perspective view

Figure H.1 All different perspectives of the auxiliary structure with its floaters carrying the sway plate structure in the construction phase.

H.2 Sketches of the resulting design

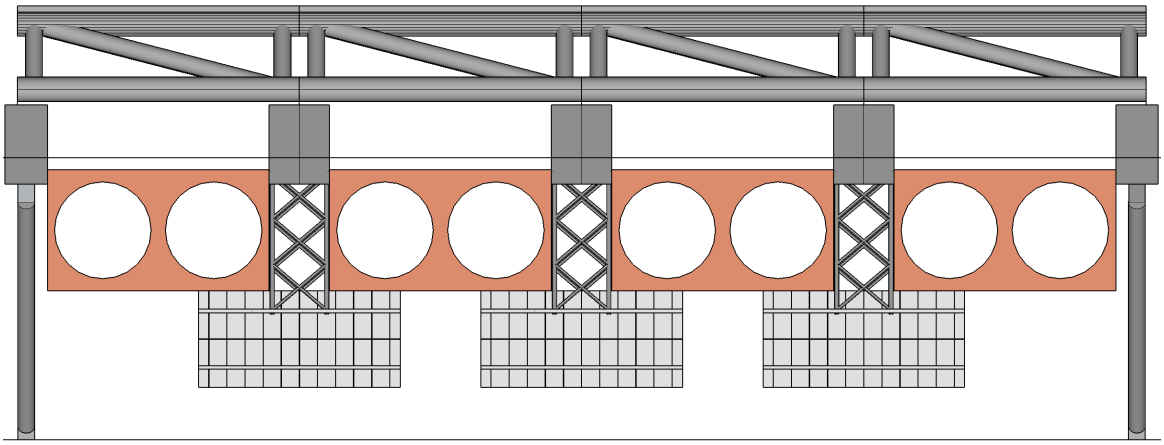

Figure H.2 Front view of one Tidal Bridge element with the resulting design

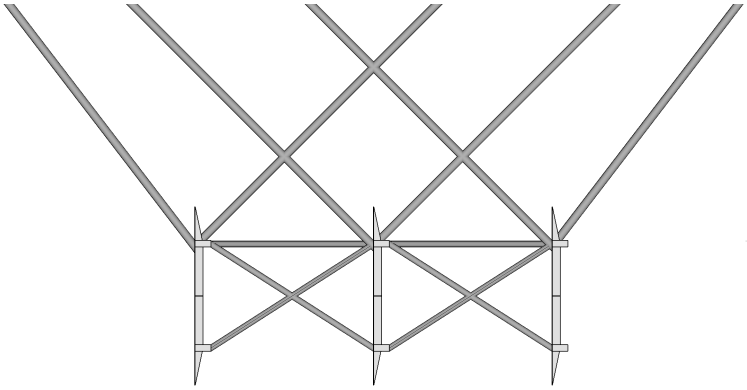

Figure H.3 Side view of one set of sway plates of the resulting design

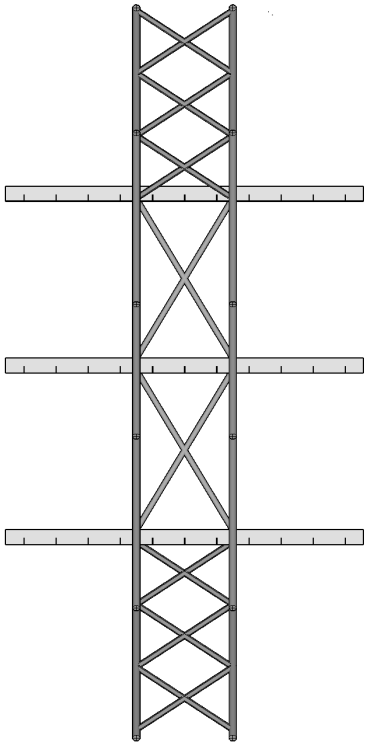

Figure H.4 Top view of one set of sway plates of the resulting design

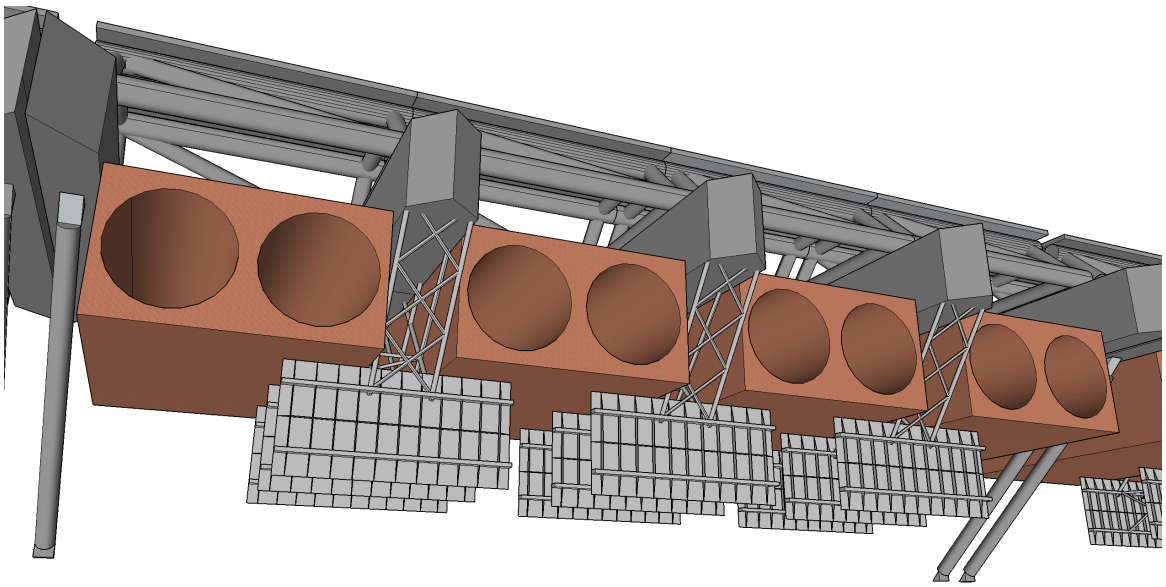

Figure H.5 Perspective sketch of the resulting design integrated in the Tidal Bridge structure

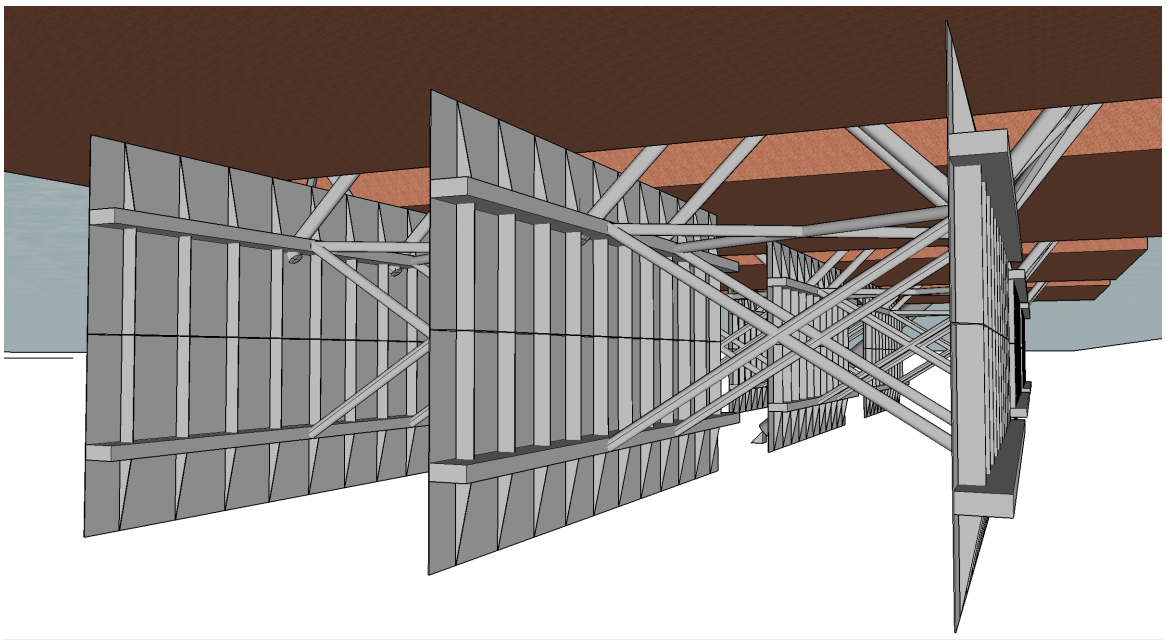

Figure H.6 Perspective sketch detail of one set of three sway plates integrated in the Tidal Bridge structure.

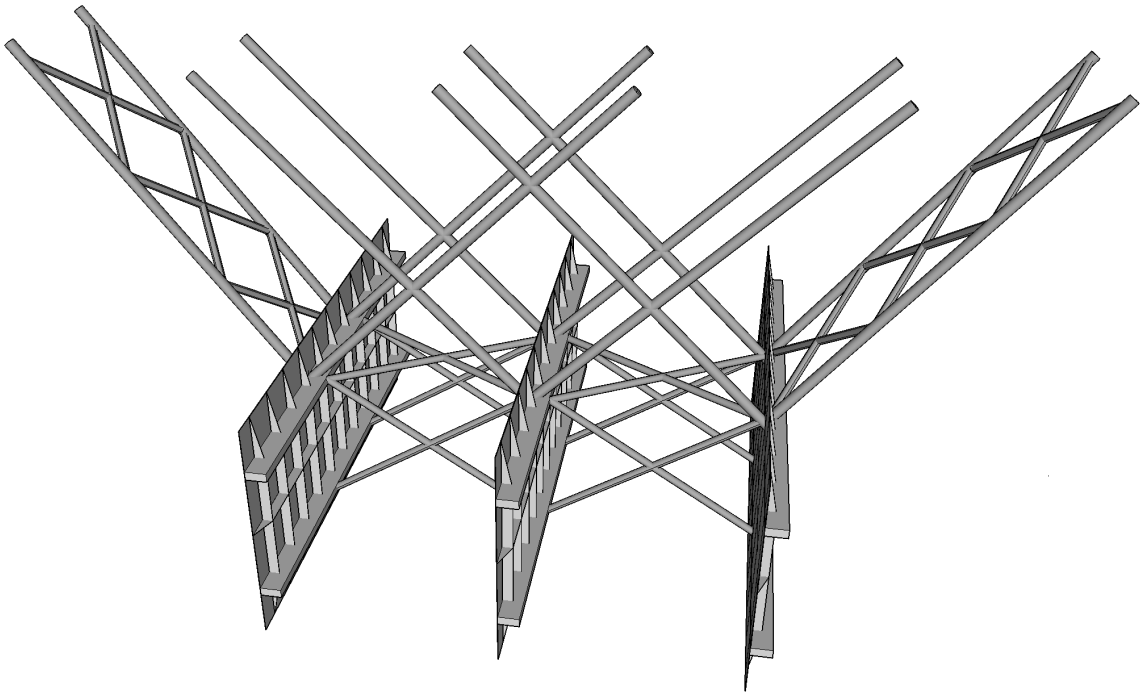

Figure H.7 Perspective sketch of one set of three sway plates.

H.3 Sketches of the pin connection

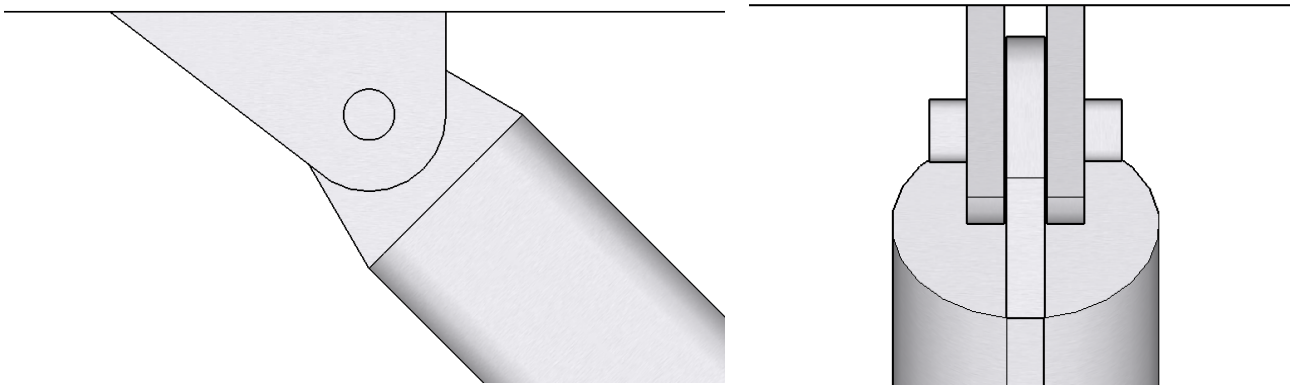

(a) Side view

(b) Front view

Figure H.8 Drawings of the pin connection between the sway plate structure and the floater

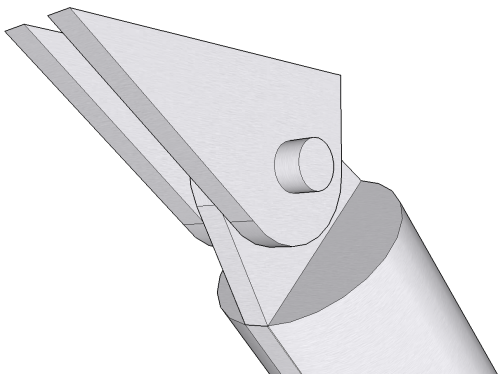

Figure H.9 Perspective view of the pin connection between the sway plate structure and the floater

I | Limitations of the report

This appendix chapter qualitatively discusses the limitations of the design report which have been split into two groups. The first groups addresses the limitations of the structural dynamics model, and the second group the limitations of the wave characteristics model.

I.1 The limitations of the structural dynamics model

The structural dynamics model has a significant role in the construct of this design. The structural dynamics model has been used to acquire knowledge about the dynamic response of the Tidal Bridge, and the model has been used to quantify the specific dynamic response. The limitations below may value some uncertainty related to the quantification of the dynamic response. However, the conclusions about the acquired knowledge of the dynamic response of the Tidal Bridge stays valid as the model has been elaborately verified. Hence, the model responds to changing parameters as it should do. The most relevant limitations are discussed first.

- **Unvalidated model:** The structural dynamics model has not been validated with experiments to check the physical accuracy. Although, the accuracy of the quantified response may be slightly off, the order of magnitude of the quantified response is not expected to be drastically different compared to the scale model and the resulting design stays valid.
- **Excluded response to irregular waves:** The structural dynamics model only examines the response to regular waves and not to irregular waves. Irregular waves may lead to short and exceptional peak accelerations which are not calculated by the used model. These may or may not become problematic depending on the user experience of such short and exceptional accelerations. This may influence the resulting design dimensions. However, this influence will not be affecting the choice for the resulting design variant over the other variants.
- **Assumed stabilizing current influence:** The results of the structural dynamics model are partly based on the assumed that the tidal currents through the strait stabilize the dynamic behaviour of the Tidal Bridge. The additional current related drag forces are quadratically dependent to the current velocity. This should lead to stabilizing the dynamic behaviour. This is a fair assumption and always valid as long as drag related instabilities do not occur. This assumption is not expected to lead to rejecting the resulting design.
- **Drag related instabilities:** The resulting design could make the total Tidal Bridge structure unstable to the current related drag forces. The Tidal Bridge is a fairly heavy structure and only enormous drag forces could induce instabilities. This effect is not expected to lead to rejecting the resulting design.
- **Neglecting the side floating elements:** The structural dynamics model only simulates the dynamics of one of the middle two elements of the four floating elements. The two unmodelled elements have a restriction in the critical degree of freedom of sway one one side of the element. This restriction is expected to lead to less dynamics than the middle two modelled elements, and hence, this limitation is not expected to lead to rejecting the resulting design.
- **Assumed open boundaries:** The influence of the adjacent floating elements has been neglected, which resulted in assuming open boundaries on the sides of the floating elements in the model. It became rather complicated to model the influence of the adjacent elements with a model that integrates the four floating

elements with their three degrees of freedom separately. Attempts to verify simplified boundary conditions that were dependent on the displacement, were not successful either. The model uses open boundaries which assumes that the adjacent element dynamically behaves identically resulting in absent inter-element forces. The additional restriction of the connections cannot increase the amount of dynamic response by adding energy to the system. The fair assumption is therefore made that the dynamic response of the Tidal Bridge that includes this inter-element connection force would show the same or smaller.

- **Introduced uncertainties due to the usage of the Morison equation:** The Morison equation quantifies the hydraulic forcing of the waves which is the driving parameter leading to the exceedance of the serviceability limits. The Morison equation consists of various contributions that introduce uncertainties in the model which are shortly discussed below:
  - **Estimated added mass:** The sensitivity study showed the importance of the inertia coefficient to the Tidal Bridge dynamic behaviour. The inertia coefficient partly consists of a contribution related to the submerged volume and partly consists of a contribution related to the added mass. Uncertainties are introduced by the determination of the added mass. The complex shape of the turbines make it difficult to make accurate predictions of the added mass. Furthermore, the geometry and shape of the turbines influence the magnitude of the added mass of the floater. Also, interference effects with the free surface and the bottom make the added mass dependent on frequency. These uncertainties may lead to a calculated dynamic response which is slightly off. However, the analysis that lead to the resulting design would not become much different and the same resulting design would have been selected with a more accurate model.
  - **Estimated drag coefficient:** The drag coefficient depends to the Keulegan-Carpenter number for the intermediate and drag dominated regime. In reality, the KC number changes upon having a different wave height, wave length and current velocity. The drag coefficient was kept constant in the structural dynamics model. The drag forces may be overpredicted in a more drag dominated regime. This leads to an slightly underestimated dynamic behaviour for situations that are more drag dominated. However, the highly inertia dominated structure is not dependent on the drag coefficient and this effect of a changing drag coefficient is negligible.
  - **Used grid approach:** The Morison equation is intended to be used for structures that have a structure length in the directions of the waves of one fifth of the wave length or smaller. The structural dynamics model makes this recommendation less imperious by dividing the structure into grid cells and evaluates the Morison equation per grid cell. The stated usage recommendation is valid for each grid cell. Simplification concerning the distribution of the added mass and the water particle accelerations over these grid cells introduces uncertainties. These uncertainties are expected to be slightly overestimating the dynamic behaviour. This effect is expected to be small. Furthermore, the over-prediction of the dynamics may turn out positively in reality.
- **Estimated radiation damping:** Vugts (1968) has performed experiments to the radiation damping of a semi-submersed floating objects like ships. These experimental results have been used to determine the radiation damping of the floater, but also for the turbine which is completely submerged. Literature shows that the radiation damping becomes less and goes to zero for objects that do not have interference effects with the free surface. The estimated radiation damping of the turbine may probably be less as the moving objects have less interference effects with the free surface. This uncertainty may underestimate the dynamic behaviour slightly. However, the sensitivity showed that the influence of the radiation damping is negligible.
- **Neglected diffraction effects:** The frontal surface area of the floaters and turbines of the total Tidal Bridge is relatively large compared to remaining area through which the waves pass the structure. The waves become reshaped due to the influence of the large structure which is called diffraction. This effect is not taken into account in the description of the wave particle kinematics. Neglecting diffraction effects overpredicts the dynamic behaviour.
- **Used interpolation:** The structural dynamics model calculates the combined acceleration caused by a defined wave height and wave length combination and outputs corresponding displacements, velocities and accelerations. These discrete model results are subsequently interpolated with cubic interpolation

to generate a continuous visual results. Interpolation estimates data that has not been modelled. The introduction of uncertainty due to presenting faulty end results is expected to be small. Many of those discrete data points is modelled in order to reduce uncertainties due to interpolation.

- **Neglected the third dimension:** The structural dynamics model approaches the dynamic problem with a two-dimensional perspective on the system. Ignored effects are: the dynamics of three extra degrees of freedom, the different pendulum lengths due to the different depths below the element, and the different pendulum angles due to the different lengths. The effects of the third dimension are expected to be very small.

I.2 The limitations of the wave characteristics model

The wave characteristics model has a significant contribution in determining the downtime of the base case and the proposed design optimizations. The list below qualitatively discusses the limitations of the wave characteristics model that may not have been fully respected. The most relevant limitations in the model are presented first.

- **Estimated near shore processes:** Many coefficients of the near shore processes have been determined with hand calculations. Approaching dissipation or diffraction with hand calculations for the situation of the Larantuka Strait proved to be difficult. The uncertainty has been visualized by the confidence intervals in the model result and presented in the end result as well. The over- or underprediction has been quantified and taken into consideration in the design process.
- **Neglecting swell waves:** The wave characteristics model assumes waves in the Larantuka Strait to be only generated by wind within an area with a radius of 600 kilometres or smaller. Swell waves generated farther away may penetrate into the strait which causes the Tidal Bridge to exceed its serviceability limits more often. These types of waves are not accounted for in the wave characteristics model and cause an underprediction of the downtime. This effect is expected to be small in the area with a moderate wind climate.
- **Used wind data:** The wave characteristics model is only dependent on one single open source data set. Uncertainties existing in this data set develop into uncertainties in the wave characteristics model. These uncertainties have not been quantified by a comparison with a different data set. Although the accuracy of the results may be off, the used reasoning that lead to the resulting design would not change.

I.3 The limitation of the chosen serviceability limits

The chosen and used serviceability limits have been found in literature. However, not much literature was available about serviceability limits of a floating bridge. Differently chosen serviceability limit may lead to a different determination of the downtime and a different geometry of the resulting design. The serviceability limits have been deducted from an American writer. Serviceability limits in Indonesia may be more tolerable and less risk averse.